

## MASTER

### Rigidized inflatable structures

#### an innovative production method for structurally optimized elements

van de Koppel, W.J.; van Dijck, S.H.M.

*Award date:*  
2013

[Link to publication](#)

#### **Disclaimer**

This document contains a student thesis (bachelor's or master's), as authored by a student at Eindhoven University of Technology. Student theses are made available in the TU/e repository upon obtaining the required degree. The grade received is not published on the document as presented in the repository. The required complexity or quality of research of student theses may vary by program, and the required minimum study period may vary in duration.

#### **General rights**

Copyright and moral rights for the publications made accessible in the public portal are retained by the authors and/or other copyright owners and it is a condition of accessing publications that users recognise and abide by the legal requirements associated with these rights.

- Users may download and print one copy of any publication from the public portal for the purpose of private study or research.
- You may not further distribute the material or use it for any profit-making activity or commercial gain

# Rigidized Inflatable Structures

An innovative production method for structurally optimized elements

REPORT



Joost van de Koppel - Stan van Dijck





# Rigidized Inflatable Structures

An innovative production method for structurally optimized elements

**Joost van de Koppel - Stan van Dijck**

Graduation committee:  
prof.dr.ir. J.J.N. Lichtenberg  
ir. A.D.C. Pronk  
Ir. A.P.H.W. Habraken  
Prof. Ir. P. von Buelow

University of Technology Eindhoven  
Architecture, Building & Planning  
Studio Slimbouwen VI



**Project:** Master thesis  
Studio Slimbouwen VI

**Title:** Rigidized inflatable structures; an innovative  
production method for structurally optimized elements

**Authors:** S.H.M van Dijck  
s.h.m.v.dijck@student.tue.nl  
www.stanvandijck.com

W.J. van de Koppel  
w.j.v.d.koppel@student.tue.nl  
www.cargocollective.com/joostvandeKoppel

**Date:** August 15<sup>th</sup> 2013

**Location:** Eindhoven University of Technology  
Faculty Building Technology  
Den Dolech 2  
5612 AZ Eindhoven

**Graduation committee:** Prof. Dr. Ir. J.J.N. Lichtenberg  
Ir. A.D.C. Pronk  
Ir. A.P.H.W. Habraken  
Prof. Ir. P. von Buelow

Eindhoven University of Technology  
Eindhoven University of Technology  
Eindhoven University of Technology  
University of Michigan



## PREFACE

The report that lies before you describes the efforts that we made in the frame of our master thesis at Eindhoven University of Technology, at the faculty of Building Technology. The idea to cooperate during our graduation was conceived during our visit to the Textile Roofs 2012 congress in Berlin. Here, Arno Pronk showed the different subjects that were available in the frame of free form design, which included a concept of a new production method for open cell structures. This subject both caught our interest, which lead to the decision to join efforts. Now, one year later, the thesis is finished and we both look back on a interesting, instructive, intensive and fun final year.

This thesis would not have been completed without the help of several different people. First of all, we would like to thank our graduation committee, with Arno Pronk in particular, for their coaching and assistance during the project. Especially the help of Prof. Ir. P. von Buelow with the ParaGen method was essential in the research. The staff of the van Musschenbroek laboratory, with Hans Lamers in particular, and the students of the Design for Manufacturing course have helped us very much with the fabrication and testing of the scale models, and would not have been realized without their help. Also, we would like to thank Arnold Voskamp from Eurocarbon, Peter van der La from Beamix, Simon van Bijsterveld from VRBZO, Harry Buskes from Carpro, Edwin Hutten from Euroresin, Teunissen B.V., Rovadi Landbouwmecanisatie and Wilbert van Dijck for the sponsoring of materials for the fabrication and their contribution to the realisation of the prototype. Finally, we want to thank Mathias Goelke from Altair Engineering for giving us the opportunity to present our research at the Altair Technology Conference in Turin.

Deze thesis beschrijft de ontwikkeling van een innovatieve productie methode voor constructief geoptimaliseerde, snede actieve constructie systemen. Het onderzoek komt voort uit een groeiende maatschappelijke vraag naar een vermindering van het materiaalgebruik in de bouw, waardoor het gebruik van grondstoffen ook wordt verminderd. Een antwoord op deze vraag is het gebruik van constructieve optimalisatie om zo het gewicht van constructieve elementen te verminderen. Echter, momenteel zijn er geen efficiënte productiemethoden welke geschikt zijn om de organische vormen kenmerkend voor constructief geoptimaliseerde elementen te maken. Vanwege de eigenschap om altijd ronde vormen aan te nemen wordt een productie methode gebaseerd op inflatables die geheel of gedeeltelijk kunnen worden verhard gezien als een veelbelovende oplossing. In dat geval bestaat de bekisting van de ruimtelijke constructie volledig uit opblaasbare structuren en is daardoor geheel gebaseerd op vorm-actieve principes. De methode gebruikt een binnenste inflatable, of secundaire mal, die als de hulpconstructie dient en tijdelijk of semi-permanent is. Tegen de buitenkant van deze secundaire mal worden opblaasbare buizen die de geoptimaliseerde structuur weergeven opgeblazen, en kunnen vervolgens geheel of gedeeltelijk worden verhard.

Het onderzoek is gestart met een literatuur studie naar de grondbeginselen van constructieve optimalisatie. Vervolgens zijn de vier snede actieve constructie systemen topologisch geoptimaliseerd d.m.v. empirische case studies, om zo hun algemene morfologische eigenschappen te bepalen. Hieruit bleek dat de relatie tussen de vorm en structuur, oftewel de structurele morfologie, van deze geoptimaliseerde elementen erg strek is. De resulterende topologie en morfologie van een optimalisatie cyclus wordt bepaald door de kracht verdeling door de ontwerp ruimte en de verschillende randvoorwaarden en prestatie eisen die op die ontwerp ruimte werken. De morfologie van een geoptimaliseerde balk kan worden herkend in elk ander geoptimaliseerd snede actief element. Ook bezit de geoptimaliseerde balk de meeste algemene morfologische eigenschappen, waardoor deze als case heeft gediend voor de voorgestelde productiemethode. Met deze topologisch geoptimaliseerde ruimtelijke balk is vervolgens een vorm optimalisatie uitgevoerd m.b.v. de ParaGen methode. Met deze parametrische methode is een populatie van 1276 verschillende oplossingen algoritmisch gegenereerd. Met de oplossing met de hoogste specifieke stijfheid is uiteindelijk een "size" optimalisatie uitgevoerd m.b.v. STAADpro.

Er zijn ook literatuur studies uitgevoerd om de meeste geschikte inflatable typologie en materiaal te bepalen voor de secundaire mal. Deze studies leidde

tot vijf typologieën die zijn geëvalueerd a.d.h.v. vier morfologische indicatoren. De vier geoptimaliseerde constructie systemen zijn geëvalueerd m.b.v. dezelfde indicatoren om ze te kunnen vergelijken met de inflatable typologieën. Dit is geresulteerd in een matrix waaruit bleek dat een recht hoge druk systeem de beste typologie is om te gebruiken als secundaire mal voor onze case. Daarnaast bleek uit de literatuur studie naar membraan materialen dat, a.d.h.v. tien relevante criteria, deze mal het beste van PVC gecoat polyester gemaakt kan worden.

De laatste stap in de onderzoeksfase was een literatuur studie naar membraan verharding methoden. Uit dit onderzoek bleek, samen met de resultaten van een aantal expert meetings, dat er geen "rigidizable materiaal" zoals gebruikt in de ruimtevaart een op een toepasbaar is in de bouw. Echter, de grootste voordelen van deze methodes, zoals de mogelijkheid tot "rigidizeren" op commando, kunnen worden benut wanneer hun opbouw wordt gecombineerd met commerciële fabricatie methoden als resin transfer moulding of vacuüm infusie.

De resultaten van de onderzoeksfase diende als de basis voor de ontwikkelingsfase, die startte met een constructieve analyse van de case m.b.v. GSA en STAADpro. Tegelijkertijd zijn er twaalf betonnen schaalmodellen gemaakt en getest van vier verschillende geometriën. Hieruit bleek dat bepaalde geometrieën nadelig zijn m.b.t. hun rechte lijnige eindige elementen model. Ook werd door de test bevestigd dat de case die gekozen was inderdaad de hoogste stijfheid had. Samen met de resultaten van constructieve analyse was alle informatie bekend voor de fabricage van het prototype. Deze is uiteindelijk gemaakt van geweven glas vezel sokken die zijn opgeblazen rondom een PVC gecoate polyester buis. De glas vezels zijn vervolgens geïmpregneerd met een polyester hars om zo de definitieve geoptimaliseerde structuur over te houden.

Met de fabricage van het prototype is de voorgestelde productie methode gedemonstreerd op ware grote. De voornaamste voordelen van elementen gemaakt met deze methode zijn het enorm lage eigen gewicht, en de snelle inzetbaarheid. Het systeem kan volledig opblaasbaar worden gehouden of kan deels of volledig worden verhard, waarvoor de mogelijke toepassingen groot zijn. Voorbeelden van toepassingen zijn elementen voor noodhulp, tijdelijke constructies, militaire constructies, en het versterken van bestaande constructies. De secundaire mal kan worden verwijderd, maar onderzoek is nog nodig naar de combinatie van een verharde geoptimaliseerde structuur en een opblaasbare binnenste tube. Hierdoor zal het geheel zich gaan gedragen als een "tensairity", waarbij de sterkte groter is dan de som van de individuele onderdelen.

This thesis describes the development of an innovative production method for structurally optimized section active structure systems. The research stems from the growing demand of society to reduce material use in the construction sector, in turn reducing resource depletion. An answer to this issue is found in the use of structural optimization to reduce the weight of structural elements. However, currently there are no efficient production methods which are suited for producing the organic shapes distinctive for structurally optimized elements. Due to its nature to conform to funicular shapes, a production method based on inflatable membranes which can be partly or fully rigidized is believed to be a promising solution. In that case the formwork of the three-dimensional structure consists entirely of inflatables and is therefore completely based on form-active principles. The method uses an inner inflatable, or secondary mould, which serves as falsework and is either temporary or semi-permanent. On the outer surface of the secondary mould, tubes which can be partly or fully rigidized are inflated and represent the optimized structural element.

The study started with an in depth literature review into the fundamentals of structural optimization. Subsequently, topology optimization by mean of empirical case studies was performed on the section active structure systems to determine their general morphological features. This showed that the relation between structure and form, i.e. the structural morphology, of these optimized elements is very strong. The resulting topology and morphology of an optimization routine is determined by the force distribution through the design space and the different constraints and performance requirements that act on that specific design space. Since the morphology of an optimized one-bay beam can be recognized in every optimized section active structure system, and most of the general morphological features are reflected in an optimized beam, it served as a case for the proposed production method. This topologically optimized three dimensional beam was then shape optimized using the ParaGen method. With this parametric method, a population of 1276 different solutions was created algorithmically. The solution with the highest specific stiffness was finally size optimized using STAADpro.

Literature reviews were also performed to determine the most suitable inflatable structure typology and envelope material for the secondary mould. This study revealed five typologies which were assessed according to four morphological indicators. The four optimized section active structure systems were assessed according to the same indicators in order to compare the inflatable typologies to the optimized structures. The resulting matrix showed that a straight

high pressure system was the best inflatable typology to use as the secondary mould for our case. In addition, the literature review into envelope materials revealed the properties and characteristics of membrane materials in general. Moreover, it showed that, according to ten criteria relevant to this research, PVC coated polyester could best be used for the fabrication of the secondary mould.

The final step in the research phase included a literature review into rigidization method used for terrestrial and space applications. This study, together with feedback from several experts, showed that no single rigidizable material for space applications can be transferred to the construction industry directly. However, their main advantages, e.g. rigidization on command, can be utilized when combining their structure with commercial manufacturing methods such as resin transfer moulding or vacuum infusion.

The results of the research phase formed the foundation of the development phase, which started with a full structural analysis of the model based on detailed requirements and conditions in GSA and STAADpro. Parallel to this analysis, twelve concrete scale models were fabricated of four different geometries. These scale models showed that certain geometries were disadvantageous compared to their finite element model which used straight members. It also showed that the geometry that was chosen as the case indeed possessed the highest stiffness. Together with the structural analysis, all the information needed for the fabrication of the prototype was known. The prototype was fabricated of braided glass fibre tubes which were inflated around an inflated PVC coated polyester tube. The glass fibre was finally impregnated with a polyester resin using hand lay-up, leaving the final rigidized optimized structure.

With the fabrication of the prototype the proposed production method was demonstrated in full scale. The main advantages of the method are its extremely low self weight and rapid deployability, which can be increased when a rigidization method use in space can be utilized. The system can either be kept inflated or can be rigidized to make the structure independent of air pressure, increasing the possible applications of the method. Rigidized inflatables can for example be used for emergency relief, temporary structures, military applications, or for the reinforcement of existing structures. The secondary mould can be removed to leave a rigid structural element, but research still has to be done into the combination of a rigid optimized outer structure and inflated inner tube. In this case, the entire structure will act as a tensairity. Here, the strength will be larger than the sum of the individual parts, rendering an extremely light weight, rapid deployable, high strength element.





PREFACE	I
SUMMARIES	II
<b>A</b> PROBLEM DEFINITION PHASE	13
<b>1 RESEARCH PLAN</b>	<b>15</b>
1.1 Motivation	15
1.2 Project framework	16
1.3 Goal	17
1.4 Defining the notions	18
1.5 Relevance	19
1.6 Theoretical framework	20
1.7 Methodology	21
<b>B</b> RESEARCH PHASE	25
<b>2 STRUCTURAL OPTIMIZATION</b>	<b>27</b>
2.1 Framework	28
2.2 Fundamentals	29
2.2.1 Introduction	29
2.2.2 Procedure	29
2.2.3 Structural optimization categories	30
2.2.4 Topology optimization	31
2.2.5 Methodologies	33
2.3 Inspire case studies	35
2.3.1 Introduction	35
2.3.2 Evaluation of the software	36
2.3.3 Beam structures	37
2.3.4 Frame structures	44
2.3.5 Beam grid systems	51
2.3.6 Slab structures	52
2.3.7 Conclusion	56
2.4 Validation of the software	57
v     2.5 ParaGen method	58
2.5.1 Introduction	58
2.5.2 The parametric model	58
2.5.3 Results	61
2.6 Synthesis	64
<b>3 INFLATABLE STRUCTURES</b>	<b>67</b>
3.1 Framework	68
3.2 Fundamentals	69
3.2.1 Introduction	69
3.2.2 Historical development	69
3.2.3 The pneu as a load bearing mechanism	71
3.2.4 Analogy with soap bubbles	72
3.3 Typologies	73
3.3.1 Introduction	73
3.3.2 Parameters	73
3.3.3 Typologies	74
3.3.4 Morphological indicators	77
3.3.5 Conclusion	78
3.4 Envelope materials	79



3.4.1	Introduction	79
3.4.2	Fabrics	80
3.4.3	Fabric materials	82
3.4.4	Coatings	84
3.4.5	Coating materials	84
3.4.6	Films	86
3.4.7	Material properties	88
3.4.8	Criteria	90
3.4.9	Conclusion	92
3.5	Synthesis	93
<b>4</b>	<b>RIGIDIZATION METHODS</b>	<b>97</b>
4.1	Framework	98
4.2	Fundamentals	99
4.2.1	Structure	99
4.2.2	Characteristics	100
4.2.3	Manufacturing methods	100
4.3	Gossamer structures	103
4.3.1	Introduction	103
4.3.2	Characteristics	103
4.3.3	Rigidization techniques	104
4.4	Rigidization techniques for Gossamer structures	105
4.4.1	Aluminium and film laminates	105
4.4.2	Second order transition change and shape memory polymer composites	106
4.4.3	Plasticizer or solvent boil off composites	107
4.4.4	Thermally cured thermoset composites	109
4.4.5	Ultra violet cured composites	109
4.4.6	Inflation gas reaction composites	110
4.4.7	Foam rigidization	110
4.4.8	Multi Criteria Analysis	112
4.5	Synthesis	115
<b>5</b>	<b>SYNTHESIS</b>	<b>117</b>
<b>C</b>	<b>DEVELOPMENT PHASE</b>	<b>121</b>
<b>6</b>	<b>STRUCTURAL ANALYSIS</b>	<b>123</b>
6.1	Introduction	125
6.2	Finite element model	126
6.2.1	Method	126
6.2.2	Linear member model	127
6.2.3	Curved member model	128
6.2.4	Composite curved member model	129
6.3	Synthesis	134
6.3.1	Conventional concrete beam	134
6.3.2	General conclusions	134
<b>7</b>	<b>SCALE MODELS</b>	<b>135</b>
7.1	Introduction	136
7.1.1	Framework	136
7.1.2	Geometries	136
7.1.3	Manufacturing methods	137
7.2	Test results	139
7.2.1	Introduction	139
7.2.2	ID: 1269	139



7.2.3 ID: 799	140
7.2.4 ID: 1259	141
7.2.5 ID: 1249	142
7.2.6 Average linear elastic regions	143
7.3 Synthesis	144
<b>8 PROTOTYPE</b>	<b>145</b>
8.1 Introduction	146
8.2 Fabrication	146
8.3 Conclusion	148
<b>CONCLUSIONS AND RECOMMENDATIONS</b>	<b>151</b>
<b>REFERENCES</b>	<b>153</b>



**A**

# **Problem definition phase**



# Research plan

## 1.1 MOTIVATION

In May 2012 we visited a congress called Textile Roofs 2012 in Berlin, together with four other students and Arno Pronk. Here, Arno showed the different graduation subjects that were available in the frame of free form design. One of these subjects included an inflatable mould which was rigidized after inflation (Figure 1.1). We also talked about the possibility of working in pairs during the master thesis, since experience showed that this often benefits the result. We were both interested in the subject described above and therefore decided to collaborate during the master thesis. The subject fits well within the frame of our master portfolios and can accommodate further development of our competencies.

We both completed one master project within the frame of lifespan, and one master project in the frame of product development. Our affinity with technique manifests itself easier within product development projects, since lifespan projects tend to stay more on the surface. We feel that this subject gives us the opportunity to explore all the different aspects of product development, from preliminary research to realization. In addition, the use of 3d modelling software is also included, mainly by structural optimization.

We feel that this subject fits within the studio Slimbouden, since the meta objective is to reduce the use of materials in construction. Therefore, this thesis could make a positive contribution to the current world wide sustainability debate.

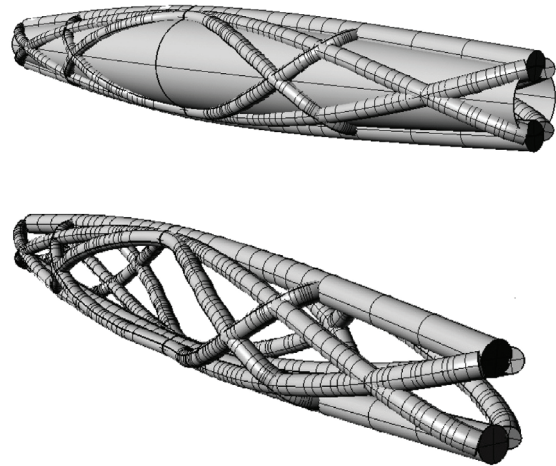


Figure 1.1: Concept

The official approval for our research subject was given at the beginning of September, which made it possible to start several weeks earlier. During the first few weeks we mainly resided in the university library trying to grasp all the different subjects that were involved. One of the first things we put on paper is the mind-map shown below (Figure 1.2). This is an early attempt of trying to map the different variables and their interdependency. This mind-map gave us insight in the different variables, and made it possible to search relevant sources more focussed.

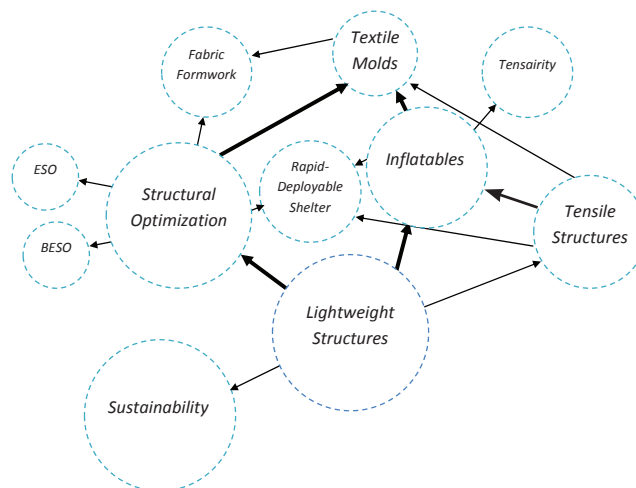


Figure 1.2: Initial mind map



## 1.2 PROJECT FRAMEWORK

The Netherlands is involved in several international covenants and agreements concerning the greenhouse effect. In 1992 the framework for climate change was concluded under supervision of the United Nations. This covenant acts as an international framework where governments can join forces to counteract the consequences of climate change (United Nations 2012). In the frame of this covenant the Kyoto Protocol was signed in 1997 by 181 countries. The protocol describes targets for reducing CO<sub>2</sub> emissions for 37 industrialized countries and the European Community. The main difference with the framework for climate change is that the protocol binds the participating countries to reduce their emissions instead of encouraging them. The protocol initiated in 2005 and obligated the participants to reduce their emissions with an average of 5.2% by 2012, where the Netherlands had to reduce by 6% (United Nations 2012). Following the Kyoto Protocol, which is no longer into effect, the European Commission wrote the Roadmap to a Resource Efficient Europe (European Commission 2012), which is one of seven flagship initiatives of the Europe 2020 strategy (European Commission 2012). It describes the necessity of moving towards a resource efficient society after decades of resource depletion based growth in wealth and wellbeing; *"If we carry on using resources at the current rate, by 2050 we will need, on aggregate, the equivalent of more than two planets to sustain us, and the aspirations of many for a better quality of life will not be achieved."* The World Business Council for Sustainable Development estimates that by 2050 we will need to use our resources, raw materials, energy, water, air, land and soil, 4 to 10 times more efficient (WBCSD 2010). Where the Kyoto protocol already caused for the decoupling of growth and the use of carbon, the roadmap 2020 is aimed at decoupling growth from resource use. In short, the main goals for the year 2020 are;

- Reducing carbon emissions by 20%
- Increasing the share of renewable energy by 20%
- Increase of energy efficiency by 20%

The roadmap describes three key sectors, nutrition, housing and mobility, which together are responsible for 70-80% of all environmental impacts. For the building industry it states that; *"Better construction and use of buildings in the EU would influence 42% of our final energy consumption, about 35% of our greenhouse gas emissions and more than 50% of all extracted materials"*. The impact of the construction sector on the environment is underlined in several studies, which is illustrated by the following indicators (WBC-

SD 2010; Lichtenberg 2006;

- The building industry is responsible for 35% of the total waste production. In the Netherlands annually about 65 millions tons of waste is produced. With more than 22 millions tons the building industry represent a major part of the total waste problem
  - 25% of all road transport of goods is building related.
  - The production of building materials represent 8-10% of the total energy consumption. The energy used in buildings represents about 33% of the national consumption.
  - The building industry is responsible for 50% of the total raw material consumption.
  - For the realization of 1 m<sup>2</sup> net floor surface 1,000 kg up to 1,500 kg of building material is applied. To compare: A mobile home weighs 80-100 kg per m<sup>2</sup>.

The indicators shown above and the current policy of the European and Dutch government show that a future sustainable society depends on developments in the construction sector. A large opportunity which can be derived from the previous, is the reduction of resources used in the construction sector (European Commission 2012). When the use of materials is decreased, the depletion of raw materials is also decreased. In addition, less building material production means less energy consumption and less building related transport, decreasing the embodied energy of buildings.

A novel method for reducing the weight of a structure or structural component is the use of structural optimization. Structural optimization is a tool which helps to integrate structure and form, in a way similar to natural or biological optimization. An optimization problem consists of minimizing or maximizing a given function, while satisfying certain constraints. It either decreases the structural weight while increasing the strength, or it decreases the weight while maintaining the same stiffness properties (Frattari 2011). Studies have shown that structurally optimized structures or structural elements can be up to 40% lighter than same sized conventional elements (Bailiss 2006; Garbett, 2008). Furthermore, dead weight reductions in beams cascade through the structural system, reducing design loads on supporting members and providing further material and embodied energy savings throughout the rest of the structure (West, 2006). However, current production methods and processes are not adequately equipped for producing elements whose shape is derived from an structural optimization analysis. The shape of supporting elements, as we know it today, is mainly characterized by rectangular, flat uniform sections. This is not



based on optimal structural efficiency, but mainly on the economic efficiency of rectangular, flat formwork that is commercially available (West, 2010; Cauberg et al., 2008). Currently, there are no production methods commercially available which can make the organic shapes distinctive for structurally optimized elements (Frattari 2011).

One method that is currently being explored is the use of fabric formwork for concrete elements. By its very nature, concrete, or any other material that solidifies, can take on almost any shape imaginable. However, traditional panelized formwork is only suited for the fabrication of flat, rectangular moulds. In the case of heavy solidifying materials, such as wet concrete, the traditional formwork is above all required to limit the outward deflection under the pressure of the concrete. Fabrics however, resist these forces solely by tension, drastically reducing the weight and size of the formwork required (West, 2006). Fabric formworks are 100 to 300 times lighter than traditional formwork and are foldable. This drastic reduction in weight and volume reduces the amount of transport needed greatly (West, 2010; Cauberg et al., 2008). A downside which has come to light is the need for additional falsework to support the fabric (Cauberg et al., 2008). In a highly industrialized manufacturing process this would not be an issue, since the formwork and additional falsework can be reused many times. However, the custom and unique nature of shapes resulting from a structural optimization analysis call for a more flexible fabric formwork system. A solution could possibly be found using inflatable structures as moulds, which are subsequently partly or fully rigidized. Due to their extremely low self weight, inflatable structures can easily be relocated, they achieve high insulation values and can realize large spans (Bektesevic, 2010). Even though the system is known to be very flexible, the collection of potential shapes is actually limited. Since inflatable structures have to adapt to force equilibrium, they have to conform to funicular shapes (Yun Chi & Pauletti). The main downside of inflatable structures is their operation and maintenance costs. Air supported systems need continuous air supply to keep their structure intact. The main problem of air inflated systems is their strong load limitation, which causes the need for large beam diameters and high overpressure (Luchsinger et al). A solution for this problem, which has already been addressed by Frei Otto and Thomas Herzog in the seventies, can be found in the rigidization of the structure after inflation. Otto described several methods which can be used for "solidified technical pneus in building construction and civil engineering". However, these methods were never really adopted by the construction industry (Otto, 1995). The only sector actively investigating the rigidization of inflatable structures nowadays is the aerospace industry.

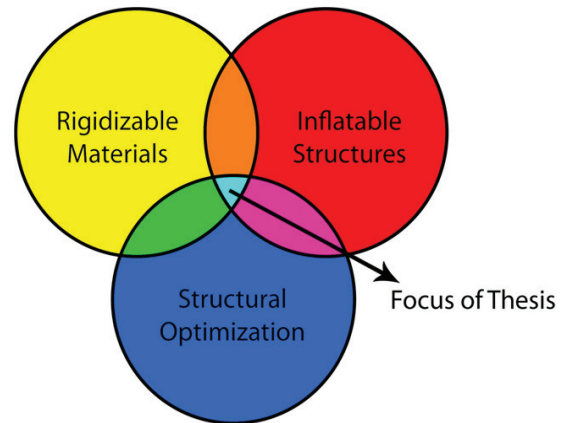


Figure 1.3: Focus of the thesis

### 1.3 GOAL

In the project framework, three main research objects can be identified; *structural optimization*, *inflatable structures* and *rigidizable materials*. These three variables meet in the focus of our thesis (Figure 1.3). The meta objective of this study is to make a positive contribution to the current sustainability debate, by reducing the use of materials in construction. The contribution of our thesis to the problem described in the project framework is the realization of a new production method, enabling the fabrication of structurally optimized elements. In other words;

**The goal is to develop a production method for structurally optimized section active structure systems, by using a rigidized inflatable structure.**

The central question of this research is therefore the following;

**In which way can a production method for a structurally optimized section active structure system be realized, using a rigidized inflatable structure?**

In order to provide an answer to the central thesis question, sub goals are derived accompanied by their corresponding research questions:

• **SUB GOAL 1:**

The main goal of this phase is to produce a case. It is important to know how a structurally optimized element looks like, and why it looks that way. In addition, the criteria that play a role in deciding which optimized structure system is best to use as a case have to be identified.

**RQ1:**

*Which structurally optimized section active structure system can best be used as a case?*

SRQ 1.1:  
What are the fundamentals of structural optimization?

SRQ 1.2:  
What are the morphological features of structurally optimized section active structure systems?

SRQ 1.3:  
Which structurally optimized section active structure system best reflects these morphological features?

• **SUB GOAL 2:**

With the case derived during RQ1, the goal is to determine how an inflatable structure can be used as falsework for the production of this optimized shape. Therefore, research has to be done into the requirements and conditions on which the structure has to conform to. Subsequently, a study into the materials and typologies of inflatable structures will be done, that will conform to these requirements and conditions. In conclusion, a consideration of suitable materials and typologies will determine which will be best to use during the rest of the research.

**RQ 2:**

*In which way can an inflatable structure be used as falsework for the production of structurally optimized section active elements?*

SRQ 2.1:  
Which requirements, conditions and properties do inflatable structures have to conform to?

SRQ 2.2:  
Which typologies of inflatable structures exist?

SRQ 2.3:  
Which materials are used for inflatable structures?

• **SUB GOAL 3**

The goal is to produce the optimized shape derived from RQ1 by rigidizing an inflatable structure, to create a solid structure independent of air-pressure. At first, the requirements and conditions of the rigidizable materials need to be determined. This will be followed by the study on rigidizable materials, and a consideration of suitable materials that will conform to these requirements and conditions.

**RQ 3:**

*Which rigidization method is best suited for producing the case derived in RQ1??*

SRQ 3.1:  
Which requirements, conditions and properties do rigidizable materials have to conform to?

SRQ 3.2:  
Which rigidization methods exist?

## 1.4 DEFINING THE NOTIONS

**Rigidizable materials:**

Rigidizable materials, as described in terms of gossamer structures, can be defined as: "Materials that are initially flexible to facilitate inflation or deployment, and become rigid when exposed to an external influence". The external influence can be of many forms such as heat, cold, ultra-violet radiation, and even the inflation gas itself (Cadogan & Scarborough, 2001). Research in the field of rigidizable materials is mainly performed by the aerospace agencies as ESA, NASA & ILC Dover. These materials are used to rigidize inflatable structures in space, to reduce the weight during space travelling.

**Inflatable Structures:**

Frei Otto describes pneumatic structures in *IL35 Pneu und Knochen* as followed:

*"A pneu is a structural system consisting of a ductile envelope which is capable of supporting tensile stress, is internally pressurised and surrounded by a medium. The pneu allows forces to be transferred over considerable distances with a minimum use of materials, and extremely wide-span structures to be erected".*

The word "pneu" (greek: Pneuma = air) is used in technology and medicine to describe objects in which an envelope contains an air volume. The term "pneu" is a term that is applicable on many areas of living and inanimate nature. Technical pneumas are for example air-filled children's balloons, hot air and gas-filled balloons, non-rigid airships, car tyres, airhouses and air & water hoses. Besides these technical pneumas, there are pneumas in inanimate nature, as mist droplets and air bubbles in water and foam. Examples in living nature are soft organisms such as bacteria, herbaceous plants, worms and animal organs (Otto, 1995). This description of a pneu according to Otto is too wide for our thesis since only technical pneumas are relevant. Therefore the term *inflatable structures* is used in our thesis, which is comparable with the technical pneumas. Inflatable structures, as described in the Dictionary of Architecture and Construction are:

*"A very lightweight enclosed structure, usually fabricated of a membrane of an impervious material and supported by the difference in air pressure between the exterior and the interior of the structure rather than by a structural framework. Fans must maintain the interior pressure slightly in excess of normal atmospheric pressure to prevent the structure from slowly deflating and*



collapsing" (Harris, 2006).

Inflatable or pneumatic structures have made a huge development over the time. The first applications were done in 1783 with hot air balloons, after stagnation in development of more than a century, the developments unfolded largely. Especially in the 1960's and 1970's, a large development on inflatable structures for shelters and temporary buildings was made. Frontiers on this field were Frei Otto and Buckminster Fuller.

#### **Structural Optimization:**

In the monograph of M.P. Bendsøe called "Optimization of Structural Topology, Shape, and Material", an overview of the fundamental ingredients for finding the optimum layout of a linearly elastic structure are presented. In this context the "layout" of the structure includes information on the topology, shape and sizing of the structure. The homogenization method allows for addressing all three problems simultaneously.

"Sizing, shape and topology optimization problems address different aspects of the structural design problem. In a typical sizing problem the goal may be to find the optimal thickness distribution. The optimal thickness distribution minimizes (or maximizes) a certain quantity such as the stress, deflection, etc., while certain constraints on variables are satisfied. The design variable is for example the thickness of the plate.

The main feature of the sizing problem is that the domain of the design model and state variables is known in advance and is fixed throughout the optimization process. On the other hand, in a shape optimization problem the goal is to find the optimum shape of this domain, that is, the shape problem is defined on a domain which is now the design variable. Topology optimization of solid structures involves the determination of features such as the number and location of holes and the connectivity to the domain.

The purpose of layout optimization is to find the optimal layout of a structure within a specified region. The only known quantities are the applied loads, the possible support conditions, the volume of the structure to be constructed and possibly some additional design restrictions such as the location and size of prescribed holes." (Bendsoe, 1995).

#### **Rigidized inflatable structures:**

Frei Otto mentioned hardened or solidified pneumatics in *IL35 Pneu und Knochen* with examples of the glass-blowing industry, and in the building industry in the form of concrete shells cast on top of pneumatics and concrete-sprayed airhouses. These solidified structures no longer require an internal pressure (Otto, 1995).

The combination of these fields has also been researched by the aerospace industry for lightweight structures in space, with a small travel volume. With the use of, for the building industry, new types of rigidizable materials. These rigidizable materials from the aerospace industry could be used for a technology transfer to the building industry.

#### **Structural optimized inflatable structures:**

Very limited research has been performed in the field of structural optimized inflatable structures. This combination has to be explored.

#### **Structural optimization using rigidizable materials:**

The combination of structural optimization and rigidizable materials is depending on a mold to rigidize the materials on. An inflatable mold could be applied. This combination has to be realized using a mold.

### 1.5 RELEVANCE

#### **Scientific Relevance:**

The focus of this thesis is based on three main research objects; *structural optimization, inflatable structures and rigidizable materials*. In each research object former research has been done. For structural optimization several interesting theses and books are published. The outcome is a shape that is not easily realized with the traditional formwork and is lacking of production methods to put it into practice. Fabric formworks are used to realize organic shapes, but besides the fabric formwork additional falsework is required to maintain the shape. The material that is reduced by structural optimization is therefore less interesting as additional falsework gives more waste than traditional formwork. To reduce the material and formwork needed to realize a structural optimized form, an inflatable structure can be applied. Research on inflatable structures is widely done and applicable for this thesis. These inflatable structures require a continuous air supply and are therefore only applicable for temporary use. By rigidizing, a specialization from the aerospace technology, this temporary form can be transformed in a solid structure. The technology transfer of rigidizable inflatable structures to non-aerospace markets is one of the current interests of aerospace agencies. The gap between a structural optimized shape and the practical realization of such a shape, by using rigidized inflatable structures, is therefore an interesting focus for this thesis. The pre-studies on each research topic are available, the combination however is unique.

#### **Societal Relevance:**

The goal of the thesis is to develop a production method for an element of a main supporting structure



which shape is determined by a structural optimization analysis, by using a rigidized inflatable structure. With this shape, determined by a structural optimization analysis, the material used to realize structures can be reduced, a way of being efficient with material and as a well known quote; Doing more with less. Material efficiency is socially relevant in multiple ways; less cost, less weight, less waste and less environmental load.

The reduction of cost will be of interest of the closely involved parties on short term, but eventually this will be of interest for the society. The reduction of weight leads to a reduction of dead weight on the total construction and as a result of this weight reduction the total weight of the structure of buildings can be reduced. This partial and total weight reduction is interesting for architects, contractors, constructor etc. to save on both material, weight and costs. The reduction of building waste and the environmental load contribute to a more sustainable environment. The extraction of raw materials and the production, transport and processing of (semi-)fabricates is reduced. The share of the building sector on environmental impacts such as desertification, soil pollution, energy consumption, air pollution and water pollution is reduced. The role of the building sector as a polluter is one of the key aspects which SlimBouwen is based on. Reducing the share of the building sector on the societal environmental problems is achieved in a sustainable and innovative way by coping with products and materials. This is of interest for the global community and is supported by the government.

To realize a material efficient shape, a structural optimization analysis is conducted. The structural optimization analysis is a specialization that is very interesting, however it is not yet widely known. A research in structural optimization will be of interest for constructors, program developers, architects etc. The application of structural optimization in the building environment can eventually lead to new products and production methods.

In this thesis two specializations are combined for the realization of structurally optimized elements. Therefore, knowledge of the two has to be brought together. The inflatable structures are made of membranes, which are commonly produced by textiles. The textile industry is willing to be innovative and to make transfers to new industries, which is underlined by the recently published "Routekaart Textiel" (Verenigde textiel industrie Nederland, 2011). The application of rigidizable materials used for inflatable structures is a specialization of the aerospace industries. There has been research to use these rigidized inflatable structures in space. Technology transfer of rigidized inflatable structures to other markets is pro-

moted by these aerospace agencies. They are actively searching for companies who are willing to transfer space technologies to commercial products or services.

The overall focus of the University of Technology Eindhoven is on sustainability and SlimBouwen. These subjects are also the focus in the SlimBouwen-Atelier and are applicable on the goal of this thesis.

## 1.6 THEORETICAL FRAMEWORK

As explained earlier, this research consists of three main research objects or variables. To make these variables researchable, a theoretical framework is described to define the boundaries of our research.

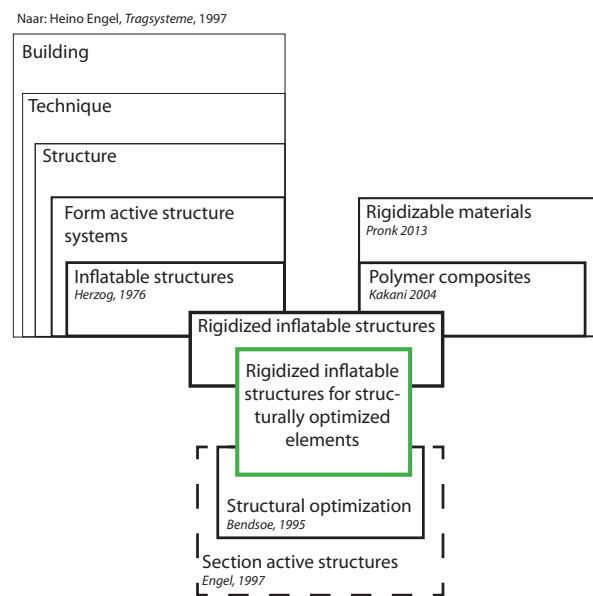


Figure 1.4: Theoretical framework

### INFLATABLE STRUCTURES

Many literature can be found concerning the classification of structures. Probably the most used is the classification of structure systems by Heino Engel (Engel, 1997). He stated that architects should have more knowledge about structural design, and that the differentiation between architectural and structural design should be dissolved.

Engel describes the building as being the sum of three "constituent agents"; form, function and technique. The technique of a building is determined by four determinants; enclosure, structure, services and transportation. The structure of a building is defined by three components; flow of forces, geometry and material. A structure system is defined only by flow of forces and geometry; "Structures are examples and hence design implements; structure systems are orders and hence design principles".

The main objective of a structure is to constrain and/or redirect forces. Four different mechanisms in

nature and technique can be identified for achieving this objective;

Adjustment to the forces	-->	Form active
Dissection of the forces	-->	Vector active
Confinement of the forces	-->	Section active
Dispersion of the forces	-->	Surface active

Pneumatic structures, as well as cable, tent and arch structures, belong to the form active structure family. They are "systems of flexible, non-rigid matter, in which the redirection of forces is effected by particular form design and characteristic form stabilization".

In this research, only the structure family pneumatic structures, or inflatable structures, will be discussed. Finally, inflatable structures can be classified in three different categories (Herzog, 1976);

- Air-inflated structures
- Air-supported structures
- Hybrid structures

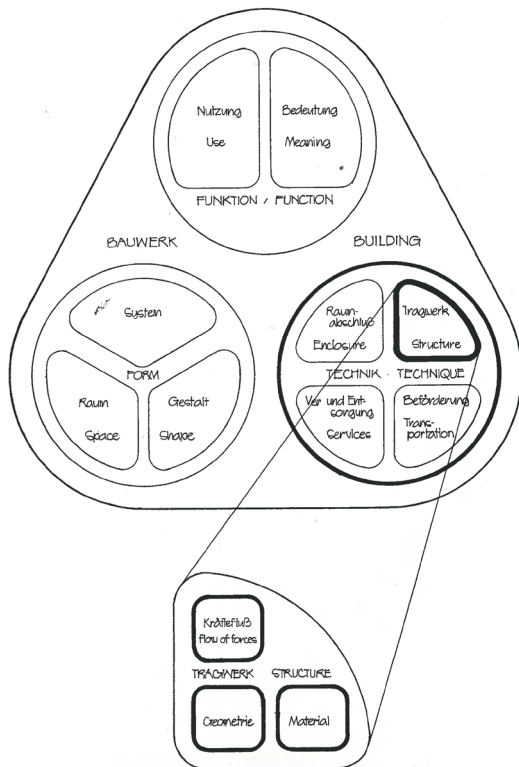


Figure 1.5: Interrelationship of building and structure (Herzog 1997)

### RIGIDIZABLE MATERIALS

Solidification is a phase transition in which a liquid turns into a solid by lowering its temperature. Besides homogeneous materials, composites can also solidify (Dantzig, 2009). Composites however, solidify due to other circumstances than lowering the temperature, which is explained in the paragraph "defining the notions". Those composites that are capable and suitable for rigidizing inflatable structures can be classified in the following three categories;

- thermosetting composite materials
- thermoplastic composite materials
- aluminum/polymer laminates

This classification is made in the frame of space inflated structures, and is therefore missing one important composite; concrete. Therefore, this classification will be expanded with the composite concrete during this research.

### STRUCTURAL OPTIMIZATION

Structural optimization has not been implemented often in construction, but mainly in aviation and the automobile industry. Very little relevant literature can therefore be found which relates structural optimization to buildings or building elements. The problem that needs to be solved however, is always the same. A structural optimization problem consists of three problems (Bendsoe, 1995);

- Topology optimization
- Size optimization
- Shape optimization

Structural optimization can be applied to almost everything within the technical environment, and is often applied in nature, in e.g. seashells. This research limits itself to weight reduction in structural elements. Therefore, only section active and surface active structure systems are considered, since form active and vector active structure systems are already regarded as light weight structures.

Structural optimization within the context of this research limits itself to topology, shape and size optimization on section active and surface active structure systems.

## 1.7 METHODOLOGY

This empirical scientific research is design oriented, and consists of a literature review and experimental research, and subsequently a product development phase. It is a descriptive and explorative study into (the coherence and relations between) the characteristics of structural optimization, inflatable structures and rigidizable materials.

First, several principles and preconditions are described after the pre-study and the investigation of relevant theories. These principles and preconditions are the spectacles through which the main variables are researched. The empirical study of the three main variables; structural optimization, inflatable structures and rigidizable materials, is done by means of literature review and experiments. The literature review will be based on primary sources such as scientific

papers and dissertations, and on secondary sources such as books. The variables are subsequently ranked and compared during the synthesis. This synthesis is used as the foundation of the product development phase. The results of the synthesis are fed back to the principles and preconditions defined at the start of the research phase.

The product development phase starts with forming a concept solution for the central thesis question, using the results from the research phase. This concept design is subsequently build, tested and analysed. The results from this cycle are used as new input for improving the concept design. This cycle is iterated numerous times to achieve the desired end result. This cyclic iterative design process is based on a model conceived by Thompke in 2003 (Thomke, 2003).

The research model (Figure 1.6) shows the different phases of the study. The model is based on the empirical cycle conceived by A.D. de Groot (de Groot, 1994). The different phases showed in the model can be linked to the five phases of the empirical cycle;

**Observation = Pre-study**

During the pre-study empirical evidence is collected and grouped. Here, the hypothesis is first formed mostly based on presumptions.

**Induction = Problem definition**

By investigating relevant theories and the pre study the hypothesis is formulated, also known as the induction phase. Here, a verifiable hypothesis is formulated in such a way that verifiable predictions can be derived from it. The hypothesis of this research is explained under the paragraph "goal".

**Deduction = Research**

During the research phase consequences of the hypothesis derived during the induction phase are inferred. Here, a rule is that every scientific prediction inferred during the deduction phase is strictly verifiable.

**Testing = Product development**

The criteria for (scientific) knowledge is the fact that one can pre-

dict the outcome of a testing procedure [18]. Therefore, during this phase models and prototypes will be made to test the hypothesis derived during the induction phase, and the predictions derived during the deduction phase.

**Evaluation = Presentation & evaluation**

During the evaluation phase, the value of the results obtained during the testing phase are put in a broader perspective. This phase is more interpretive than the previous phases, and is therefore more subjective.

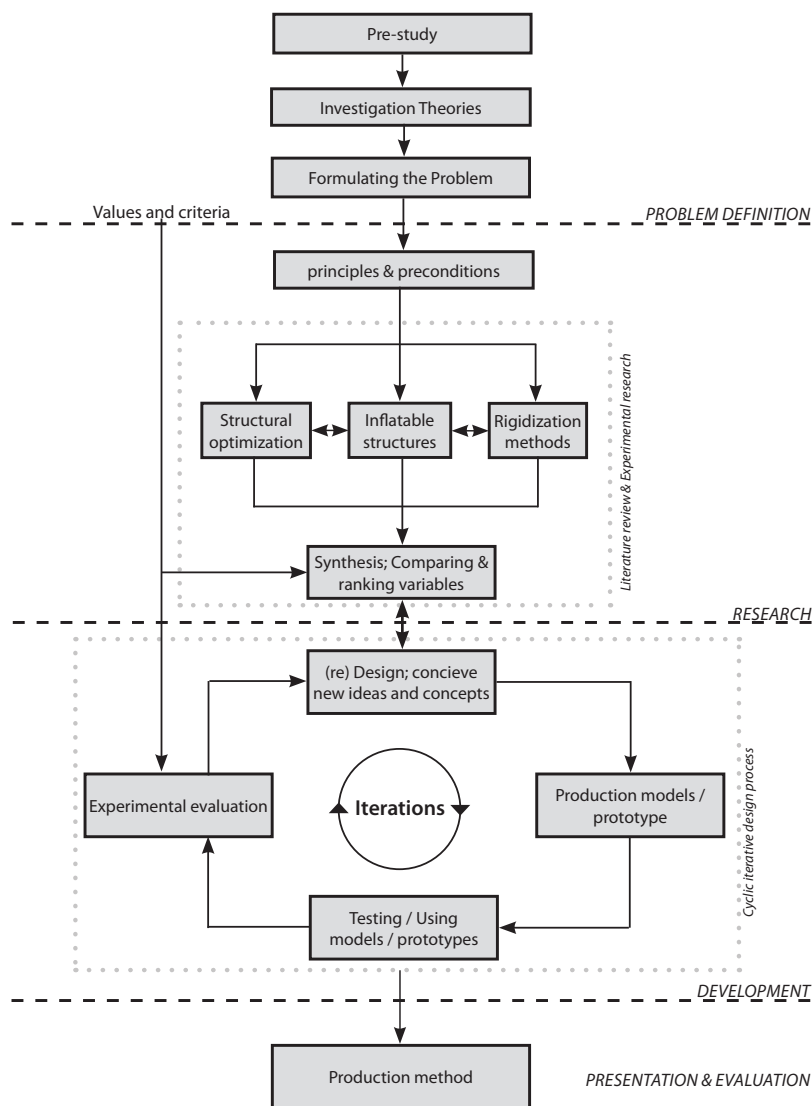


Figure 1.6: Research model







**B**

## **Research phase**



# 2

## Structural Optimization



As stated in the research plan, the main goal of the study of the research object “Structural Optimization” is to produce a case for the development phase. The corresponding research question is therefore;

RQ1: Which structurally optimized section active structure system can best be used as a case?

Several other questions are embedded in this central question. First of all, the fundamental principles of structural optimization have to be understood. In this case, the study will limit itself to the basic theoretical principles; i.e. the mathematical aspects are outside of the scope of this research. Subsequently, an empirical study using SolidThinking Inspire 9.0, validated by Topostruct and Patran, will reveal the morphological features of structurally optimized section active structure systems. Finally, using the ParaGen method developed by Assoc. Prof. Peter von Buelow at the Taubman College of Architecture and Urban Planning at the University of Michigan, a case is derived which best reflects these morphological features. To summarize;

**SRQ 1.1:**

What are the fundamentals of structural optimization?

**SRQ 1.2:**

What are the morphological features of structurally optimized section active structure systems?

**SRQ 1.3:**

Which structurally optimized section active structure system best reflects these morphological features?

It is important to define some of the notions described in the approach above.

### SECTION ACTIVE STRUCTURE SYSTEMS

The classification of structure systems by Heino Engel was already explained in chapter one, especially in the context of pneumatic structures. In the frame of structural optimization it is imperative since section active structure systems form the basis of the optimization process. Habraken (2010), defines lightweight structures as following; “The aim of lightweight structures is to minimize material use with as a result lower self weight that preserves strength, stiffness and stability. Minimizing the material use is realized by using the material as efficient as possible”. When looking at the different structure systems described by Engel (1997), form active and vector active systems can be categorized

as lightweight structures. In addition, surface active systems can also be categorized as lightweight structures depending on the shape of the structure<sup>1</sup>. Therefore, structural optimization within the context of this research limits itself to topology, shape and size optimization on section active structure systems. Indeed, from a material saving point of view, this is where the most profit is to be gained.

### MORPHOLOGICAL FEATURES

Morphology, is a contraction of the Greek words “morphé” meaning form, and “logos” meaning study. According to the new Oxford Dictionary of English (1998) it means; “the study of forms and things”. It is field of study which focuses on many topics, especially in biology; “the study of the size, shape, and structure of animals, plants, and microorganisms and of the relationships of the parts comprising them” (Britannica 2013).

The main gap in the definition above, is the fact that the research subjects in the frame of this study are not animals, plants and microorganisms, but section active structure systems which are, naturally, structural in nature. Structural morphology is a term coined by Michael Burt in 1989 for a new IASS working group called the “Structural Morphology Group”. The design of any construction system can be classified according to four parameters; forms, forces, material and structure (Figure 2.1). Structural morphology can be defined as the direct relation between the study of form and structure, which is affected by the behaviour of the material and the flow of forces (Motro<sup>2</sup>, 2009).

The morphological features, in the context of this thesis, can now be defined as the distinctive attributes or aspects that determine the structural morphology of an optimized section active structure system.

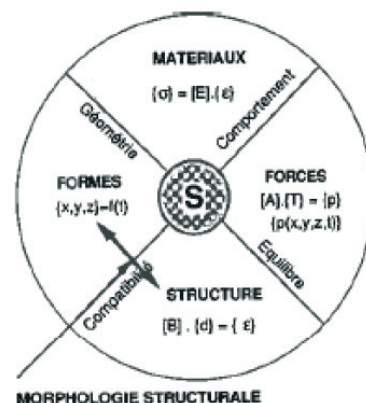


Figure 2.1: Conceptual scheme of the position of Structural Morphology in the design of a construction system (Motro, 2009)

1. For example, the concrete shells which are characteristic for the work of Heinz Isler are lightweight structures.
2. René Motro, Pieter Huybers, Francois Gabriel and Ture Wester founded the Structural Morphology Group during the IASS Copenhagen Symposium in 1991 (Motro, 2009)

## 2.2.1 INTRODUCTION

Optimization is a branch of mathematics which seeks to obtain the best result under given circumstances. An example could be to find the quickest route across the TU/e campus when using the footbridges, or in the case of structural optimization, minimizing the weight while satisfying certain requirements. Optimization can be applied to solve a wide array of engineering problems, but in this thesis it is limited to section active structure systems as explained in chapter one. The first steps in the field of optimization were made by an Australian inventor called Mitchells in 1904, and has grown to be a full fledged branch of mathematics today. In the literature many different definitions can be found, but an excellent general notion of optimization is given by Rao (1996);

*“In design, construction, and maintenance of any engineering system, engineers have to take many technological and managerial decisions at several stages. The ultimate goal of all such decisions is either to minimize the effort required or to maximize the desired benefit. Since the effort required or the benefit desired in any practical situation can be expressed as a function of certain decision variables, optimization can be defined as the process of finding the conditions that give the maximum or minimum value of a function”.*

Structural optimization is a specific field of optimization which seeks to generate a component which possesses an optimal structural performance. It is a sub field of design optimization, which optimizes a component by maximizing its *utility* while satisfying predetermined *functional requirements* and *performance constraints*. Structural optimization is the design optimization of a component, where the utility, functional requirements and performance constraints are structural in nature (Kumar 1993).

Utility is a measure of the structural performance, effectiveness and desirability of a component. Maximizing the utility could mean maximizing the stiffness, maximizing the manufacturability, minimizing the weight or minimizing deflection. Functional requirements are specifications that define the intended use of a component and the conditions under which it will operate. Common functional requirements are size and weight limitations, material properties, locations and type of supports and location, directions and magnitude of loads. The performance constraints define the range of acceptable structural behaviour of the component. Examples are the allowable stress level, maximum weight, maximum deflection etc. (Chapman 1994). Structural optimization problems

can either be solved analytically or numerically. Given the large number of variables that exist in optimization problems, analytical methods are often not possible. Most methods used today are therefore numerical methods which seek a global optimum, or give multiple “pretty good” solutions. Numerical methods can not find an exact answer to a problem, however, they can handle very complex problems which would otherwise be unsolvable.

## 2.2.2 PROCEDURE

The first step in any structural optimization routine is to turn the qualitative problem description, e.g. minimizing the weight while maintaining stiffness properties, into a quantitative mathematical statement which can be solved numerically. This is usually done by completing the following steps (Olason & Tidman 2010; Chapman 1994);

1. **Definition design variables.**  
The design variables are the parameters which control the design of the component. They represent the properties of the component which are allowed to vary during optimization. In most structural optimization problems the design variables are the density and orientation of an element.
2. **Developing objective function.**  
The objective function either calculates the utility of a design or minimises the cost, depending on the algorithm which is used. First, a set of design variables are given an initial value, which corresponds to a particular component design. Subsequently, the structural behaviour of that particular component is calculated. At last, the utility or cost of the design is determined.
3. **Creating design constraints.**  
Design constraints consist of functional requirements and performance constraints. They determine whether or not the proposed design is feasible or.
4. **Setting side constraints**  
Sometimes side constraints are set to determine the allowable range of the design variable values, and thus the range of possible designs.

A more specific definition of structural optimization can now be derived from the previous. Since the design variables control the components design, *structural optimization procedures attempt to find the set of design variable values which maximizes an objective function which is subjected to a set of design constraints* (Chapman 1994).



After the quantitative statement is developed, actual optimization begins. The entire routine is controlled by an optimization algorithm and is iterative. The algorithm chooses an initial set of design variable values randomly. These design variable values are put through the objective function, which basically consists of a modeller and a structural analysis program. The modeller translates the variable values to a design<sup>1</sup>, which is subsequently analysed to determine its structural behaviour<sup>2</sup>. The results are then used to determine the utility or the cost of the design. The initial design variables values are then altered based on these results, to try to maximize the utility or minimize the cost. The entire routine iterates until an optimal solution is found. The optimization routine is displayed schematically in Figure 2.2.

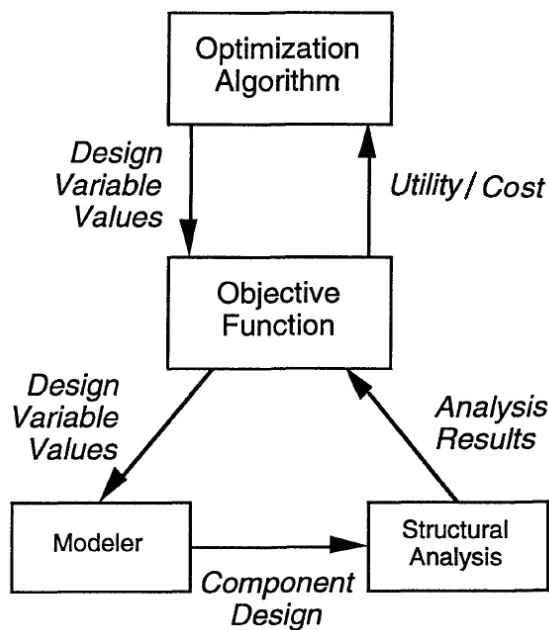


Figure 2.2: Interaction between structural optimization subroutines (Chapman 1994)

### 2.2.3 STRUCTURAL OPTIMIZATION CATEGORIES

In the literature, three main categories of structural optimization can be identified (Christensen & Klarbring 2009; Chapman 1994; Olason & Tidman 2010). To which category the problem belongs depends on which component attributes are controlled by the design variables. The problem can either be a size, shape or topology optimization.

#### Size optimization

Size optimization is often considered to be the simplest form of structural optimization. The shape and

topology of the component which has to be optimized are known and constant. The design variables control the size of the elements and are therefore allowed to vary during optimization. Figure 2.3 shows a sizing optimization where the diameter of the elements are the design variables.

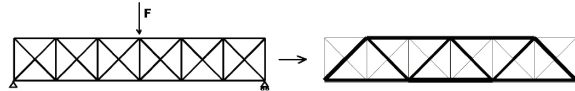


Figure 2.3: Size optimization (Olason & Tidman 2010)

#### Shape optimization

In the case of shape optimization, only the topology of the component is known and kept constant. Shape optimization, as well as size optimization, will not result in new holes or split body parts. The size and shape of the component have to be determined and are therefore the design variables. According to Chapman, in almost every shape optimization the design variables control the place of the control points of the component and thus control the size and shape. It is important to see that often size optimization occurs automatically when performing a shape optimization. Examples of shape optimization are the determination of hole diameters or radii of fillets.

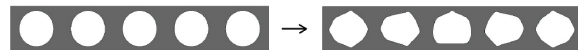


Figure 2.4: Shape optimization (Olason & Tidman 2010)

#### Topology optimization

Topology optimization is often considered to be the most difficult form of structural optimization. Here, the topology, shape and size of a particular component are yet to be determined; "In addition to controlling the design's outer boundary, the design variables must create and remove, as well as define the size and shape of, any number of holes in the design's interior" (Chapman 1994). Topology optimization problems are usually tackled using a so called 0-1, or black and white, representation of the problem (Rozvany 2001). This is elaborated upon in the following paragraph. Often, shape and size optimization occur automatically when performing a topology optimization.

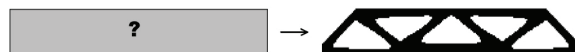


Figure 2.5: Topology optimization (Olason & Tidman 2010)

1. The model is usually a finite element mesh which describes the components size, shape and topology. For example, Optistruct uses Hypermesh and ParaGen uses a parametric model developed with Generative Components.
2. Most structural analysis are performed using a finite element analysis.

## 2.2.4 TOPOLOGY OPTIMIZATION

### TOPOLOGY

Topology is a contraction of the Greek words “Tospos”, meaning place, and “Logos”, meaning study. It is a relatively young branch of mathematics dealing with the properties of objects that are maintained when that particular object is deformed. It studies the most basic properties of space, such as orientation, connectedness and compactness, which are preserved under continuous deformation (BRON). A more intuitive definition could be to describe it as modeling clay mathematics. The study of topology started in 1736 with the publication of Leonhard Euler’s paper on the Seven Bridges of Köningsberg. The ancient city of Köningsberg in Prussia was divided by the Pregel River, which divided the city in two sides and enclosed two large islands in the middle of the city. The two mainlands and the two islands were connected to each other by seven bridges. The problem was to find the path which led through the entire city while crossing every bridge only once. There were no other means of crossing the river. Euler proved that there was no solution to this topological problem (Figure 2.6).

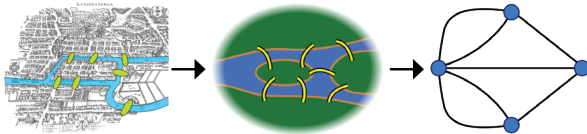


Figure 2.6: Seven bridges of Köningsberg

When combining the definition of optimization by Rao (1996) with the previous definition of topology, we can define topology optimization as follows;

*Topology optimization is the process of finding the conditions that give the maximum or minimum value of a function describing the properties of a space which are preserved under continuous deformation.*

### TOPOLOGY OPTIMIZATION

Topology optimization is relatively new field of structural mechanics. It has two main sub fields; Layout Optimization (LO), which addresses problems with very low mass targets, and Generalized Shape Optimization (GSO), addressing high mass targets. As discussed earlier, optimization problems can be solved analytically or numerically. Given the high number of variables, analytical methods are not plausible and are therefore outside the scope of this research. Generalized shape optimization can be categorized based on the type of topology involved

(Rozvany 2001);

- Isotropic-Solid/Empty (ISE)
- Anisotropic-Solid/Empty (ASE)
- Isotropic-Solid/Empty/Porous and/or Composite (ISEP/ISEC/ISECP)

The ISE topology is the most important one, since it occurs in most optimization problems. The goal is to find the optimal distribution of material in a given design space, where an element can either be solid or empty. A problem is usually discretized into finite elements using the finite element method. The resulting problem is subsequently solved using an optimization method, where the goal is to determine which elements are solid and which are empty. This is also called a “black and white topology” or a “0-1 topology” (Rozvany, 2001; Olason & Tidman 2010; Chapman 1994).

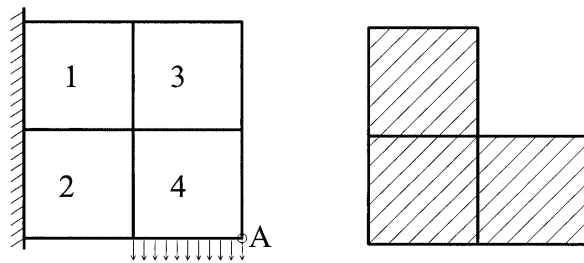


Figure 2.7: Simple ISE topology problem with a mass target of 0.75. Left; problem statement. Right; Optimal solution (Rozvany 2001)

The two main optimization methods for solving the problem described above are the “Density Method”, also known as the SIMP<sup>1</sup> method, and the “Homogenization Method”, also known as the OMP<sup>2</sup> method. In addition, evolutionary methods<sup>3</sup> will be discussed shortly in paragraph 2.3.5 since the ParaGen method is based on the fundamental steps commonly used in genetic algorithms (Buelow 2012).

### THE DENSITY METHOD

The density method is the main solving strategy used by Altair’s Optistruct, and therefore also SolidThinking Inspire 9.0 (Pupat 2013). Here, the material density is the design variable which can vary continuously per element between 0 and 1. The relation between the stiffness of the material is assumed to be linear with the density of the material. This corresponds with an engineers intuition; e.g. steel which is denser than aluminium is also stiffer than aluminium. Since the density is allowed to vary between 0 and 1, fictitious values of intermediate density are possible. These are unwanted since this would require the use of different materials in the design space. Therefore, intermediate densities are penalized to make the result behave more like an ISE topology (Pupat 2013);

1. Solid Isotropic Microstructures with Penalization  
 2. Optimal Microstructures with Penalization  
 3. Examples of such methods include ESO and BES0; (Bi-directional) Evolutionary Structural Optimization





Olason & Tidman 2010; Rozvany 2001). This penalization is done using the “power law representation of elastic properties”:

$$s = \rho^p \quad \text{where;}$$

- s = Relative stiffness
- $\rho$  = density
- p = penalization factor

Here, a value of 1 represents the standard linear relation between the stiffness and the density. When increasing the power<sup>1</sup>, the penalization of intermediate

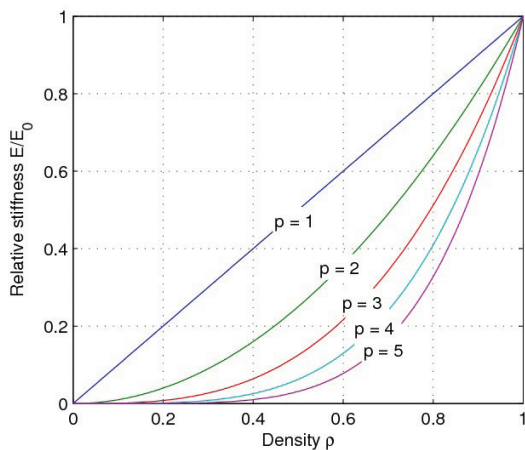


Figure 2.8: Relative stiffness as a function of the density with different penalization factors (Adopted from Olason & Tidman 2010)

densities will be stronger (Figure 2.8).

The main advantage of the density method is the fact that only one free variable per element is necessary, reducing the need for high computational power. Also the method is suited for dealing with any combination of design constraints.

#### HOMOGENIZATION METHOD

Due to the non-intuitive aspects of the intermediate densities involved in the density method, it took almost a decade for its adoption as a full fledged solving strategy for topology optimization. Therefore, other methods were researched to give the intermediate densities a more physical form. The homogenization method, or OMP method, uses an optimal microstructure build of a porous composite material. It is the main solving strategy used in the topology optimizer “Topostruct” (Paragraph 2.6.1). The type of microstructure used depends on the specific problem statement. Examples are solids with square or rectangular holes or layered microstructures. Since the macroscopic properties of the microstructure are not isotropic, an additional design variable is necessary; the orientation. Depending on the type of microstructure

	SIMP	OMP	NOM
Microstructure of elements	solid, isotropic	optimal nonhomogeneous	nonoptimal nonhomogeneous
additional penalization	yes	yes	no
homogenization necessary	no	yes	yes
no. of free parameters per element	1	2D*: 3 or 4 3D: 5 or 6	
available for:	all combinations of design constraints	compliance	all combinations of design constraints
penalization adequate	yes	yes	no

\*orthogonal or nonorthogonal rank-2 laminates

Figure 2.9: Characteristics of the density and homogenization method for ISE topologies in General Shape Optimization (Adopted from Rozvany 2001)

used and the nature of the model, the number of free variables per element varies between three and six. The downside of this higher number of free variables is the need for a high computational capacity. In addition, the homogenization method is only suited for problems statements which involve minimizing a components compliance (Chapman, 1994; Rozvany, 2001; Olason & Tidman 2010). A summary of the characteristics of both optimization methods is shown in Figure 2.9.

#### TOPOLOGY OPTIMIZATION IN PRACTICE

Topology optimization is becoming increasingly more popular. Its adoption in the automotive and aeronautic industry has accelerated the development of commercial software such as Ansys, Optistruct, Solidthinking Inspire, Genesis, MSC/Nastran, MSC Construct and Tosca<sup>2</sup>. In the automotive industry, topology optimization is used to reduce the weight of different components, while maintaining the same stiffness properties. In the aeronautic industry, the acceptance of topology optimization as a tool for reducing the weight of aircraft components was slower due to the more complex support and loading conditions (Krog et al. 2002).

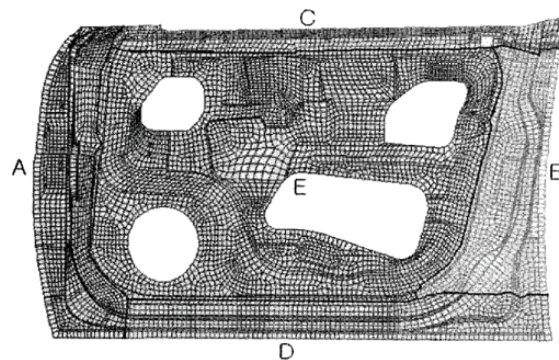


Figure 2.10: Result of topology optimization on the inner panel of a car door (Lee et al, 2003)

1. The value of p usually varies between 2 and 5 (Olason & Tidman 2010; Rozvany 2001)
2. All of these programs use the density method as described above, except Tosca which uses an evolutionary method (Rozvany 2008)

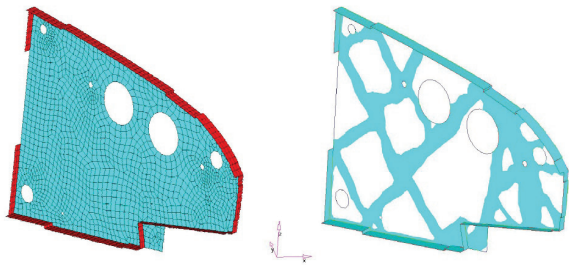


Figure 2.11: Result of topology optimization on an Airbus A380 wing component (Krog et al. 2002)

The adoption of topology optimization, and in a broader sense, structural optimization, in the building industry has been very slow. On the one hand, this is due to the fact the most software which is commercially available is especially tailored to fit the demands of the automotive and aeronautic industries (Dombernowsky & Sondergaard 2009). On the other hand, this is caused by the lack of adequate production methods to produce the shapes distinctive for structurally optimized elements. Several researchers have studied the potential of topology optimization in architecture over the last years. Frattari (2012) investigated the subject to derive a design methodology for the creation of structural forms. He also pointed out the same shortcomings related to the production of such forms. In addition, multiple studies can be found on the use of fabric formwork for structurally optimized concrete structures (West 2005; Orr et al. 2010; Cauberg et al. 2008). Dombernowsky & Sondergaard (2012) used a CNC milling machine to produce formworks of polystyrene foam (Figure 2.12). All of these studies however are focussed on the rigidization of the formwork by concrete. In this research, other rigidizing materials are also considered.

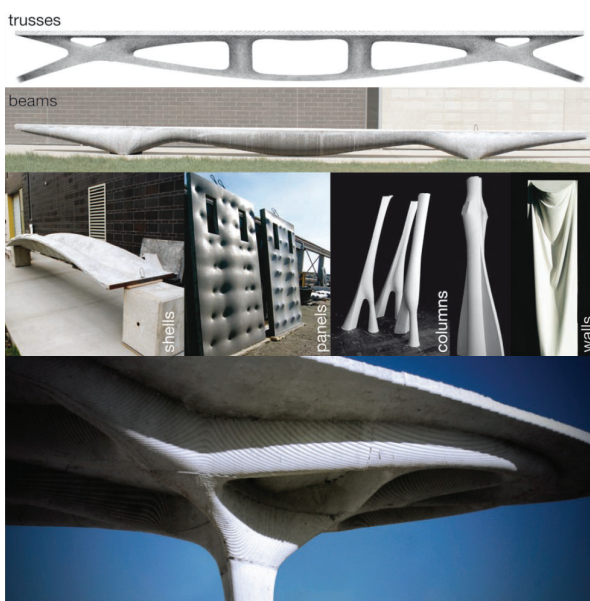


Figure 2.12: TOP: Examples of fabric formed concrete structures by C.A.S.T (West 2009). BOTTOM: Prototype pavilion by Dombernowsky & Sondergaard (2012)

## 2.2.5 METHODOLOGIES

Over the last few years, several methodologies have been developed to aid in the design process of structurally optimized forms. Early models include flow charts used in the automotive and aeronautic industries. The model below describes the design process for a wing component of an Airbus A380. The component is optimized using Optistruct and associated software. Even though this model is specifically tailored for the design of an aircraft component, it is very similar to newer methodologies used for the automotive and building industry.

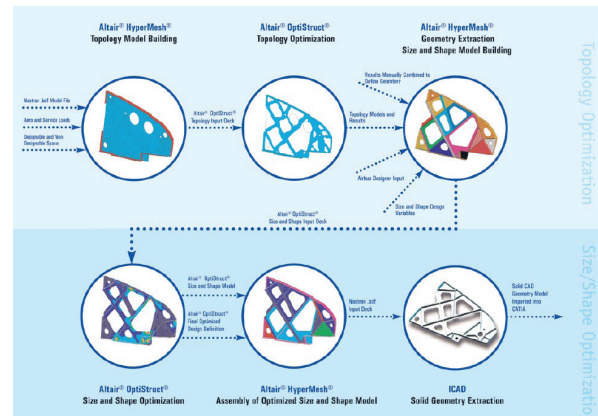


Figure 2.13: Design process of an aircraft component (Krog et al. 2002)

Basically, every methodology can be partitioned in two parts; topology optimization in the concept design and size and shape optimization during the detailed design (Krog et al. 2002; Olason & Tidman 2010; Frattari 2011). In the concept phase, following an analysis of the solid model, the topology, shape and size of the component are determined based on preliminary requirements and constraints. When the resulting topology is satisfactory, the design moves towards the detailed phase where the final shape and size are determined based on detailed requirements, constraints and other boundary conditions. Here, materials and profiles are assigned and the design is checked in accordance with the code.

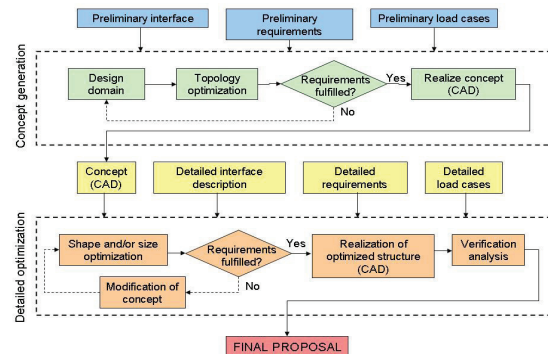


Figure 2.14: Design process methodology for Saab Microwave Systems (Olason & Tidman 2010)



## PARAGEN

ParaGen, a contraction between Parametric and Genetic Algorithm, is a method developed to explore parametric geometry based on aspects of performance and visual criteria. It is a response on the rapid developments in the field of generative design, where a wide range of designs are quickly generated, however, without informing the designer about the performative aspects of the geometries. The method is based on the fundamental steps used in a genetic search; selection, reproduction, crossover, mutation and fitness (Buelow 2012; Nevey & Alvarez 2002). It is a cyclic process (Figure 2.15) which produces a range of pretty good solutions.

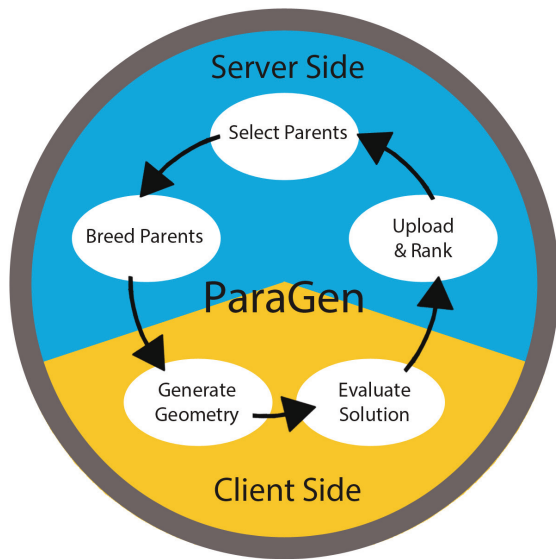


Figure 2.15: The ParaGen cycle (Buelow 2012)

A genetic algorithm (GA), in the context of structural optimization, is an optimization technique based on the theory of natural selection. It breeds an initial, randomly created, population of candidate solutions over a number of generations. The candidate solutions are coded into binary strings which can be seen as chromosomes known in biology. Each binary number corresponds to a gene, where the value of the number corresponds to an allele. The genes in the chromosome, or the binary number in the candidate solutions, corresponds to a certain trait of that particular solution, just as a gene can determine a persons hair colour. The candidate solutions are evaluated through a fitness function<sup>1</sup>, which measures how well the candidate can solve the problem at hand. According to “survival of the fittest” candidates that are better suited for solving the problem, have a higher chance of passing their genetic information onto future generations, meaning they have a higher chance

of getting picked. In this manner, each generation will be better suited to solve the problem, since only strong candidates are allowed to breed. An optimal solution is found when new children no longer show significant improvements (Chapman 1994; Nevey & Alvarez 2002).

The ParaGen method follows the following steps<sup>2</sup>;

- **Selecting parents**

This selection can be made algorithmically by the program based on the fitness of the candidates or interactively by the designer based on intuition and/or aesthetics. An important feature is that multiple fitness functions can be used simultaneously, e.g. finding the least weight and fewest members. An initial population is always generated randomly by the program.

- **Breeding parents**

The breeding is normally between two parents which are among the “fittest” of the population. However, one parent breeding and even randomly created candidates are also possible.

- **Developing the geometries**

New child data sets are uploaded into a parametric modeler<sup>3</sup> containing a script which describes the range of possible geometries.

- **Evaluation of the possible solutions**

The geometries created in the previous step are subsequently analysed in some simulation software<sup>4</sup>. Here, quantitative data is collected to feed the fitness function and help the designer in the decision making process.

- **Ranking the solutions**

The solutions with their accompanying quantitative and qualitative data are uploaded to a web page interface. The designer can then filter the solutions using any number and combination of parametric variables and/or performance values.

In this research, the ParaGen method is used for the detailed design phase; meaning it will be used for size and shape optimization. The fitness function, parametric model and other input necessary for the ParaGen method will be explained in paragraph 2.5.

1. A fitness function is for example minimizing the compliance.
2. For an elaborate description we refer to the full paper of Mr. von Buelow (Buelow 2012)
3. In this research Generative Components by Bentley Systems was used
4. In this research Staad Pro by Bentley Systems was used

## 2.3.1 INTRODUCTION

To determine the morphological features of structurally optimized elements, a parameter study was performed using SolidThinking Inspire 9.0 (paragraph 2.4.4). A morphological overview is given varying the 10 different constraints that are available in Inspire. The four results that display the biggest difference in morphology are displayed and explained. The starting point of this parameter study are the section active structure systems (Engel 1997). First beam and frame structures are discussed. Beam grid structures are not elaborated since from the study into beam and frame structures it can be assumed that the optimization of this structure system is a combination of the results of beam and frame structures. Slab structures are discussed shortly as they are in essence a beam or frame with a very high width to height ratio.

In Inspire, the optimization of an element can be constrained by ten different constraints. As explained in paragraph 2.4.4, the mass target can take any value between 0 and 100. For practical reasons, the possible mass targets in this parameter study are restricted to 20, 40 and 60 percent. Obviously, the possible choices of materials is almost infinite. Here, the possible materials are limited to concrete, foam and steel since they possess a wide array of mechanical properties. Load types are restricted to point loads and distributed forces, torques and pressures are not applicable.

All the other constraints can take any value available in Inspire. The manufacturing constraints, symmetry and draw direction, are given to show a complete overview. In this study they are not used, since the manufacturing method has yet to be developed. Also, during this stage of the study frequency targets are not applicable and are therefore not used.

The different section active sub-groups are studied according to six main parameters or phenomena which were found to have the most influence on the results; load type, support type, height to length ratio, width to height ratio, continuous variant and design space. Other parameters and constraints proved to have less or almost no impact on the topology and morphology of the result.

## Morphological overview

	Constraint	Value			
P1	Mass target	20	40	60	
P2	Material	concrete	foam	steel	
P3	Load	point		distributed	
P4	Support type	hinged		fixed	
P5	Support place	none	plane	edge	point
P6	Symmetry	none	symmetric	cyclic	cyclic symmetric
P7	Draw direction	single draw	split draw	stamping	
P8	Frequency target	none	maximum	minimum	
P9	Thickness control	none	minimum	minimum + maximum	
P10	Gravity	on		off	

### 2.3.2 EVALUATION OF THE SOFTWARE

The case studies discussed in this paragraph are performed using Solidthinking Inspire 9.0, which is developed by Altair Engineering. The program is developed to enable design engineers, architects and product designers create and investigate structural forms very quickly and efficiently. The program uses the powerful hyperworks suite from Altair on the background. A problem statement is first discretized using Hypermesh, and subsequently optimized using Optistruct in the background (Palmer & Nelson 2011).

Optistruct is the main topology optimization solver from Altair, and has been used in the aerospace and automotive industries for several decades. The Hyperworks suite uses Hypermesh as a preprocessor to discretize a CAD model. Optistruct itself does not have a graphical interface. Therefore, the entire problem statement is made in Hypermesh, i.e. boundary conditions, properties etc. This problem statement is then solved using Optistruct. The results are then exported to the postprocessor Hyperview (Figure 2.16).

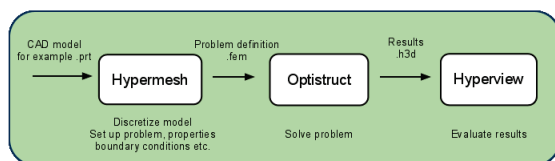


Figure 2.16: An overview of the workflow in Hyperworks (Olason & Tidman 2010)

Optistruct was first released in 1993 and has been improved ever since. The software is capable of performing a wide range of different finite element analysis, including static and non linear analyses. The program is capable of performing topology optimization on 2D and 3D elements, but also shape and size optimization. Depending on the problem statement, it used either the density method or homogenization method. Shape optimization is always performed using the perturbation vector approach. Multiple fitness functions can be used for optimization, either separate or simultaneously. However, in order to meet the demand for faster and simpler software, Altair developed Inspire, which is a trimmed down version of Optistruct.

Inspire uses Optistruct in the background for topology optimization, which in turn uses the density method. Right now, Inspire always optimizes for stiffness maximization. However, Altair already indicates that the next version will allow for minimizing mass under stress and / or displacement constraints (Pupat 2013). For the empirical case studies performed in this paragraph it was necessary to generate accurate solutions quickly, and to be able to change parameters eas-

ily. Given the large quantity of different optimization that had to be performed, the time of one iteration, or optimization cycle, had to be as short as possible. For this purpose, Inspire 9.0 turned out to be the ideal software.

Inspire has a very clear user interface (Figure 2.17), causing first time users to quickly generate initial results. The program has a graphical interface where basic design space can be drawn. However, we mostly used rhinoceros 4.0 and Solidthinking Evolve to generate the design space, which can then be imported into Inspire. It has to be noted that Inspire has an option to export results directly to Evolve for post-processing. Also, files can be saved as multiple different extensions including STL files for 3D printing.

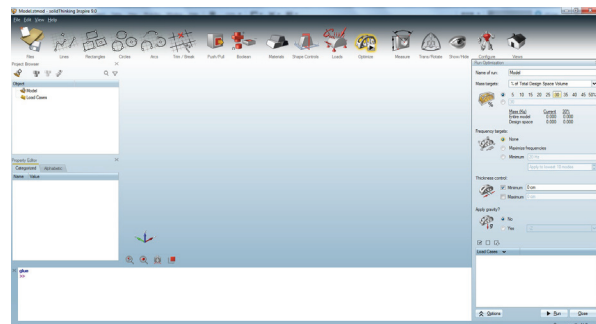


Figure 2.17: The user interface of Inspire 9.0

The required step for an optimization routine are roughly the same every time;

- Generating the design space
- Setting boundary conditions (Material properties, supports, mass target etc.)
- Optimization
- Analysing the result

The main advantage of the software is the ability to quickly generate accurate results, ready for post-processing. In this way, the designer can acquire a better understanding of the structural performance of the part in an early stage of the design process. The user interface is very clear and does not leave much room for error. The main downsides we encountered were some bugs in the software causing it to crash during certain actions. However, Solidthinking indicated that these would be solved in the next version. In addition, right now Inspire can only for stiffness maximization.



### 2.3.3 BEAM STRUCTURES

The first section active sub-group described by Engel are the beam structures (Figure 2.18). The starting point for the study into the morphological features

of this group is a one-bay beam with dimensions described in Figure 2.19. The other sub-systems, as displayed in Figure 2.18, will be discussed subsequently.

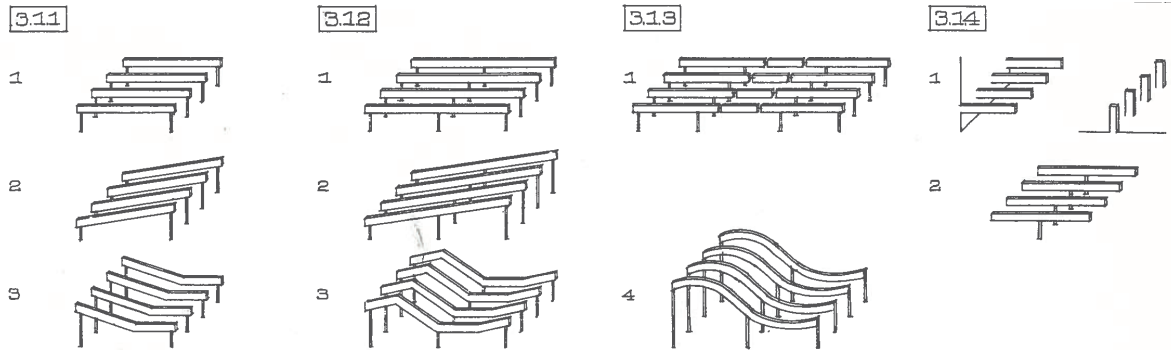


Figure 2.18: Beam structures (Engel 1997)

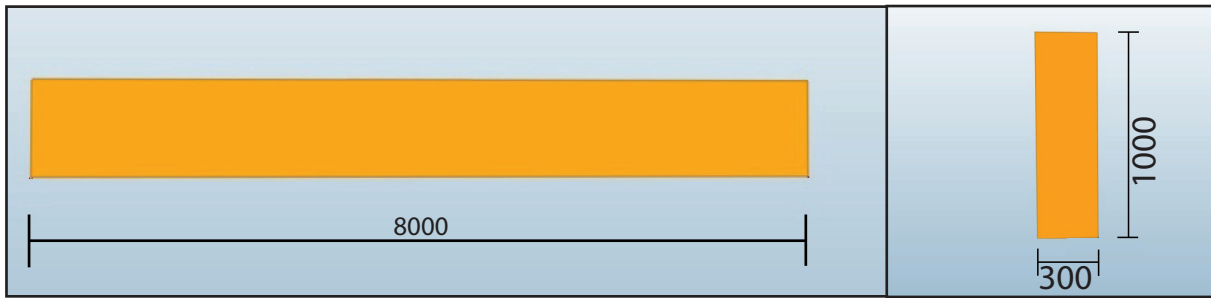


Figure 2.19: Front and side view of the design space

	A		B		C		D	
	PARAMETER	VALUE	PARAMETER	VALUE	PARAMETER	VALUE	PARAMETER	VALUE
Mass target	P1	<input type="radio"/> <input checked="" type="radio"/> <input type="radio"/>	P1	<input checked="" type="radio"/> <input type="radio"/> <input type="radio"/>	P1	<input checked="" type="radio"/> <input type="radio"/> <input type="radio"/>	P1	<input type="radio"/> <input checked="" type="radio"/> <input type="radio"/>
Material	P2	<input checked="" type="radio"/> <input type="radio"/> <input type="radio"/>	P2	<input type="radio"/> <input checked="" type="radio"/> <input type="radio"/>	P2	<input checked="" type="radio"/> <input type="radio"/> <input type="radio"/>	P2	<input checked="" type="radio"/> <input type="radio"/> <input type="radio"/>
Load	P3	<input checked="" type="radio"/> <input type="radio"/>	P3	<input type="radio"/> <input checked="" type="radio"/>	P3	<input checked="" type="radio"/> <input type="radio"/>	P3	<input type="radio"/> <input checked="" type="radio"/>
Support type	P4	<input checked="" type="radio"/> <input type="radio"/>	P4	<input checked="" type="radio"/> <input type="radio"/>	P4	<input type="radio"/> <input checked="" type="radio"/>	P4	<input type="radio"/> <input checked="" type="radio"/>
Support place	P5	<input type="radio"/> <input checked="" type="radio"/> <input type="radio"/>	P5	<input type="radio"/> <input checked="" type="radio"/> <input type="radio"/>	P5	<input checked="" type="radio"/> <input type="radio"/> <input type="radio"/>	P5	<input checked="" type="radio"/> <input type="radio"/> <input type="radio"/>
Symmetry	P6	<input checked="" type="radio"/> <input type="radio"/> <input type="radio"/> <input type="radio"/>	P6	<input checked="" type="radio"/> <input type="radio"/> <input type="radio"/> <input type="radio"/>	P6	<input checked="" type="radio"/> <input type="radio"/> <input type="radio"/> <input type="radio"/>	P6	<input checked="" type="radio"/> <input type="radio"/> <input type="radio"/> <input type="radio"/>
Draw direction	P7	<input checked="" type="radio"/> <input type="radio"/> <input type="radio"/> <input type="radio"/>	P7	<input checked="" type="radio"/> <input type="radio"/> <input type="radio"/> <input type="radio"/>	P7	<input checked="" type="radio"/> <input type="radio"/> <input type="radio"/> <input type="radio"/>	P7	<input checked="" type="radio"/> <input type="radio"/> <input type="radio"/> <input type="radio"/>
Frequency target	P8	<input checked="" type="radio"/> <input type="radio"/> <input type="radio"/>	P8	<input checked="" type="radio"/> <input type="radio"/> <input type="radio"/>	P8	<input checked="" type="radio"/> <input type="radio"/> <input type="radio"/>	P8	<input checked="" type="radio"/> <input type="radio"/> <input type="radio"/>
Thickness ctrl	P9	<input checked="" type="radio"/> <input type="radio"/> <input type="radio"/>	P9	<input checked="" type="radio"/> <input type="radio"/> <input type="radio"/>	P9	<input checked="" type="radio"/> <input type="radio"/> <input type="radio"/>	P9	<input checked="" type="radio"/> <input type="radio"/> <input type="radio"/>
Gravity	P10	<input type="radio"/> <input checked="" type="radio"/>	P10	<input checked="" type="radio"/> <input type="radio"/>	P10	<input checked="" type="radio"/> <input type="radio"/>	P10	<input checked="" type="radio"/> <input type="radio"/>

Figure 2.20: Morphological overview

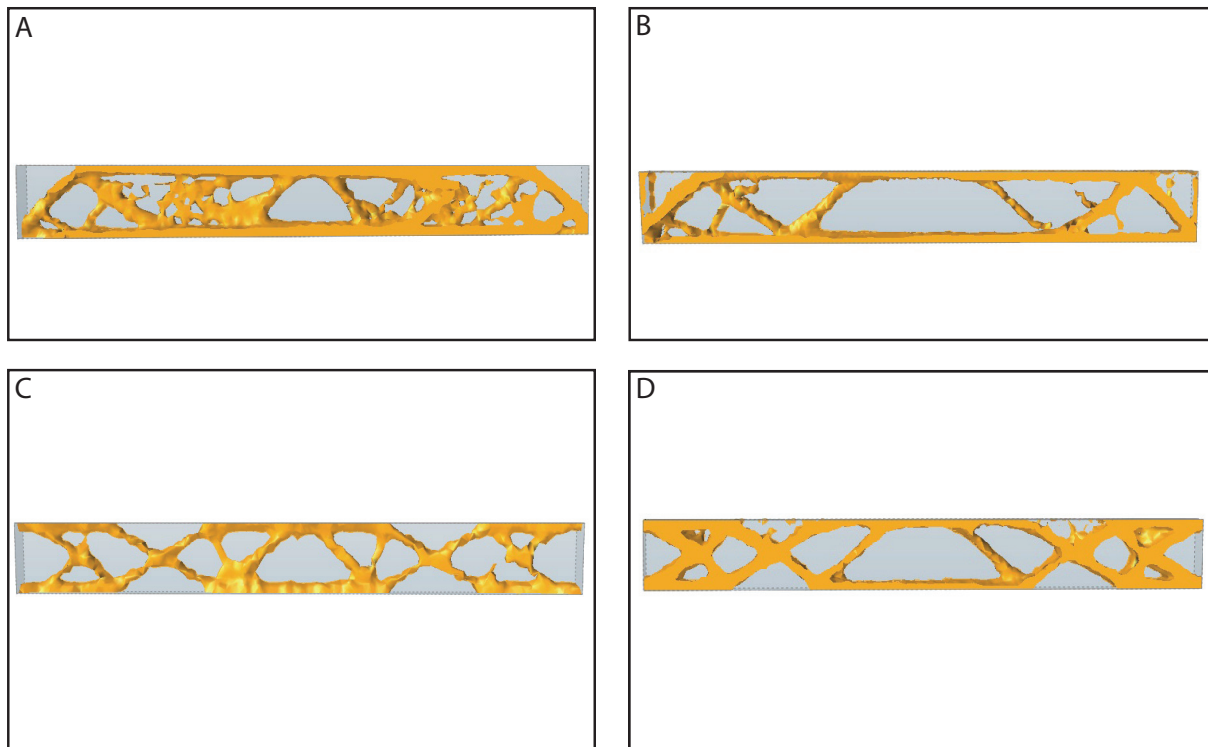


Figure 2.21: Characteristic results of topology optimization on a one-bay beam

The Figures displayed on this page show the results of the parameter study done in Inspire 9.0 on the one-bay beam shown in Figure 2.21. A, B, C and D show the widest range of results, meaning that varying other constraints will influence the outcome less than the constraints varied in these specific results. The relation between structure and form, the structural morphology, of these optimized beams is very strong. If one understands the structural behaviour of any given problem, you can understand any result that Inspire gives you.

The constraints that have the most influence on the outcome are the place and type of supports used. In result A and B a hinged support on the bottom edge of the beam was used, where in C and D the beam was fixed at both ends. Since a hinged support is unable to absorb a moment, the moment tends to zero near the supports. Therefore, little material is necessary near the supports. This is the other way round when a fixed support constraint is used. Here, the moment tends to zero near 1/4 and 3/4 of the length (Figure 2.21), explaining the lack of an upper and lower flange. In both cases, one result is influenced by a point load (A and C) and one by a distributed load (B and D). At the location of the point load, an inverted V-shaped member appears which directs the forces at an angle of 45 degrees. This particular feature does not appear when a distributed load is used, since, naturally, the load is already distributed over a larger surface. When moving from a centred point load towards a distributed load (by adding more point loads), the two bars

of the V-shaped member move further and further apart. The value of the loads applied does not make a large difference on the resulting topology of the element. Further structural analysis should determine whether or not the element is structurally sound.

The mass target constraint determines the volume fraction that is kept during optimization. In the results shown above, mass targets of 20 and 40 percent were used. In general, mass targets do not influence the resulting topology much, but have more influence on member sizes. Also, the material choice does not influence the result much. However, when the gravity constraint is used, which should only be activated in case of materials with a high density, the material choice does influence the result significantly. It has to be noted that thickness control, that is a minimum size or a minimum and maximum size constraint, can improve the result of any problem. By improving we mean making the resulting topology more clear.

In figure 2.22 the four different results are depicted beneath one another. Hereby, it becomes clearly visible that all the results can be partitioned in four segments. Since the beam is eight meters long, every segment is two meters. This makes sense, since forces are usually distributed at an angle of about 45 degrees. With a given height of one meter, a segment becomes two meters wide. From the reasoning above, we can assume that the height to length ratio of a beam plays an important role in the optimization process. In addition, the same assumption can be made with regard

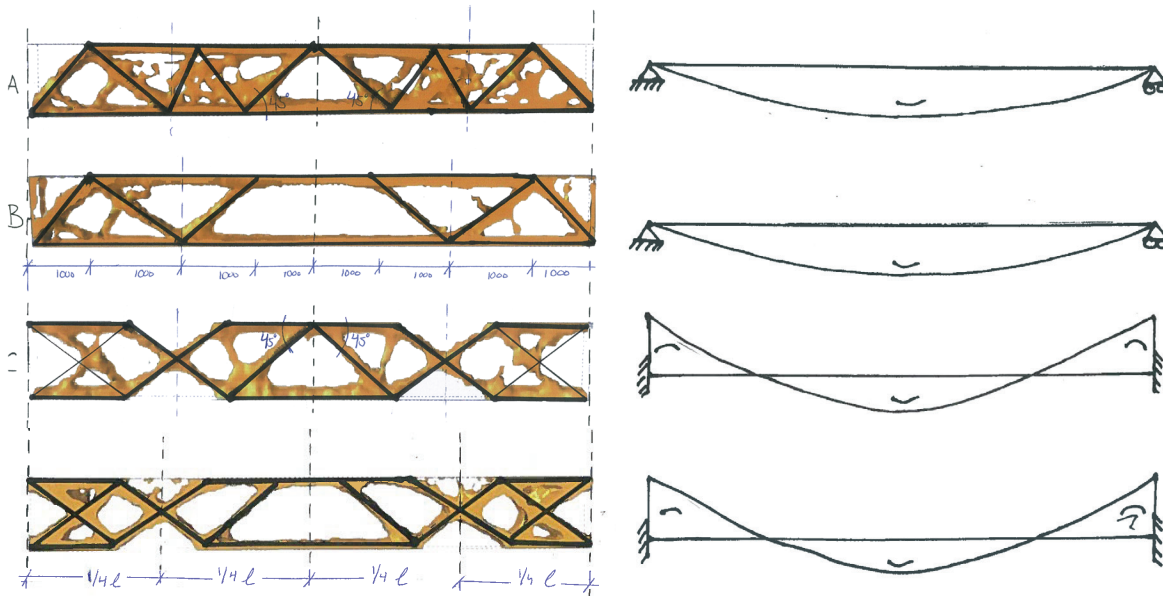


Figure 2.22: LEFT: Interpretation of the results, RIGHT: moment diagrams

to the width to height ratio. To determine which influence increasing or decreasing these ratios have on the results, they were modelled in Inspire.

#### SLENDERNESS

Figure 2.24 shows different height to length ratios<sup>1,2</sup> of result B of a one-bay beam, starting with a ratio of 1 up to 1/18. In this case, the beam is supported at the bottom ends of the beam, where the left side is fixed and the right side is hinged. When the height is the same as the length the forces cannot be transferred at an angle of 45 degrees. The force is transferred via a straight line from the point load to the supports. Material between the supports and the line from the

load to the support is removed, which results in an arch. With a ratio of 1/2 the loads can be transferred at an angle of 45 degrees which also results in arch, but with a higher curvature than the previous one.

Starting with a ratio of 1/4 up to a ratio of 1/10 a similar stable topology emerges. By stable we mean that varying the topology slider (Figure 2.23) does not result in any significant changes in the topology of the component. From 1/12 the topology starts to be unclear. Applying thickness control, mainly minimum size, can improve the result up to a certain level. Minimum size eliminates members with a size lower than the specified minimum member size, giving a clearer result. However, from a ratio of 1/14 and lower this has little effect.

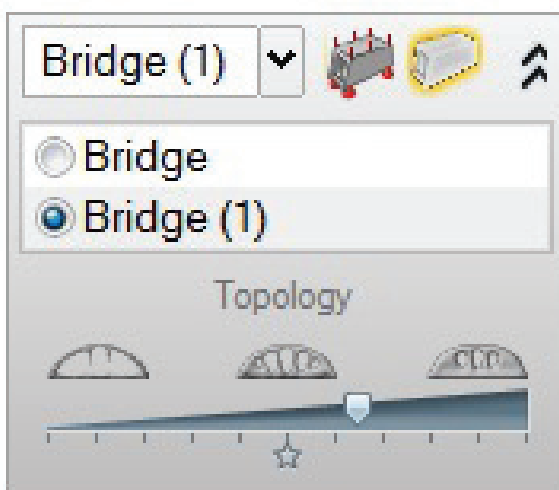


Figure 2.23: Topology slider

Figure 2.25 shows the different height to length ratios of result D. Here, both ends of the beam are fixed, which leads to a different topology than result B. When the height and length are equal, the forces will still be distributed at an angle of 45 degrees, since they do not have to be transported to the bottom ends of the beam. Therefore, almost 75% of the design space is removed. With a ratio of 1/2 and 1/4 the same topology appears, only now approximately 50% of material is removed due to the larger length of the beam. From 1/6 the topology starts to change, leading to a clear topology at a ratio of 1/8. This topology stays constant up to a ratio of 1/16. It only changes in the second and third quarter where an additional cross appears. Elsewhere, the topology does not change, the beam merely gets stretched. The fact that

1. The design space has the following ratios; Height to length ratio =  $h/l = 1/8$ , Width to height ratio =  $b/h = 3/10$
2. According to Jellema 3: Draagstructuur, a rule of thumb for hinged concrete beams is a height to length ratio of 1/10 - 1/12.





the topology stays constant for lower ratios is due to the type of supports used in this case. Fixed supports appear to lead to more stable and constant topologies after optimization than hinged supports.

**B**

PARAMETER	VALUE
P1	● ○ ○
P2	○ ● ○
P3	○ ●
P4	● ○
P5	○ ● ○
P6	● ○ ○ ○
P7	● ○ ○ ○
P8	● ○ ○
P9	● ○ ○
P10	● ○

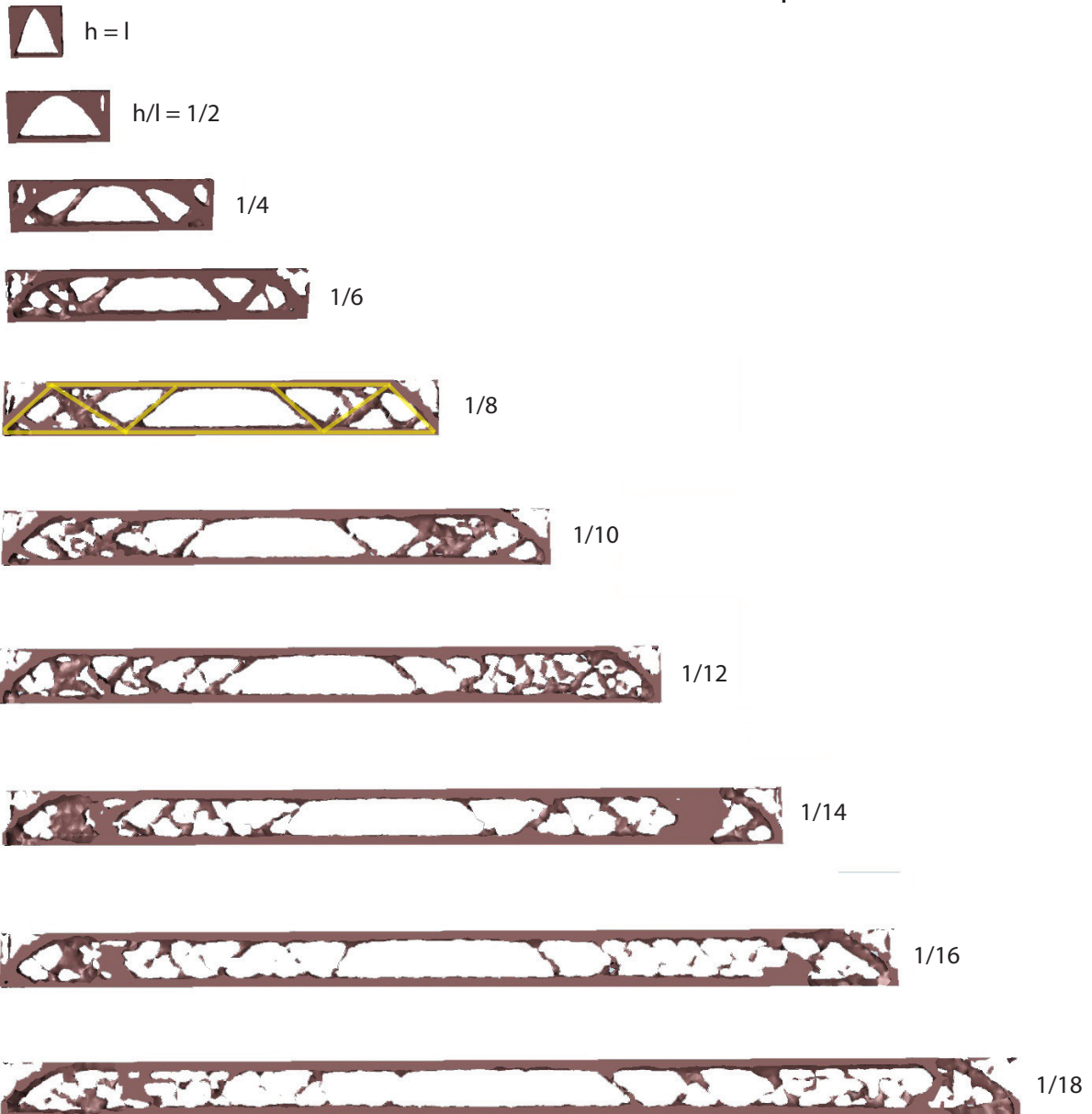


Figure 2.24: Height to length ratios of result B

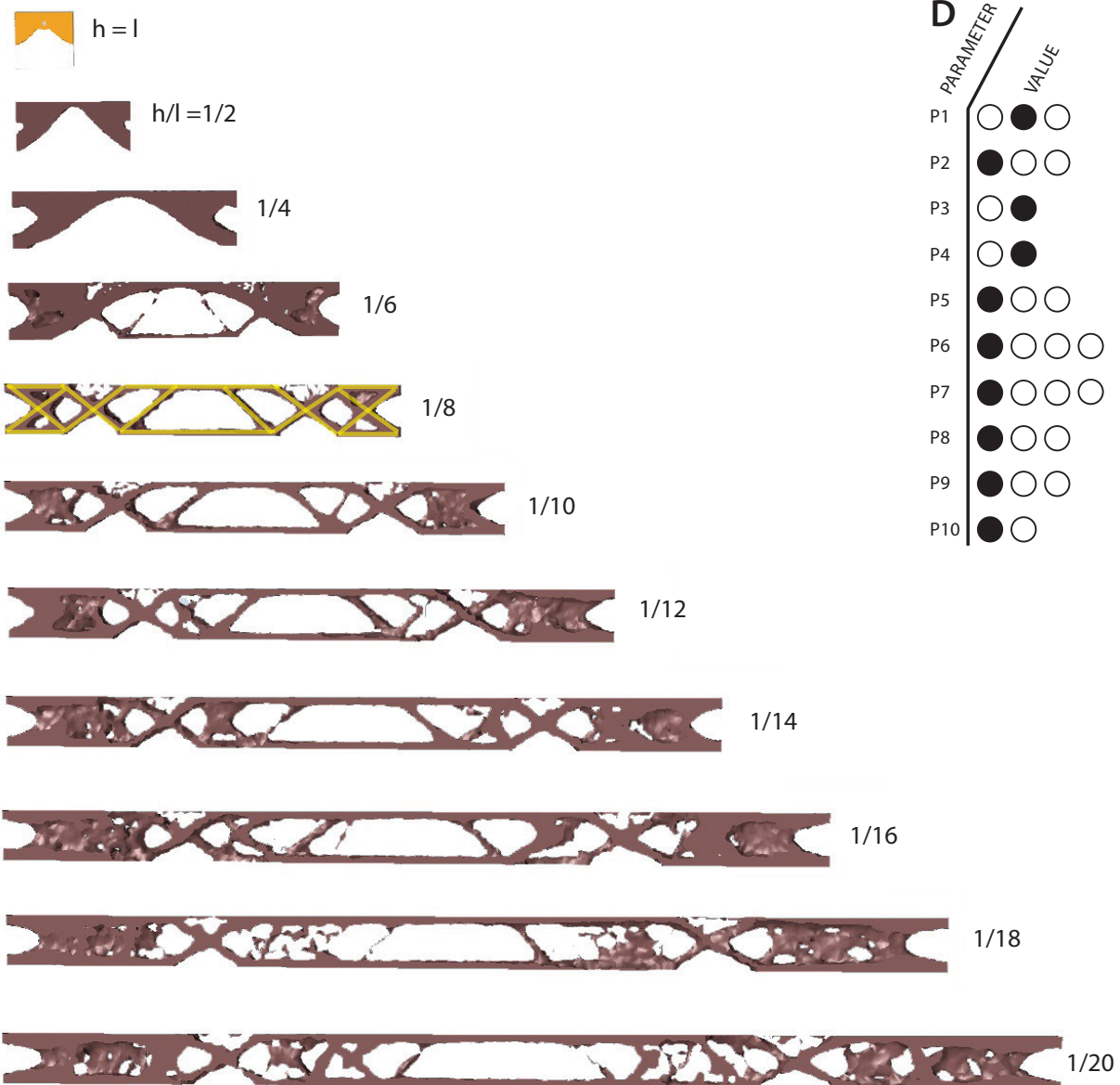


Figure 2.25: Height to length ratios of result D

### CONTINUOUS BEAMS

All the previous cases discussed beams on two supports. Naturally, beams are often continuous and are therefore supported by multiple supports. To gain insight in the behaviour of topologically optimized continuous beams, result B and D discussed earlier were optimized when constrained by multiple supports. These optimized continuous beams show results which are strongly related to the beams on two supports. The topologies of hinged and fixed beams derived earlier are clearly recognizable in the continuous beams (Figure 2.26).

Obviously, where there is an extra support there is a V-shaped member to direct forces to the support. A notable detail is the cross near the supports of the hinged beam. In the case of a beam on two supports, this feature only exists with a fixed beam, since the

moment tends to zero at that point (Figure 2.22). This is also the case with both continuous beams, as is showed in Figure 2.26.

### WIDTH TO HEIGHT RATIO

Besides the height to length ratio, the width to height ratio is also an important feature. When this ratio is lowered, the beam will move from a 2D structure to a 3D structure. Eventually, when the width is increased further, it will become a slab which is a different structure system subgroup. Figure 2.27 shows the result of increasing the width to height ratio of a hinged beam. In between the supports holes appear in transverse direction, due to the moment tending to zero locally, resulting in a local 3D structure. The diagonal members in the middle of the beam are maintained, causing the element to stay 2D in the middle.

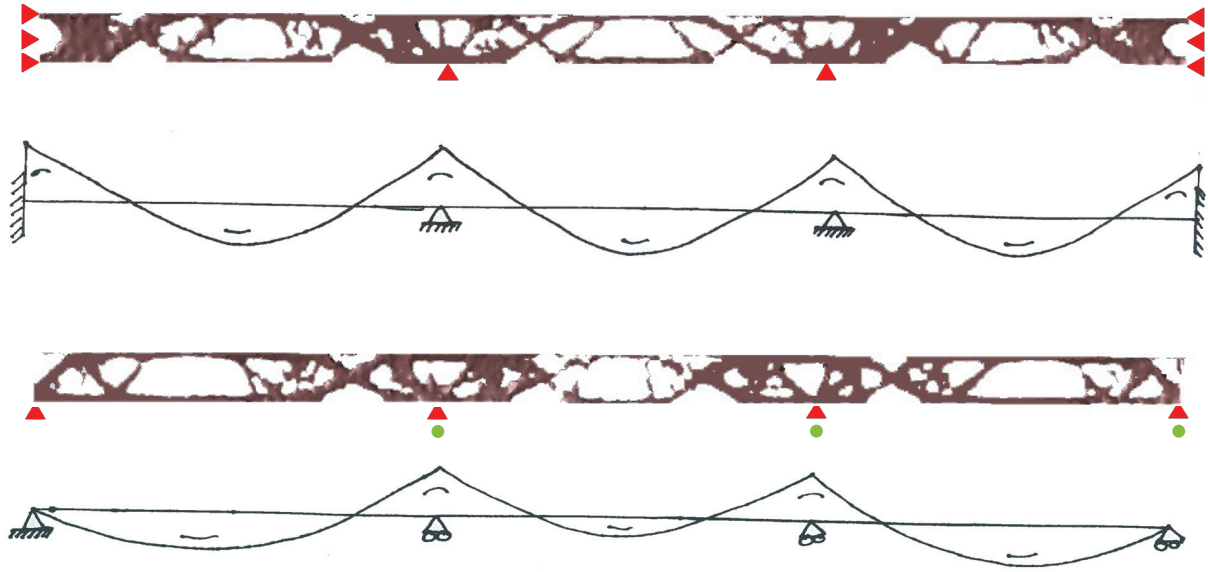


Figure 2.26: Continuous beams with moment diagrams

When the width is increased further this combination of a 2D structure in the middle, and a 3D structure near the supports becomes more and more evident. This structural morphology appears with all combinations of constraints. In this case a distributed load was used, but the results can be generalized for point loads also. As in the case of the parameter study into the height to length ratio, a beam with hinged supports appears to be unstable. It is difficult to reach convergence when increasing the width while maintaining the

same height. The clear topology that emerged with the standard design space, is not translated to design spaces with a higher width to height ratio.

With a ratio of 3/10, as shown in Figure 2.27, the result is similar to a typical 2D truss. The first signs of a 3D structure are already visible with a ratio of 2/5. Besides holes in the longitudinal direction, holes in the transverse direction of the beam also appear. The holes appear where the moment tends to zero. The

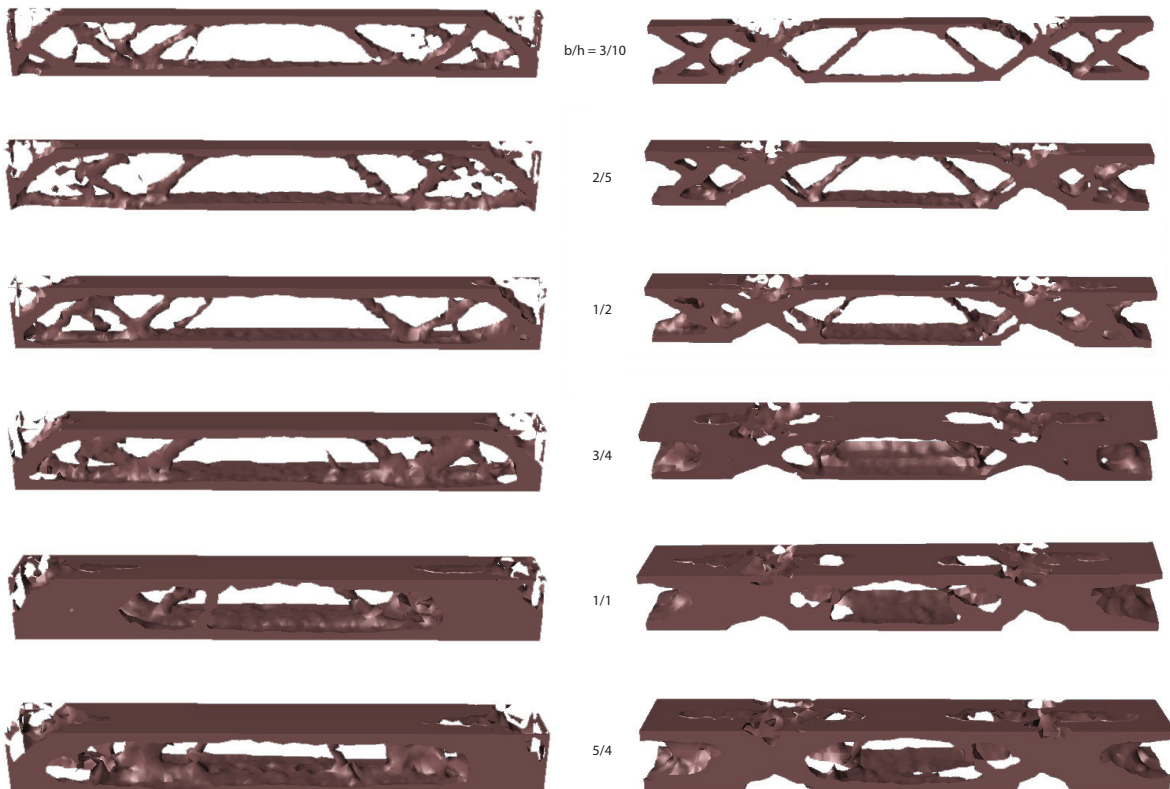


Figure 2.27: Different width to height ratios: Left result B, Right result D



topology of the beam stays constant from  $2/5$  up to approximately  $8/10$ . Here, the middle members also move to the edge of the beam. This is clearly visible at a ratio of 1. The results are constant for the remainder of the ratios. Ratios higher than  $5/4$  are not shown, since they are never used in practice due to the buckling problem.

A big difference compared to a hinged beam is the clear and stable topology that emerges in the case of a fixed beam. The topology of the 2D element is translated to a 3D element, independent of the width to height ratio. When we take a closer look at result D where the width and height are equal, we see that most members can be connected and run in a helical form around the beam (Figure 2.28), not unlike the tensairity principle. The middle diagonal members are the only ones that are not continuous. The continuity of the members could be advantageous looking from a production point of view.

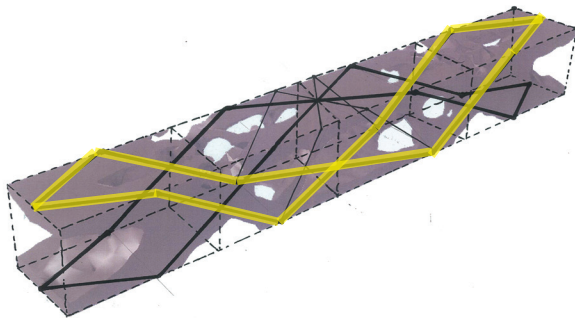


Figure 2.28: Result D; continuity of the members

#### ALTERNATIVE DESIGN SPACES

All the results thus far have used an initial design space with a rectangular cross section. From a production point of view, it is important to gain insight in the behaviour of an element when a design space with a curved cross section is used, since inflatable structures have to conform to funicular shapes. The model with a height to length ratio of  $1/8$  and a width to height ratio of 1 is used as a base. The top Figure shows the front and side view of the design space, the second Figure is a hinged beam and the third shows the result with fixed supports.

In Figure 2.29, a square section is used with curved vertices (radius of 0.2 meters) as a first step to approach a round section. Making the vertices curved does not affect the result much compared to the result with a square section. The similarities in the resulting topology are clearly visible. This was not the result when the vertices were curved up to a point where the resulting cross section was round. Here, Inspire removes material at the sides of the design space. The resulting shape is similar to a standard I-beam. To counteract this, a hole was used in the middle of the design space. Hereby, the result is again similar to the

result with a square section design space. Even when the design space is tapered as in Figure 2.31, the results are similar. It has to be noted that the result can be improved by using symmetry constraints.



Figure 2.29: square section with curved vertices

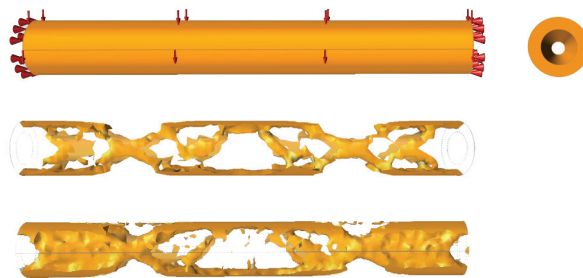


Figure 2.30 : round cross section

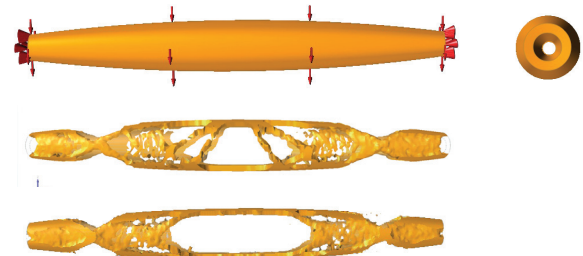


Figure 2.31: Tapered design space

#### CONCLUSION

The following conclusions can be derived out of the previous parameter study (Appendix E);

- The support type has a large influence on the resulting topology. Less material is needed where the moment tends to zero.
- Members connect at an angle of approximately 45 degrees since forces also disperse at this angle.
- The difference in topology between an optimization problem with a distributed and a point load are the middle diagonal members that connect in the case of a point load, and are apart in the case of a distributed load.
- The value of the force used does not influence the resulting topology.
- Mass target does not determine the resulting topology, but influences component attrib-



utes that mostly deal with size and shape optimization.

- Material (isotropic) choice has very little influence on the outcome of topology optimization, unless the gravity constraint is used in combination with high density materials.
- Fixed supports lead to more stable topologies than hinged supports.
- Increasing the slenderness of a one-bay beam does not result in new topology, the result only gets stretched.
- Stable slenderness ratios:  
Hinged:  $1/4 < h/l < 1/10$   
Fixed:  $1/8 < h/l < 1/16$
- Fixed supports are better suited for optimized beams with a high slenderness ( $h/l < 1/10$ ).
- In the case of a continuous beams the topology

of a one-bay beam merely gets copied.

- Beams with fixed supports become completely 3D when the width to height ratio is increased.
- The members of a 3D beam run in helical form around the beam and are continuous, forming a closed structure

As was shown in this paragraph, many different forms of optimized beams exist. However, these conclusions show that most optimized beams are derivatives from one another. The one-bay beam is the basis for all other forms of optimized beams, and is therefore used as a representative case for optimized beam structures. Due to manufacturing constraints, the circular beam is used since it was shown that it has the same morphology and topology as his square-edged counterpart.

### 2.3.4 FRAME STRUCTURES

The second section active sub-group described by Engel are the frame structures (Figure 2.32). The starting point for the study into the morphological features of this group is a one-bay frame with dimensions described in figure 2.34.

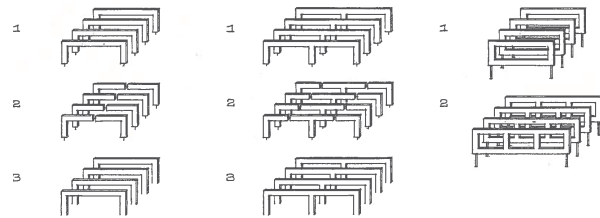


Figure 2.32: Frame structures (Engel 1997)

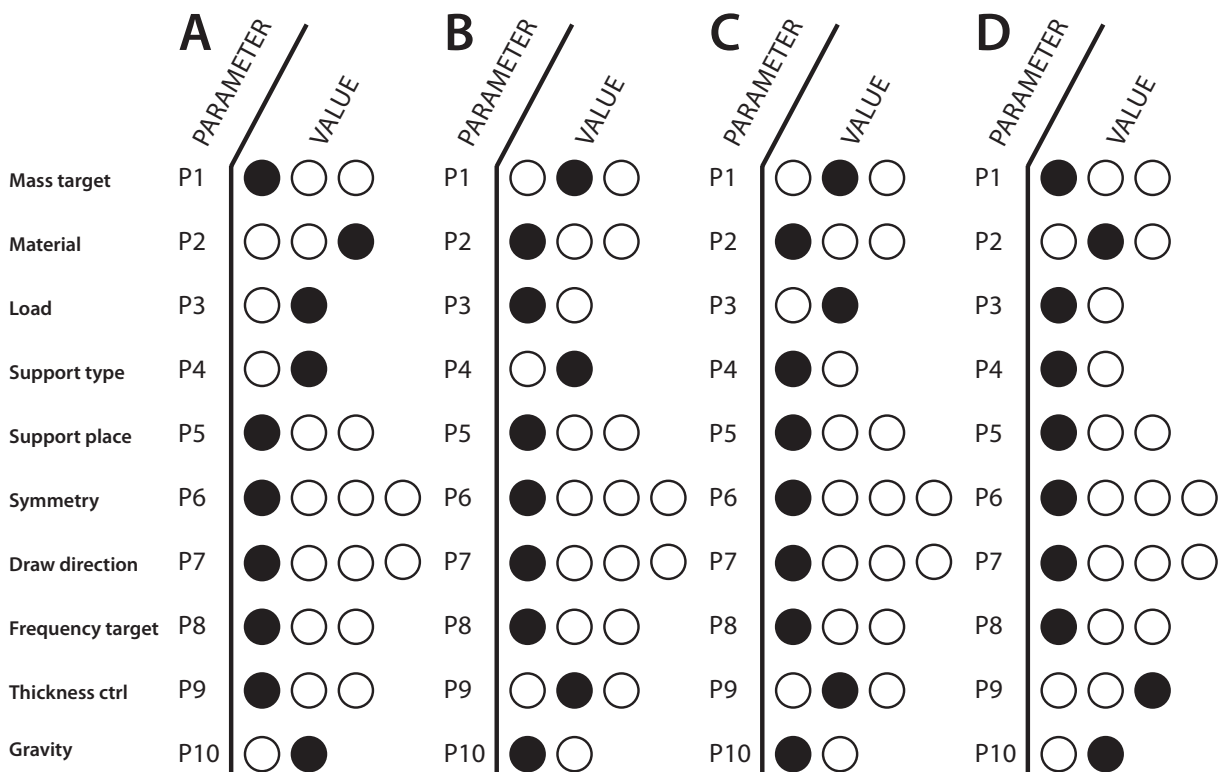


Figure 2.33: Morphological overview

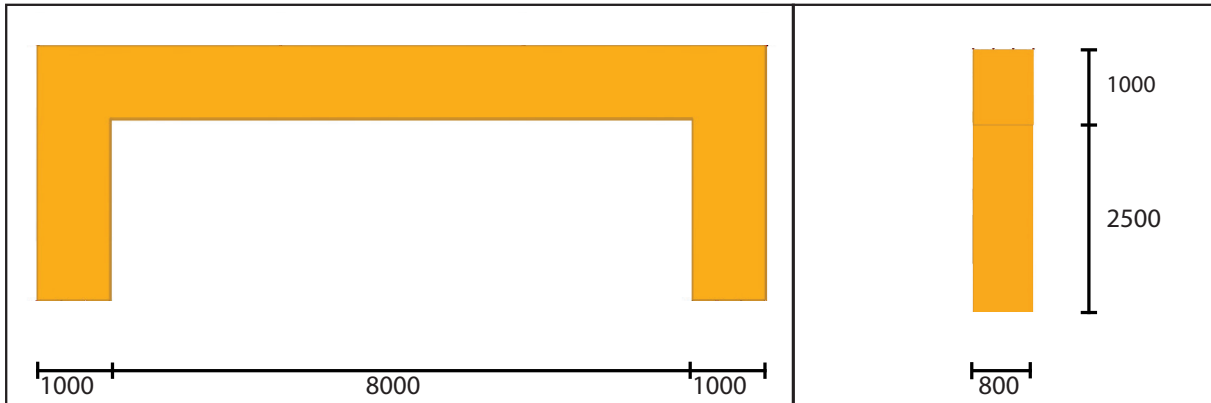


Figure 2.34: Front and side view of the design space

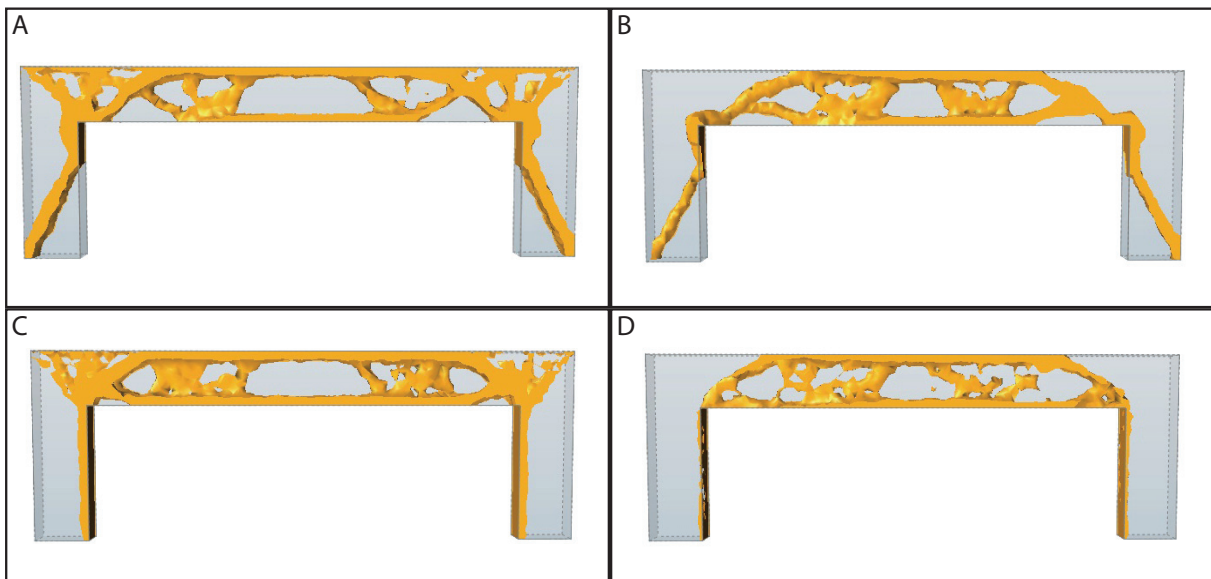


Figure 2.35: Characteristic results of topology optimization on a one-bay frame

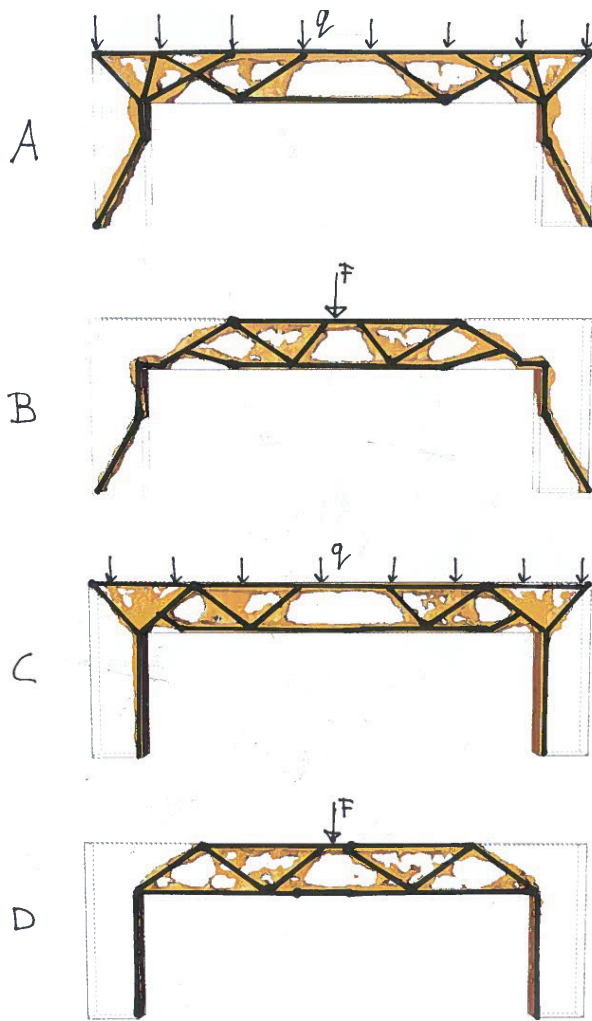
The figures displayed on this page show the results of a parameter study on the one-bay frame shown in figure 2.35. A, B, C and D show the widest range of results, meaning that varying other constraints will influence the outcome less than the constraints varied in these specific results.

In result A and B, the frame was supported by fixed hinges at the bottom, where in result C and D roller supports were used. Both A and C are constrained by a distributed force, and B and D by a point load. Result A through D of the optimized one-bay beam are clearly visible in these optimized frames. The top beam is identical to a one bay beam, especially in the case of a roller support. In the case of a roller support, the outcome can be seen as an optimized beam with very high supports. The same morphological features can therefore be recognized. In addition, the same conclusions as in the case of one bay beams apply with regard to mass targets, material choice and gravity.

In result A and B the previously discussed beams

are also clearly recognizable. Due to a different supporting mechanism, the resulting morphology is also different. The topology however, is almost identical to result C and D. The basic shape result A and B is an arch. The distributed load in result A is supported by a truss structure that transfers the forces to the arch shape. Result A has a clear topology, where the fixed beam discussed in the previous paragraph is clearly recognizable. The main difference between result A and B is due to the difference in load type. In the case of a point load, the moment near the edges is smaller, reducing the need for many material.

Figure 2.36 shows an interpretation of the main structural lines in the four results. Depending on the forces applied on the structure, the truss-like shape is determined. The forces applied are being distributed at an angle of 45 degrees towards the arch shape. From this arch shape these forces are distributed down to the foundation.



e 30]

Stan van Dijck & Joost van de Koppel

Figure 2.36: Sketches of the main supporting structure of the one-bay frame results

### MOMENT DIAGRAMS

At first a moment diagram of an one-bay frame with a distributed load is sketched, this is a similar structure as in result A, only with a larger span. The moment diagram of a distributed loaded frame has 4 points in which the moment is zero. These zero-moments are on the arch like shape of the frame. At these points little material is necessary causing only a single bar to appear. An arch like shape would be much more optimal to reduce the amount of material used. At the edges the structure has to transfer a large moment, which leads to a large amount of material.

The moment diagram of a point loaded frame has also 4 points in which the moment is zero and these zero-moments are also on the arch like shape of the frame like in the distributed load. The outcomes of the moment diagram are very similar to the distributed load, except in the edges is the necessary amount of material reduced, due to a smaller moment. The smaller moment is an outcome of a linear moment-

line instead of a parabolic line, in which the moment increases greatly as the length increases.

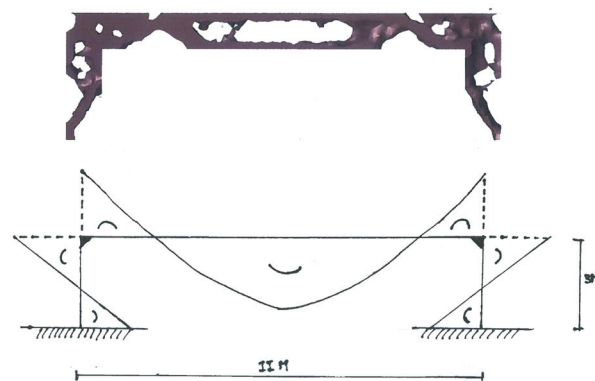


Figure 2.37a: Moment Diagram of a one-bay frame with a distributed load

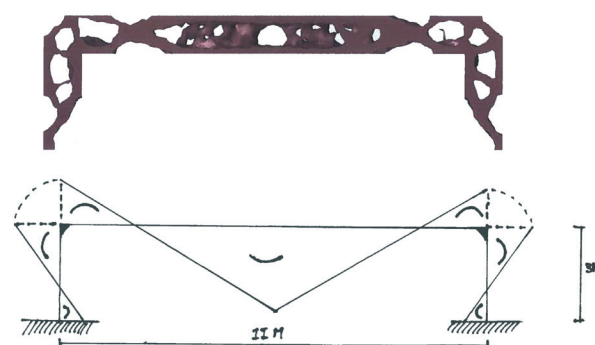


Figure 2.37b: Moment Diagram of a one-bay frame with a point load

### SLENDERNESS

The relation between the height and length is important for the optimization of a structure. This overview gives a clear view on the difference in topology when this ratio differs. The overview is based on result A, the only difference is that the mass target is set to 40% instead of 20%. Result A, with mass target 40% has a height / length ratio of 1/8.

This basic shape is extended and shortened in steps of 2 meters. The topology in the beam part of the shape is the same in most cases, it only gets stretched or shrunk over the entire length. The topology in the upper corners of the shape changes to transfer the forces from the beam part to the column part. The ideal shape would be an arch, but this is prevented by the design space. Therefore the corners are becoming more solid in the case of larger spans.

The shapes derived from the optimization with a ratio of 1/10 or higher have the topology that is stretched over the length. These topologies are typical for one-bay frames.

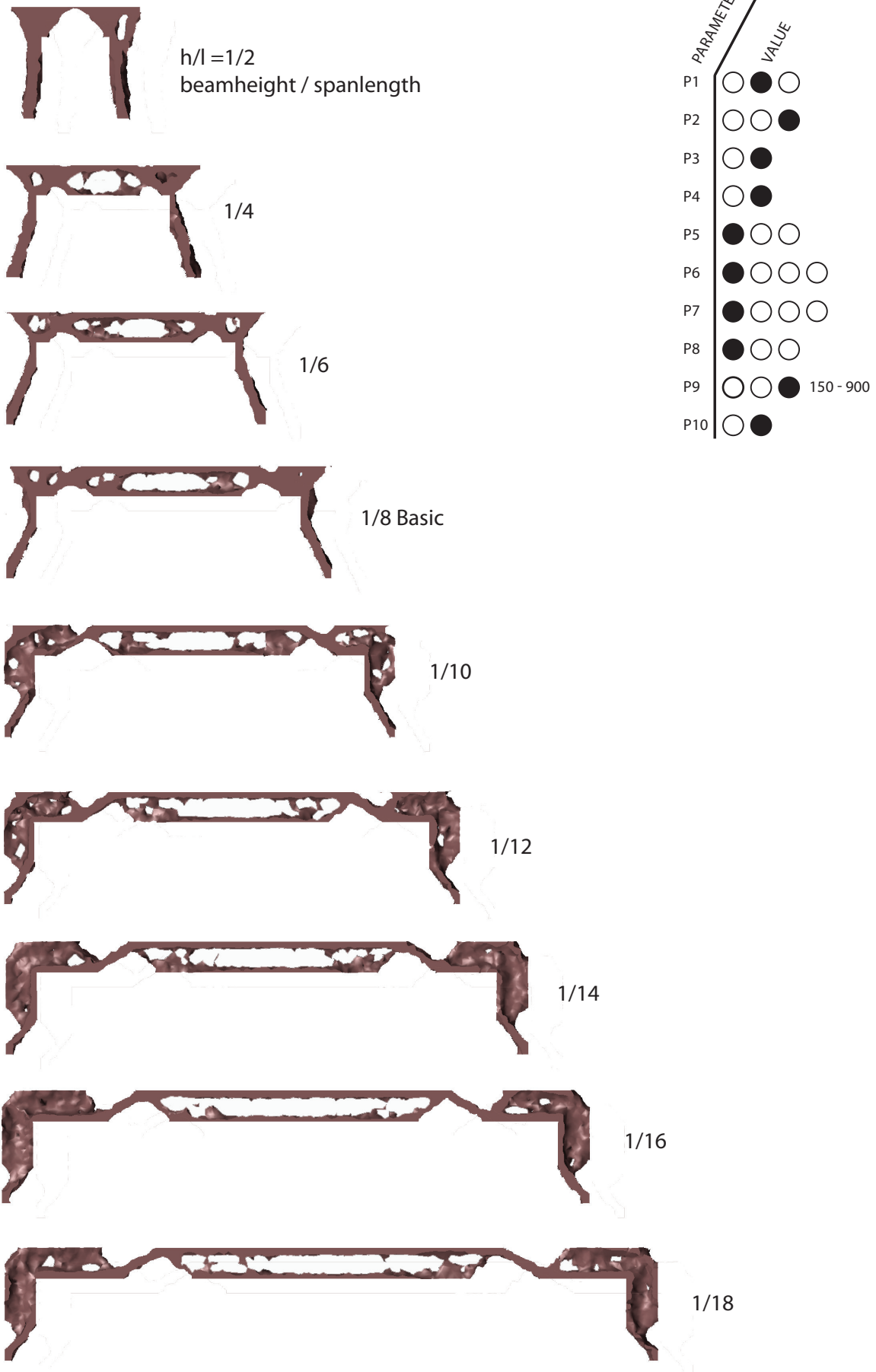


Figure 2.38: Height to length ratios of result A



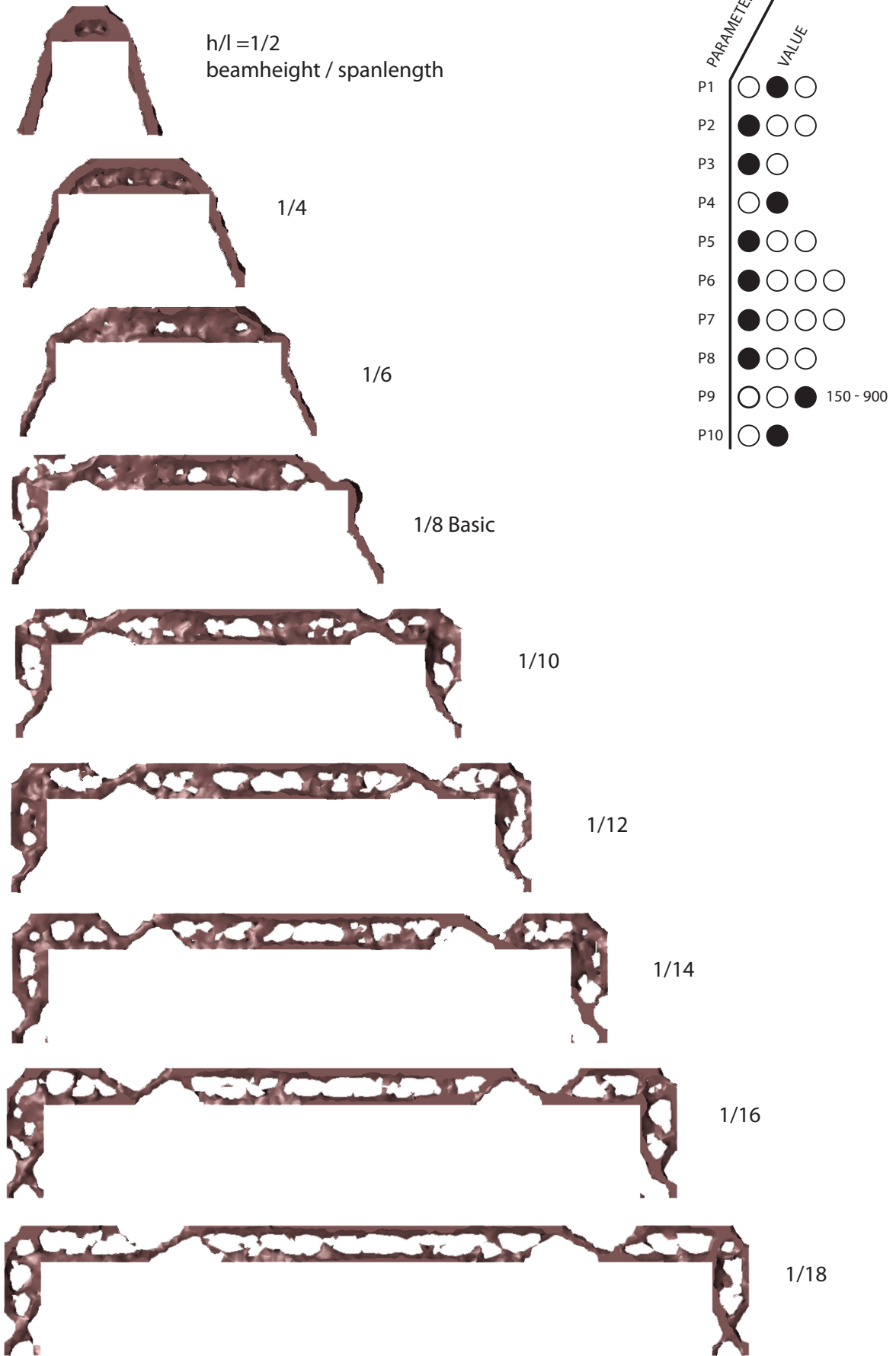


Figure 2.39: Height to length ratios of result B



Figure 2.40: Multipanel frame with a distributed load



Figure 2.41: Multipanel frame with a point load

The point-loaded frames have a clear truss structure which transfers the forces from the point load to the foundation. The arch shape can be drawn in every model. At the arch line, the moment changes direction, which allows the structure to have one single bar to transfer the forces. The moment diagram of the frames is illustrated before. The models with ratios 1/8 till 1/14 have a clear topology that has minor changes. If we compare the models with the moment diagram, it can be noticed that the applied material on the edges is necessary to distribute the moment.

#### MULTIPANEL FRAMES:

The frames in this phase are extruded with an extra column, meaning they are continuous. Both spans are 10 meters, so they are similar to the previous one-bay frames. A distributed load is applied on the multipanel frame. The structure is similar to the results of previous optimizations on the outer sides. The forces of the two point loads form an equilibrium in the central column, resulting in a straight column. A truss shape structure on top of the central column forms the connection between these two frames. The arch shape of the two portals is noticeable, but partly replaced by the central column and truss system, this is a result of the equilibrium between the two frames.

A multipanel frame with a point load is optimized in figure 2.41. This frame is very similar to the multipanel frame with a distributed load. The topology in this optimization is more clear than in the distributed load. As in one-bay frames with a point load, the amount of material in the edges is minimal. The central part is similar to the multipanel frame with a distributed load, consisting of a straight column with a truss system on top forming an equilibrium between the two frames.

#### WIDTH TO HEIGHT RATIOS

To achieve 3d cases realizable with inflatables, a topology optimization of the frame structures with different widths has to be performed. The outcome of a topology optimization with a small width of 400 mm, as shown in the illustrations will be a 2D structure. As the width increases the structure shape will be three-dimensional. The frame with a width of 800 mm is the basic model used in previous studies and results in a 2d structure. As the width of a structure is more than 1200 mm the structure becomes a 3d shape. From a production point of view the 3d models are more likely to be produced. These 3d shapes can have an inner inflatable on which the outer inflatables are attached and eventually can be rigidized. By increasing the width of the structure to values of 2400 mm or larger the basis of the structure will exist of three arches that are connected in several directions. The topology of these structures becomes unclear and large parts are solid.

The next phase in the optimization of frames is to adjust the design space to the outcomes of these studies. Therefore the design space is changed in an arch shape, where the form follows the function. The arch shapes can be realized in 2d and 3d structures.

#### OPTIMIZING THE DESIGN SPACE

The design space of the previous optimized frames was based on three perpendicular attached beams. One of the remarkable and repetitive outcomes of the optimized frames was that the basis of all these frame was the arch shape. By the three rectangle beams' design space, the arches were interrupted. This leads to a less efficient and less optimized structure.

Therefore the design space is redesigned to allow the arch shape to be continuous. This results in a more efficient way of material use, as shown in the



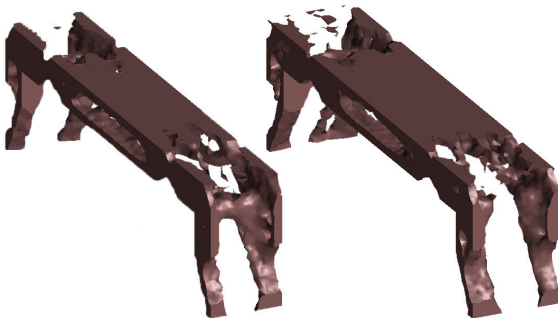
Width = 400 mm

Width = 800 mm



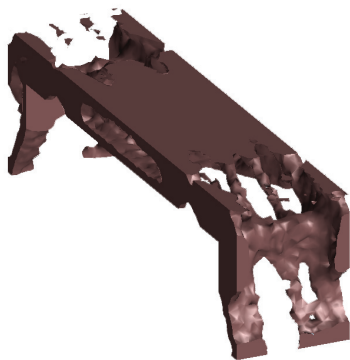
Width = 1200 mm

Width = 1600 mm



Width = 2000 mm

Width = 2400 mm



Width = 2800 mm

Figure 2.42: Width to Height ratio of result D

illustrations. If the arch shape is interrupted, the moment increases near the edges. Besides that the moment becomes larger, a larger span also results in a larger moment.

In structures with small spans this has less consequences for the structure. As the span increases, the moment in the edges increases, and if the arch is interrupted, this will lead to additional material to transfer the forces at the edges. The differences in material and topology are clearly visible between the original frame shape and the arch shaped frame. The reduction of material used in percentage in structures with large spans is greater than in structures with smaller spans if the arch shape can be continued as shown in Figure 2.43.

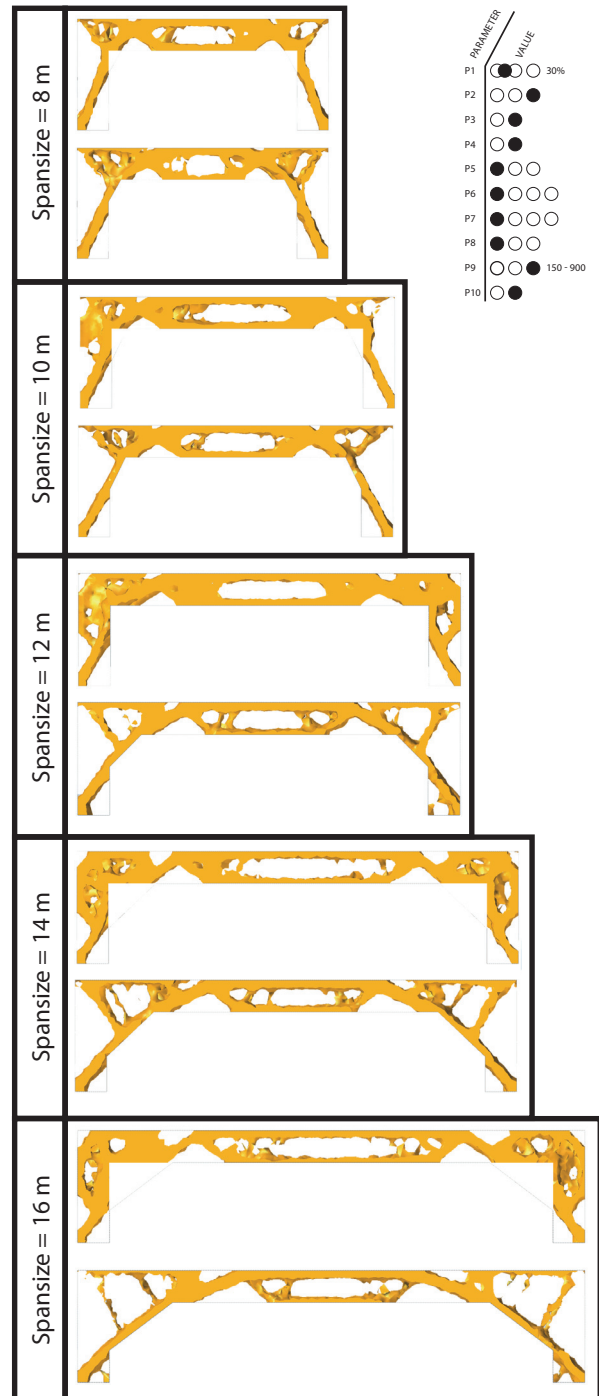


Figure 2.43: Optimized design space applied on multiple spans of Result A



## CONCLUSION

The following conclusions can be derived out of the previous parameter study;

- The type of load has the largest influence on the resulting topology and morphology. Less material is needed where the moment tends to zero.
- The topology of the one-bay frames is based on an arch shape to transfer the forces through the structure to the support points.
- The optimized horizontal part of the beam is topologically the same as an optimized one bay beam constrained by similar parameters.
- The type of supports used have little influence on the resulting topology.
- Members of the horizontal part of the frame connect at an angle of approximately 45 degrees since forces also disperse at this angle.
- The difference in topology between an optimization problem with a distributed and a point load are the middle diagonal members that connect in the case of a point load, and are apart in the case of a distributed load.
- The value of the force used does not influence the resulting topology.
- Mass target does not determine the resulting topology, but influences component attributes that mostly deal with size and shape optimization.
- Material (isotropic) choice has very little influence on the outcome of topology optimization, unless the gravity constraint is used in combination with high density materials.
- Increasing the slenderness does not result in new topology, the result only gets stretched. The larger the slenderness, the larger the moment near the edges, the more materials is needed near the edges.
- Stable slenderness ratios:  
 Distributed load:  $1/10 < h/l > 1/18$   
 Point load:  $1/8 < h/l > 1/14$
- In the case of a continuous frames the topology of a one-bay frame merely gets copied.
- Frame structures become completely 3D up to an increased width of 2400 mm. However, the members are never continuous since it is not a closed structure.
- The traditional design space of a one-bay frame is exists out of three perpendicular attached beams. By adjusting the design space and rounding the inner edges, the arch shape can be continuous which leads to a more efficient use of material.

These conclusions show that optimized frame structures are always derivatives from each other. From a technical en environmental point of view, it makes much more sense to use an optimized frame

structure with an optimized design space as a representative case.

## 2.3.6 BEAM GRID SYSTEMS

The third section active structure system group described by Engel (1997) are the beam grid systems. This group can be sub-divided into homogeneous grids, gradated grids and concentric grids (Figure 2.44). A beam grid systems is a collection of multiple beam structures, which together form a new section active structure system. Since this system is composed of multiple beam structures, an optimized beam grid system is also a collection of multiple optimized beam structures. Figure 2.45 shows a basic beam grid composed of beams with a length of eight meters. This grid was optimized in Inspire to show that the result is a collection of optimized beam structures discussed in paragraph 2.5.2: continuous beams.

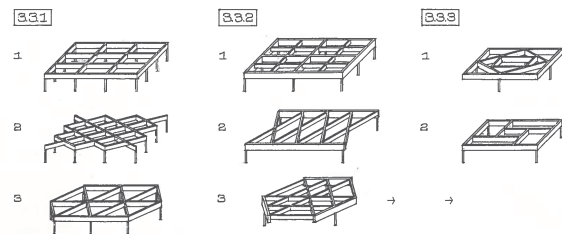


Figure 2.44: Beam grid systems (Engel, 1997)

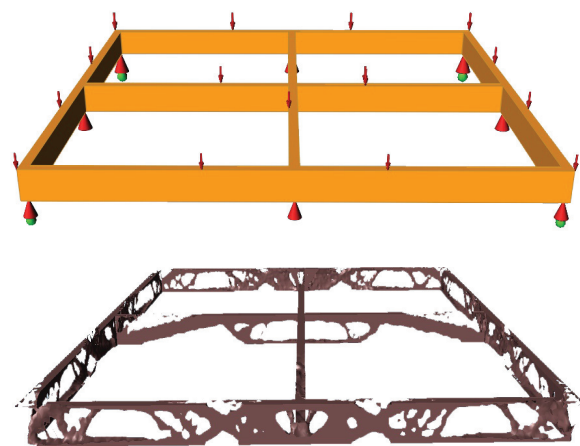


Figure 2.45: Top; Design space beam grid system , Bottom; Optimized beam grid system

The optimized beam grid shown in figure 2.45 on the right is strongly related to the optimized continuous beam discussed in paragraph 2.5.2. In fact, the individual beams in a beam grid behave exactly as a continuous beam structure, using the same principles and structural morphology. Therefore, the same morphological features that were identified in paragraph 2.5.2 apply in the case of beam grid systems.



A noticeable aspect of the optimized beam grid are the two centre beams. Their morphology and topology differs from the beams discussed in 2.3.3, which is due to the type of supports used. In this case, the beam is supported by fixed hinges at both ends, since all the middle supports of the beam grid are fixed hinges. When optimizing an individual beam with a length of 16 meters which is supported by fixed hinges at both ends (figure 2.46), the result is exactly the same as the centre beams of the beam grid shown in figure 2.45.



Figure 2.46: Top; Design space continuous beam , Bottom; Optimized continuous beam

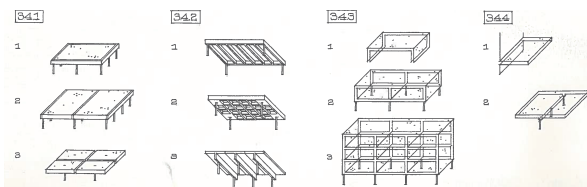


Figure 2.47: Slab structures (Engel, 1997)

### 2.3.7 SLAB STRUCTURES

The fourth and final section active sub group are the slab structures (figure 2.47). As stated in the introduction, a slab structure can be seen as a beam or frame structure with a high width to height ratio. The separate structure systems that were studied are mathematically speaking closely related. When increasing the width of a beam structure while maintaining a constant height, the geometry will move towards a slab structure. When increasing the height of a slab structure while keeping the width constant the result will be similar to an optimized frame structure. Figure 2.48 shows the initial design space which was the starting point of the parameter study. Figure 2.49 shows the morphological overview with the four characteristic cases.

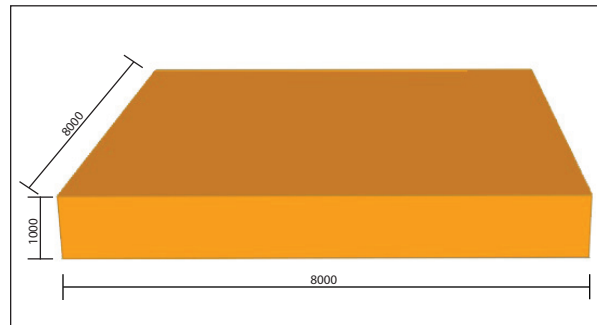


Figure 2.48: Design space for slab structures

	A		B		C		D	
	PARAMETER	VALUE	PARAMETER	VALUE	PARAMETER	VALUE	PARAMETER	VALUE
Mass target	P1	<input type="radio"/> <input checked="" type="radio"/> <input type="radio"/>	P1	<input checked="" type="radio"/> <input type="radio"/> <input type="radio"/>	P1	<input checked="" type="radio"/> <input type="radio"/> <input type="radio"/>	P1	<input type="radio"/> <input checked="" type="radio"/> <input type="radio"/>
Material	P2	<input checked="" type="radio"/> <input type="radio"/> <input type="radio"/>	P2	<input checked="" type="radio"/> <input type="radio"/> <input type="radio"/>	P2	<input checked="" type="radio"/> <input type="radio"/> <input type="radio"/>	P2	<input checked="" type="radio"/> <input type="radio"/> <input type="radio"/>
Load	P3	<input type="radio"/> <input checked="" type="radio"/>	P3	<input checked="" type="radio"/> <input type="radio"/>	P3	<input checked="" type="radio"/> <input type="radio"/>	P3	<input type="radio"/> <input checked="" type="radio"/>
Support type	P4	<input type="radio"/> <input checked="" type="radio"/>	P4	<input type="radio"/> <input checked="" type="radio"/>	P4	<input checked="" type="radio"/> <input type="radio"/>	P4	<input checked="" type="radio"/> <input type="radio"/>
Support place	P5	<input checked="" type="radio"/> <input type="radio"/> <input type="radio"/>	P5	<input checked="" type="radio"/> <input type="radio"/> <input type="radio"/>	P5	<input type="radio"/> <input type="radio"/> <input checked="" type="radio"/>	P5	<input type="radio"/> <input type="radio"/> <input checked="" type="radio"/>
Symmetry	P6	<input checked="" type="radio"/> <input type="radio"/> <input type="radio"/> <input type="radio"/>	P6	<input checked="" type="radio"/> <input type="radio"/> <input type="radio"/> <input type="radio"/>	P6	<input checked="" type="radio"/> <input type="radio"/> <input type="radio"/> <input type="radio"/>	P6	<input checked="" type="radio"/> <input type="radio"/> <input type="radio"/> <input type="radio"/>
Draw direction	P7	<input checked="" type="radio"/> <input type="radio"/> <input type="radio"/> <input type="radio"/>	P7	<input checked="" type="radio"/> <input type="radio"/> <input type="radio"/> <input type="radio"/>	P7	<input checked="" type="radio"/> <input type="radio"/> <input type="radio"/> <input type="radio"/>	P7	<input checked="" type="radio"/> <input type="radio"/> <input type="radio"/> <input type="radio"/>
Frequency target	P8	<input checked="" type="radio"/> <input type="radio"/> <input type="radio"/>	P8	<input checked="" type="radio"/> <input type="radio"/> <input type="radio"/>	P8	<input checked="" type="radio"/> <input type="radio"/> <input type="radio"/>	P8	<input checked="" type="radio"/> <input type="radio"/> <input type="radio"/>
Thickness ctrl	P9	<input type="radio"/> <input checked="" type="radio"/> <input type="radio"/>	P9	<input checked="" type="radio"/> <input type="radio"/> <input type="radio"/>	P9	<input checked="" type="radio"/> <input type="radio"/> <input type="radio"/>	P9	<input type="radio"/> <input checked="" type="radio"/> <input type="radio"/>
Gravity	P10	<input type="radio"/> <input checked="" type="radio"/>	P10	<input type="radio"/> <input checked="" type="radio"/>	P10	<input type="radio"/> <input checked="" type="radio"/>	P10	<input type="radio"/> <input checked="" type="radio"/>

Figure 2.49: Morphological overview for slab structures

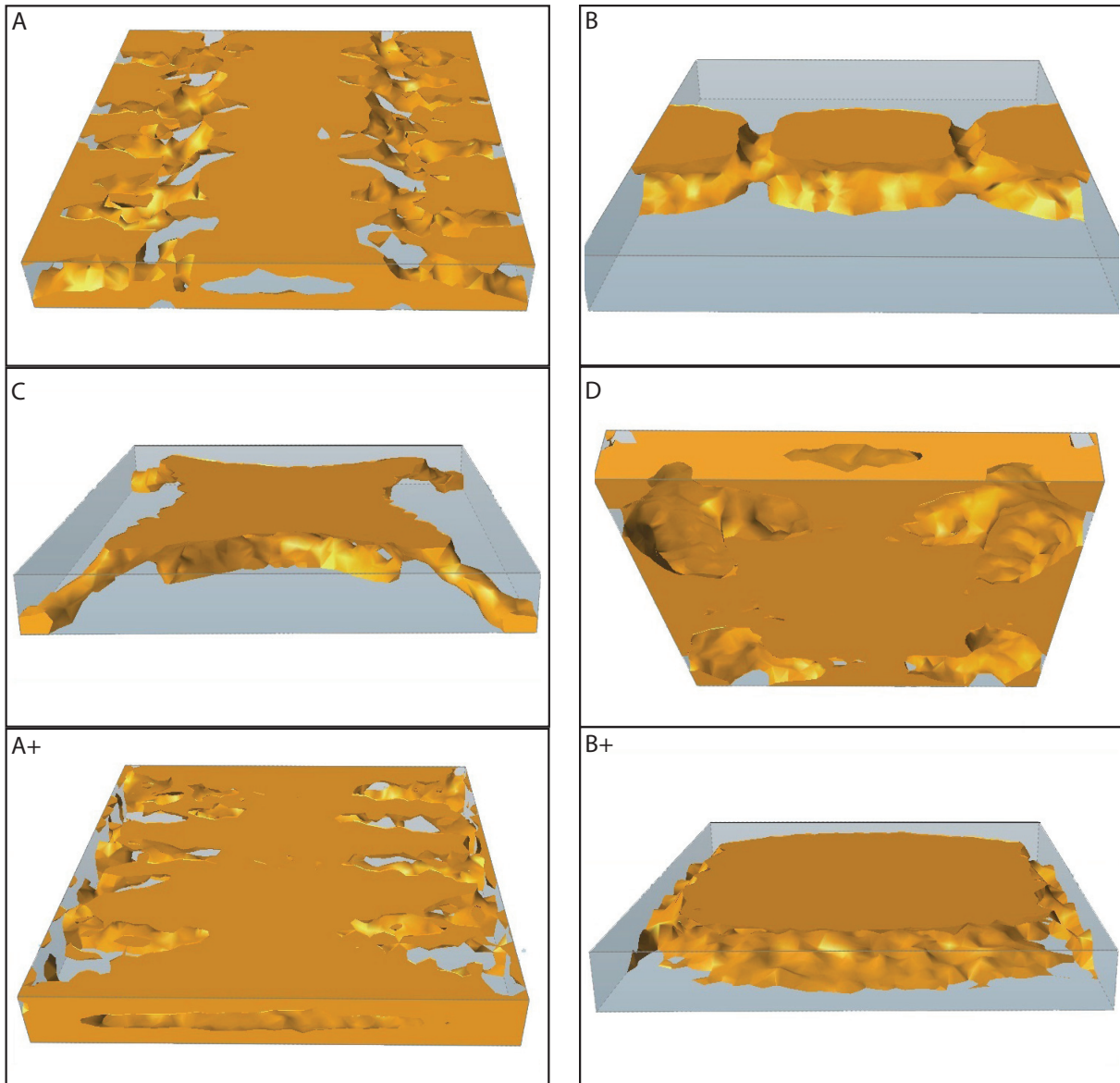


Figure 2.50: Characteristic results of topology optimization on a slab

The figure above shows the characteristic result of topology optimization on a slab. Again, the result show the widest array of outcomes, meaning that varying other constraints will have less effect on the outcome. Some conclusions that were derived during the optimization of beams, frames and beam grids are also applicable on slab structures. As in the previous section active sub-groups, material choice has very little effect on the outcome of an optimization cycle. Also, gravity only influences the outcome when a material with a high density is used. The mass target does not influence the resulting topology, but influences component attributes that mostly deal with size optimization, and to a lesser extent also shape optimization.

Result A shows a slab with fixed supports, which is constrained by a distributed load. Basically, this is the

one bay beam discussed in paragraph 2.5.2: *width to height ratio* with a very high width. The 3d nature of the optimized beam width a ratio of 1/1 is not translated to the slab shown in figure 2.50X;A. The morphology of the optimized beam is only recognizable at the two edges of the slab. In the middle, arched ribs appear. The result is therefore similar to a conventional ribbed slab. When changing the distributed load to a centre point load, the result changes significantly (Figure 2.50;B). A large part of the material is removed since it is not necessary for transporting the load to the supports. Also, less material is needed where the moment is zero, as explained in paragraph 2.5.2 and 2.5.3.

Result A+ and B+ are the same as A and B, where the fixed supports are replaced by hinged supports along the bottom edges. The resulting morphology



is again unclear, as is often the case when optimizing a component with hinged supports. Again less material is needed where the moment tends to zero, which is near the supports. The slab is hollow, resulting in a three dimensional structure over the entire cross section.

Result C and D show a 4-point supported slab, where the supports are located at the corners of the design space. Both in the case of a distributed and a point load the resulting topology is very clear. Result C can be explained using figure 2.22 in paragraph 2.3.3. Here, a beam supported by fixed hinges is optimized when constrained by a distributed load. When looking at result C of the optimized slab, the same morphology and topology is recognizable between two opposite supports. Basically, result C is the combination of two optimized beams supported by fixed hinges. The same rationalization can be made in the case of a distributed load (result D). Only now, more material is needed near the edges resulting in ribs appear the edges.

#### SLENDERNESS

The figure below shows two different height to

length ratios of the six characteristic results. When moving towards a larger span, i.e. a smaller ratio, the different result all become more and more solid. Jel-ema 3; Draagstructuur, gives rules of thumb for the thickness (height) to length ratio of in situ and prefab floors, which is generally between 1/25 and 1/35. The optimized slabs with a ratio in the range of 1/25 to 1/35 show very similar results. Basically, two different topologies can be recognized, which are the result of the type of support used. With a fixed support, holes appear near 1/4 and 3/4 of the span, where the moment tends to zero. In the case of a hinged support, the moment tends to zero near the supports, explaining the lack of material. This comparison of different ratios with different slabs shows that optimized slabs become more solid when the ratio decreases (i.e. the span increases while the height is constant). This implies that a slab with a common span<sup>1</sup> can already be considered as an optimized structure system.

Besides decreasing the height to length ratio, the height can also be increased while keeping the length constant. In that case the design space will become a cube, and the optimized element is similar to a frame structure discussed in paragraph 2.3.4 with a high

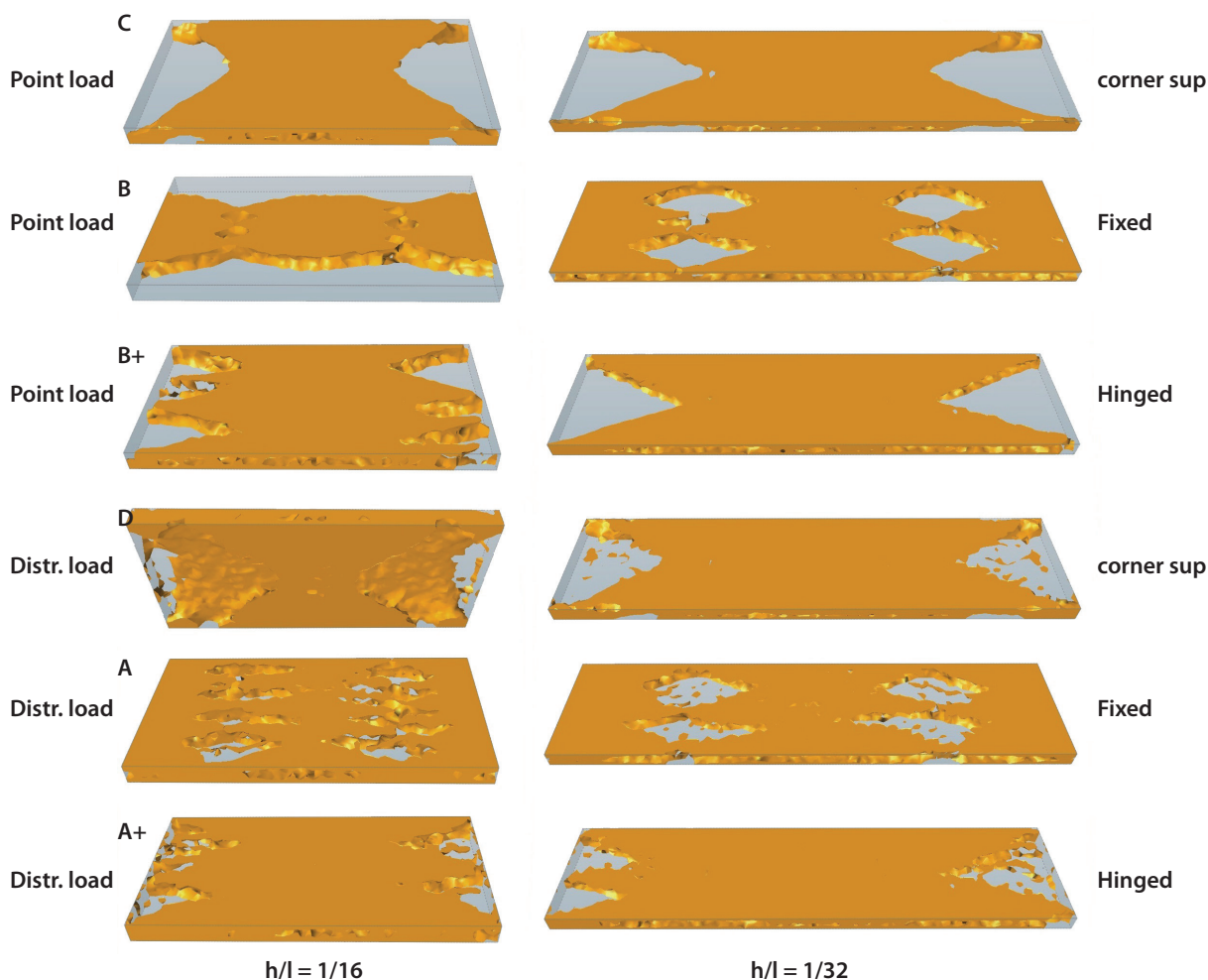


Figure 2.51: Increasing the slenderness of an optimized slab



width (Figure 2.42).

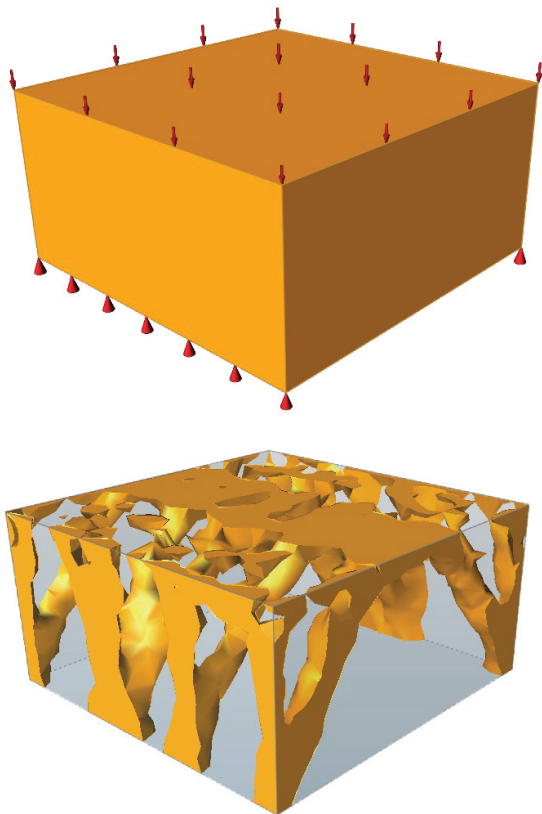


Figure 2.52: Slab structure with a high height to length ratio

#### WIDTH TO HEIGHT RATIO

The relation between the width and the height of these slab structures can be derived from observations and conclusions made during the study into the other section active structure systems. When the width of the element is very small with respect to its height<sup>2</sup>, the element is considered a beam structures and therefore behaves as such. When the width is increased the morphology and topology of the optimized element will move towards the result showed in figure 2.53. A slab which is supported at its corners is symmetrical about two axes. Increasing the width therefore produces the same result as increasing the length. In the case of a fixed support or a hinged support the morphology and topology of an element with width  $x$  simply gets copied.

#### CANTILEVERED SLABS

The final section active sub group are the cantilevered slabs and beams. Again, there is a strong relation between the two since a cantilevered slab is a cantilevered beam with a high width. Just like optimized 2-point supported beams, optimized cantilevered beams have the same morphology and topology as their commercially available counterparts (Figure 2.54). This means that truss like cantilevered beams, such as the one depicted below, can be considered as topologically optimized structures. When increasing the width towards a cantilevered slab, the same phenomenon occurs as when increasing the width of a uniform slab (Figure 2.55).

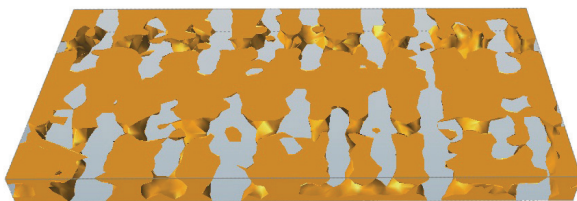


Figure 2.53: Result A with a width of 16 meters.

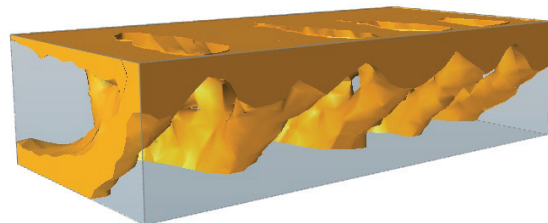


Figure 2.55: Optimized cantilevered slab

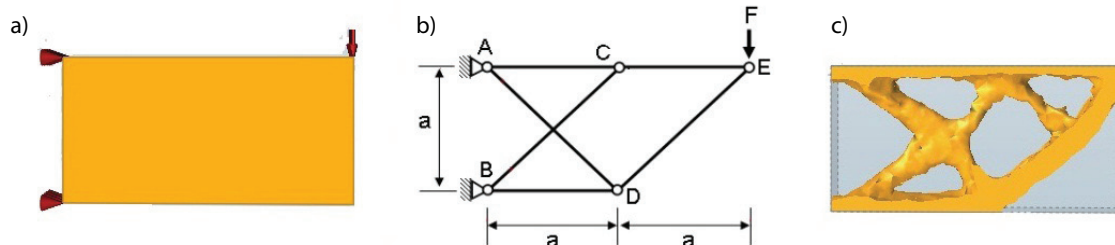


Figure 2.54: a) Design space of a typical cantilevered beam problem; b) Typical solution of a cantilevered beam problem; c) Topology optimization by Inspire

1. A common span as defined by Jellema 3; Draagstructuur.  $1/25 < H/L < 1/35$
2. As defined in paragraph 2.5.2:  $W/H < 3/2$





## CONCLUSION

The following conclusions can be derived out of the previous parameter study;

- Material (isotropic) choice has very little influence on the outcome of topology optimization, unless the gravity constraint is used in combination with high density materials.
- The value of the force used does not influence the resulting topology.
- Mass target does not determine the resulting topology, but influences component attributes that mostly deal with size and shape optimization.
- Support type has a large influence on the resulting topology. Less material is needed where the moment tends to zero.
- A uniform slab is a derivative from a one-bay beam which is constrained by the same parameters.
- When the length of a slab is increased, while maintaining a constant height, up to a height to length ratio which is common for floors, only the type of supports used still influences the resulting topology.
- A slab with a height to length ratio which is commonly used in floors can be seen as an optimized structure.
- An optimized slab with a high height to length ratio is an optimized frame structure.
- Increasing the width of an optimized slab structure does not result in new topology, the result merely gets copied.

Slab structures display a wider variety of results than beam and frame structures and therefore make it harder to find a representative case. Slabs with hinged supports are less stable and give generally more unclear results. Therefore, they will be less likely to be produced and are thus excluded from further elaboration. Since the morphology and typology of a one-bay beam is the basis for most optimized section active structures, and is clearly recognizable at the edges of a slab with fixed supports, it will serve as a representative case for slab structures.

### 2.3.8 CONCLUSION

From the separate conclusions derived from the separate analysis of the four section active structure systems defined by Engel (1997), generalizations can be made. When we compare the separate conclusions, the following morphological features appear to be generally applicable to topologically optimized section active structure systems:

- The type of supports used has the greatest

influence on the resulting topology of an optimization problem (except in the case of frame structures); little material is necessary where the moment tends to zero.

- Fixed supports lead to more stable topologies than hinged supports.
- The main difference between the type of load used are the two middle members (except in the case of slabs); far apart in the case of a distributed load and close together in the case of a point load.
- Members connect at an angle of approximately 45 degrees since forces also disperse at this angle.
- Increasing the slenderness does not result in new topology (except slab structures), the result only gets stretched.
- The mass target does not determine the resulting topology, but influences component attributes that mostly deal with size and shape optimization.
- The value of the force(s) used also does not influence the resulting topology, but influences component attributes that mostly deal with size and shape optimization.
- Material choice has very little influence on the outcome of topology optimization.
- In the case of continuous systems, or slabs with a high width, the topology of its one-bay counterpart merely gets copied.

The relation between structure and form, the structural morphology, of these optimized elements is very strong. The resulting topology of an optimization process is determined by the force distribution through the design space and the different constraints and performance requirements that act on that specific design space. The most important conclusion that can be derived out of the previous paragraphs is that the topology of the one-bay beam discussed in paragraph 2.3.3 can be recognized in almost every optimized section active structure system; the horizontal part of a frame structure, beam grid structures, and slab structures. It is the basis for every other optimized section active structure system. Therefore, many morphological features that apply for beam structures also apply for other section active structure systems. Since an optimized beam structure is the basis for other section active elements, and reflects many of the morphological features which apply to optimized section active structure systems in general, it will serve as a case for the remainder of this thesis.

For the validation of solidthinking Inspire 9.0, the one-bay beam discussed in paragraph 2.5.2 was also optimized using Topostruct. The same constraints and boundary conditions were used (Figure 2.56), ensuring the validation of the software.

Topostruct is developed by Sawako Kaijima and Panagiotis Michalatos (Michalatos & Sawako), and is an open source topology optimizer. The program was developed using the methods and ideas discussed in Martin Bendoe’s book “*Topology Optimization, Theory, Methods and Applications*”. Therefore, the main solving strategy used is the homogenization, or OMP, method discussed in paragraph 2.1 (Bendoe, 2004). The software is intended for designers and (non) engineers who want to familiarize with topology optimization and gain insight in the structural behaviour of materials. It has a very clear and accessible interface and is therefore ideal for producing quick results. Basically, one chooses between a 2d or 3d model, specifies the geometry (design space), applies support, load and

density regions and sets the target density (mass target). Post optimization, one can plot stress lines per section and animate the displacement. Also, to avoid checkerboarding and improve the final shape, tools such as filtering and subdivision can be used.

Figure 2.56 shows the results of topology optimization of the one-bay beam discussed in paragraph 2.5.2 using Topostruct. For each case, A, B, C and D, the results of Topostruct are compared to the result of Inspire 9.0. The top Figure of each case shows the set up of the model, i.e. design space, load region and support regions. The second Figure is a fog representation of the density, and the third shows the rendered iso surface of that density. The fourth Figure is the optimized case in Inspire. The morphology of the result of case A is slightly different using Topostruct. This is due to fact that hinged supports generally give more unclear results. The topology however is very similar. For cases B, C and D, the morphology as well as the topology are identical.

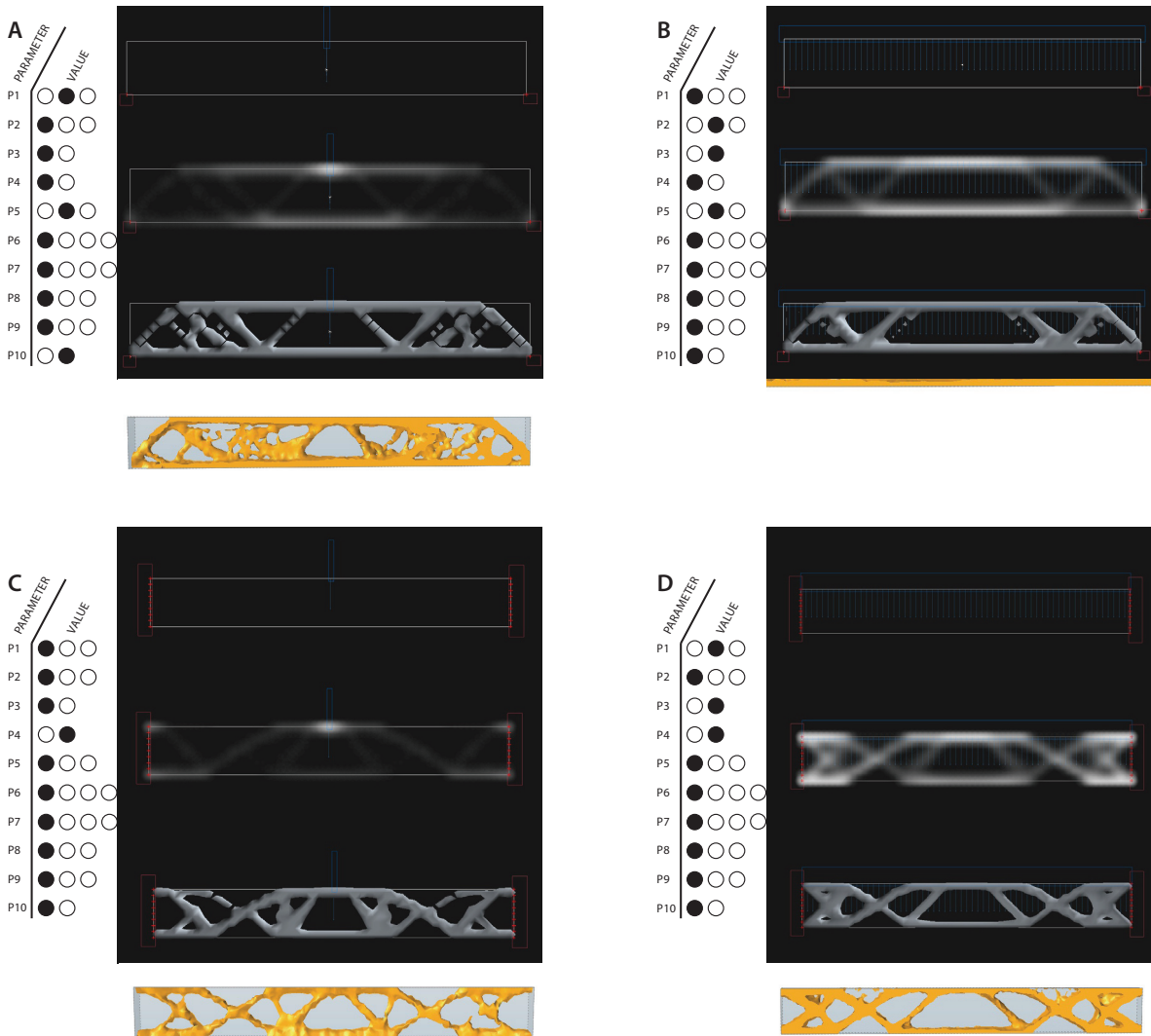


Figure 2.56: One-bay beam optimization using Topostruct

## 2.5.1 INTRODUCTION

As concluded in paragraph 2.5.6. the optimized one-bay beam structure is the basis for the section active structure systems, and reflects many of the morphological features which apply to optimized section active structures in general. The one-bay beam structure will serve as a case in further study. In addition the link between optimized structures and inflatables is of importance for the case. Even though inflatable structures are known to be very flexible, the collection of potential shapes is actually limited. Since inflatable structures have to adapt to force equilibrium, they have to conform to funicular shapes. Therefore a study in shapes that are based on funicular shapes is performed with Inspire at the end of paragraph 2.5.2. At first the square section of a one-bay beam is changed into a square section with curved vertices. Since the result with curved vertices is not satisfying, a complete round shape is optimized, resulting in an I-shape. To counteract this, a hole was used in the middle of the design space to derive a optimized shape with a hollow space inside, which makes it possible to apply an inflatable inside the beam. Two cases are derived from the optimized shape with a hollow space inside and a point load. These cases are named circular beam (figure 2.57) and tapered circular beam (figure 2.58) and are used in further research.

The circular beam is used as a case for the ParaGen method, since its morphology and topology is very similar to the square edged optimized beam. This is not the case for the tapered beam, which has a more unclear topology (figure 2.58). In the appendix an approximation of the members and point coordinates can be found of the tapered beam.



Figure 2.57: Circular beam



Figure 2.58: Tapered circular beam

## 2.5.2 THE PARAMETRIC MODEL

## BREEDING OF THE PARENTS

The ParaGen method is a cyclic process and starts with the breeding of parents. At the start of the cycle there are no parents to select, therefore the no parent breeding method is used. This implies that all of the values are randomly generated and chosen to fit within the range required for each variable used in the parametric modeller.

Since the topology is determined with Inspire, the values can be approximated. The range in which the values can vary can be determined with a certain precision based on the model. A requirement for the range of the variable values is that the values can at least cover the member size given from the Inspire model. Important for the determination of the range of values is that the hollow inside of the beam needs to be retained. Therefore, the maximum deflection towards the hollow inside of the beam is limited.

Before determining the midpoints of the parametric points the Inspire model has to be studied on the basic shapes that can be recognized. At first the baselines are sketched and at each intersection a variable value is assigned. The model consists out of four lines that are applied over the entire length of the beam; the blue lines, and six circular lines that cover the inner X shapes; the red, green and purple lines (figure 2.59). The midpoints of the variable values are estimated on the black dots, these are intersections, midpoints or endpoints of arcs.

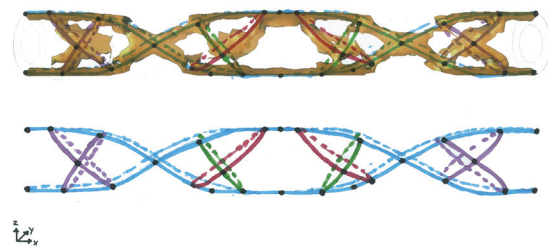


Figure 2.59: Basic structure shapes of the circular beam

To estimate the midpoints of the variable values, the Inspire model is exported to AutoCAD. With the use of guidelines the midpoints are estimated in the X, Y and Z direction. The midpoints of the values are ordered in a Microsoft Excel file, which describes the X, Y and Z values of each variable value and the domain in which they are allowed to vary. Figure 2.61 give an isometric view of the beam with the corresponding points. Only one quarter of the points of the beam have to be approximated, since it is symmetrical about two axes.

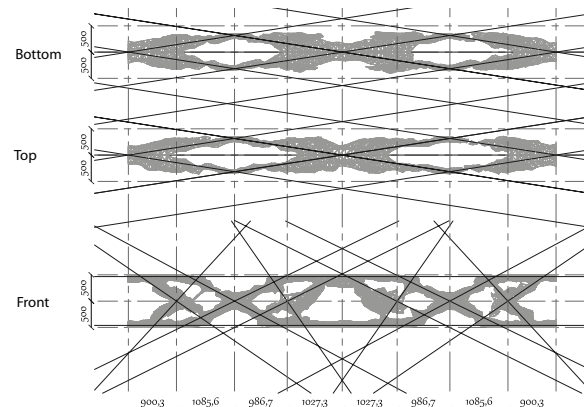
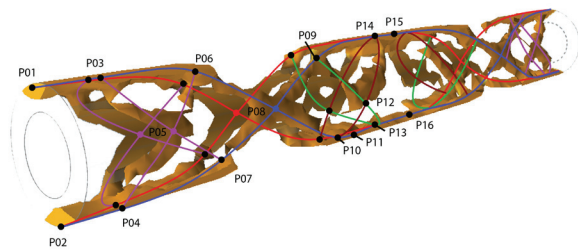


Figure 2.60: Estimation of values for the circular beam



Values	X			Y			Z		
	-	+	0	-	+	0	-	+	0
P01	0	0	500	950	0	0	500	950	0
P02	0	0	500	50	0	0	500	50	0
P03	253	460	950	0	0	0	0	0	0
P04	493	420	50	0	0	0	0	0	0
P05	900	356	500	0	0	0	0	0	0
P06	1260	300	896	0	0	0	0	0	0
P07	1352	275	185	0	0	0	0	0	0
P08	1986	184	500	0	0	0	0	0	0
P09	2721	299	865	0	0	0	0	0	0
P10	2461	286	239	0	0	0	0	0	0
P11	2811	313	50	0	0	0	0	0	0
P12	2973	339	500	0	0	0	0	0	0
P13	3278	386	50	0	0	0	0	0	0
P14	3869	480	950	0	0	0	0	0	0
P15	4000	500	950	0	0	0	0	0	0
P16	4000	500	50	0	0	0	0	0	0

Variability	X			Y			Z		
	-	+	0	-	+	0	-	+	0
0	0	0	0	500	500	50	900	1000	0
0	0	0	0	500	500	50	0	100	0
100	153	353	100	460	560	50	900	1000	0
100	393	593	100	420	520	50	0	100	0
200	700	1100	100	356	456	50	450	550	0
200	1060	1460	100	300	400	100	796	996	0
200	1152	1552	100	275	375	100	85	285	0
300	1686	2286	150	184	334	50	450	550	0
300	2421	3021	100	299	399	100	765	965	0
200	2261	2661	100	286	386	100	139	339	0
200	2611	3011	100	313	413	50	0	100	0
300	2673	3273	150	339	489	150	350	650	0
300	2978	3578	100	386	486	50	0	100	0
300	3569	4000	100	480	580	100	850	1050	0
0	4000	4000	0	500	500	50	900	1000	0
0	4000	4000	0	500	500	50	0	100	0

Figure 2.61: Midpoint values for the circular beam

### GENERATING GEOMETRY

With the point coordinates obtained from the previous study of the Inspire model a parametric model can be created with Generative Components by Bentley Systems. The parametric model is created with a script which describes the transactions to perform.

The first transaction that has to be made is the import of the data from the Excel file which contains the point coordinates and their variable domain. The X, Y and Z values are imported and the range of these values is set in the script by the transaction of GraphVariables. The range is determined by setting the lowest and highest possible value.

The next transaction is to place a point on the combination of the X, Y and Z values. These points are set to invisible for the clarity of the model. Since the model is symmetric the points are mirrored in the X and Y direction. To mirror the points, the X value is subtracted of the total length of the beam, which is 8000 mm, the Y value is subtracted of the total width of the beam, which is 1000 mm.

This transaction is followed by the adding of lines between the points, based on the lines that are determined in the previous paragraph. The outcome will be a line-model that is based on the circular beam and tapered circular beam. This line-model is ready to be exported to the simulation software. Therefore the following transactions are applied. Capture an image for the web-interface with a defined iso view to

compare the solutions, see figure 2.62. The last step in the parametric modeling software is to export a .dxf file that is used for the simulation software.

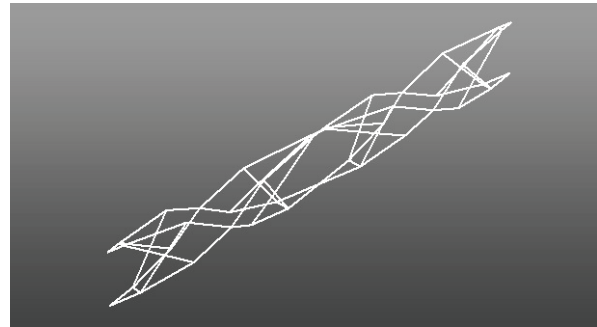


Figure 2.62: Generative Components parametric line model

### EVALUATE SOLUTIONS

The .dxf file that is exported out of Generative Components is imported into simulation software capable of performing a finite element analysis. The simulation software that is used in the ParaGen method is StaadPro from Bentley Systems. With this simulation software the structural performances can be analysed. The set-up of the StaadPro model is as follows;

- Center point load of 50 kN
- Continuous members (fixed moment connections)
- Fixed supports
- Material: steel

For now, steel was used as a material. As long as the materials are isotropic the material choice does not effects the resulting shape much, only the size of the members, as was the case in Inspire.

With these properties the randomly generated initial population is evaluated in StaadPro. Every solution is analysed and uploaded into a database with its corresponding performance values. Besides the X, Y and Z coordinates of the points the following performance values are determined<sup>1</sup>;

- Number of nodes [#]
- Number of members [#]
- Total member length [m]
- Maximum member length [m]
- Average member length [m]
- Deflection in X [cm]
- Deflection in Y [cm]
- Deflection in Z [cm]
- Direction of largest deflection [cm]
- Weight [kg]
- Modal frequency [Hz]

1. More performance values are possible such as stress levels, lighting conditions, acoustic values etc. (Buelow 2012)

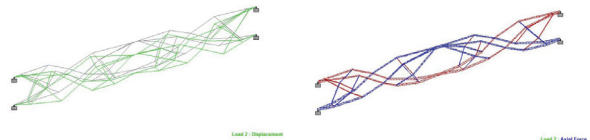
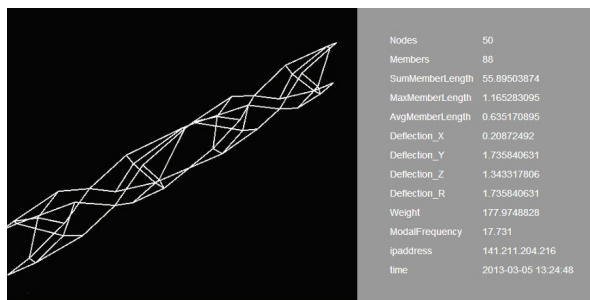


Figure 2.63: Example of StaadPro output, uploaded in the online database (id\_tag: 1, ORIB)

### RANKING SOLUTIONS AND SELECTING PARENTS

The solutions are uploaded to a web server which displays the solutions through a graphic interface. These solutions are provided with their quantitative and qualitative data. The quantitative data of the solutions are given by the simulation software. With this graphic web based interface the collected solutions can be filtered or sorted by any, or any combination, of either parametric input or performance values derived from simulation software. Here, a fitness function is used as a test to access the fitness of every solutions. Every combination of performance values can be used as the fitness function, for example;

- **Lowest weight vs. highest stiffness**
- highest modal frequency vs. lowest members
- lowest weight vs. lowest deflection
- etc.

In our case, the goal is to minimize the weight while obtaining the highest possible stiffness. With this fitness function, a final population of 2664 individual solutions was created algorithmically. These solutions were analysed to determine whether or not the results were satisfactory.

The analysis showed that a problem in the set up of the parametric model has caused the points to shift in a non uniform manner (Figure 2.64). With respect to the optimization of the production method, the points have to be bound to a hypothetical tube in the x-direction. Now, the points move non uniformly in

the x-plane, as is shown in figure 2.64. Hereby, the use of an inner inflatable as falsework will be very difficult, since its surface is locally double curved, causing the need for complicated cutting patterns.

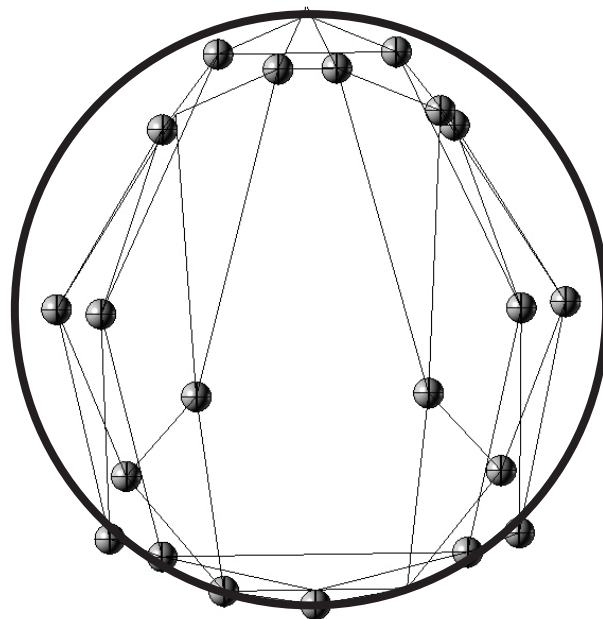


Figure 2.65: Non uniformity of points after optimization (id\_tag: 1, ORIB)

To counteract this problem, a new parametric model was made in Generative Components. Now, the points are bound to the surface of a hypothetical tube (Figure 2.65), limiting the number of free variables to 2; the elevation in the x-direction [x] and the angle [α]. This leads to better output with respect to the production method, but also reduces the necessary computational capacity due to the lower number of variables. In addition, the middle diagonal members have now been joined together since this leads to a more efficient redirection of forces. Also, crossmembers have been added in the top and bottom of the beam. The analysis of the first scale model showed that the points shown in figure 2.67 are the weakest. Local buckling can occur easily since there is not enough material to transport shear forces. Therefore, crossmembers were added, creating a stiffer geometry.

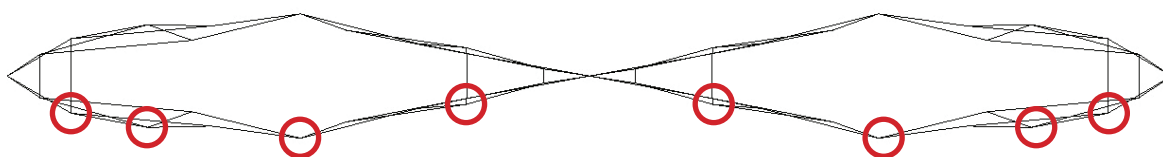


Figure 2.64: Non uniform shifting of points(id\_tag: 1, ORIB)

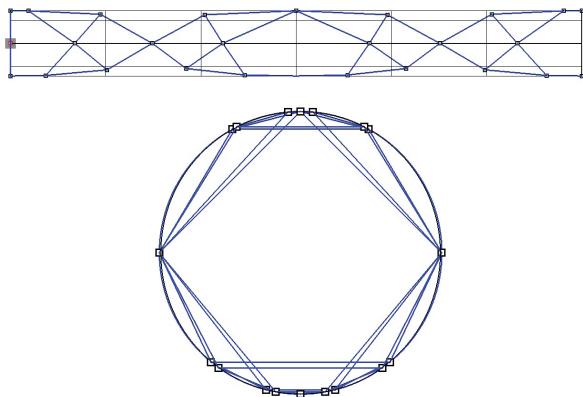


Figure 2.66: New parametric model; points on a hypothetical tube

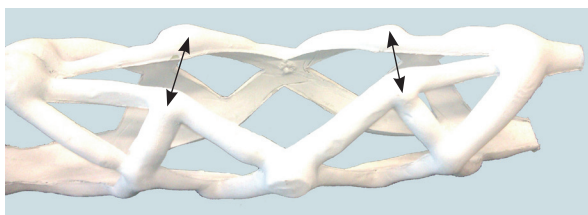


Figure 2.67: Weak point of the original geometry

### 2.5.3 RESULTS

With this new model an initial random population was created. This time the results were satisfactory, showing no unwanted deviations. Therefore, ParaGen ran until convergence was reached while optimizing for two different fitness functions; minimal weight and highest stiffness. Ultimately, a population of 1276 different solutions was created and stored in the SQL database.

In paragraph 2.5.2 the different performance data that is determined by ParaGen was explained. Four of these are of special interest, and therefore the best performing solutions of these performance objectives are showed<sup>1</sup>.

1. Lowest total member length
2. Lowest deflection in Y-direction
3. Lowest weight
4. Highest modal frequency (stiffness)

In the different solutions the initial parametric model is also shown, together with the domain in which the points were allowed to vary. The points in the upper flange and in the middle have not moved significantly in the y-direction. In fact, the two solutions optimized with a fitness function with a structural nature (2 & 4) have not moved at all. The middle points of the two solutions optimized for material reduction (1 & 3) have shifted a small distance in the positive

and negative y-direction. The solution with the lowest total member length differs the most from the initial geometry. This is mainly due to the fact that this initial geometry is generated using Inspire, which does not account for lowest total member length. Inspire optimized for maximizing the structural performance while minimizing the weight, which is similar to solutions 2, 3 and 4.

Solutions 2 and 4 seem to be stretched towards the center of the beam. All of the points have moved towards the middle. This means that the position where the moment tends to zero is more towards the middle of the beam than the Inspire model indicated.

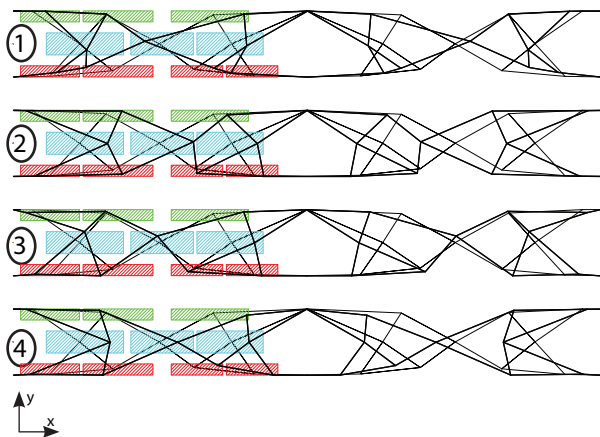


Figure 2.68: Best performing solutions for different fitness functions.

As explained earlier, we are searching for a solution with the least weight, while having the highest stiffness. Naturally, the weight of an structure is very dependent on the material that is used. For this optimization cycle, ParaGen used steel as a material, which has very different properties than the materials that we are hoping to use. However, also based on conclusions drawn from the previous analysis using Inspire, the material choice does not effect the topology or shape of the geometry, but mostly the size of the elements. Therefore, the correct material properties will be used when performing the size optimization using GSA.

The entire population which has been generated by ParaGen is stored using an online database. This database can be accessed at any time and used to search and evaluate the different data. First, the solutions with the lowest weight and those with the highest stiffness were analysed separately. Subsequently, to find the best performing solutions, a scatter diagram (Figure 2.71) was used, plotting the weight on the x-axis and the stiffness on the y-axis. The modal frequency is used as a measure for stiffness; the higher the frequency the higher the stiffness. The values of

1. Full data sheet of these solutions can be found in the appendices



the frequency are flipped, so that the best performing solutions can be found near the origin.

ParaGen initially optimized for weight minimization as the primary fitness function. Later, the set up was switched to optimize for stiffness maximization. It has to be noted that light structures typically have a higher stiffness and heavy structures typically have a low stiffness. This means that when optimizing for either of the two fitness functions, the other is also being optimized secondarily. Table 2.1 shows the top 20 lightest solutions starting with the lightest one; idtag 981 with a weight of 126.8 kg. The mean weight of this top 20 is 130.33 kg with an mean modal frequency of 23.76 Hz. Table 2.1 shows the top 20 solutions with the highest stiffness, starting with idtag 1259 with a frequency of 33.7 Hz. Here, the mean weight is 143.14 kg with a mean frequency of 31.15 Hz. These numbers underline the fact that ParaGen initially ran for weight minimization, and later switched to stiffness maximization. The solutions with the least weight are relatively less stiff than the stiffest solutions are heavy. The lightest solutions are on average 23.7 % less stiff than the stiffest solutions, while the stiffest solutions are on average only 10% heavier than the lightest solutions. However, as we explained earlier, we are looking for solutions which perform good at both fitness functions. Therefore, a scatter diagram was used to evaluate the top three performing solutions (Figure 2.71).

	idtag	Weight	Modal Frequency
1	981	126,8	20,5
2	936	126,8	21,2
3	953	128,1	24,3
4	836	128,1	24
5	1091	128,5	25,7
6	986	130,2	28,7
7	843	130,6	24,5
8	1046	130,8	25,7
9	903	130,9	18,9
10	922	131	23,8
11	951	131	23,8
12	1215	131	27,1
13	1095	131,1	25,9
14	707	131,2	19,1
15	811	131,7	21,2
16	1145	131,7	23,6
17	714	131,7	21,5
18	1065	131,8	25,4
19	817	131,8	25,1
20	989	131,8	25,1

mean	<b>130,33</b>	<b>23,76</b>
------	---------------	--------------

	idtag	Weight	Modal Frequency
1	1259	146,6	33,7
2	1207	133,3	32,9
3	1132	139,6	32,8
4	1233	152,8	32,5
5	1269	132,8	32,5
6	1226	143,8	32,1
7	1066	139,5	31,6
8	1254	144,9	31,6
9	1276	144,3	31,3
10	1127	146,5	31,1
11	1264	146,2	30,5
12	1194	141,7	30,5
13	1251	144,6	30,4
14	1248	138,9	30,3
15	1273	137,2	30,3
16	1249	143,2	30,3
17	1257	155,1	29,9
18	1212	148,2	29,7
19	1177	136,1	29,5
20	1203	147,5	29,5

mean	<b>143,14</b>	<b>31,15</b>
------	---------------	--------------

Table 2.1: Top 20 performing solutions for; TOP: lowest weight, BOTTOM; highest stiffness.

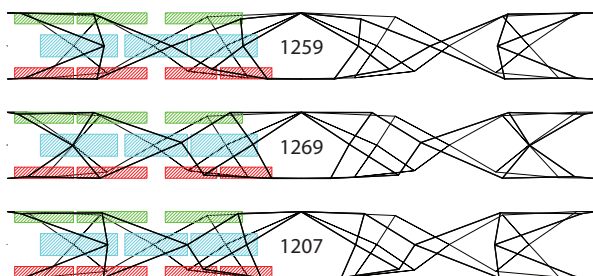


Figure 2.69: Three best performing solutions

The three best performing candidates are shown in figure 2.69. Naturally, they have a very similar morphology, with the largest variations occurring in the cross in the first and fourth segment. Since the structural performance of these three solutions do not differ much, the best candidate will be chosen based on aesthetics and compatibility with the proposed production method.

idtag	weight [kg]	frequency [Hz]
1207	133.3	32.9
1259	146.6	33.7
1269	132.8	32.5

Figure 2.70: Weight and modal frequency of top three performing solutions

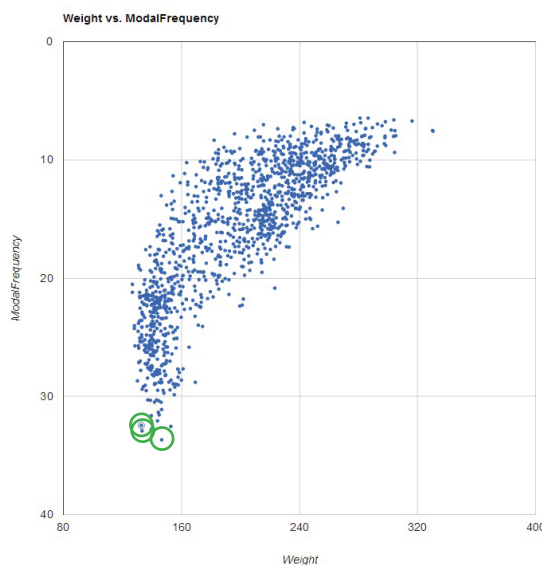


Figure 2.71: Scatter diagram for weight vs. stiffness.



Solution 1259 is significantly heavier than the other two solutions, making it less favourable. Also, P09 and P10 (Appendix A) have shifted more inwards than the other two. These points are connected with a linear member in the y direction to their mirrored counterpart. In this model, all members are linear which is the most efficient route for transporting forces. However, in the real model these members are curved. Therefore, the further these points have shifted inwards, the more the result differs from the actual curved model. Based on these two observations id. 1259 can be considered less ideal than the other two solutions.

The weight and frequency of id 1269 and id 1207 are almost identical. Therefore, the choice between these two is based on their morphology. The main difference in the position of the points can be found in the first and fourth segments. In the case of result 1269, P05 has not shifted much. Hereby, the members form a cross which runs continuously around the circumference of the model. With id 1207 this is not the case since P05 has shifted along the x-axis. From a manufacturing point of view this is less favourable since the joints between members become more complex. Therefore, id 1269 will serve as a case for the remainder of this research.



The main goal of this phase was to produce a case;

**RQ1:**

*Which structurally optimized section active structure system can best be used as a case?*

The first step of the form finding process included the topological optimization of section active structure systems. The optimization of these structure systems was assumed to lead to the largest reduction in material, since form-, vector- and surface active systems can already be considered as lightweight structures. Empirical case studies are performed on the four section active structure systems;

- beam structures
- frame structures
- beam grid systems
- slab structures

The goal of these case studies was to reveal the morphological features of the four separate section active structure systems and the morphological features of topologically optimized section active structure systems in general. The empirical case studies were performed using solidThinking Inspire 9.0. The density method is the main solving strategy used in Inspire, which uses Altair OptiStruct and HyperMesh in the background. During optimization, the material density is the only design variable and is allowed to vary continuously between 0 and 1. The relation between the stiffness and the density of the material is assumed to be linear. Fictitious values of intermediate density are penalized using the power law representation of elastic properties to make the result behave more like an ISE topology. For validation purposes, topological optimization on the section active structures was also performed using Topostruct, which uses the homogenization method as a solver. Case studies were carried out using a morphological overview describing all the different constraints that can be applied on a given design space in Inspire 9.0, and the possible or characteristic values they can assume. Varying one parameter at a time, an empirical case study was performed revealing the influence of the individual constraints on the outcome of a topological optimization.

The type of supports used, i.e. the degrees of freedom and location, have the most influence on the resulting morphology of topologically optimized section active structure systems. Less material is needed where the moment tends to zero, reducing the area of the cross section locally. In the case of frame structures the type of support has less influence, especially when the height to length ratio is equal to or larger than 1/10. With these larger spans, an optimal design space would allow the structure to form an arch at the

inner side. With larger spans, larger moments occur which need to be transported via the corners of the frame towards the supports, leading to larger cross sections near the corners. In this context, the type of support has little influence on the moment distribution in the horizontal part of the frame. It has to be noted that fixed support generally lead to more clear and stable topologies than rolled and pinned supports. Point loads lead to denser member distributions than distributed loads, except in the case of slab structures. With respect to beam and frame structures, forces caused by a point load will be transferred by two diagonal members towards the bottom flange. These members, as well as most other members in optimized structures, connect at an angle of about 45 degrees since forces also disperse at this angle. When incrementally increasing the number of point loads, the resulting morphology will move towards the morphology of an optimized structure constrained by a distributed load, meaning that the middle diagonal members move further apart.

The slenderness and height to width ratios were also studied to gain insight in the behaviour of the optimization routine when the proportions of the design space change. The separate structure systems that were studied are mathematically speaking closely related. When increasing the width of a beam structure while maintaining a constant height, the geometry will move towards a slab structure. When increasing the height of a slab structure while keeping the width constant the result will be similar to an optimized frame structure. For the intermediate height to width ratios in between the three structure systems no general morphological features were found. Increasing the slenderness, i.e. height to length ratio, of beam and frame structures does not result in new topology. The result of its one-bay counterpart merely gets stretched. However, there are certain limits where further increase of the slenderness will lead to unclear topologies. These limits are mainly determined by the type of supports and type of load that is used. In addition, making a beam or frame structure continuous also does not result in new topology. Here, the result of its one bay counterpart gets copied. The same generalization can be made regarding slabs with high widths. Mass targets, material choice and the value of the load(s) used have little influence on the resulting topology of an optimized structure, but influence component attributes that mostly deal with size and shape optimization.

The relation between structure and form, i.e. the structural morphology, of these optimized elements is very strong. The resulting topology and morphology of an optimization routine is determined by the force distribution through the design space and the



different constraints and performance requirements that act on that specific design space. The morphology of an optimized one-bay beam can be recognized in every optimized section active structure system. Many morphological features that apply for an optimized beam structure therefore also apply for frame structures, beam grid systems and slab structures. Therefore, shape and size optimization will be performed on the optimized circular beam (Figure 2.72), which in turn will serve as the case for the proposed production method.



Figure 2.72: Optimized circular beam structure

The optimized three dimensional beam was used as a basis for the development of the parametric model, which in turn forms the basis for the ParaGen method. The model consisted of 46 nodes, of which 42 were parametric. The nodes were bound to the surface of a hypothetical tube, limiting the number of free variables to 2; the elevation in the x-direction ( $x$ ) and the angle ( $\alpha$ ). Compared with a model using 3 free variables, this lead to better output with respect to the proposed production method, and also reduced the necessary computational capacity. In addition, due to computational limitations the model was schematized using linear instead of curved members. The FEA model used a center point load of 50 kN, fixed supports, continuous members with fixed moment connections and the material properties of ASTM A-36 steel. Pipe profiles were used with selected diameter and wall thicknesses resulting from the structural analysis. With this set up a total population of 1276 individual solutions were created algorithmically and stored in the SQL database. ParaGen optimized for two different fitness functions, i.e. minimal weight and highest modal frequency (stiffness). With the plot function a scatter diagram was created to find the most promising solutions which performed well for both objectives.

The three most promising solutions were analysed according to their morphology and the proposed production method. Solution 1269 was assessed to be the best solution, since it deviated the least from its curved counterpart.

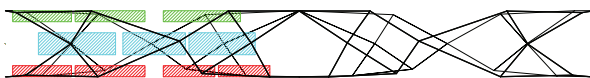


Figure 2.73: Definitive structurally optimized case



# 3

## Inflatable structures

The main goal in this chapter is to determine in which way an inflatable structure can be used as falsework with respect to the proposed production method. Therefore, the main research question in this chapter is;

**RQ 2:**

*In which way can an inflatable structure be used as falsework for the production of structurally optimized section active elements?*

The first step towards the answer of this question is to determine the fundamentals of pneumatic structures. Subsequently, the different typologies of inflatable structure that exist are revealed and compared to the optimized section active structure systems. In addition, the materials which are used for inflatable structures are mapped and analysed to determine which one is best suited for our case. This is done by answering the following sub questions;

*SRQ 2.1:*

*Which requirements, conditions and properties do inflatable structures have to conform to?*

*SRQ 2.2:*

*Which typologies of inflatable structures exist?*

*SRQ 2.3:*

*Which materials are used for inflatable structures?*

The fundamentals of inflatable structures are revealed by performing an in depth literature review into the requirement, conditions and properties of inflatable structures. This leads to the criteria which are used in the literature for the classification of the different inflatable typologies. These typologies are then assessed according to several morphological indicators found in the literature. The same morphological indicators are used to assess the optimized section active structure systems. Hereby, a balanced consideration can be made to determine which inflatable typology is best suited as falsework in the production method for our case. Together with the results of the in depth literature review into membrane materials, it forms an profound answer to research question two.

As explained in paragraph 1.4, the term inflatable structures is used instead of pneumatic structures. The term pneumatic structures is too broad for our research, since it also includes entities such as plants and human cells. Therefore, this research limits itself to technical pneumatic structures, i.e. inflatable structures. The criteria that are used for the decision making process in this chapter are derived using results from the literature reviews. Since the comparison that is made in this chapter has never been done before, the criteria could not be taken directly from the lit-

erature. Therefore, the criteria were determined by the authors themselves, based on the results of the literature review.

## 3.2.1 INTRODUCTION

Pneumatic structures are among the most common and efficient structural systems in living and inanimate nature. It consists of a ductile envelope which is capable of supporting tensile stress and is internally pressurized with respect to its surrounding medium. Examples of pneumatic structures in living nature include bacteria, worms, certain herbaceous plants and even animal, thus also human, organs. In inanimate nature, examples are water and mist droplets and water and soap bubbles. In a technical context, mankind have been using pneumatic structures for over 3000 years. The filling of animal skins with meat to produce sausages, or with air to form a ball are all examples of technical pneumatics. Nowadays, well known examples include car tires, balloons and airhouses (Figure 3.1) (Otto 1995; Herzog 1976).



Figure 3.1: 1) Inflatable in living nature, the ringworm; 2) Inflatable in inanimate nature, the soap bubble; 3) Technical inflatable, the bubbletree (Adopted from <http://www.bubbletree.fr/bbtree/racine/default.asp>)

Since the term pneumatic structures also include the structural system of for example a water filled balloon, scientist often do not agree about the correct terminology. Nonetheless, the notion has become generally accepted. In the context of this research, only technical pneumatics are discussed in relation to structural optimization, and are therefore referred to as *inflatable structures*.

Inflatable structures are often referred to as natural of biological structures, since they possess many attributes often found in nature. For example, inflatables are soft, funicular and light, where attributes often found in technology are hard, square edged and heavy (Figure 3.2). Technical pneumatics possess the same biological features as natural pneumatics. The potential of these pneumatics as a mould for structurally optimized section active structure systems is emphasized by its strong relationship with common attributes found in nature, since these optimized elements also have a strong relationship with natural forms as well (paragraph 2.3.1).

Nature	soft	round	light	flexible	multi-functional	structure optimized	transient
Technology	hard	square-edged	heavy	rigid	mono-functional	material optimized	durable

Figure 3.2: Nature versus technology: Pneumatic structures have many attributes of nature (Adopted from Luchsinger et al. 2005)

## 3.2.2 HISTORICAL DEVELOPMENT

The development of inflatable structures have had some ups and downs since its inception in the 18<sup>th</sup> century. According to the literature, the first technical application of a pneumatic structure, i.e. the first inflatable structure, is the hot air balloon developed by the Montgolfier brothers in 1783 (Otto 1995; Herzog 1976; Chi & Pauletti; Topham 2002). This achievement marked the start of a period where many people attempted these manned balloon flights. The balloons were made of paper, canvas or silk and were filled with hot air and later gas for buoyancy. Later in the 19<sup>th</sup> century engineers started to equip their balloons with propellers to enable controlled flight. This advancement led to a new benchmark in the development of inflatable structures; the first airworthy dirigible by Alberto-Santos Dumont in 1898. During the same period, John Boyd Dunlop also patented a very important invention; the pneumatic tire. This was actually already invented in 1845 by Robert William Thomson who also patented his idea. However, his patent expired without notice. When Dunlop reinvented the inflatable tire in 1888, the timing was just right due to developments in the rubber industry and the emergence of transport and trade.

In 1918 Frederick William Lanchester had his idea to transfer the dirigible technology to architecture

patented. His idea was to create inflatable structures on the ground for campaign hospitals. The patent was approved but due to a lack of funds and appropriate membrane materials it was never constructed. This last problem was solved in 1935 with the invention of nylon by Dupont. This led to the adoption of inflatable shelters and decoys during the second world war. When the war ended, America needed an extensive network of radars across the country to accommodate the increase of military air operations. To protect these radars against weather influences they had to be covered by a structure which did not interfere with the radar signals. This led to the development of the first ground-anchored inflatable structures by Walter Bird in 1948. Engineers now saw the potential of inflatable structures which meant the start of academic research into the subject during the sixties and seventies. Especially Richard Buckminster Fuller and Frei Otto have made significant contributions in the field of inflatable structures. These years were the heyday of inflatable structures. All over the world people were experimenting with this "new" construction technology. Groups such as Ant Farm (Figure 3.4) and Utopie (Figure 3.5) experimented on a "trial and error" basis as well as designing utopian concepts of inflatable structures. The popularity of inflatables in those days was underlined by the world expo 1970 in Osaka, Japan. A large number of the pavilions build for this expo included some form of inflatable, also due to the high seismic activity in the region. One of the most prominent examples is the Fuji pavilion, which was the largest inflatable structure build thus far.

Inspired by the success of the expo in Osaka, engineers started to construct large span roofs for stadiums in the United States and Canada in the seventies, eighties and nineties. However, due to high maintenance and sometimes even deflation of the structures they were used less and less. With the emergence of computer aided design, inflatables are making a come back. However, stand alone applications are often avoided. Inflatables nowadays are often used in combination with a primary stiff structure (Nicholas Grimshaw, Eden project), using only the advantages of this structure system (Otto 1995; Herzog 1976; Topham 2002; Engel 1997; Chi & Pauletti).



Figure 3.3: Richard Buckminster Fuller - NYC Dome. Example of 1970's utopian inflatable structure

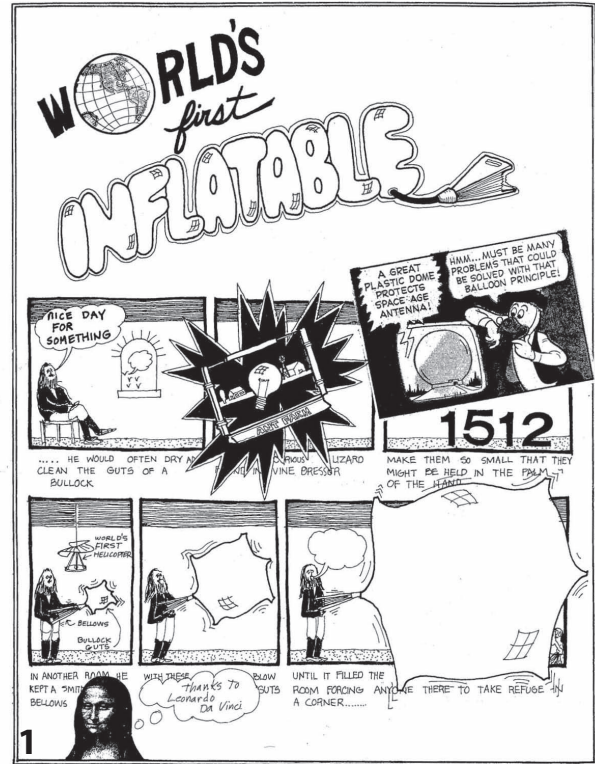


Figure 3.4: 1) Page two of the Inflatocookbook by Ant Farm; 2) Ant Farm - 50x50 Foot Pillow, used as a medical pavilion at the Rolling Stones free concert at Altamont in 1969

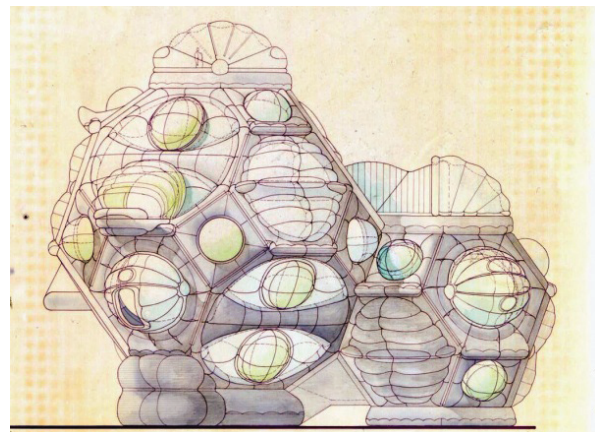


Figure 3.5: Utopie - Habitation Pneumatique Experimentale. Utopian design by Jean Paul Jungmann, Jean Aubert & Antione Stinco

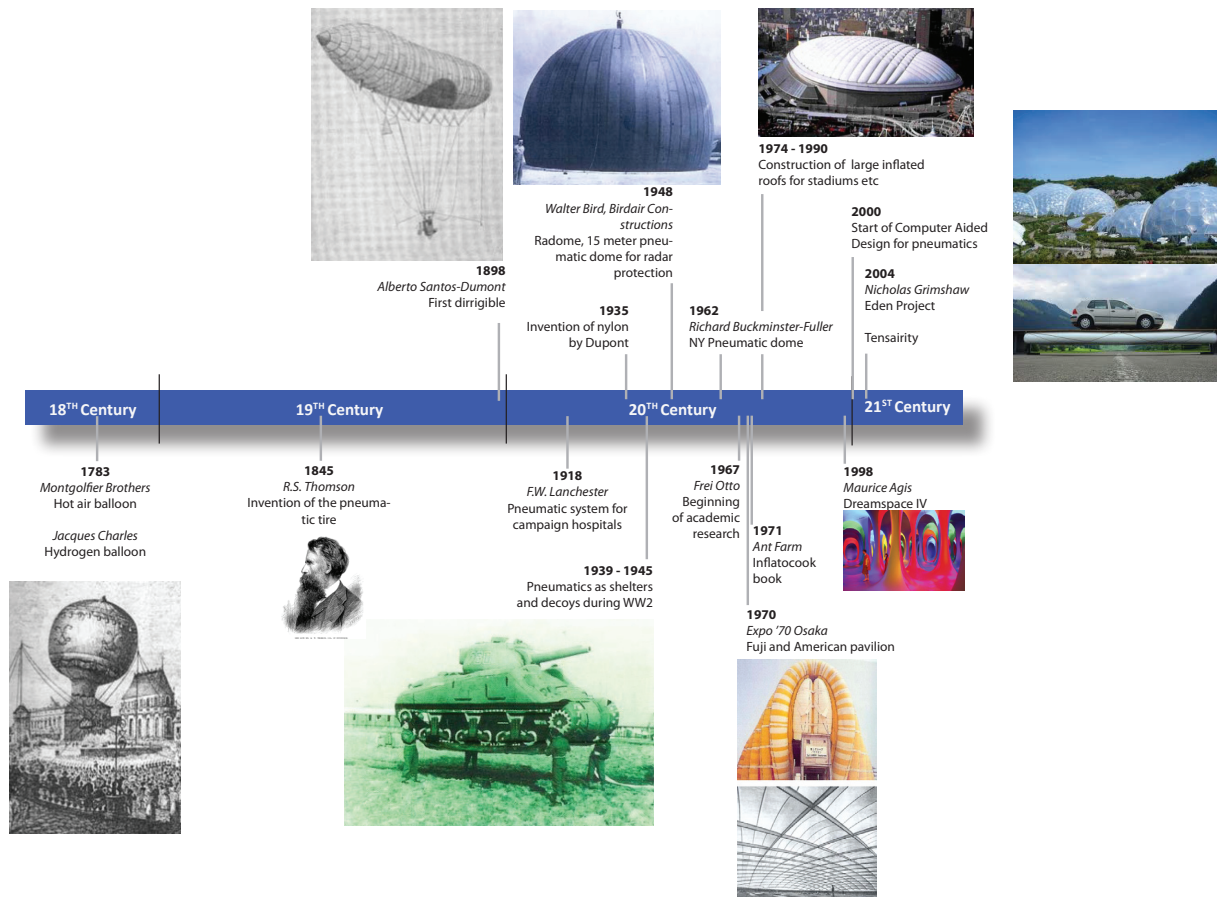


Figure 3.6: Timeline describing the most significant developments in the history of inflatable structures

### 3.2.3 THE PNEU AS A LOAD BEARING MECHANISM

A pneumatic structure is initially a flexible membrane material, only capable of absorbing tension, which is stressed by a pressure difference. Any pneumatic structure consists entirely or partially out of the following principal elements (Otto 1995);

- Envelope
- Content
- Medium
- Internal bracing
- Pressure difference

The envelope of a pneu in the context of this research refers to the type of membrane used, which is explained in paragraph 3.4. The content of a pneumatic structure refers to the material used to achieve the pressure difference needed for stabilization of the pneu, this could be air but also the rigidizable materials elaborated in chapter four. Since this study limits itself to the exploration of technical pneumas for structurally optimized section active structures, these will now be referred to as *inflatable structures*.

Every inflatable structure is capable of resisting external forces, often wind pressure or suction and snow

loads. However, the most important loading is the internal pressure. Here, according to Herzog (1976);

*“The stressing medium (content) becomes the supporting medium and therefore a structural element. The resulting structure becomes a pneumatic load bearing structure.”*

Initially, there are two types of inflatable structures. Determined by the number of membrane layers between the occupied space and the exterior, an inflatable is either a single or a double load bearing membrane structure. In addition, inflatable structures can be classified as open or closed (Figure 3.7). Almost all inflatable structures known to man are termed closed structures. Examples of open structures are sails, parachuted and kites (Otto 1995; Herzog 1976; Holslag 1972). However, the literature disagrees whether or

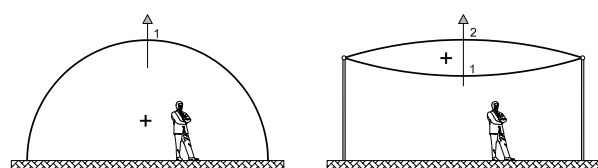


Figure 3.7: Left; closed single membrane structure with an open membrane. Right; closed double membrane structure with an closed membrane





not the latter can be defined as an inflatable at all. A final general classification can be made according to the type of membrane used; open or closed (Figure 3.7).

Based upon the previously described elements and types of inflatable structures the number of combinations that can be made is almost indefinite. However, all pneumatic structures, in living and inanimate nature and technical pneus, have to conform to funicular shapes. This means that they always conform to the following equation (Herzog 1976);

$$p = \sigma (1/r_1 + 1/r_2) \quad (1)$$

where:

P = Pressure

$\sigma$  = Surface tension

$r_1$  = The largest radius of curvature of the surface

$r_2$  = The smallest radius of curvature of the surface

From (1) several properties inherent to pneumatic structures can be derived. The equation shows that pneus with a smaller radius have a higher internal pressure, and therefore a lower surface tension. This can be proven easily by an experiment where two soap bubbles of unequal size are connected by a tube. Here, the smaller bubble inflates the larger bubble meaning that it must have a higher inner pressure (Wolf 1968). If the two radii  $r_1$  and  $r_2$  are equal the resulting pneu will be synclastic. If one of the two radii is at least twice as large as the other, we speak of a monoclastic shape. If the shape is double curved, but in opposite directions, we speak of an anticlastic shape (Figure 3.8) (Holslag 1972; Herzog 1976).

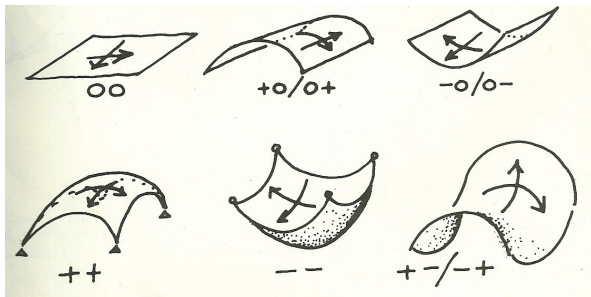


Figure 3.8: Zero-, syn-, anticlastic surfaces (Holslag 1972)

Since decreasing the radius of curvature will reduce surface tension and thus the required tensile stress of the membrane, cables are often spanned across inflatable structures. This will divide the surface into sections with a lower radius of curvature. The cables will transfer the major forces towards the foundation, where the membrane itself acts as an secondary structure (Figure 3.9) (Engel 1997).

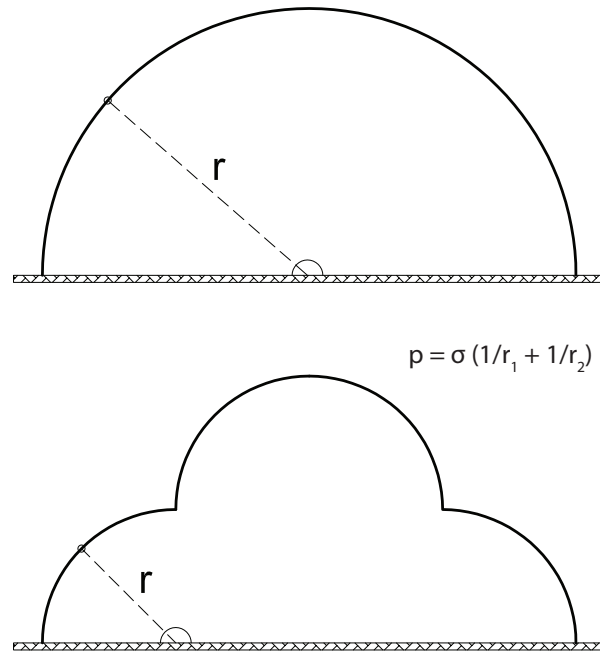


Figure 3.9: Effect of a cable net on the radius of curvature

### 3.2.4 ANALOGY WITH SOAP BUBBLES

Inflatable structures are usually constructed of cutting patterns, since it is not yet possible to construct them out of an elastic material. These patterns are flat membranes which can be fixed together by several different techniques. Nowadays, they are usually generated by the press of a button with the aid of computer programs such as Rhino Membrane, GSA, Formfinder and Forten4000. Before those programs existed, engineers used models based on soap bubbles to approach the correct shape. In fact, equation (1) is based on soap bubbles.

Engineers looked at soap bubbles because they are an "ideal" pneumatic structure. Since the envelope of a soap bubble is a soap film, it is not capable of absorbing any point loads. Therefore, the soap molecules will flow until a steady state occurs where the surface tension is equal in all directions. In this state the average curvature will be zero and the potential energy will be as less as possible. The largest possible volume has been enclosed using the least amount of surface; *minimal surface* (Holslag 1972; Herzog 1976).

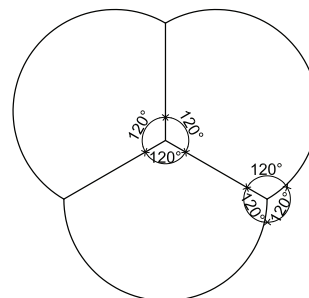


Figure 3.10: Soap bubbles always meet at an angle of 120 degrees

Engineers also studied agglomerations of soap bubbles to determine the most efficient position of external cables or internal membranes. Studies have shown that soap bubbles always join at an angle of 120 degrees, where a maximum of three individual bubbles can meet in one point in two dimensions (Figure 3.10), or four in three dimensions. The main advantage of using the minimal shape of a soap bubble as a model for an inflatable structure is the equal and minimal surface tension in every point. This will reduce creasing at the edges of the inflatable. This theory is not always useful, since in reality many more forces will act on an inflatable opposed to just internal pressure (Holslag 1972).

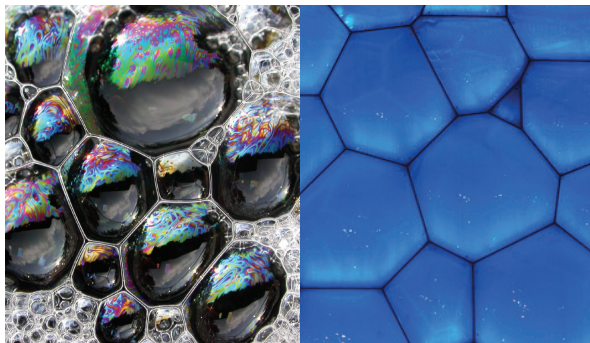


Figure 3.11: LEFT; Agglomeration of soap bubbles. RIGHT; facade of the Beijing National Aquatics Center.

3.3.1 INTRODUCTION

Many different classifications of inflatable structures can be found in the literature, using different sets of criteria. In this paragraph, an overview of the different criteria is given, leading to a comprehensive classification of inflatable typologies. This final classification combines multiple sources found in the literature to come to an overview. The five typologies found will ultimately be compared to the optimized section active structure systems to determine the best suitable combinations.

3.3.2 PARAMETERS

Inflatable structures can be categorized according to several different parameters. Holslag (1972) discusses 18 parameters which define an inflatable structures, divided among three main parameters; energysystems, membranes and anchors. Between the different combinations that can be made using these parameters, over 23 million variations are possible. However, millions are not plausible since several parameters are mutually exclusive. Herzog (1976) describes a more complete methodology for the classification of inflatable structures. The features of inflatables are arranged into four groups according to the type and nature of the features;

- structural system
- structural type
- structural form
- structural kind

The structural system defines a static system where neither the dimensions and proportions, nor the materials are known. The structural type describes the possible secondary elements that might be used. When the proportions of the structure are known, we speak of a structural form. Here, the structure is “formalized” but not materialized. When the structure is not yet fully defined, the term structural kind is used. When all the features and characteristics of the inflatable are known, we speak of a load bearing structure (Herzog 1976). Using this methodology, 1 492 992 different alternatives can be derived. Again, certain parameters are mutually exclusive, resulting in 250 560 plausible alternatives.

Certain key characteristics can be recognized in the methodology described above, which result in *inflatable structure typologies*. The structural system, consists of the following parameters;

- Formation of membranes
- Kind of pressure
- Kind of additional support

Herzog uses these three parameters to describe the different inflatable typologies. However, most other authors only use the first two parameters.

number	feature	group	characteristics	variety
1	formation of membranes	structural system	a) single      b) double	2
2	kind of pressure		a) positive      b) negative	4
3	kind of additional support		a) no      b) point      c) linear	12
4	formation of additional stabilizing elements	structural type	3 b: a) rosette b) ring c) bulged surface 3 c: d) cable e) truss f) arch	28
5	arrangement of additional stabilizing elements		3 b: a) single b) in row c) crossed d) radial e) irregular 3 c: f) single g) one way h) radial i) tangential k) two-way l) three- (and more) way m) irregular	148
6	formation of tertiary support	structural form	3 b, c: a) no b) tension c) compression d) bending	580
7	dimension of main directions of expansion	structural kind	a) one b) two c) three	1 740
8	kind of curvature		a) single b) synclastic c) anticlastic	5 220
9	kind of membrane material	structural kind	a) elastic b) thermoplastic c) non-elastic/ adjustable d) non-elastic/rigid	20 880
10	degree of span		a) up to 20 m b) 20 - 100 m c) more than 100 m	62 640
11	kind of addition		a) no b) one direction c) two directions d) three and more directions	250 560

Figure 3.12: Classification of inflatable structures according to 11 parameters (Herzog 1976)

### 3.3.3 TYPOLOGIES

In the literature, several different classifications of inflatable structures can be found. Even though they seem to differ at first, they are all very similar. The number of possible inflatables is almost indefinite based on the possible combinations of features. However, a general classification can be made based upon certain key characteristics which determine the inflatable typology (Figure 3.12).

A first differentiation is made between the level of the pressure difference between the inflatable and the atmospheric pressure. We distinguish low pressure systems from high pressure systems. Low pressure systems typically have a pressure difference of 0 to 0.01 bar (or 0 to 100 mmWK). High pressure systems have a pressure difference of 0.2 bar and higher<sup>1</sup> (200 mmWK and higher). Often an initial distinction is made between air-supported structures and air-inflated structures. However, in this research the first differentiation is maintained since it gives a more black and white representation. In the case of low pressure systems, we can distinguish two different typologies; single membrane structures<sup>2</sup> and double membrane structures<sup>3</sup>. In the case of a single membrane structure the accessible space is also the pressurized space. In the case of a double membrane structure the accessible space is not pressurized. Both typologies can be stabilized using positive or negative pressure, or a combination of both. However, it has to be noted that in the case of negative pressure, meaning a relative overpressure of the exterior, the inflatable structure cannot form a solid by itself. Therefore it will always need a secondary structure for stabilization. On these grounds, some authors question whether or not an inflatable stabilized by negative pressure is an inflatable in the first place.

High pressure systems, also referred to as air tube systems, are often classified as a single typology. However, based upon their morphology, they can be classified into three different typologies which can all be stabilized in five different manners; i.e. straight structures, buckled structures and arched structures.

#### SINGLE MEMBRANE STRUCTURES

The main attribute which is distinctive for this typology of inflatable structures is the fact that the accessible space is also the pressurized space. This space is usually pressurized using a medium under low pressure. The structure needs a continuous air supply to prevent it from deflation. Cable nets are often used to reduce the radius of curvature and thus the sur-

face tension. The forces which act on the structure are transported towards the bottom edges. This typology is mostly used for temporary structures due to its high maintenance demand.

#### DOUBLE MEMBRANE STRUCTURES

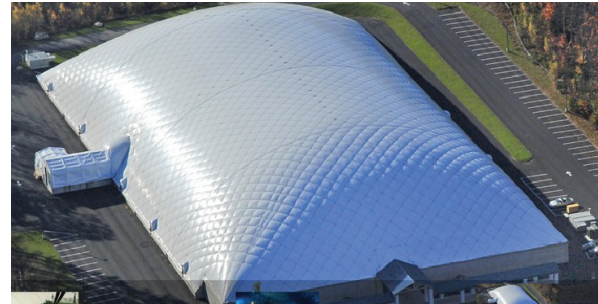


Figure 3.13: Single membrane structure; an indoor tennis hall.

This typology is characterized by its two layers which are identical and mirrored with respect to each other. Here, the accessible space is not pressurized, eliminating the need for continuous air supply. The pressure difference is only necessary to stabilize the cushion, since a primary structure is always necessary to prevent the membrane from becoming a sphere. The inflatable itself does not contribute to the stability of the overall structure. Therefore, double membrane structures are mostly used for roof structures.

#### STRAIGHT, BUCKLED AND ARCHED HIGH PRESSURE



Figure 3.14: The Allianz Arena; the facade is a double membrane structure

#### SYSTEMS

High pressure systems differ from the previously discussed typologies mainly due to their high pressure difference. Their morphology is characterized by linear, tubular members which can be straight, buckled or arched. They have a high curvature in one direction, and a small or zero curvature in the other direction. In the direction of little curvature they are able to transfer transverse forces, and are therefore often used as beam, frame or grid structures. However, compared to other structures which can transfer transverse forces, they are not very efficient. Therefore, they are often used in situations where fast and light (de)as-

1. The pressure difference in an inflatable structure normally does not exceed 7 bar (Herzog 1976)
2. Also referred to as Air Controlled Indoor Systems or air supported halls (Engel 1997)
3. Also referred to as Air Cushion Systems (Engel 1997)

sembly, light weight and low volume are decisive factors. Since the membrane is only able to absorb tensile forces, the pressure forces caused by the load case have to be compensated by pre-tensioning the membrane. Therefore, the pressure difference used in these inflatables is high (approximately 0.2 - 7 bar). Since no inflatable is 100% airtight (due to leakage through the fibres), they have to be reinflated every three to six months, depending on the volume, material and pressure difference ( Engel 1997; Holslag 1972; Herzog 1976).

### DEVICES FOR STABILIZATION

Low pressure systems can be stabilized using either positive or negative pressure or a combination of both. In the case of negative pressure, a secondary structure is necessary since an inflatable under negative pressure is not able to form a solid by itself (Engel 1997). In addition, negative pressure results in concave shapes which are disadvantageous in relation to snow and water pools. Due to these features negative



Figure 3.15: Inflatable arch by the U.S. Army for temporary shelters.

pressure systems are almost never used in practice.

High pressure systems can be stabilized as an individual element, or by combination or addition. When multiple high pressure systems are added together so that they are separable by disconnecting the connection mechanism, they form a discontinuous high pressure system (Herzog 1976), also referred to as a structural space envelop by Engel (1997) (Figure 3.17). When the individual elements are only separable by

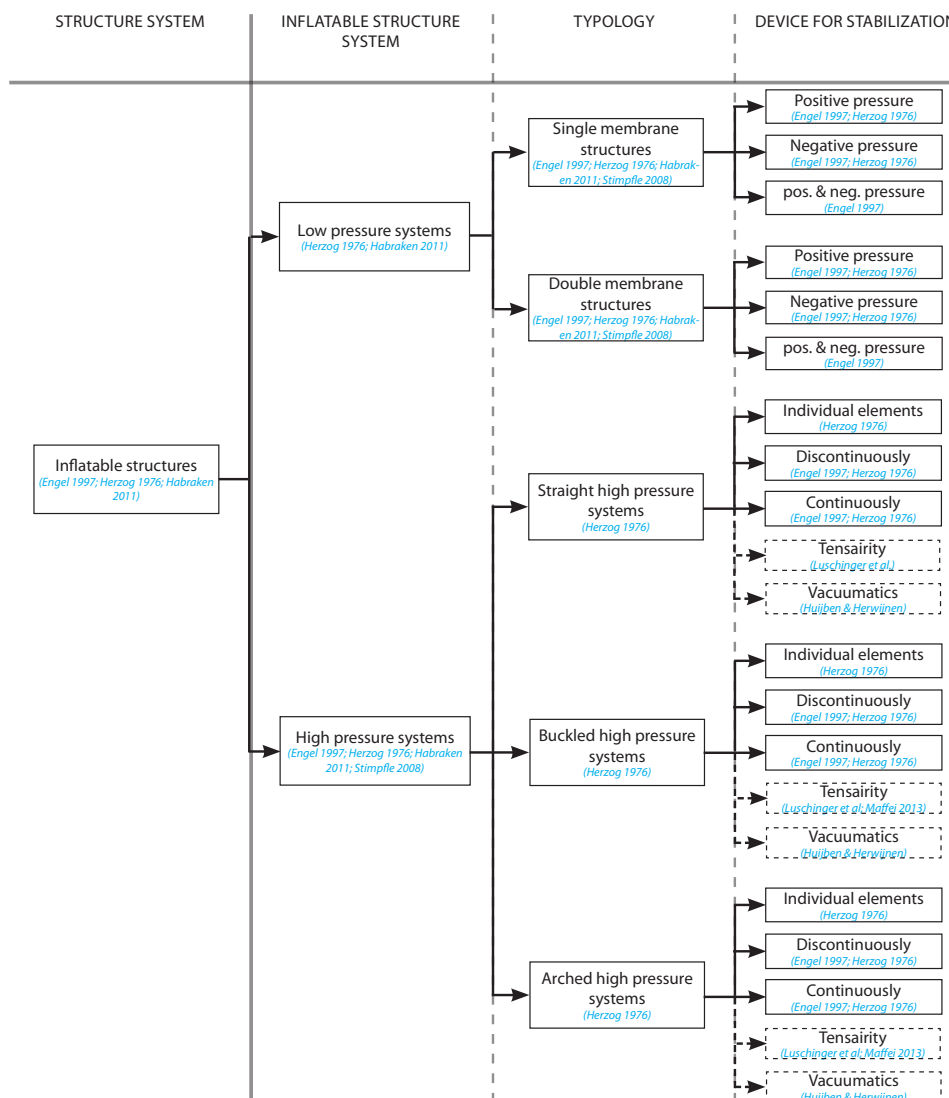


Figure 3.16: Overview of the inflatable structure typologies and their devices for stabilization



destroying the other elements the inflatable is continuous, also known as a load bearing skeleton (Engel 1997) (Figure 3.17).



Figure 3.17: TOP; Fuji Pavilion during Expo '70, a discontinuous high pressure system. BOTTOM; Example of a continuous high pressure system.

### TENSAIRITY

Two special devices for the stabilization of inflatable structures are tensairity and vacuumatics. Tensairity is result of an attempt to counteract the biggest downside of high pressure inflatables; load restriction. As discussed earlier, high pressure systems are not very efficient compared to other structure systems capable of transferring transverse forces. An inflatable shelter with a width of 25 meters and a height of 11 meters result in air beams with a diameter of 76 cm and an overpressure of 5.5 bar. Due to this pressure, the membrane must be able to absorb very high tensile forces resulting in the need for expensive high tech fibres (Luchsinger et al.).

Tensairity uses low pressure (50 - 500 mbar) to stabilize compressive elements against buckling. Typically, a large fraction of the section of any compressive element is necessary to stabilize the element against buckling. Due to the low pressure inflatable, the compressive element is fixed. Therefore, the element can be stressed to its yield limit, causing a large reduction in the cross section of the element. In addition, cables that spiral around the inflatable are pre-tensioned also leading to minimal cross sections. In this manner, the load bearing capacity of a standard air beam can be doubled, while positive attributes such as light weight and rapid deployability are maintained.

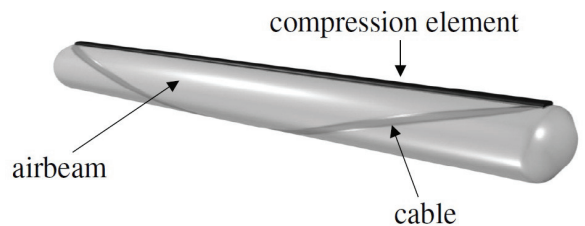


Figure 3.18: TOP; Basic elements of Tensairity (Luchsinger et al.) BOTTOM; Tensairity beam (Airlight Ltd.)

Until now, the technology has only been used in combination with straight higher pressure systems (Figure 3.18). However, the technology is also suited for buckled and arched structures (Maffei 2013).



Figure 3.19: Prototypes of tensairity arches by Roberto Maffei (Maffei 2013)

### VACUUMATICS

Vacuumatics is a method developed at Queen's University in Belfast by John Gilbert and William A. Hanna. It uses a double layer membrane with a granular filling, which is frozen in a pre-determined geometry by the relative over pressure of the exterior. Initially, the structure is flexible and incapable of absorbing forces. When the air between the two membranes is extracted, the granular filling is packed tightly together. The more air is extracted, the higher the relative overpressure of the exterior, the stiffer the structure. A big advantage of this method is the reversible nature of the process. When air is reintroduced, the structure becomes flexible again, and the whole cycle can be repeated.

At Queen's University, several case studies were performed (Figure 3.20) using six different geometries, nine membrane materials and six different filling materials. However, due to funding problems the potential of the method was never fully explored. However, recently a new research into the possibilities of vacuumatics started at Eindhoven University of Technology. In this case the focus is mainly on using



vacuumatics as a flexible formwork for concrete structures (Figure 3.21). According to Huijben (2012), certain disadvantages prevent vacuumatics from being a successful stand alone application. However, Delft University carried out a case study on a foot bridge using the principle of vacuumatics (Figure 3.22) (Knaack et al. 2008).

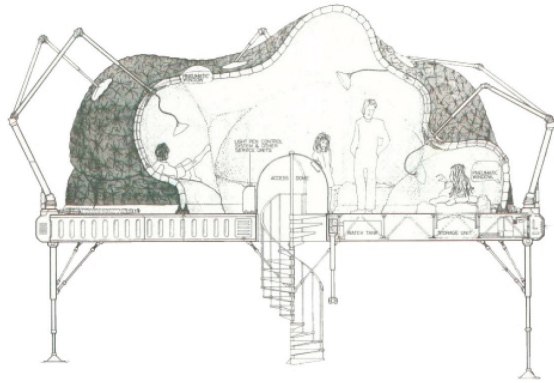


Figure 3.20: John Gilbert and William A. Hanna - a method by which the occupant can mould the shape of his room as desired.

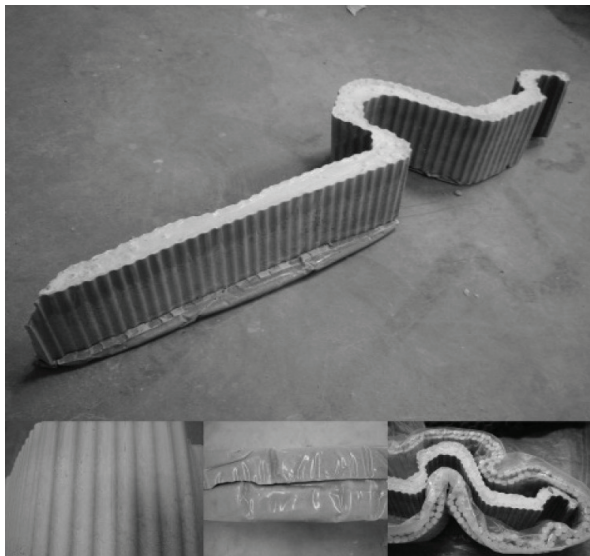


Figure 3.21: Vacuumatics for flexible concrete formwork (Huijben 2012)



Figure 3.22: Deflated bridge by the TU Delft (Knaack et al. 2008)

### 3.3.4 MORPHOLOGICAL INDICATORS

The parameters discussed in the second paragraph of this chapter define inflatable structures according to their characteristics. However, the goal of this study into inflatables is to determine which inflatable structure best reflects the morphological features of structurally optimized section active structure systems. Therefore, the typologies found in the previous paragraph have to be assessed according to their morphological features (Herzog 1976). When the morphological features of inflatables and optimized structure systems are studied, they will function as criteria to determine which inflatable is best to use in which case.

- Membrane

The first important feature has already been discussed briefly. An inflatable can be termed open or closed. In the context of this research all inflatables are closed structures since open structures such as sails and parachutes are outside its scope. Therefore, this feature will not be considered. Besides the structure, the membrane itself can also be open or closed. When the membrane forms a closed loop, it is termed closed (tubes, cushions etc.). In all other cases the membrane is open, as explained in paragraph 3.2.3.

- Proportion

As discussed earlier, soap bubbles can be seen as "ideal" pneumatic structures. A bubble always has the form of a sphere, which is equal in three dimensions. However, by using cutting patterns of inelastic material inflatable structures can also assume other shapes. Therefore, an important morphological feature is the proportion of the inflatable. We recognize three different types; two equal dimensions and one larger, two equal dimensions and one smaller, and three equal dimensions (Figure 3.23). Naturally there will be gray areas with intermediate values. In general, the relationship with the highest ratio is decisive (Figure 3.23).

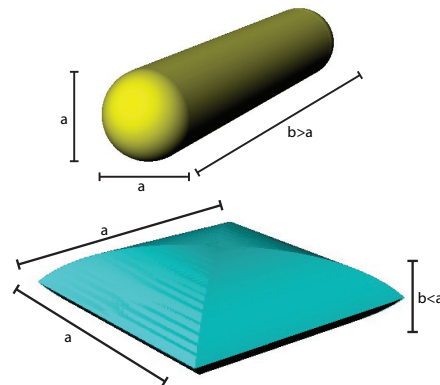


Figure 3.23: TOP; one dominant dimension. BOTTOM; two dominant dimensions

1. Disadvantages such as a sudden loss of pressure results in an immediate collapse of the structure

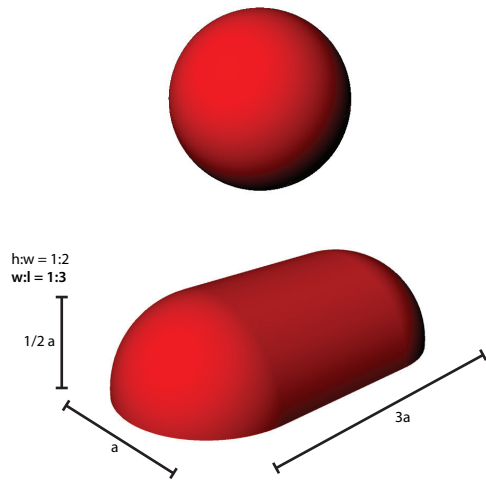


Figure 3.24: TOP; the sphere, all dimension are of similar size. BOTTOM; Different dimensions; the width to length ratio is decisive

- Curvature

As explained earlier, an inflatable can be monoclastic, synclastic or anticlastic (Figure 3.8)

- Pattern of the element

The pattern of the elements is also a feature. An inflatable can either be straight, buckled or arched. This feature should not be confused with the curvature. For example, an inflatable structure can be monoclastic and arched, but also anti clastic and arched.

The last feature is the type of connection that is used between the elements. Here, we distinguish two types of connections; addition and combination. The main difference is that in the case of an addition, the inflatables can be separated by decoupling the connection mechanism. In the case of a combination, one or more inflatables will have to be destroyed. At first, this feature will not be considered, since the typologies will first be treated as individual elements. However, when linking the inflatables to optimized structure systems this feature will be of importance.

### 3.3.5 CONCLUSION

The morphological features explained before can be given a code for each value that they can assume;

- Type of membrane [M]: Open [O] or Closed [C]
- Proportion [PP]: one dominant dimension [1<sub>2</sub>], two dominant dimensions [2<sub>1</sub>], three equal dimensions [3]
- Curvature [CU]: Monoclastic [M], Synclastic [S], Anticlastic [A]
- Pattern [PA]: Straight [S], Buckled [B], Arched [A]
- Connection [CO]: Combination [C], Addition [A]

When we assess the typologies found in the pre-

vious paragraph according to these morphological features, we come to the overview shown below. This overview will be essential for determining which inflatable best reflects the morphological features of structurally optimized section active structure systems (§ 3.5).

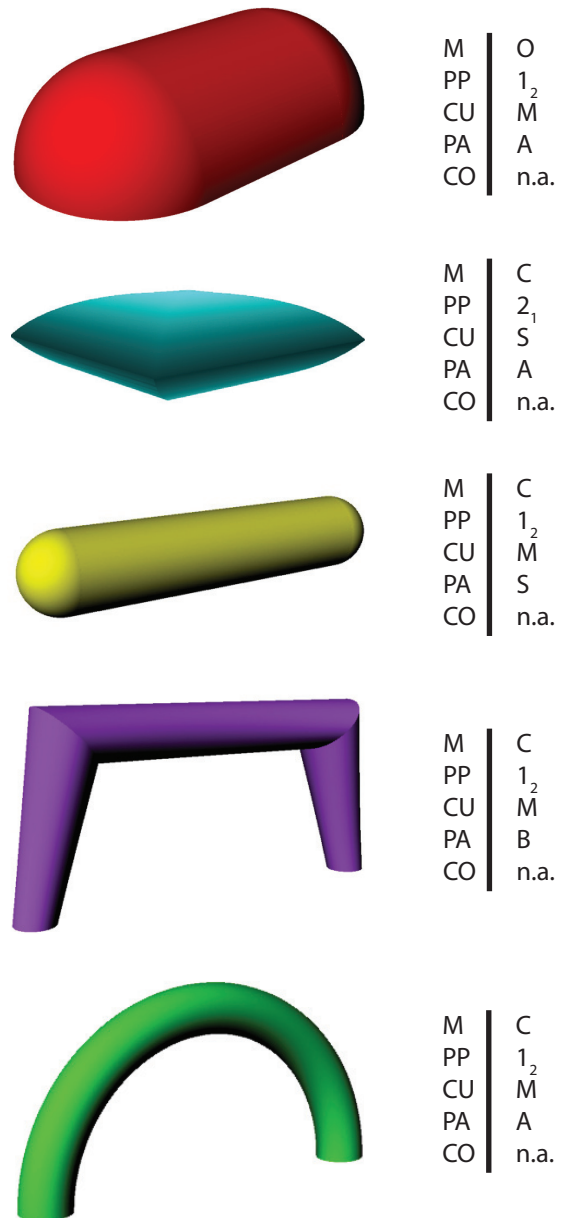


Figure 3.25: Morphological features of inflatable structure typologies

### 3.4.1 INTRODUCTION

As described by Frei Otto and in paragraph 3.2.3, a pneumatic structure consists out entirely or partially out of the following principal elements: Envelope, Content, Medium, Internal bracing, pressure difference. In this paragraph the envelope of a pneumatic structure or in other words the lightweight covering materials are described.

There are several kind of classifications for architectural envelope materials in defined by different authors as Frei Otto, Thomas Herzog, Tony Reid and Turlogh O'Brien, Arjan Habraken and Rogier Houtman. Out of these classifications an overview is made to classify all the materials and to summarize the work of the previously named authors (Figure 3.26).

At first the envelope materials are divided in isotropic and anisotropic materials. Isotropic materials show the same strength and stretch in all directions. Anisotropic materials have direction orientated properties (Herzog, 1976). Instead of a division in isotropic and anisotropic materials, the envelope material could also be divided into films and fabrics.

The reinforced films and films are isotropic materials. Reinforced films are combination of materials in contrast to the films, which are made of one basic material. Anisotropic materials are divided in two kind of fabrics; the coated fabrics and the uncoated fabrics. Coated fabrics are fabrics with a special coating that is suitable for only a few fabrics, therefore only a few combinations of materials are possible. Coated fabrics improve the performance of the fabric and the material becomes more isotropic. Uncoated fabrics can be divided in a several types of fibres of which the fabric is made of. At first the fabrics will be discussed.

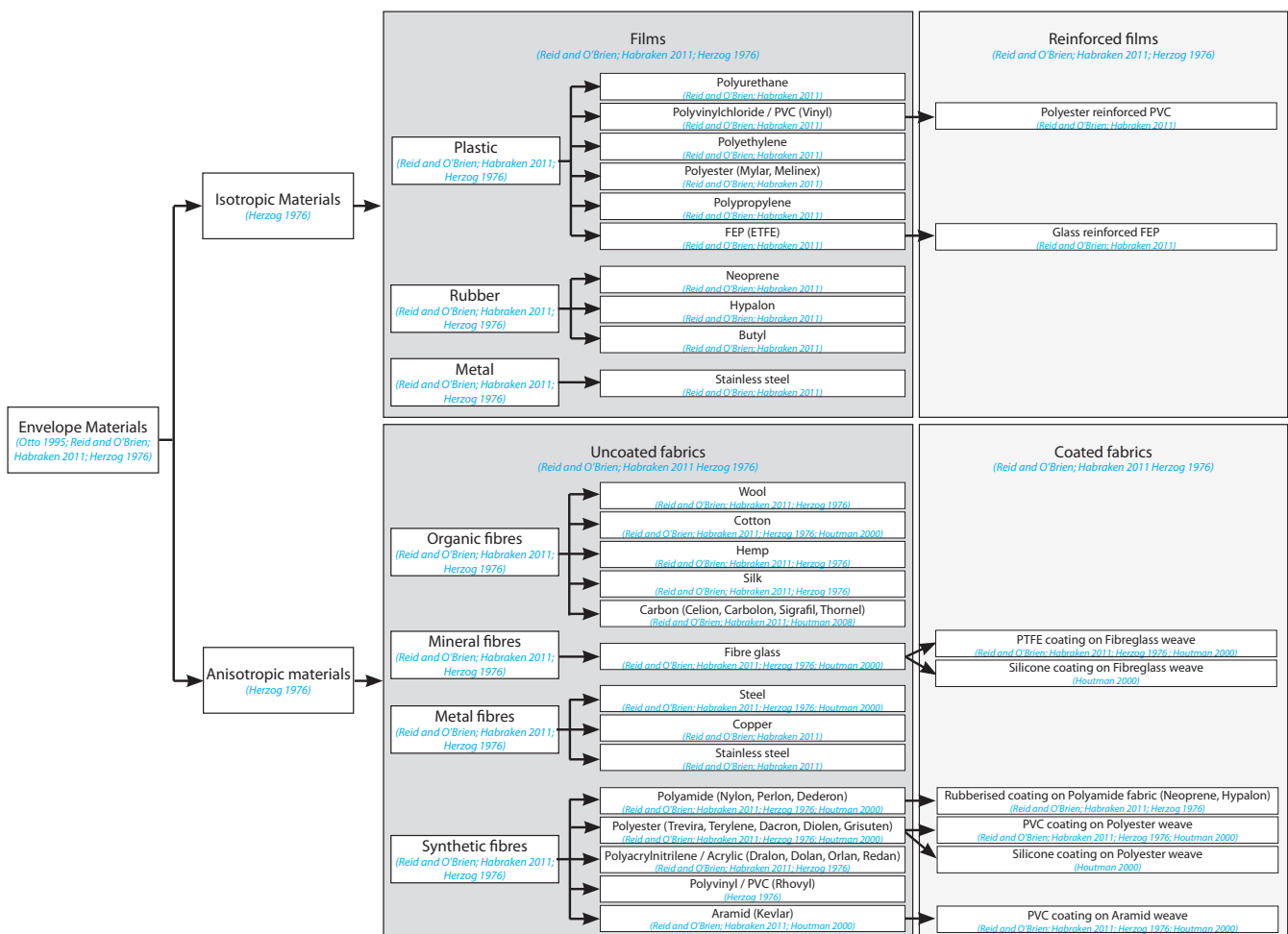


Figure 3.26: Overview of architectural envelope materials



### 3.4.2 FABRICS

Fabrics are constructed by a number of different processes. At first the yarns are produced by the spinning, drawing and twisting together of fibres. These yarns are woven in two perpendicular directions to each other, the warp direction and the weft direction, resulting into fabrics. In most cases the fabrics are coated on both sides to protect the fabric and to make it water tight.

#### FIBRES AND FILAMENTS

Yarns consist out of other elements known as fibres or filaments. There are natural fibres and chemical fibres. Natural fibres have a restricted length and are bound up in strands and are called spin fibres. Chemical fibres have an endless length and are called filaments. The diameter of natural fibres is smaller than 0.1 mm, where chemical fibres can have larger diameters. For chemical fibres the shape of the cross-section can differ, natural fibres on the other hand can only have a round shape. The choice to apply a certain fibre for a membrane on a project is mostly influenced by the costs, although there are several fibres applicable. An overview of the mostly applied fibres is shown in figure 3.26 and the most important fibres with or without a coating will be discussed in the following paragraphs.

#### YARNS AND THREADS

Out of the fibres and filaments comes the basic component in the weaving process, the so called yarns. In some cases yarns may be twisted together into threads which are then used for weaving. For the inflatable structures a thread with a circular cross-section is the best to have. Spin fibres need to be stabilised by twisting around the centre of the thread. Filament do not need to be twisted around the centre. To decrease the elasticity of the thread, the fibres need to be more twisted. By the amount of twisting, the mechanical properties of a thread can be determined precisely.

#### FABRICS

Woven fabrics are anisotropic surface forms with two right angled preferential directions whose angles can be displaced. The directions of the weaving are the so-called warp direction and weft direction. In the weaving process the threads are stretched in the warp direction, and another yarn is passing backwards and forwards through the warp threads in the weft direction. See figure 3.27.



Figure 3.27: Warp- and weft direction of a fabric (Habraken 2011)

There are several ways to establish a woven fabric. The basic method of weaving is the so-called basket weave, where each weft thread passes over and under each warp thread alternately and vice versa (See figure 3.28 A). Another method is the panama weave in which two or more weft threads together pass over and under the same amount of warp threads together alternately and vice versa (See figure 3.28 B).

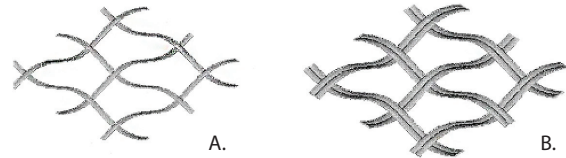


Figure 3.28: A. Basket weave and B. Panama weave (Houtman 2000)

Besides the basic methods there are a lot of varieties possible, like passing three warp threads underneath and one above, or two weft threads woven into one stronger warp thread. In this way the tear strength of a fabric can be increased. For structural use the basic methods are more sufficient and therefore only the basket weave and panama weave are used for membrane structures. The panama weave has a better mechanical behaviour than the basket weave because of the multiple threads that are used. A fabric made from many thin fibres will have a smaller deformation than an equal weight fabric with less but thicker fibres. The application of thinner fibres will decrease the thickness and increase the density of the fabric, while the weight is kept equal per square meter. This is an effect of the more straight orientated fibres which results in a higher E-modulus. Thicker fibres have a lower E-modulus and these fibres are easier to stress out possible folds. (Reid and O'Brien; Houtman, 2000; Herzog, 1976; Habraken, 2011)

A property of fabrics is the **nonlinearity**, this means that the ratio between stress and strain is not linear. In figure 3.29 a typical result is shown for a fabric that is tested uni-axial, the stress and strain are displayed. (Houtman, 2000; Wesdorp, 2005)

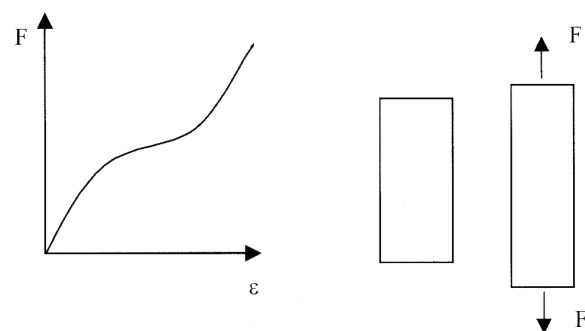


Figure 3.29: Typical stress-strain curve uni-axial loaded (Houtman, 2000)



The fabrics are **anisotropic** materials as the threads in the warp direction are more straight while in the weft direction the yarns are woven in afterwards. Because the weft threads are less straight, the weft threads will stretch first when a load is applied, and the fabric has a lower stiffness in the weft direction. In figure 3.30 several strips are cut out of the fabric, but a different orientation of the fibres is regarded which leads to different stress-strain graphs. (Houtman, 2000; Wesdorp, 2005; Herzog, 1976)

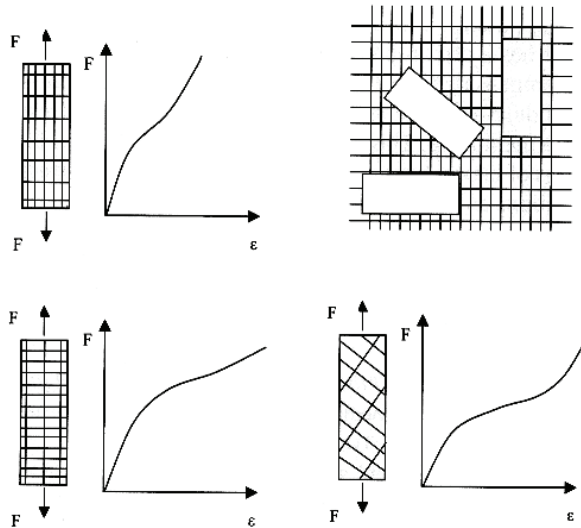


Figure 3.30: Anisotropy shown in different fibre orientations (Houtman 2000, Wesdorp 2005)

By prestressing the threads in the weft direction before coating the fabric, the threads will have a more equal undulation what will reduce the differences in the weft and warp stiffness. This will improve the stiffness in the weft direction and the fabric will become more isotropic. This also will reduce the need for re-tensioning because the stretch that normally occurs in the weft direction is limited. An example is shown in figure 3.31. (Habraken, 2011; Houtman, 2000; Wesdorp, 2005)

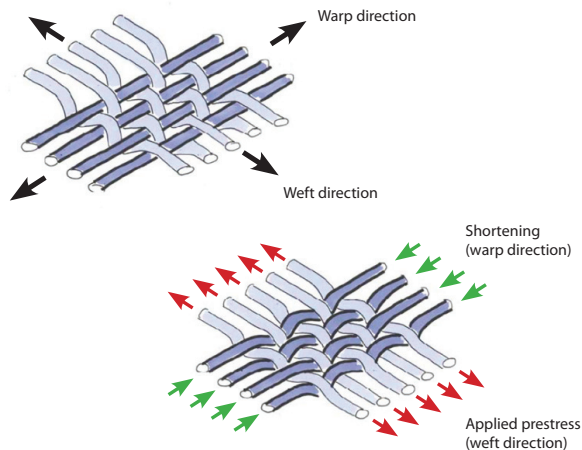


Figure 3.31: Fabric with and without prestressed threads in the weft direction (Habraken 2011)

Another considerably important property of fabrics is the **non-elasticity**. The non-elasticity is explained by the same test examples as shown in the anisotropic graphs, but then the tests are carried out more than once on the same strips of the fabric. The figure 3.32 shows a different unloading curve as a loading curve, and therefore when the second loading cycle starts, the second loading curve differs from the first loading curve, as well as the second unloading curve differs from the first unloading curve. By repeating the loading cycle, each loading and unloading curve is different, even though the differences are decreasing. The applied load determines the size of the elongation.

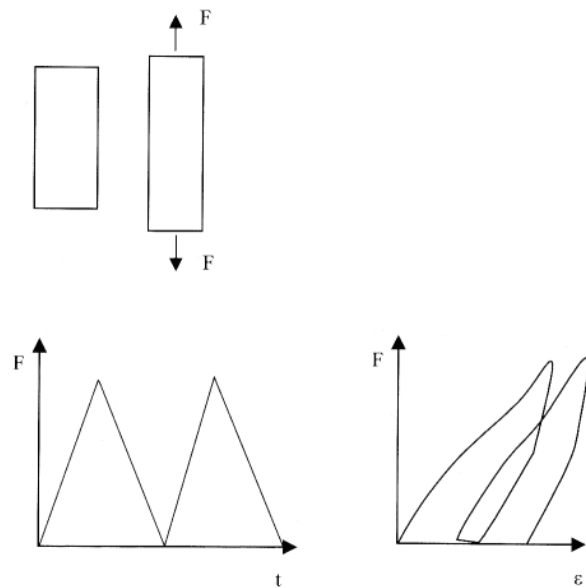


Figure 3.32: Non-elastic behaviour of woven material (Houtman 2000, Wesdorp 2005)

The stress-strain behaviour from a fabric that is heat set and coated under warp tension shows large differences both in warp and weft direction and in uni-axial and biaxial tension. The performance of the fabric can be even more balanced when the fabric is heat set and coated under weft tension as shown in figure 3.34. The other properties of uncoated fabrics, such as tear-propagation resistance and flexibility are also affected by the coating. When fibres are woven non-perpendicular it is called biaxial. A triaxial weaving consists out of a biaxial weave with a axial weave and has even better stiffness properties. (Veldman, 2005) (See figure 3.33)

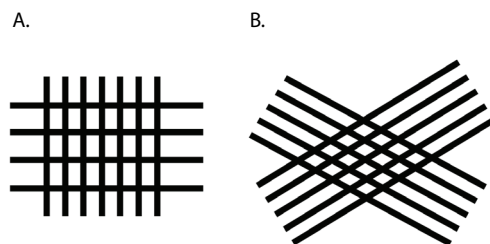


Figure 3.33: A) Uni-axial weave B) Biaxial weave (Wesdorp, 2005)



The uncoated fabric is primarily responsible for strength and elasticity. The other important requirements, such as flame resistance, resistance to UV-radiation, insensitivity to mechanical influences and

chemicals must be provided by the coating. More information about the properties of coated fabrics will be given in paragraph 3.4.5.

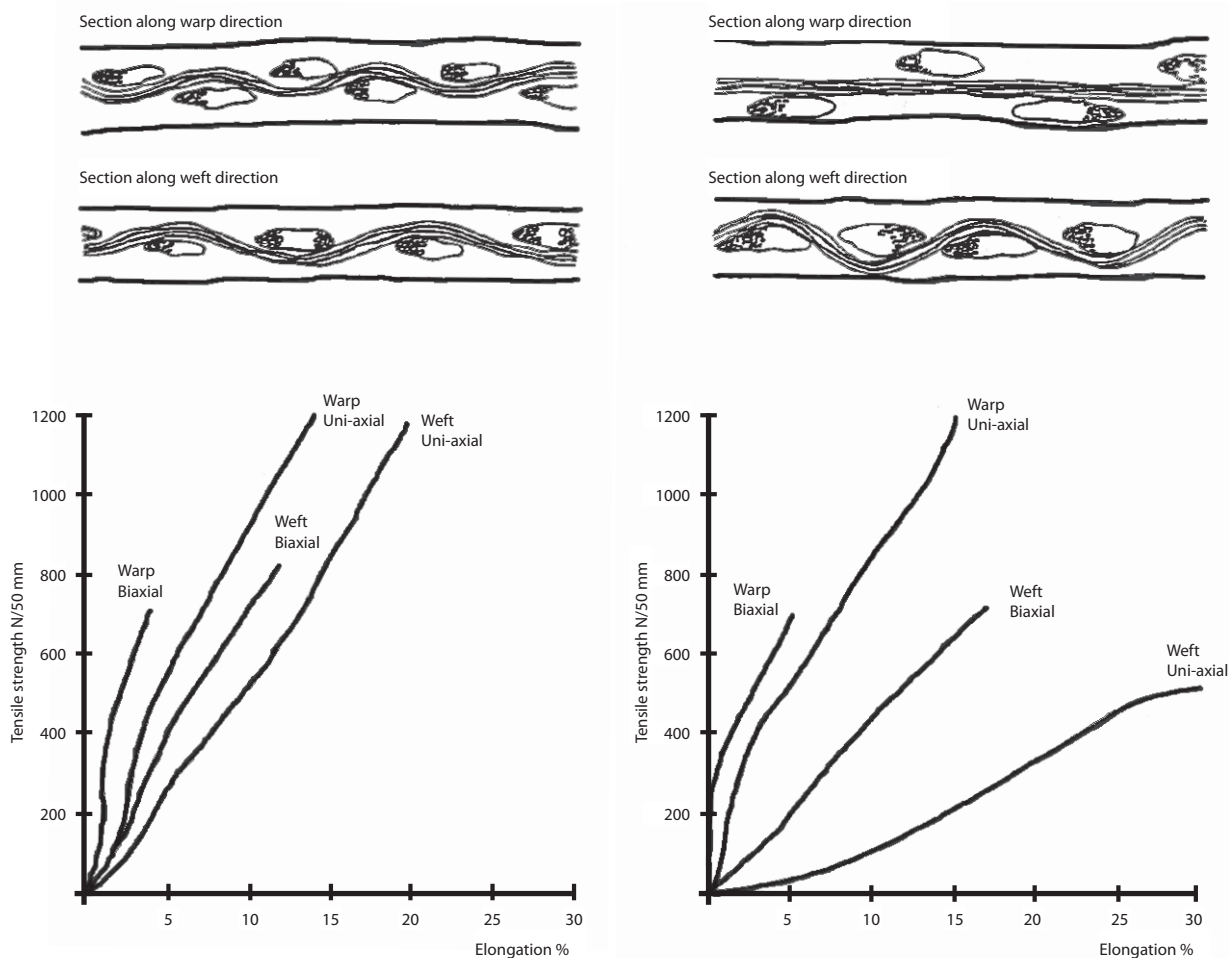


Figure 3.34: Structure and behaviour of similar fabrics heat set and coated under warp tension (left hand side) and under weft tension (right hand side) (Skelton, 1972)

### 3.4.3 FABRIC MATERIALS

Fabric materials are used in architectural membranes and the most common used fibres are described in this paragraph. Furthermore fibres are applied in gossamer structures. These high end fibres possess high performance properties. At first the architectural materials are described.

#### COTTON FIBRE

Organic fibres are seldom used today for pneumatic structures, the only organic fibre that is applied in membrane structures is the cotton fibre. The organic properties of this fibre make it subject to fungi and moisture. The expected lifetime is 4 years, if permanently used. The durability of organic fibres have a considerable lower durability and a less favourable elasticity than mineral or synthetic fibres. (Reid and O'Brien; Houtman, 2000; Herzog, 1976)

#### POLYAMIDE FIBRE

The polyamide fibre, also known as Nylon, has a bad resistance against UV-radiation, swells in the length direction when it gets wet and is herewith of little importance for textile architecture. This fibre has a high strength, low modulus and high extension. (Reid and O'Brien; Houtman, 2000; Herzog, 1976)

#### POLYESTER FIBRE

The polyester fibre has a high strength, medium modulus and medium extension. The mechanical properties decrease by the influence of sunlight and ageing takes place. The polyester fibre is a standard product in the textile architecture and is together with fibreglass the most common used fibre. The fibre has a large reserve-capacity and wrinkles and folds can be easily removed by re-tensioning the structure. (Reid and O'Brien; Houtman, 2000; Herzog, 1976)

### GLASS FIBRE

The glass fibre has the lowest elasticity under loading of the architectural textiles. Because of this low elasticity their spatial deformability is relatively low. The angle displacement of the fabric threads and thus their ability to adapt to synclastic or anticlastic surfaces is also low, so that a very accurate cutting pattern is necessary. For this research it is of great importance that the fabric can adapt to synclastic and anticlastic surfaces. The metal fibres have an even greater strength and for this reason their adaptability is even lower, that is why metal fibres are hardly applied in practice. Ageing exerts little influence on the fibre-glass what has a tremendous impact on the expected lifetime of the structure. Subjection to moisture decreases the tensile strength of fibre glass. (Reid and O'Brien; Houtman, 2000; Herzog, 1976)

### ARAMID FIBRE

The aramid fibre, or the most well-known Kevlar fibre, has a high tensile strength and is chemically resistant. A great disadvantage is the low elastic strain and the bad resistance against high temperature and UV-radiation. This fibre is less stiff than carbon fibres, which makes the fibres less brittle and the strength to weight ratio is higher. (Reid and O'Brien; Houtman, 2000)

### CARBON FIBRE

Carbon fibres or graphite fibres are materials consisting out of fibres composed mostly of carbon atoms. These atoms are bonded together in crystals that are more or less aligned parallel to the long axis of the fibre. These fibres are woven together into a fabric. Carbon fibres have excellent properties, such as high stiffness, high tensile strength, low weight,

high chemical resistance, high temperature tolerance and low thermal expansion. In comparison to glass fibres and plastic fibres these fibres are relatively expensive. Due to its high stiffness and low elasticity, the material is somewhat brittle and not foldable. (Meijer, 2007)

### VECTRAN FIBRE

Vectran fibres have a high strength and modulus, low creep, and good chemical stability and are thermally stable at high temperatures. Vectran fibres have a melting point of 330°C, with progressive strength loss from 220°C. The fibres have a high resistance to UV-radiation and can be used outside for long term. (Kuraray America, 2006)

### PBO FIBRE

PBO or zylon fibre is a super fibre with the highest strengths and modulus that almost doubles the aramid fibres. Zylon has superior creep resistant and is very heat resistant, with a decomposition temperature of 650°C and has extremely high flame resistance. PBO-fibres show a decrease in strength with exposure to UV-radiation, humidity and strong acids. PBO products for outdoor use have to be protected by covering materials. PBO fibre is quite flexible and has very soft hand, in spite of its extremely high mechanical properties. (Toyobo, 2005; Yamashita et al., 2003)

An overview of the properties of fibres is shown in table 3.1.

Material	Density (g/cm <sup>3</sup> )	Tensile strength (N/mm <sup>2</sup> )	Tensile strain (%)	Elasticity (N/mm <sup>2</sup> )	Remarks
Cotton	1.5-1.54	350-700	6-15	4500 - 9000	- Only for temporary use of interest
Polyamide 6.6 (Nylon)	1.14	Until 1000	15-20	5000-6000	- When exposed to light only average resistance to ageing - Swelling when exposed to moisture - Only of little importance in textile architecture
Polyester fibre (Trevira, Terylene, Dacron, Diolen)	1.38-1.41	1000-1300	10-18	10000-15000	- Widely spread, together with fibreglass a standard product in textile architecture
Glass fibre	2.55	Until 3500	2.0-3.5	70000-90000	- When exposed to moisture, reduction of breaking strength - Brittle fibres, therefore is spun into filaments of 3 µm diameter - Together with Polyester a standard product in textile architecture
Aramid fibre (Kevlar)	1.45	Until 3000	2-4	130000-150000	- Special fibre for high-tech products
Polytetrafluorethylen (Teflon, Hostaflon, Polyflon, Toyoflon etc.)	2.1-2.3	160-380	13-32	700-4000	- High moisture resistance - Remarkable anti adhesive - In air non-combustible - Chemical inert
Carbon fibres (Celion, Carbolon, Sigrafil, Thornel)	1.7-2.0	2000-3000	< 1	200000-500000	- Special fibres for high-tech products - Very low expansion coefficient - Non-combustible
Vectran fibres	1.4	1100-3200	3.8	-	- Special fibres for high-tech products
PBO fibres (Zylon)	1.54	5800	2.5	-	- Special fibres for high-tech products - Non-combustible

Table 3.1: Material properties of the base material of fabrics (Houtman 2000; Sobek and Speth, 1993; Toyobo, 2005; Meijer, 2007; Kuraray America, 2006;)

### 3.4.4 COATINGS

The fibres are described in the previous paragraph from which the fabric is woven. To create durable and water tight membranes, most of the fibres need a coating on both sides. The coating process has to be designed to achieve a good penetration of the fabric, good adhesion and an adequate thickness over all parts. The strength of the seams is indicated by the adhesion of the coating to the fabric. Coatings are usually applied in three stages, at first primers or lubricants are applied, then the main bulk coats are

applied, and at last the surface finishes are added. Several coatings are available, but the most common coatings are PVC-, PTFE- and silicone coatings. Fabrics are often coated for the following reasons: Protecting yarns against damage; Make it water- and wind proof; Protect against UV-radiation; Prevent the adhesion of dirt; Welding different parts of the membrane together; Coating can contain colour pigments. This will also be discussed by the material properties in paragraph 3.4.7.

### 3.4.5 COATING MATERIALS

#### PVC COATING ON POLYESTER WEAVE

The PVC coating on polyester weave is together with PTFE coating on fibreglass weave the most common used coating. The PVC coating is mostly applied on a polyester weave. The tensile strength of a polyester weave with PVC coating is reasonably high what makes the fibres useful for mechanical prestressing. Thereby the not extremely high elasticity modulus allows to stress out wrinkles and folds. To reduce the ageing process and make it repelling dirt an acrylic coating or a teflon top layer is applied (PVF-film) or merged (PVDF-merging). The difference in application is the time the structure has to stand, permanent or temporary. Permanent structures (15-20 years) use heavy coated fabrics with for example a teflon top layer and for folding structures a PVDF coating will be more desirable. With these coatings the material is considered to be fire-resistive. (Houtman, 2000; Herzog, 1976; Habraken, 2011)

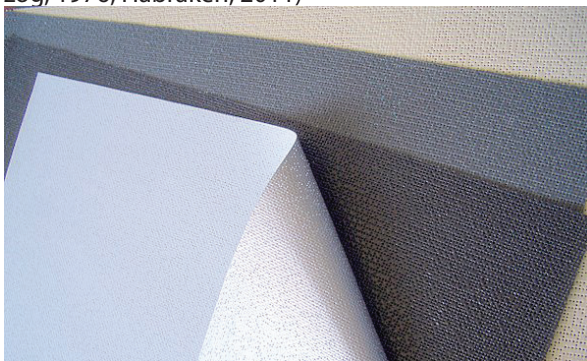


Figure 3.35: PVC coated polyester fabric



Figure 3.36: PVC coated polyester fabric

#### PVC COATING ON ARAMID WEAVE

The aramid fibre is an interesting lightweight building material used for air tubes, which is researched by S.L. Veldman. It is produced by Eurocarbon and the so-called braided sleeve uses a triaxial weave. The outcomes are high-pressure air tubes which can take on the support function of a beam, an arch or a grid becoming a type of frame structure. The aramid fibres are braided into sleeves of tubes and have an inner coating to create a seamless airtight inflatable structure of approximate 30 psi. On the outside a PVC coating is applied to protect the fibres from UV-degradation. (Houtman, 2000; Wesdorp, 2005; Veldman 2005; Habraken, 2011)

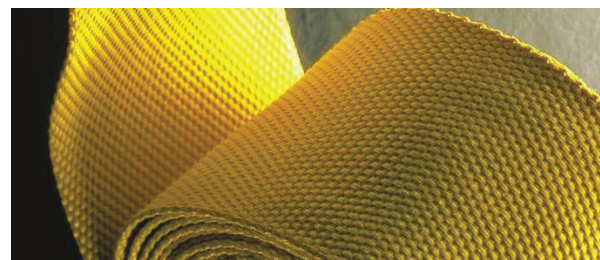


Figure 3.37: Aramid fibre



Figure 3.38: The (over)braiding process of Eurocarbon B.V.



Property	Polyester fabric			Fibreglass fabric	
	PVC	PVC	PVC	PTFE	Si
Coating	PVC	PVC	PVC	PTFE	Si
Top coating	Acrylic	PVF-lamination	PVDF-merging		
Expected lifetime	8-10 years	12-15 years	12-15 years	>30 years	>30 years
Ageing resistance	Average	Good	Good	Very good	Very good
Self-cleaning	Average	Good	Good	Very good	Average
Transparency	Good	Good	Good	Good	Very good
Fire-retardant	Good	Average	Good	Very good	Very good
Foldable	Very good	Average	Good	Bad	Average

Table 3.2: Properties of coated fabrics (Houtman, 2000; Houtman, 1996)

#### PTFE COATING ON FIBREGLASS WEAVE

Polytetrafluorethylene is most applied coating on fibreglass weavings. The PTFE coated glass fibre consists of yarns of glass fibres that are coated with a teflon coating. Teflon coated fibreglass weave is the most permanent of the coated architectural fabrics. It has a lifetime of over 30 years since the material is not subject to ageing as a result of UV-radiation. The tensile strength of glass fibres is high, but the thin glass fibres are brittle and restricted in their flexibility. A very precise production process is required, since the material is not able to stretch out the wrinkles and folds due to its higher E-modulus. Therefore the application of the fabric is only for permanent structures and it is not re-locatable. The coated fabric is non-combustible, dirt repellent and can reach translucency's up to 25% (Houtman, 2000). Drawbacks are the significantly higher price than for example a polyester membrane and the difficulty of welding two parts of coated fabric together. (Houtman, 2000; Herzog, 1976; Habraken, 2011)



Figure 3.39: PTFE Coated fibreglass



Figure 3.40: PTFE Coated fibreglass on the Riyadh Stadium

#### SILICONE COATING ON FIBREGLASS WEAVE

The applications of silicone coating on fibreglass weaves are rare. Fibreglass coated with silicone rubber is less likely to be damaged during transportation and erection than fibreglass coated with Teflon, due the silicone rubber is more flexible. The light transmission of the silicone coating on fibreglass is claimed to be as much as 25% for the architectural membrane and 90% for the thin liner material. The silicone coating provides a good water protection for the fibreglass and assures a lifetime of over 30 years as well. The price of a silicone coated fibreglass is said to be between the PTFE coated fibreglass and PVC coated polyester. (Houtman, 2000)



Figure 3.41: Silicone Coated fibreglass



Figure 3.42: Silicone Coated fibreglass for air-supported structures



Fabric / Coating	Weight (g/m <sup>2</sup> )	Fire retardant	Tensile strength warp/weft (N/50mm)	Tensile strain warp/weft (%)	Tear strength (N)	Bending capacity	Seam strength (N/50mm)
Polyester/PVC Type 1	800	B1	3000/3000	15/20	350	Very good	2400 (30mm, 70°C)
Type 2	900		4400/3950	15/20	580		2850 (60mm, 70°C)
Type 3	1050		5750/5100	15/25	950		3350 (60mm, 70°C)
Type 4	1300		7450/6400	15/30	1400		4600 (60mm, 70°C)
Type 5	1450		9800/8300	20/30	1800		4600 (60mm, 70°C)
Fibreglass/PTFE	800 1270	A2 A2	3500/3000 6600/6000	7/10 7/10	300 570	Sufficient	6000 (60mm, 70°C)
Fibreglass/Si	800 1270	A2 A2	3500/3000 6600/6000	7/10 7/10	300 570	Good	
Aramid/PVC	900 2020	B1 B1	7000/9000 24500/24500	5/6 5/6	700 4450	Good	4800 (30mm, 70°C)
PTFE/-	520	Non combustible	2000/2000	40/30	500	Very good	
Cotton- Polyester- /	350 520	B2 B2	1700/1000 2500/2000	35/18 38/20	60 80	Very good	

Table 3.3: Properties of coated fabrics (Houtman, 2000; Houtman, 1996)

### 3.4.6 FILMS

In contradiction of fabrics, films do not exist out of fibres, but are extruded from a homogeneous thermoplast. For this reason films can be categorized as isotropic materials. Isotropic materials show the same mechanical properties in all directions. Films are often thinner and have a smaller strengths as fabrics. Therefore the maximum span of films is much smaller as the maximum span of fabrics. In general unreinforced films are not used very much as architectural coverings. Films are often made of plastic, rubber or metal and usually have a low air permeability.

Reinforcing the films increases the properties of the membrane, but reinforced films are not often used for lightweight structures. These reinforced films consist out of the conventional film material and reinforcing it with an open weave fabric. The fabric is usually laminated between two thin layers of film material. This method is also often used for materials used in gossamer structures and will be explain in the chapter of rigidizable materials. The most common reinforced foils for architectural purposes are PVC-, PTFE- and ETFE-films. In gossamer structures film materials as Mylar, Kapton and FEP are used.

#### PVC

Properties as a low stiffness and its sensitivity to temperature changes makes the PVC-film not suitable for outdoor applications. Therefore PVC films are mostly applied for temporary internal use and for small spans. The tensile strength of PVC films varies from 6.9 to 25 N/mm<sup>2</sup>. (Habracken, 2011; Herzog, 1976)

#### PTFE

PTFE-films have minimum and maximum use temperatures of -240°C to 260°C and a melting temperature of 327°C. In addition, PTFE-films provide superior creep resistance at high temperatures, excellent low-temperature toughness, excellent chemical stability and exceptional flame resistance. In contrast to PFA, FEP and ETFE the PTFE-films are not processable as a thermoplast. PTFE has one of the lowest coefficients of friction against any solid. The tensile strength of PTFE-films varies from 21 to 34 N/mm<sup>2</sup>. (DuPont, Fluoroplastic Comparison - Typical Properties)

#### FEP

FEP-films have an excellent chemical stability, excellent non-stick properties and the maximum use temperature is 200°C and the melting temperature is 260°C. FEP-films share PTFE's useful properties of low friction and non-reactivity, but are more easily formable due to their thermoplastic procesability. FEP is softer than PTFE and it is highly transparent and resistant to sunlight. The tensile strength of FEP-films is 23 N/mm<sup>2</sup>. (DuPont, Fluoroplastic Comparison - Typical Properties)

#### PFA

PFA-films and FEP-films are very similar, except that PFA has the advantages of higher use temperature of 260°C and a melting temperature of 306°C, and a higher tensile strength of 25 N/mm<sup>2</sup>. PFA is similar to FEP in terms of its mechanical properties. These two are both superior to PTFE with regards to their flexibility, making them useful for tubing applications.



However, their ability to endure repetitive folding (flex life) is actually lower than PTFE's own. PFA has a higher flex life than FEP. PFA is more affected by water absorption and weathering than FEP, but is superior in terms of salt spray resistance. (DuPont, Fluoroplastic Comparison - Typical Properties)

#### ETFE

ETFE-films is effectively the high strength version of FEP, PFA and PTFE, often featuring slightly diminished capacities in other fields as thermal and electrical properties by comparison. The ETFE film has a minimum and maximum use temperature of -185°C to 150°C and a melting temperature of 267°C. The tensile strength is considerably higher as the previous films and varies from 40 to 46 N/mm<sup>2</sup>. ETFE is by far the most commonly used material for transparent closed pneumatic structures. It has a lifetime of about 25 years. (DuPont, Fluoroplastic Comparison - Typical Properties; Habraken, 2011)

#### PET (Mylar)

In gossamer structures Mylar is used, this is a polyester film made of Polyethylene terephthalate (PET). Mylar polyester film retains good physical properties over a wide temperature range (-70°C to 150°C). The tensile strength of Mylar is in the range of 20-24 N/mm<sup>2</sup>. (DuPont, Properties of Mylar)

#### POLYIMIDE (Kapton)

Polyimide films possess a combination of properties that make it ideal for a variety of applications in many different industries. Polyimide films have the ability to maintain its excellent physical, electrical, mechanical and thermal properties over a wide temperature range with a maximum of 500°C, and has an excellent chemical resistance. The tensile strength of the Kapton Type 100 HN Film is 231 N/mm<sup>2</sup>. (DuPont, Properties of Kapton)

Tensile strength and elongation properties of films are shown in table 3.4.

Film	Tensile strength (N/mm <sup>2</sup> )	Elongation (%)
PVC	17 - 25	240 - 255
PTFE	21 - 34	300-500
FEP	23	325
PFA	25	300
ETFE	40 - 46	150-300
PET	20 - 24	91-116
POLYIMIDE	231	72-83

Table 3.4: Properties of films (DuPont; PVC.org)

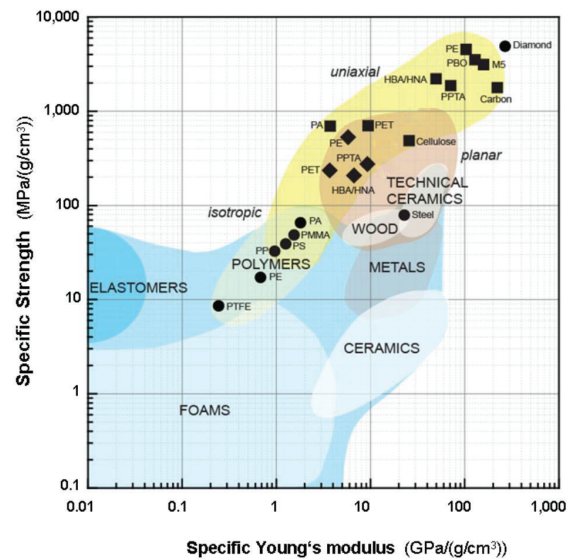


Figure 3.43: Material performances (Meijer, 2007)



### 3.4.7 MATERIAL PROPERTIES

The material properties of coated fabrics are separated in properties mainly influenced by the fabric, and properties influenced by the coating. To eventually choose a material for the case, the material has to full fill certain requirements. These requirements are often determined on the material properties. In figure 3.44 the relationship between the composite properties of a coated fabric and the separate properties of the fabric and the coating are set out.

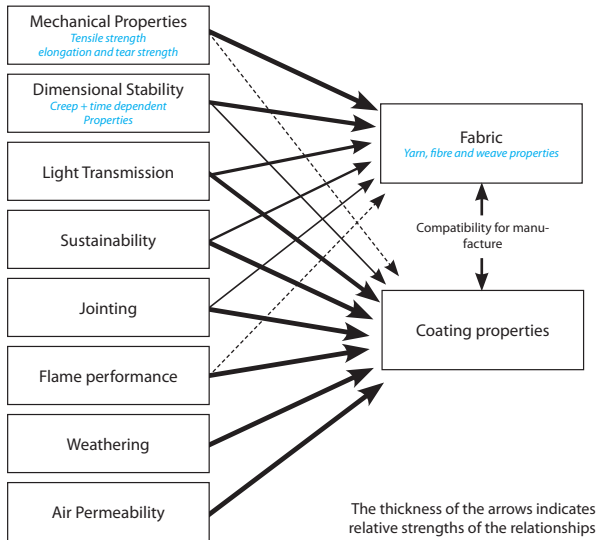


Figure 3.44: Properties of coated fabrics and their relationship to the fabric and coating, based on Reid and O'Brien.

#### MECHANICAL PROPERTIES

The short-term mechanical properties which are primarily interesting for lightweight structures are the tensile strength, tensile modulus, elongation, tear strength, adhesion strength and tear propagation. For coated fabrics these mechanical properties are primarily determined by the fabric even though the coating will have a certain influence as well. Important is the way these properties are maintained with age and when permanently stressed or under cyclic loading.

The **tensile strength** is an important property for the envelope material since the material is used as a primary structural element. The construction and non-homogeneity of the applied materials make an exact definition of the tension strength not clearly definable. The tensile strength is usually given in kp/5 cm. The actual strength of a woven fabric depends on the number of threads per cm, on the thread denier and the type of weave. The required tensile strength differs by low or high pressure systems. Low pressure inflatables require strength values of 200 to 600 kp/5 cm and thicknesses of 0.7 to 1.2. High pressure inflatables require strength values of 1000 kp/5 cm and thicknesses of several millimetres.

The **tensile modulus**, also known as the Young modulus or elastic modulus, is a measure of stiffness of an elastic material and is a quantity used to characterize materials. The tensile modulus enables the calculation of the change in the dimension of a material under tensile or compressive loads. The tensile modulus is of particular importance to the accuracy of the cutting pattern and erection tolerances.

The **elongation** of the material is required to be not too great, otherwise the envelope material will lose its shape. In the previous example of PVC coated polyester fabrics the percentage of elongation of material is also much higher as with a permanent load of 80% instead of 50% which will lead to the short term breaking of the material.

The **tear strength** is a measure of a fabric's ability to stand up to damage that has the form of tearing, which rather takes place than direct tensile failure.

For fabrics the **adhesion strength** is of importance to specify the resistance of adhesion of the coating to mechanical separation from the woven fabric generated by tensile forces. This is also called the peeling test. By increasing the adhesive strength, the tear propagation resistance is also negatively influenced, therefore a equilibrium between tear propagation strength and adhesion strength is required.

The **tear propagation** resistance gives information regarding the tear propagation load at which a sample, which is already notched on one edge, tears on. The tear propagation resistance is also influenced by the fabric form, the type of weave, the formula of coating paste and the twist of the thread. Herzog defines a rule of thumbs for the tear propagation resistance; in general one can estimate the tear propagation resistance at 10 to 15% of the tensile strength. (Reid and O'Brien; Herzog, 1976; Habraken 2011)



#### DIMENSIONAL STABILITY

When a coated fabric is stressed over a period of time, the dimensional stability is mainly depended on the basic fibre material and not the yarn or weave construction. The dimensional stability is influenced by several factors as load weight and loading period, weathering and temperature. A coating has influence on the dimensional stability due to its function to protect the fabric. Important for the choice of a fabric is that the dimensional stability of the fabric will not largely decrease over time.

Coated fabrics are influenced by the **loading period**. A property of coated fabrics is that the long term tensile strength is considerably lower than the tensile strength in a short term. Testing showed that the envelope will break by a lower value than its tensile strength when it is loaded for a longer period. For example Herzog refers to test showed that PVC coated polyester fabrics will tore, under permanent loads of 80% of the tearing strength, after some hours or days. With a permanent load of 50% of the tearing strength there is no reduction in strength after 10000 hours.

Also fabrics that are exposed to **UV-radiation** will largely decrease in strength over time. The difference between several fibre material in strength reduction is large. The coating has an large effect in limiting the loss of strength caused by the UV-radiation.

The **temperature** has influence on the strength and elongation of a fabric over time. When the temperature increases the strength and stiffness decrease and the elongation increases. In any case one can state that temperatures of  $-25^{\circ}\text{C}$  to  $+70^{\circ}\text{C}$  are normal for coated fabrics and within this range the influence on strength and stretch behaviour is low. Tests by Herzog and Krummheuer have shown a reduction of 10-20% in strength at a temperature of  $70^{\circ}\text{C}$  compared to those tested at  $20^{\circ}\text{C}$ .

**Weathering** conditions as humidity and moisture influence the dimensional stability of a woven fabric. The influence of weathering on the material properties of fabrics has large differences.

For an estimation of long-term strengths of coated fabrics based on short term results Hearle has suggested a general rule of thumb that the short term strength should be reduced by 10% for each factor of 10 that the service life exceeds the testing time (Reid and O'Brien; Herzog, 1976; Habraken, 2011; Haerle, 1969).

#### LIGHT TRANSMISSION

For envelope materials some degree of light transmission is often required. The light transmission is not required to determine the case, but might be of interest if a rigidization method is considered which demands transparency for rigidization.

#### SUSTAINABILITY

The sustainability of materials is often expressed by the Life Cycle Assessment (LCA). The LCA method is not yet applied on all of the membrane materials and therefore a comparison is not possible. Recent studies on LCA values of membranes materials, started last year by frontiers in the membrane materials for architectural purposes. These frontiers are gathered by Tensinet, to perform a LCA analysis of all membrane materials for architectural purposes. An LCA analysis on ETFE is performed. PVC coated polyester is recycled by Taxyloop and is improved in the last decade with regards to sustainability.

#### FLAME PERFORMANCE

The flame performance is of importance for emergency cases. The performances are almost entirely governed by the properties of the coating and a little influenced by the fabric. Important factors for assessing flame performance are flame resistance, smoke generation, toxic fumes and integrity of seams (Reid and O'Brien; Herzog, 1976).

#### WEATHERING

The durability and weathering characteristics of coated fabrics are mainly determined by the choice of coating material. Weathering characteristics are temperature, UV-radiation, oxidation, moisture, aggressive chemicals and organic growth. These characteristic can decrease the performances of coated fabrics until it is unable to full fill its requirements. The influence of weathering over time is also referred to by the dimensional stability. The properties of coatings on polyester and fibreglass fabrics are shown in table 3.3 and the influence of weathering on fibres is in the remarks of table 3.1. (Reid and O'Brien; Herzog, 1976)

#### AIR PERMEABILITY

For inflatable structures the envelope material is required to have a low air permeability. A low enough permeability for inflatables with uncoated fabrics is difficult to achieve. Therefore coatings on fabrics are used to achieve a very low air permeability, and a fairly heavy coating is required for high pressure structures to prevent air loss over a period of time. Other significant factors that influence the pressure are an applied load and the performance of the seams. (Reid and O'Brien)

## JOINTING

Several ways of jointing of envelope materials are possible and are primarily dependent on the basic material and sometimes on its coating. Joints can be separable and inseparable. At first the **inseparable** joints are described.

Herzog describes six possible types of inseparable joints;

- Sewing
- Welding
- Cementing
- Vulcanising
- Riveting
- Clamping

At first the three most commonly used methods will be described, followed by the less used methods.

**Sewing** mostly is applied for jointing uncoated fabrics. Sewing is one of the most applied jointing techniques when not very high strengths are required, and there are no requirements on low air permeability. By sewing coated fabrics wrinkles occasionally occur in the joints and this requires extra attention.

**Welding** is considered as one of the best joining techniques and is the most widely used technique. Three different methods of welding are possible; hot key, high temperature welding and high frequency welding. Welded joints are usually stronger than the basic material and the adhesive strength of the coating to the fabric is the limiting factor. Welded joints show considerable reduction in strength at high temperatures.

**Cementing** or the so-called gluing usually have very high strengths. The cemented area is often stronger than the bond between fabric and coating. As like the welded joints, the adhesive strength of the coating to the fabric is in many cases the limiting factor for determining the strength of cemented joints. Cementing joints are decreased in strength by higher temperatures. Cementing joints are often used in high pressure structures where sewn joints would leak.

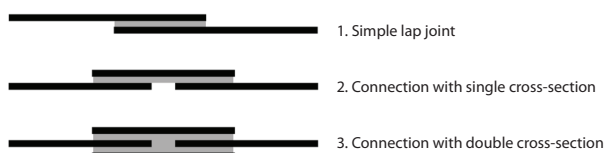


Figure 3.45: Welded and cemented joints

**Vulcanising** can be used for joining together rubber skins or rubberised fabrics.

**Riveting** is little used and is achieved by using pop-rivets placed at short intervals, while the inner fabric is pressed against the outer fabric at the point of overlap. This joining technique is not airtight.

**Clamping** is also a joining technique that is expensive and additional material is required. Metal clamps are equally deformed when applied, by using an air pistol at short intervals.

Herzog describes the following **separable** joints;

- Zip fasteners
- Press fasteners
- Lacings
- Peg joints
- Connecting strips
- Different combinations of clamps, springs, rings material loops or membrane belts with inserted cables, link chains etc.

These separable joints must be as airtight as possible when they lie between zones of different pressure. If several individual inflatable structures are joined together and the same pressure applies inside the building as outside, then the bondings only have to satisfy mechanical requirements.

## ANCHORAGE

The possibilities of anchorage of the inflatable structures to the ground or other structural elements are too wide to describe, and a case-dependent solution is required to be developed.

## 3.4.8 CRITERIA

In this chapter the materials and their properties and performances are elaborated. The goal is to have a well-argued choice of material for the production phase. Therefore, based on a set of criteria, the most suitable material for the secondary mould has to be determined. As explained earlier, the inflatable structure can be distinguished in two types of inflatable moulds.

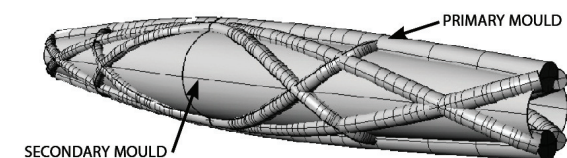


Figure 3.46: Model with primary and secondary mould

The inflated structure consists of the secondary mould, which is the low-tech inner inflatable tube and, and the primary mould which is the rigidizable structural element. Here, the main function of the secondary mould is to serve as falsework for the primary mould. It forms a circular shape on which the prima-



ry moulds are fixed and it has to adopt the bending forces of the structure. The function of the primary moulds is to transfer the tensile and compressive forces to the support points. Since functions of the moulds differ, the requirements on the material differ, and for each mould a set of criterium can be determined.

The envelope materials for lightweight structures may be required to have a wide range of properties which contain several incompatibilities. The required properties that are needed, determine the choice of material and therefore the type of fabric or films. However, it is often not possible to completely satisfy all these requirements in one material so that a compromise is generally necessary. A possibility to satisfy the required properties is to select coatings, fabrics or films that meet the different aspects of the requirements. Therefore, the level of satisfaction of the required properties is determined by their performance on the different criteria. Many criteria can be found in literature with different importance for the material choice. Therefore, a selection of criteria has to be made and their corresponding weight factors have to be determined. Here, the performance of a material on the criteria can have a certain value, and materials can be rated on their compatibility for the secondary mould. Also, a distinction has to be made on materials that are incompatible on beforehand, to have a smaller selection of possible materials.

#### SECONDARY MOULD

The secondary mould is the inner inflatable, on which the outer tubes are fixed. A wide range of envelope materials can be considered, but only few materials are suitable. An exclusion of several materials can be made for further elaboration based on major drawbacks of the material.

Some major drawbacks are found in literature for an exclusion of several materials for the case. The first drawback is that it is not possible to use a film or a uncoated fabric because the films are not strong enough and the fabrics are not sufficiently durable and impermeable. So, it becomes necessary to use a coated fabric or a reinforced film. Though, reinforced films are not often used in lightweight structures and are mainly applied if a high light transluence is required. A requirement that is not relevant for the secondary mould and therefore the coated fabrics are preferable. Besides uncoated fabrics and films, the high tech materials are of no interest for the secondary mould based on their low availability and high costs. Eventually, a first exclusion of envelope materials based on the previous arguments is made for the secondary mould. The coated fabrics are the most suitable materials of all the possible envelope materials. The following envelope materials are considered:

- PVC Coated Polyester
- PVC Coated Aramid
- PTFE Coated Fibreglass
- Silicone Coated Fibreglass

After the first exclusion of materials, criteria have to be formulated with their corresponding weight factors. Naturally, the corresponding weighing factors are somewhat subjective since the criteria are case specific and there are no direct references.

1. Cost
2. Simplicity to manufacture
3. Availability
4. Mechanical properties
5. Foldability
6. Air permeability
7. Dimensional stability
8. Lifetime
9. Maintenance
10. Flame performance

The ten criteria described above are considered as the most important criteria for a thoughtful consideration of envelope materials for the secondary mould.

#### WEIGHT FACTORS

The criteria described above are ordered from the most important to the least important. For a uniform weighing of factors there are four possible values per criterium; bad, acceptable, good and excellent. These represent the performance of the material in comparison with the other materials. Here every material can take any value per criterium, with the exception that the best performing material can score excellent in any given criterium. The weight factors are as follows:

Criteria	Weight factor
1,2,3	3
4,5,6,7	2
8,9,10	1

Table 3.5: Weight factors

Since the secondary mould is a low-tech inflatable, requirements are focussed on the production of a low budget and easy to manufacture mould, which satisfies the requirements. Criteria as cost, simplicity to manufacture and availability are of great importance due to the budget. The following criteria as mechanical properties, foldability, air permeability and dimensional stability are focussed on the material performances. The less important criteria are based on the performance of the material over time, which only influences the case after years.

### 3.4.9 CONCLUSIONS



The multi-criteria table shows that the PVC Coated polyester is the most satisfying material on the requirements of the secondary mould. Therefore, the **PVC Coated polyester** will be applied as envelope material for the secondary mould.

The envelope material for the primary mould is derived from a consideration of the most satisfying combinations of rigidizable materials and envelope materials. This consideration is made in chapter 5 Synthesis.

Criterion	W.F	PVC Coated Polyester	PVC Coated Aramid	PTFE Coated Fibreglass	Silicone Coated Fibreglass
Low cost	3	excellent <sup>1,2</sup>	bad <sup>3</sup>	acceptable <sup>1,2</sup>	good <sup>3,9</sup>
Simplicity to manufacture	3	excellent <sup>2,4</sup>	bad <sup>2,5,6</sup>	acceptable <sup>2,3</sup>	good <sup>3</sup>
Availability	3	excellent <sup>1,2,3,4</sup>	bad <sup>2,3,5,6</sup>	excellent <sup>1,2,3</sup>	bad <sup>3</sup>
Mechanical properties	2	good <sup>2,3,8,9</sup>	excellent <sup>2,3,5,6,9</sup>	good <sup>2,3,8,9</sup>	good <sup>3,9</sup>
Foldability	2	excellent <sup>2,3,4,9,10</sup>	good <sup>3,7,10</sup>	bad <sup>2,3,4,9,10</sup>	good <sup>3,9,10</sup>
Air permability	2	good <sup>8</sup>	good	good <sup>8</sup>	excellent <sup>4,8</sup>
Dimensional stability	2	good <sup>2,3,8</sup>	good <sup>2,3,8</sup>	excellent <sup>2,3,8</sup>	good <sup>3,8</sup>
Lifetime	2	good <sup>2,3,8,10</sup>	good <sup>5,6</sup>	excellent <sup>2,3,8,10</sup>	excellent <sup>3,10</sup>
Maintenance	1	acceptable <sup>3,10</sup>	acceptable	excellent <sup>3,10</sup>	acceptable <sup>3,10</sup>
Flame performance	1	good <sup>3,10</sup>	good <sup>5,6</sup>	excellent <sup>3,10</sup>	excellent <sup>3,10</sup>

TOTAL POINTS	73	46	62	61
--------------	----	----	----	----

- 1) van der Vegt, A.K., Govaert, L.E. 2003
- 2) Habraken 2011
- 3) Houtman 2000
- 4) Herzog 1976
- 5) Wesdorp 2005
- 6) Veldman 2005
- 7) Meijer 2007
- 8) Reid, O'Brien
- 9) Sobek, W., Speth, M. 1993
- 10) Houtman 1996

	Value derived out of the literature
	Value determined by authors
excellent	4 points
good	3 points
acceptable	2 points
bad	1 point

The main goal of the research into inflatable structures was to determine in which way an inflatable structure could be used as falsework to support the fabrication of structurally optimized elements, i.e. research question 2. The synthesis of this chapter is partially independent, and partially interdependent on the synthesis of the chapter 2. Since the research follows a funnel, the syntheses of the different chapters become more and more interdependent.

#### RQ 2:

*In which way can an inflatable structure be used as falsework for the production of structurally optimized section active elements?*

Pneumatic structures are among the most common and efficient structures in living and inanimate nature. It consists of a ductile envelope which is capable of supporting tensile stress and is internally pressurized with respect to its surrounding medium. Technical pneus, or inflatable structures, were first used in hot air balloons since 1783 by the Montgolfier brothers and are studied ever since. Basically, an inflatable structure consists of the following principal elements;

- Envelope
- Content
- Medium
- Internal bracing
- Pressure difference

The envelope refers to the membrane material used to establish the pressure difference between the content (often water or air) and the surrounding medium (often water, air or vacuum). The content becomes the supporting medium and therefore a structural element, where the resulting structure becomes a load bearing inflatable structure. Even though inflatable structures are known to be very flexible, the collection of potential shapes is actually limited. Since inflatable structures have to adapt to force equilibrium, they have to conform to funicular shapes. However, their inflated shape can be manipulated by pulling or pushing other elements on the envelope. In addition, by the use of cutting patterns complex shapes can be fabricated. The collection of potential inflatable shape or typologies can be classified according to several parameters. By determining the formation of the membranes, the kind of pressure and the kind of additional support, five main inflatable typologies are distinguished;

1. Single membrane structures
2. Double membrane structures
3. Straight high pressure systems
4. Buckled high pressure systems
5. Arched high pressure systems

These five typologies can be assessed according to four morphological indicators necessary to compare the typologies to optimized structures. An inflatable envelope can either be termed open or closed depending on the continuity of the membrane. The structure itself can also be open or closed, however, closed inflatable structure such as sails are outside the scope of this research. The second criterium is the proportion of the structure, where the dominant direction is determined, followed by the type of curvature. The fourth and final criterium is the pattern of the structure, which is either straight, buckled or arched.

Structure [S]	open [O]		closed [C]
Proportion [PP]	1 dominant [1 <sub>2</sub> ]	2 dominant [2 <sub>1</sub> ]	3 equal [3]
Curvature [CU]	mono [M]	syn [S]	anti [A]
Pattern [PA]	straight [S]	buckled [B]	arched [A]

Table 3.6: Morphological indicators

The five typologies were assessed according to these criteria and finally compared to the optimized section active elements to determine which typology can best be used as falsework.

#### CRITERIA

The criterium concerning an open or closed membrane of the inflatable is compared to an open or closed structure of the optimized element. Here, an open or closed optimized structure must not be confused with an open or closed inflatable structure, since all inflatable structures are closed. Per definition, the combination of a closed structure and an open membrane is not possible.

Naturally, many different forms of optimized section active structure systems<sup>1</sup> can be the subject of a design and production process. However, it makes no sense to compare each separate case with every inflatable typology. Therefore, one representative<sup>2</sup> case of every optimized structure system was selected during the case studies in Inspire;

- Circular one-bay beam with fixed supports  
The members of the optimized circular beam run in helical form around the beam, making it a closed structure. The beam has two equal dimensions, and one larger dimension which is therefore dominant. The pattern of the beam is obviously straight.
- One-bay frame structure with an optimized design space  
A frame structure has no continuous members and therefore does not form a closed structure. It has 2 dimensions of similar size and one dimension which is larger. Here, the arched pattern and the



monoclastic curvature of the interior is clearly visible.

- Uniform slab with fixed supports

The members of this slab are not continuous and therefore do not form a closed structure. Per definition, a slab has two dimensions of similar size and one dimension that is significantly smaller. In between the two edge beams, arched members run from side to side. Therefore, the interior of the slab (in other words the underside) is monoclastic.

Beam grid structure systems are not treated separately, since they are simply a composition of beam structures.

### THE MATRIX

Now that all the different variables are revealed and explored, they can be compared to each other. This is done in the form of the matrix displayed in figure 3.48. Here, the values of the parameters are used as criteria to determine which inflatable typology best reflects the morphological features of structurally optimized section active structure systems. Common values, i.e. attributes, are marked green. Hereby, the most promising combinations can be spotted at one glance. Of course, other factors also influence the “utility” of a combination. However, by using this matrix the most promising combinations are filtered out easily. The designer himself should then see if the proposed inflatable typology is actually the best typology to use as a secondary mould based on case specific requirements and boundary conditions.

The matrix shows that if one would like to construct an optimized beam structure, the best inflatable typology to use as a secondary mould is a straight high pressure system. The two other high pressure systems also have many common features. However, their pattern makes them less suited for constructing an optimized beam structure. Therefore, the pattern of the elements is in this case the decisive criterium.

In the case of a frame structure, the best inflatable typology to use is a single membrane structure. In the case of this structure system, the nature of the structure (open or closed) is the decisive criterion. One could argue to use an arched high pressure system instead. Especially when rigidizable materials with a high density are used, a high pressure system could be a better solution since it is able to transfer larger loads. Also, when a frame with a smaller span is the case, the arch pattern is not yet clearly visible. In this case, a buckled high pressure system could be a better solution. This shows that the matrix should only

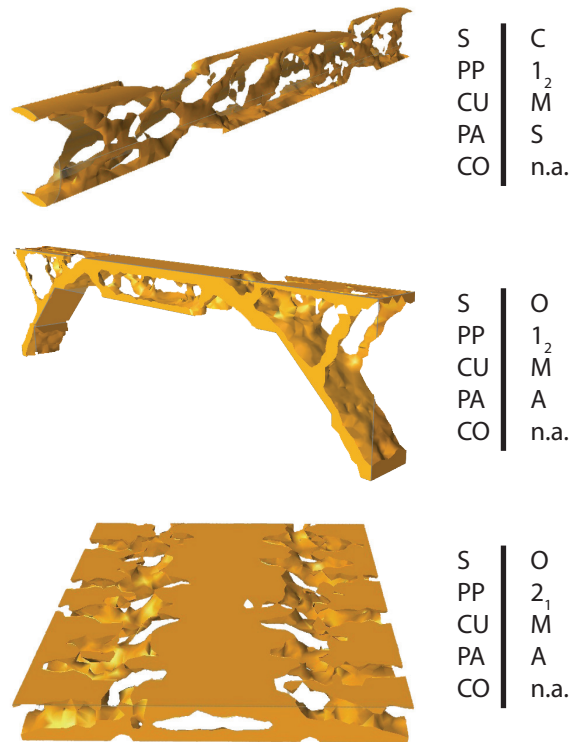


Figure 3.47: The representative structure systems assessed according to the four criteria.

be used as a guideline to point out promising solutions. The best combination always depends on case specific requirements and boundary conditions.

In the case of a slab not one combination has a match in all four criteria. Here, the decisive criterion is the proportion of the optimized structure and inflatable. Since the proportion of double membrane structures and uniform slabs match they are the best combination, even though single membrane structures have an equal number of common features. The use of a single membrane structure would lead to an inefficient use of membrane material due to difference in proportion.

### MEMBRANE MATERIALS

Membrane materials can be divided into isotropic materials, or films, and anisotropic materials, or fabrics, which can either be coated or uncoated. Some major drawbacks are found in the literature regarding the strength and permeability of films and uncoated fabrics. Films are typically not strong enough and the uncoated fabrics are not sufficiently durable and permeable. So, it becomes necessary to use a coated fabric or a reinforced film. Though, reinforced films are not often used in lightweight structures and are mainly applied if a high light transmittance is required, which is not the case for the secondary mould. In ad-

1. For example varying constraints such as support type or slenderness leads to different morphologies  
 2. See chapter 2.5

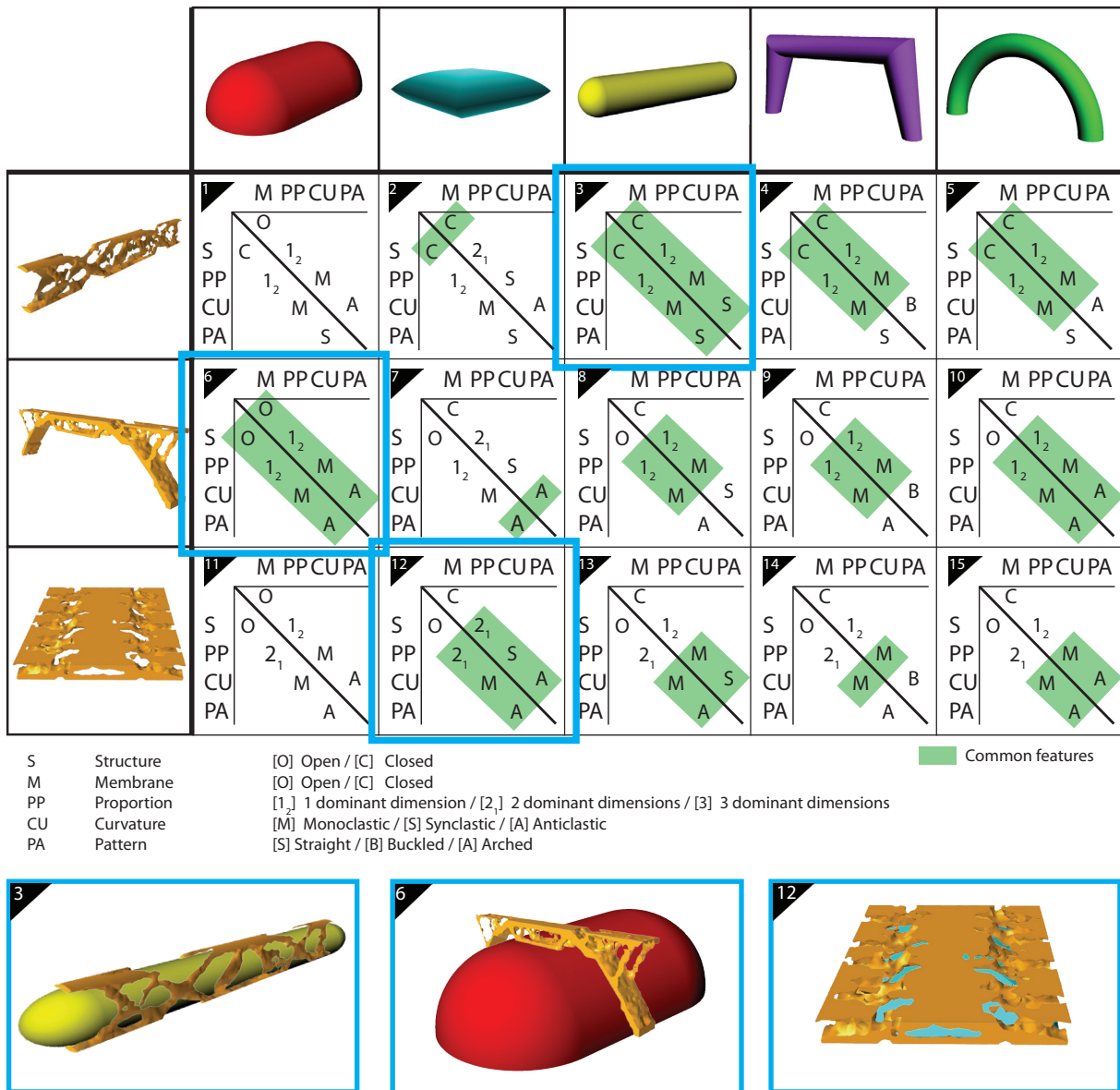


Figure 3.48: Matrix describing the most suitable combinations of inflatable typologies and optimized elements

dition, some high technology fibres, such as Vectran and PBO, used mainly in the aerospace industry can be considered to specific and expensive for our purpose. Therefore, the following envelope materials were considered and assessed according to ten relevant criteria;

- PVC Coated Polyester
- PVC Coated Aramid
- PTFE Coated Fibreglass
- Silicone Coated Fibreglass

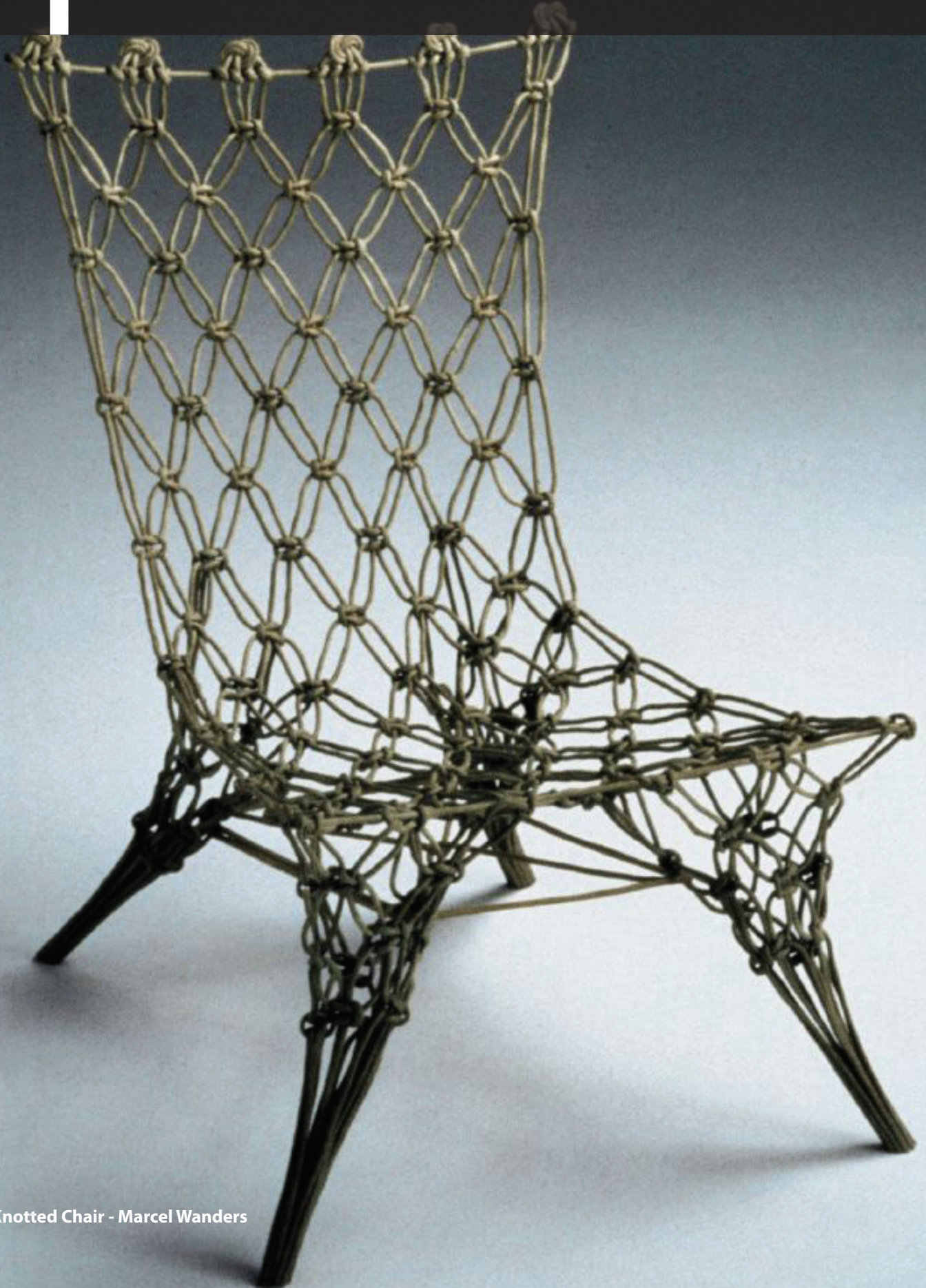
The criteria were assigned different weight factors displaying their relevance. Here, the cost, manufacturing complexity and availability were the most important criteria, rendering PVC coated polyester to be the best solution.





# 4

## Rigidization methods



Knotted Chair - Marcel Wanders

The main goal of the third research topic is to reveal which rigidizable materials exist, and determine which one is best suited for our purpose.

### Which rigidization method is best suited for producing the case derived in RQ1?

The answer to this question will result from an analysis into the requirements and conditions of rigidizable materials, and an in depth literature review into the state of the art of rigidizable materials. Parallel to the literature reviews several experts in the field of rigidizable materials were consulted to evaluate the results. The corresponding sub-research questions are therefore the following;

#### SRQ 3.1:

Which requirements, conditions and properties do rigidizable materials have to conform to?

#### SRQ 3.2:

Which rigidization methods exist?

It is important to closely define the boundaries of the study into rigidizable materials, since essentially every material that solidifies could be a rigidizable material. Pronk (2013) defines four materials that can make the transition from fluid to solid, and are suited for rigidizing a membrane;

- Concrete / cement based composites
- Ice / water
- Polymer composites
- Glass

Ice and glass are omitted from further investigation for obvious reasons. Concrete and cement based composites are also considered unfeasible mainly due to weight issues. The focus of the study into rigidizable is therefore on polymer based composites. Within the field of polymer composites three main sub categories can be distinguished; i.e. particle and fibre reinforcement and structural composites (Budinski & Budinski 2002). Assessing these sub groups on the type of reinforcement used leads to six different typologies of polymer composites (Figure 4.1). Here, woven fabrics represent the largest typology in products such as carbon-epoxy or glass fibre-epoxy composites. Examples of composite products using structural reinforcements are sandwich panels and honeycomb panels.

Our case calls for a lightweight rigidizable composite materials which can be rigidized on command. This research therefore focuses on continuous fibre reinforced composites, due to their structural performance, compatibility with available production methods and possibility to case specific tailoring due

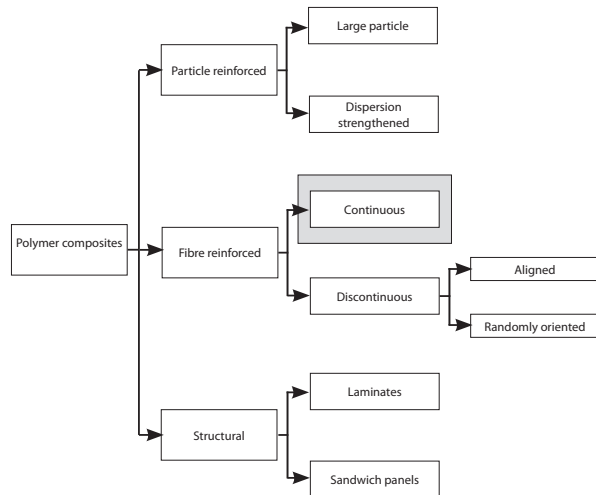


Figure 4.1: Classification of composite types (Kakani 2004)

to different weaving techniques.

An important field of study of these composites is the space industry where several rigidization techniques have been studied since the 1950's for the rigidization of inflatable structures in space (Gossamer structures). First the basic structure and characteristics of polymer composites will be explained, followed by a review of manufacturing methods used for the fabrication of commercially available continuous fibre reinforced composites. In addition, a thorough review of the state of the art of rigidizable materials for space application is performed.

## 4.2.1 STRUCTURE

Due to rapid developments in computer aided design and computer aided engineering people now have very powerful tools for designing structures with single or even double curvature. These shapes require materials with an unusual set of properties which cannot be met by conventional construction materials such as steel or concrete (Kakani 2004). Especially in the aerospace sector engineers are search-



Figure 4.2: Aeroplane composite part by Kaman Composite Structures

ing for materials with a low density, high strength and stiffness, and corrosion resistant (Figure 4.2).

A composite is by definition composed of two or more different materials, with the whole being stronger than the sum of the parts. Woody plants and trees are examples of composites found in nature. The first man made composites were documented on Egyptian tomb paintings and described bricks which were made from a combination of mud and straw. The first artificial composite was patented in 1909 under the name Bakelite, after its American inventor Leo Baekeland. A good definition of a composite material is given by Kakani (2004);

*“A composite is considered to be any multiphase material that exhibits a significant proportion of the properties of both constituent phases such that a better combination of properties is realized, also termed the principle of combined action.”*

Polymer composites generally consist of a matrix material which ensures curing, and a fibrous reinforcement. Depending on the nature of the matrix material, it is either termed thermoplastic or thermosetting. Thermoplastics have the distinct advantage of having a reversible curing process. When the material is heated above its glass transition temperature (second order) it will become fluid. This process of reheating can be repeated as many times as desirable without performance loss. Examples of thermoplastic matrix materials generally used for polymer composites are (Budinski & Budinski 2002);

- Polyetherimide
- Polyphenylene sulfide

- Polyether sulfone

In most cases a thermosetting matrix material is used. Often used materials are (Budinski & Budinski 2002);

- Epoxy
- Unsaturated polyester
- Phenolic
- Polyimide

As explained in Figure 4.1, the fibre reinforced can either be continuous, discontinuously aligned or random discontinuous. This study limits itself to continuous fibrous reinforcements since it is important to be able to control the direction of the fibres. Typically, reinforcements make up 20% - 50% of the weight of commercial composites. However, weight fractions up to 70% are also possible (Budinski & Budinski 2002). Typical reinforcement materials, which were already discussed in chapter 3.4, are;

- Polypropylene
- Aramid
- Graphite
- Glass
- Metal
- PBO
- Vectran

In these composites, the matrix material transfers the loads to the fibres which absorb the stress. The bonding between the matrix and the fibres determine the strength of the composite. The higher the aspect ratio<sup>1</sup> the stronger the composite. Therefore, longer continuous fibres yield stronger and stiffer composites than shorter discontinuous fibres. A minimal fibre length is necessary to achieve an effective composite, which is determined using the following relation (Budinski & Budinski 2002);

$$l_c = \frac{\sigma_f d}{2\tau_c} \quad 1.1$$

where;

- $l_c$  = critical length
- $\sigma_f$  = Ultimate tensile strength of the fibre
- $d$  = fibre diameter
- $\tau_c$  = fibre - matrix bond strength<sup>2</sup>

Typically, when the length of the fibre is at least fifteen times the critical length (1.1) it is called continuous. These fibres can be oriented in one, two or three directions (§ 3.4.2). An optimal fibre distribution ensures that fibres are woven in such a manner that

1. The aspect ratio is the relation between the length and the diameter of the fibre.
2. Or the shear yield strength

their longitudinal direction faces the areas of highest stress. Fibres are much stronger in their longitudinal direction than their transverse direction (Table 4.1). Therefore, for single or double curved structures biaxial or triaxial weaves are preferred over uniaxial weaves since they are better suited for absorbing bending and torsion moments which are typical for curved structures.

Material	Longitudinal tensile strength [N/mm <sup>2</sup> ]	Transverse tensile strength [N/mm <sup>2</sup> ]
Glass - Polyester	700	20
Carbon - epoxy	1000	35
Kevlar - epoxy	1200	20

Table 4.1: Longitudinal and transverse tensile strength for some unidirectional fibre reinforced composites (Kakani 2004)

#### 4.2.2 CHARACTERISTICS

Composites have characteristics which differ from traditional construction materials. Some important characteristics are listed below (Kakani 2004);

1. Composites have higher specific strength and stiffness properties than all other materials (Table 4.1). Here, specific means the tensile strength or modulus divided by the density of the material. This yields a measure for how strong or stiff the material is compared to its weight, which is a very important property of composites.
2. Composites can be tailored to meet case specific requirements by changing the orientation, distribution and properties of the fibres used.
3. The strength of a composite is greater than the sum of the strength of the parts by which it is comprised.
4. The matrix material is the bonding and shaping agent which is initially fluid. Therefore, polymer composites can take on almost any shape when using the correct production technique.
5. The components of a composite differ strongly from each other and are mutually insoluble.
6. The manufacturing principle of composites has been borrowed from nature. For example in wood cellulose fibres are bonded by lignin.
7. The main strength of a composite is acquired through the bond between the matrix and the fibres.

These general characteristics render polymer composites a widely spread material in the aerospace and

automotive industry. These branches are continuously searching for light weight, high strength materials, pushing the boundaries of innovation. In the construction industry, composites are not used very often. The last few years some companies are using carbon sheets for reinforcing existing concrete structures which no longer meet the current building code.



Figure 4.3: Reinforcing an existing concrete bridge with carbon fibres (Freyssinet France)

#### 4.2.3 MANUFACTURING METHODS

Numerous manufacturing methods exist for the fabrication of all sorts of shapes and sizes of composite parts. Some methods are aimed at large quantities of similar elements, and some are better suited for producing smaller batches or prototypes. The following overview describes some relevant fabrication methods, and gives an overview of other available methods.

##### HAND LAY-UP

The most low-tech manufacturing method for producing composite parts is the hand lay-up method. Fibrous reinforcements are placed by hand over a mould and are then saturated with resin. This process is repeated until the desired thickness is achieved. This method is typically used for low quantity series, when it is not viable to produce a metal or composite mould, and when a high dimensional stability is not necessary. (Budinski & Budinski 2002; Manufacturing processes, n.d.).

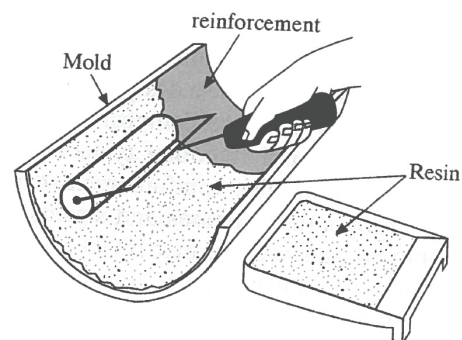


Figure 4.4: Hand lay-up method (Budinski & Budinski 2002)



An alternative of the hand lay-up method is the use of a spraying gun to speed up the process. Here, a chopper is incorporated in the gun to chop the fibres. At the nozzle the fibres are mixed with a resin and sprayed on a mould. Obviously this method is only suited for producing composite with discontinuous fibres.

#### RESIN TRANSFER MOULDING (RTM)

Due to the manual labour involved, the hand lay-up method is often considered to slow and labour intensive for high volume industrial purposes. Here, Resin Transfer Moulding or RTM is often used. This method uses two matching mould which fit tightly together, made of some kind of metal or composite. A preform is placed in between the two mould parts, after which the part is ready for injection. A resin and catalyst are mixed in the dispensing equipment right before it enters the part. Often the resin is injected under compression (3.5 - 7 bar), however Vacuum Assisted RTM (VARTM) is rapidly evolving since it does not require heat to cure (Fabrication methods, 2007). Very low viscosity resin is used to ensure proper saturation of the dry reinforcement. The main advantages of this method include fast cycle time, high dimensional stability, low cost and high surface smoothness. In addition, the method is suited for producing complex double curved parts. Disadvantages include the higher cost for the moulds, which also limit the size of possible parts. Also, the possible types of reinforcement are limited since a full saturation of the parts needs to be guaranteed (Manufacturing processes, n.d.).

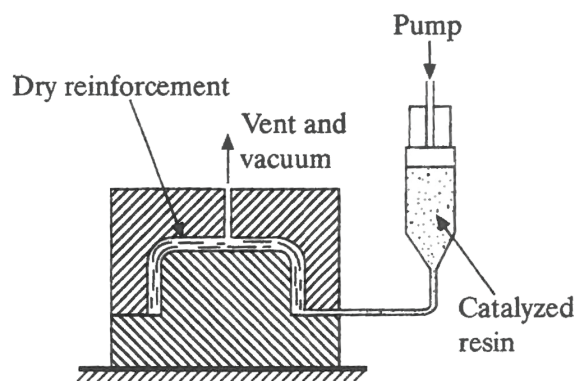


Figure 4.5: Resin Transfer Moulding (Budinski & Budinski 2002)

#### VACUUM BAG FORMING

This method was developed in order to eliminate the need for expensive matching metal mould as in resin transfer moulding. Here, atmospheric pressure is used to do the forming. Vacuum bag forming uses sheet moulding compounds (SMC) which are formed over a male mould using a bladder which is pulled over the mould using atmospheric pressure (Figure 4.6) (Budinski & Budinski 2002). Here, the resin (SMC) is introduced into the mould before the vacuum. A

variation to this method is Vacuum Infusion Processing (VIP), where the resin is introduced into the mould after the vacuum has pulled down the bag. The reinforcement is placed by hand onto the mould making this method slower than vacuum bagging using SMC's. However, since the resin introduced after the vacuum there is no room for excess resin rendering very dense parts. Also, large parts are possible using VIP with very complex shapes (Manufacturing processes, n.d.).

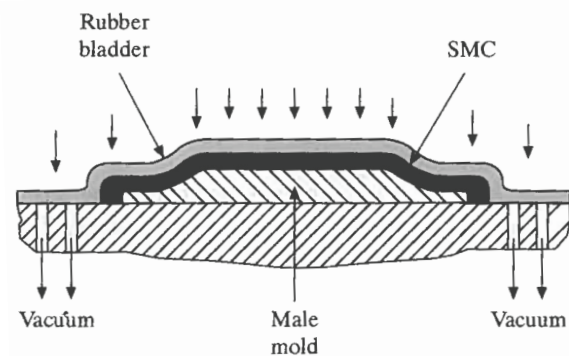


Figure 4.6: Vacuum bag forming (Budinski & Budinski 2002)

#### FILAMENT WINDING

This method uses continuous fibres, often glass, which are wound around a mandrel (Figure 4.7). The fibres are dipped in a resin bath just before they are placed on the mandrel. A head which leads the fibres moves up and down the mandrel placing the fibres in a predetermined configuration. The method can be highly automated and repeatable, and is therefore often used for large quantities. Parts often produced using filament winding include golf club shafts, fishing rods, pipes and other parts which require a high circumferential strength (Budinski & Budinski 2002, Fabrication methods 2007).

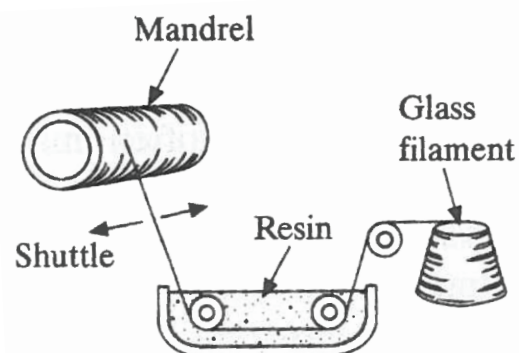


Figure 4.7: Resin Filament winding (Budinski & Budinski 2002)

#### COMPRESSION / INJECTION MOULDING

Compression moulding is a manufacturing process used for quantities between 10.000 and 200.000 parts.

It uses very expensive but highly durable metal dies and can produce parts very quickly and highly automated (Figure 4.8). The method uses sheet moulding compounds (SMC) or bulk moulding compounds (BMC) which are a dough like resin and chopped fibre paste.

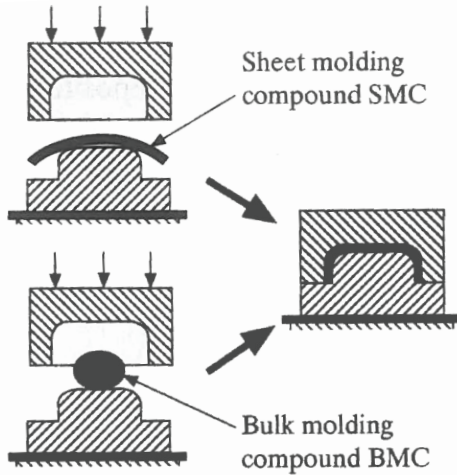


Figure 4.8: Compression moulding (Budinski & Budinski 2002)

#### PULTRUSION

This method employs resin impregnated fibres which are pulled through forming dies, and finally through a heated die where it takes its final shape. The process is continuous, relatively simple and low cost. It is used to produce structural parts such as I-beams or pipes. The method yields smooth parts with consistent quality and do not need post processing (Budinski & Budinski 2002, Fabrication methods 2007).

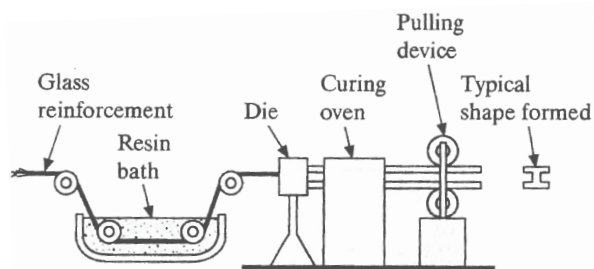


Figure 4.9: Pultrusion (Budinski & Budinski 2002)

#### AUTOMATED FIBRE PLACING (AFP) & AUTOMATED TAPE LAYING (ATL)

AFP can be considered the most complex method since it uses an articulated robotic head which can lay up to 32 tows of prepreg simultaneously. It is used to produce very complex parts where a high accuracy is required, such as sails (Figure 4.10). ATL has the advantage of being even faster since it uses a prepreg tape instead of single tows. This method is highly versatile and allows breaks in the process and easy direction changes (Fabrication methods 2007).

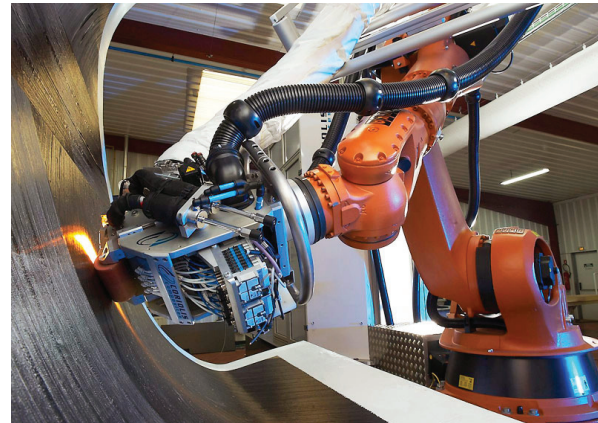


Figure 4.10 : Automated fibre placing by Lorient, 2011

#### CONCLUSION

The most important and most used commercial manufacturing techniques for fibre reinforced composites were briefly discussed in this paragraph. Of these seven techniques, filament winding, compression moulding and pultrusion are used for large quantities and highly automated processes, and are therefore outside the scope of this research. In addition, AFP and ATL can be considered to specific and expensive for our purpose. Therefore, the most promising manufacturing methods which could be used to produce the shape derived in RQ1 are hand lay-up, resin transfer moulding and vacuum infusion. These methods are suited for producing small quantities or prototypes, and are characterized by low cost and low complexity.

## 4.3.1 INTRODUCTION

As explained in the previous chapter, the extensive research of inflatable structures started in the 1960's. The study of these lightweight structures was not limited to applications on earth, but also found its way into the aerospace industry. Here, inflatable structures are used to construct (very) large lightweight structures in space. Their high potential as a successful construction method for space structures, especially compared to conventional mechanical structures, is due to their light weight, low cost and ability to be packed into small volumes (Cadogan et al 2001; Defoort et al. 2005; Freeland 1998; Marcos 2003). These so called "Gossamer Structures" are used for several applications in space, such as;

- Solar sails
- Sunshields (Figure 4.11)
- Solar arrays (Figure 4.11)
- Antennas
- Radars
- Mirrors

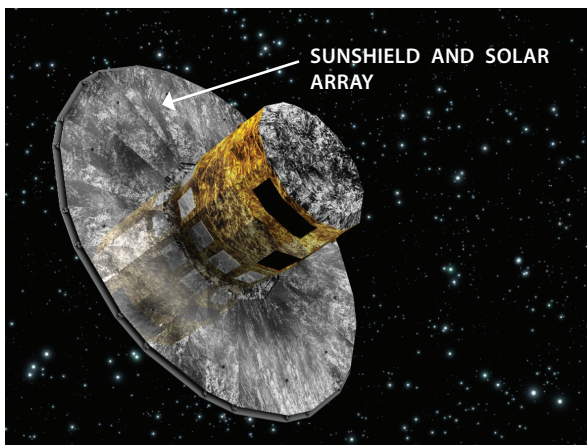


Figure 4.11: The GAIA telescope (Render by ESA)

Like inflatable structures for terrestrial purposes, Gossamer structures use some sort of inflation medium which is pressurized compared to its surrounding environment for deployment. Therefore, Gossamer structures inevitably lose this inflation medium through the fibres of the membrane material. In addition, micrometeorites which exist in the harsh space environment cause small punctures in the membrane. Therefore, space crafts have to carry an inflation device which keeps the pressure difference stable. This is not a problem for short term applications, or applications where pressurisation is a basic function<sup>1</sup>. It is generally said that Gossamer structures which will operate in space longer than one week will have to be rigidized (Defoort et al. 2005). Hereby, the structure no longer relies on a pressure difference for structural

1. For example space habitats
2. For example resin

integrity. To achieve this rigid structure which is independent of a pressure difference, so called "rigidizable materials" are used. A rigidizable material, as defined by Cadogan et al. (2001) in terms of Gossamer structures, is;

*"Materials that are initially flexible to facilitate inflation or deployment, and become rigid when exposed to an external influence"*

Here, an external influence can be heat, cold, ultra-violet radiation or the inflation medium itself.

## 4.3.2 CHARACTERISTICS

The extensive research of Gossamer structures for the past 50 years has led to several rigidization methods with different advantages and disadvantages. Most methods have been tested in laboratories, where promising techniques were also tested in vacuum chambers to simulate space conditions. However, only one method was demonstrated in space thus far. In the 1960's a rigidizable balloon satellite called Echo II used stressed aluminium for rigidization (Figure 4.12

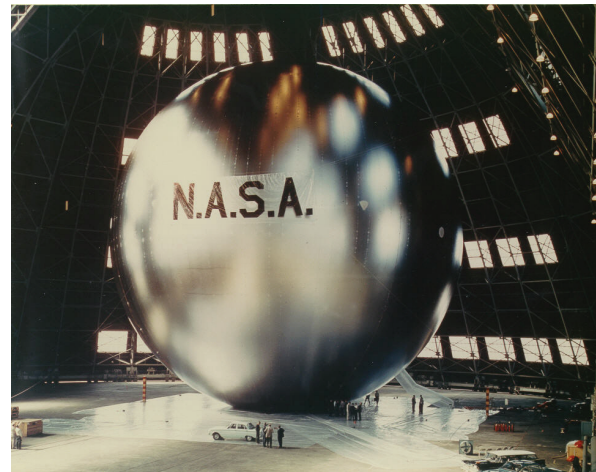


Figure 4.12: Echo II balloon satellite developed by the NASA

The methods for rigidization have stayed the same. However, the base materials which constitute the different methods are under continuous development, enhancing their performance. This is shown by the development of high tech fibres such as Kevlar, Kaptan, Zylon and Vectran. Basically, a rigidizable material, being composite in nature, consists of the following principal elements (Cadogan et al. 2001; Marcos 2003);













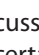
- Matrix
- Reinforcement(s)
- Supporting polymer film layer(s)






The matrix is the material that is responsible for rigidization, which is often some sort of resin or epoxy. The reinforcement is used to reinforce the matrix. Its thickness, number and properties can be tailored to meet case specific requirements. A reinforcement that is often used is graphite (carbon). The matrix together with the reinforcement is often called the pre-preg, which stand for pre-impregnated fabrics. The supporting polymeric films are used as restraint layers to maintain the desired shape, and as a gas seal.

By varying the number, properties, thickness and combination of these layers different performance characteristics can be achieved. This is necessary since different applications entail different material performances, mainly with respect to the structural performance of a rigidizable material. However, there are requirements which apply to rigidizable materials for Gossamer structures in general (Marcos 2003; Cadogan et al. 2001; Defoort et al. 2005; Jenkins 2005; Freeland 1998);

-  Rapid, predictable and controlled rigidization process
-  High specific strength and stiffness materials
  - Minimal energy required from the spacecraft for deployment and rigidization
  - Near zero coefficient of thermal expansion (CTE)
-  Allow rigidization in a wide range of thermal environments
-  No adverse effects from packaging or deployment
-  Long storage life (2+ years)
  - Limited outgassing
-  No shape deformation from deployment or rigidization process
-  Reversible
-  Compatible with associated materials
-  Simple to manufacture (compatible with manufacturing process / availability of material)
-  Low cost
-  Upscaling possible
-  Light weight
-  Compaction ability
  - High resistance to the space environment (vacuum, UV, atomic oxygen, electrons, protons)

A rigidizable material in terms of Gossamer structures should ideally meet all the requirements discussed above. However, this is not possible since certain requirements contradict one another in terms of material properties. Therefore, in the design of a rigidizable material, one should determine which requirements are decisive or most important.

At first, one might think that the detailed and specific requirements that apply to rigidizable materials

in space have nothing in common with requirements for rigidizable materials for earthbound applications. However, those requirements with a globe  in front, are also favourable for rigidizable materials for the construction industry. This shows that there is a high correlation between the requirements for rigidizable materials in terms of Gossamer structures and the construction industry, even though the two are fundamentally different. However, there is a difference between which requirements are normative. This will be discussed at the end of this chapter.

### 4.3.3 RIGIDIZATION TECHNIQUES

Based upon the nature of the phenomena that induces rigidization, rigidization technologies can be classified into three different categories (Defoort et al. 2005; Cadogan et al. 2001). These three technologies lead to seven different rigidization methods which will be discussed in the next chapter;

#### MECHANICAL RIGIDIZATION

This rigidization technology uses a pressure difference high enough to stretch a metallic layer in the envelope of the inflatable above its yield limit, rigidizing the structure. This technology knows only one rigidization method;

1. aluminium and film laminates.

#### PHYSICAL RIGIDIZATION

This technique uses a thermoplastic composite material which is initially flexible, and is cooled below its glass-transition temperature, basically freezing the matrix. Two rigidization methods can be derived;

2. Second order transition change and shape memory polymer composites
3. Plasticizer or solvent boil off composites

#### CHEMICAL RIGIDIZATION

This technique uses heat, UV radiation, a gaseous catalyst or foam for rigidization. In the case of foaming in space, the foam is also used in combination with other methods, for performance enhancement. Four methods can be derived;

4. Thermally cured thermoset composites
5. Ultra-violet cured composites
6. Inflation gas reaction composites
7. Foam rigidization

These seven rigidization methods will be discussed extensively in the this chapter. In addition, based on the requirements discussed in the previous paragraph, the most promising method will be determined.

4.4.1 ALUMINIUM AND FILM LAMINATES

Aluminium and film laminates is the only rigidization method that has ever been demonstrated in space (Figure 4.14). It is often considered the most simple rigidization method, and its principle has been unchanged since the 1906's. This method is comprised of thin layers of aluminium and polymeric film. The polymeric film used was often *Mylar*, but nowadays *Kapton* is often used due to its superior properties. The polymeric film is bonded to the aluminium by an adhesive. In most cases the aluminium is sandwiched in between the polymeric layers, but to improve the structural performance, the other way around is also possible. Often, a multi layered insulation blanket (MLI) is also used to protect the support tube laminate, i.e. the aluminium laminate, from the space environment (Cagogan et al. 2001; Jenkins 2005; Marcos 2003). A typical cross section of an aluminium laminate is shown in figure 4.13.

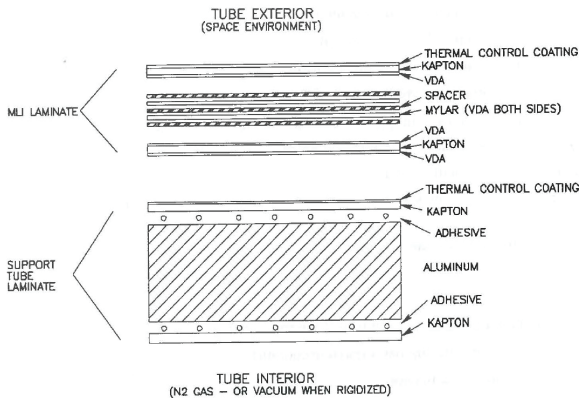


Figure 4.13: Typical cross section of an aluminium laminate (Jenkins 2005)

The two outside polymeric layers of the aluminium improve the tear resistance of the laminate and also function as an air tight seal. The laminate forms thin walled structures such as tubes and spheres. The method works due to the inflation pressure which stresses the aluminium just above its yield limit, into its plastic deformation range. Hereby, wrinkles are eliminated and the entire structure is rigidized. At this stress level, the polymeric film is still in its elastic deformation range. When the pressure is removed the material will contract slightly towards its original shape, putting the aluminium layer in compression thus essentially pre-stressing it. This phenomena reduces the overall load carrying capacity of the structure, but can be minimized by increasing the ratio of aluminium to polymeric film (Cadogan et al. 2001; Jenkins 2005; Defoort 2005).

EXAMPLES

As explained earlier, aluminium laminates are the only rigidization method ever demonstrated in space. NASA LaRC developed a 30 meter satellite called Echo

II in the late 1950's. They used a 1100-0 aluminium foil sandwiched between layers of Mylar. The method proved to work very well since Echo II orbited the earth for over five years.



Figure 4.14: Echo II balloon satellite by NASA LaRC, launched January 25 1964

The following pro's and con's apply for aluminium laminates in general. These advantages and disadvantages relate to the requirements for the construction industry. Therefore, any (dis)advantages relating to space applications only are omitted.

ADVANTAGES

- Most simple rigidization method that currently exists
- Rigidization is rapid and predictable
- Long storage life
- Reversible (not indefinitely)

DISADVANTAGES

- Thickness limitations of the aluminium layer (Thickness should not exceed 0.1 mm due to degradation by folding), therefore only suitable for carrying relatively low axial loads. Not suitable for carrying high compressive or bending loads.
- Defects due to packaging possible in the form of wrinkles resulting in shape deformation
- Rigidization pressure close to burst pressure, therefore increasing the risk
- Aluminium layer has a high CTE, therefore MLI blanket always necessary.

Property	Value
Materials used	- Aluminium 1100-0 or 3003-0 - Polymeric film (Kapton)
Modulus	68900 N/mm <sup>2</sup>

Table 4.2: Properties of aluminium laminates

#### 4.4.2 SECOND ORDER TRANSITION CHANGE & SHAPE MEMORY POLYMER COMPOSITES

Second order transition change materials use thermoplastic materials which are heated above their glass transition temperature ( $T_g$  or second order) for inflation, and are then cooled back down below their  $T_g$  for rigidization. Here, the matrix material is thermoplastic or lightly cross-linked, which is applied as a coating on a fibrous reinforcement. The fibres used as reinforcement are often glass, carbon, PBO or aramid. On the inside of the rigidizable structural material a bladder is applied which serves as an air tight seal. On the outside a restraint layer is applied which maintains the shape during inflation (figure 4.15). In most cases an MLI blanket is also used to protect the structure against the space environment, but also to enable a more controlled curing of the rigidizable structural material. In addition, the MLI blanket also prevents the structure from heating up softening post rigidization (Marcos 2003; Cadogan et al. 2001; Defoort et al. 2005)

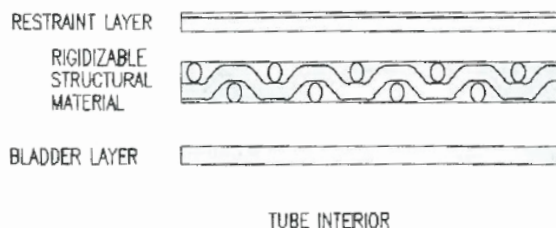


Figure 4.15: Typical cross section of an SOTC composite (Jenkins 2005)

The maximum operational temperature of the structure naturally needs to be below the  $T_g$  of the thermoplastic matrix that is used to prevent softening of the structure. The number, thickness and properties of the reinforcement layers can be tailored to enhance structural performance.

A special class of SOTC composites exist where the thermoplastic or lightly cross-linked matrix exhibits shape memory behaviour. Here, the structure is heated above a set temperature ( $T_s$ ) on the ground, cooled down below the  $T_g$ , heated again to a temperature above its  $T_g$  but below its  $T_s$ , and finally folded, packed and cooled again. Upon inflation, the structure will automatically restore to its original set shape when heated above the  $T_g$  (Cadogan et al. 2001; Marcos 2003).

#### EXAMPLES

Several examples exist of SOTC composites with and without shape memory behaviour. NTT Japan has proposed a rigidizable structure which uses a fibrous

thermoplastic matrix reinforced with glass fibres. They used four layers of fabric each consisting out of 15 strings of glass fibres in the weft direction, and 25 strings of polyamide fibre in the warp direction. The composite needed to be heated up 225 degrees<sup>1</sup> during five minutes before cooling and achieving rigidization. Also, a pressure of 19.6 kPa was necessary to force the matrix into the reinforcement. An overview of the proposed method is shown in figure 4.16 (Marcos 2003).

Structure:	Inflatable tube								
Manufacturer:	NTT Network Innovation Laboratories (Japan)								
Dimension:	✓ Long: 16 mm (1), 9,6 m (1) ✓ Diameter: 140 mm (1), 300 mm (1)								
Materials:	<table border="0"> <tr> <td style="padding-right: 10px;">Prepreg</td> <td>✓ 4 layers of co-woven fabric with 15 strings of glass fiber in weft and 25 strings polyamide fiber in warp, with fiber directions of 0°, ±45° and 90° (unknown origin)</td> </tr> <tr> <td></td> <td>✓ 995 g/m<sup>2</sup></td> </tr> <tr> <td style="padding-right: 10px;">Others</td> <td>✓ Bladder: FEP film 0,05mm</td> </tr> <tr> <td></td> <td>✓ Restraining layer: glass fiber fabric impregnated with a teflon resin. 0,1 mm.</td> </tr> </table>	Prepreg	✓ 4 layers of co-woven fabric with 15 strings of glass fiber in weft and 25 strings polyamide fiber in warp, with fiber directions of 0°, ±45° and 90° (unknown origin)		✓ 995 g/m <sup>2</sup>	Others	✓ Bladder: FEP film 0,05mm		✓ Restraining layer: glass fiber fabric impregnated with a teflon resin. 0,1 mm.
Prepreg	✓ 4 layers of co-woven fabric with 15 strings of glass fiber in weft and 25 strings polyamide fiber in warp, with fiber directions of 0°, ±45° and 90° (unknown origin)								
	✓ 995 g/m <sup>2</sup>								
Others	✓ Bladder: FEP film 0,05mm								
	✓ Restraining layer: glass fiber fabric impregnated with a teflon resin. 0,1 mm.								
Rigidization process:	<ol style="list-style-type: none"> <li>1. Inflation with gas at 19,6 kPa.</li> <li>2. To heat to 225°C during 5 min.</li> <li>3. To cool at room temperature</li> </ol>								
Development summary:	Rigidizable material for space inflatable structure is proposed, with low tack and long shelf life. Durability and foldability were evaluated and validated. Heating / restraint / MLI system must be developed. Laminates with more than three layers are necessary because each cloth becomes a uni-directional material after rigidization. Mass can become excessive.								

Figure 4.16: Overview of proposed method for a SOTC composite rigidizable material (Marcos 2003)

Multiple studies were also performed regarding SOTC with shape memory behaviour, including studies by ILC Dover (Cadogan et al. 2001) and L'Garde Inc (Guidanean & Lichodziejewski 2002). The latter included the development of a 7.3 meter long truss which weight only 4 kg.



Figure 4.17: SOTC with shape memory truss (Guidanean & Lichodziejewski 2002)

1. Other examples exist where the  $T_g$  is much lower, ranging from 30 to 50 degrees Celsius (Guidanean & Lichodziejewski 2002)



The following pros and cons apply for SOTC and SMP polymer composites in general. These advantages and disadvantages relate to the requirements for the construction industry. Therefore, any (dis)advantages relating to space applications only are omitted. It has to be noted that the literature disagrees on the need for auxiliary equipment when deploying a SMP composite structure. Cadogan et al. notes that the self deployment stress generated by the SMP is relatively low, and will therefore also need an augmentation device. Other authors state this is not necessary (Marcos 2003; Guidanean & Lichodziejewski 2002; Defoort 2005). In addition, Cadogan (2001) states that near zero CTE is possible, while Defoort et al. (2005) states that the CTE of the resins is a serious drawback.

#### ADVANTAGES

- Fully reversible
- Long storage life
- Self deployable
- High strength and stiffness possible due to tailoring of the composite
- Near zero CTE possible

#### DISADVANTAGES

- Power required for heating the material above  $T_g$
- Complexity of the method (material design and methods of application)
- Size limitations when using SMP
- Uniform heating required, therefore many control functions necessary
- CTE of the resin
- Working temperature needs to be below the  $T_g$

1 Material used	
Matrix	Resin - TP 275 ( $T_g = 100\text{ }^\circ\text{C}$ ) - TP 277 ( $T_g = 75\text{ }^\circ\text{C}$ ) - CTD DP-7AR ( $T_g = 92\text{ }^\circ\text{C}$ ) - L'Garde L5 resin ( $T_g = 43\text{-}53\text{ }^\circ\text{C}$ )
Reinforcement	- Glass - Carbon - PBO - Aramid
Supporting films	- FEP - Kapton

2 Typical compressive properties 24 x 24 5HS, 1K tow GR / TP 275 Areal Density: 225g/m <sup>2</sup>	
Strength (warp)	117 N/mm <sup>2</sup>
E-Modulus (warp)	43400 N/mm <sup>2</sup>
Resin content by weight	41%
Ply thickness	0.12 mm

3 Typical compressive properties Unidirectional GR / TP275	
Strength (warp)	350 N/mm <sup>2</sup>
E-Modulus (warp)	103000 N/mm <sup>2</sup>
Resin content by weight	39%
Ply thickness	0.12 mm

Table 4.3.2 and 4.3.3: Typical properties of an SMP SOTC composite material (Cadogan et al. 2001)

#### 4.4.3 PLASTICIZER OR SOVENT BOIL OFF COMPOSITES

Plasticizer and solvent boil off composites use a fibrous reinforcement, often glass or carbon, which is impregnated with a water-soluble resin which combined forms the prepreg. Its structure is similar to second order transition change composites, where the restraint layer needs to be permeable to the softening agent, i.e. the space environment. Before deployment, the material is kept in an environment which prevents the softening agent from evaporation (high humidity, atmospheric pressure etc). When the material is exposed to the space environment, the softening agent evaporates, leaving a rigid structure. Because of its simplicity, this method has been widely studied for the use in Gossamer structures. Also, after deployment rigidization can be reversed simply by re-wetting the material. However, a major downside of the method is the large loss of mass (upwards of 20%) due to evaporation of the softening agent, limiting the possibilities of the method (Cadogan 2001; Defoort et al. 2005).

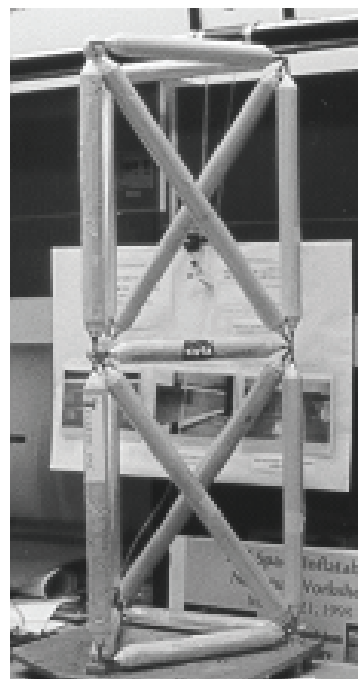


Figure 4.18: Rigidizable truss using solvent boil off of composites (Guidanean & Williams 1998)

## EXAMPLES

Several studies were performed using this rigidization method. One interesting study was done by JPL/L'Garde Inc. and NASA in 1998 (Guidanean & Williams 1998). This study focussed on the development of an inflatable rigidizable truss with complex joints (Figure 4.18). For the rigidization method they used a composite material consisting of a fabric and a water-soluble resin. Testing of the truss showed promising results regarding stiffness and compression properties.

The deployment of the truss developed by JPL was also tested in a vacuum chamber. Here, the material was initially stored in a pressurized box to prevent the material from premature rigidization. This phenomenon is caused by the fact that the boiling point of a liquid, such as water, decreases when the ambient pressure increases (Figure 4.19). The high vacuum that exists in space, causes the matrix softening agent to evaporate at much lower temperatures than on earth. This decreases the possibilities for this rigidiza-

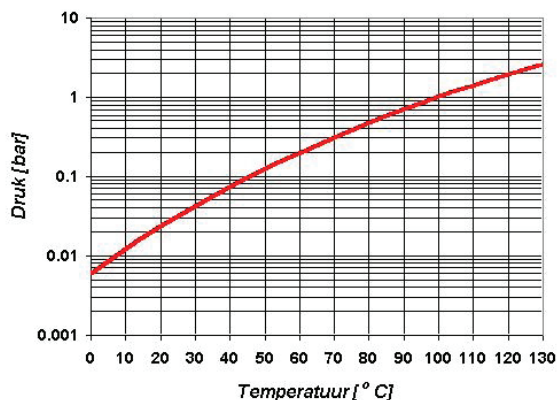


Figure 4.19: Relation between the temperature and vapour pressure of water

tion method for terrestrial applications significantly. The main advantages of this method is the reversibility, package-ability and ability for tailoring due to its laminar design. However, the large mass loss due to evaporation of the solvent is a large downside. In addition, the very nature of the method and the influence that induces rigidization limit its possibilities for terrestrial applications drastically. Therefore, this method will be omitted from further investigation.

### 4.4.4 THERMALLY CURED THERMOSET COMPOSITES

This class of rigidizable materials have only been studied extensively for the last decade. Right now, they are probably the most promising for space applications. It didn't receive much attention during the first decades of rigidizable material research, due to

the unavailability of suitable materials. This changed with the development of high strength fibres such as Carbon, Kevlar, Zylon and Vectran (Cadogan et al. 2001).

The structure of a thermally cured thermoset composite is similar to thermoplastic and solvent boil off composites. Kapton is used as a gas seal on the inside, and as a restraint layer on the outside. Usually the heater assembly layer is incorporated in the restraint layer. The rigidizable structural materials is a prepreg of a fibre reinforced matrix, often carbon/epoxy. The material rigidizes when heated to a specific temperature (Usually between 120 °C and 180 °C (Marcos 2003)) for a specific amount of time (one to several hours). The heat required for rigidization can either be by solar radiation or by embedded heaters. The latter was developed by ILC Dover inc during the nineties and has the major advantage that the curing process is very controlled and uniform. In most cases a MLI blanket is required to contain the heat during rigidization, and to protect the material against the space environment. The composite can be tailored to meet specific requirements by changing weave styles, layer orientation and number and thickness of layers (Cadogan et al. 2001; Marcos 2003; Defoort et al. 2005; Jenkins 2005).

## EXAMPLES

ILC Dover inc. has done much research in the field of thermally cured composites. Recently they developed an inflatable sunshield in space (ISIS). This sunshield consists out of a diamond shaped membrane supported by thermally cured inflatable booms, which deploy out of a rectangular fixed box (Figure 4.20). The boom have a length of 1.94 m, 4.21 m and 5.54 m and a diameter of 130.18 mm. Some details of the study are given in figure 4.21.

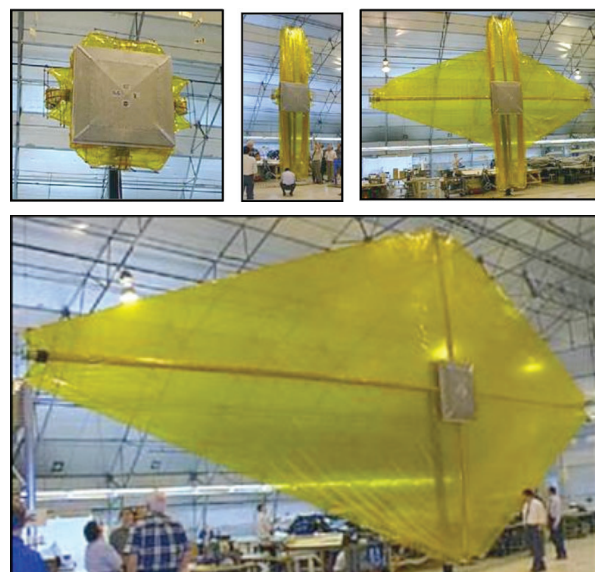


Figure 4.20: Inflatible Sunshield In Space (ISIS) by ILC Dover inc. for the Next Generation Space Telescope (NGST).



Structure:	ISIS sunshield booms				
Manufacturer:	ILC Dover, Inc. (EEUU)				
Dimension:	<ul style="list-style-type: none"> <li>✓ Long: 1,94 m - 4,21 m - 5,54 m</li> <li>✓ Diameter: 130,18 mm</li> </ul>				
Materials:	<table border="0"> <tr> <td style="vertical-align: top;">Prepreg</td> <td> <ul style="list-style-type: none"> <li>✓ 0,305 mm thick 12x12 square weave AS4 carbon fiber fabric impregnated with high latency epoxy resin (own development)</li> <li>✓ 45-50% fiber volume fraction</li> <li>✓ CTE: <math>1,8 \times 10^{-5} / ^\circ\text{C}</math></li> </ul> </td> </tr> <tr> <td style="vertical-align: top;">Others</td> <td> <ul style="list-style-type: none"> <li>✓ Bladder: 0,025 mm Kapton VN film</li> <li>✓ Heater/restraint: 0,051 mm Kapton VN film, and a resistance alloy wire heater for prepreg curing with a capacity of 155 W/m<sup>2</sup></li> <li>✓ End caps: machined ULTEM polyetherimide PEI</li> <li>✓ MLI: Inner and out layers are 0,051 mm Kapton film, VDA coated on the internal side only. Between these are five layers of 0,0076 mm Kapton film, VDA coated both sides. Each of these layers are separated from each other by a thin Dacron spacer fabric</li> </ul> </td> </tr> </table>	Prepreg	<ul style="list-style-type: none"> <li>✓ 0,305 mm thick 12x12 square weave AS4 carbon fiber fabric impregnated with high latency epoxy resin (own development)</li> <li>✓ 45-50% fiber volume fraction</li> <li>✓ CTE: <math>1,8 \times 10^{-5} / ^\circ\text{C}</math></li> </ul>	Others	<ul style="list-style-type: none"> <li>✓ Bladder: 0,025 mm Kapton VN film</li> <li>✓ Heater/restraint: 0,051 mm Kapton VN film, and a resistance alloy wire heater for prepreg curing with a capacity of 155 W/m<sup>2</sup></li> <li>✓ End caps: machined ULTEM polyetherimide PEI</li> <li>✓ MLI: Inner and out layers are 0,051 mm Kapton film, VDA coated on the internal side only. Between these are five layers of 0,0076 mm Kapton film, VDA coated both sides. Each of these layers are separated from each other by a thin Dacron spacer fabric</li> </ul>
Prepreg	<ul style="list-style-type: none"> <li>✓ 0,305 mm thick 12x12 square weave AS4 carbon fiber fabric impregnated with high latency epoxy resin (own development)</li> <li>✓ 45-50% fiber volume fraction</li> <li>✓ CTE: <math>1,8 \times 10^{-5} / ^\circ\text{C}</math></li> </ul>				
Others	<ul style="list-style-type: none"> <li>✓ Bladder: 0,025 mm Kapton VN film</li> <li>✓ Heater/restraint: 0,051 mm Kapton VN film, and a resistance alloy wire heater for prepreg curing with a capacity of 155 W/m<sup>2</sup></li> <li>✓ End caps: machined ULTEM polyetherimide PEI</li> <li>✓ MLI: Inner and out layers are 0,051 mm Kapton film, VDA coated on the internal side only. Between these are five layers of 0,0076 mm Kapton film, VDA coated both sides. Each of these layers are separated from each other by a thin Dacron spacer fabric</li> </ul>				
Rigidization process:	<ol style="list-style-type: none"> <li>1. Inflation with gas at 25,5 kPa</li> <li>2. To warm to 125-150°C. 35W/m<sup>2</sup> during 25 min.</li> <li>3. To cure at 125-150°C. 20W/m<sup>2</sup> during 45 min.</li> <li>4. To cool under 90°C and to vent the gas</li> </ol>				

Figure 4.21: Overview of proposed method for the ISIS by ILC Dover inc. (Marcos 2003)

#### ADVANTAGES

- Predictable and controlled rigidization process
- High specific strength and stiffness
- No adverse effects from packaging
- Long storage life (2 years at room temperature)

#### DISADVANTAGES

- MLI blanket necessary for heat containment
- Availability of suitable matrix materials
- Not reversible
- Much energy required for heating

Material used	
Matrix	Epoxy
Reinforcement	<ul style="list-style-type: none"> <li>- Glass</li> <li>- Carbon</li> <li>- PBO</li> <li>- Kevlar</li> </ul>
Supporting films	<ul style="list-style-type: none"> <li>- Kapton</li> <li>- Mylar</li> </ul>
Prepreg density	368 g/m <sup>2</sup>

Typical compressive properties	
Strength (warp)	606 N/mm <sup>2</sup>
E-Modulus (warp)	57200 N/mm <sup>2</sup>
Strength (weft)	591 N/mm <sup>2</sup>
E-Modulus (weft)	61400 N/mm <sup>2</sup>

Typical tensile properties	
Strength (warp)	692 N/mm <sup>2</sup>
E-Modulus (warp)	64800 N/mm <sup>2</sup>
Strength (weft)	685 N/mm <sup>2</sup>
E-Modulus (weft)	74500 N/mm <sup>2</sup>

Table 4.4: Typical properties of an thermally cured thermoset composite material (Cadogan et al. 2001)

#### 4.4.5 ULTRA VIOLET CURED COMPOSITES

UV cured composites are in many ways identical to the previously discussed thermally cured thermoset composites. The main difference is the influence that induces rigidization; ultra violet light opposed to heat. Typically, the fibre reinforced matrix cures at wavelengths between 250 and 380 nm. The source of UV light can either come from the sun or from a source inside the structure, with the latter rendering a more predictable and controlled rigidization process. The curing time can range between several minutes to several hours, depending on the type of matrix used. The most important attribute of rigidization by UV light is the fact that the materials used need to be transparent to the UV light. Therefore, minerals such as glass and quartz are common reinforcement materials. This property prevents the use of high performance fibers such as carbon, Kevlar, Vectran or PBO and the use of an MLI blanket. Therefore, UV cured composites do not exhibit the same structural performance as thermally cured composites. It has to be noted that design modifications can be made which allow the use of high performance fibres. However, this makes the manufacturing process much more complicated (Marcos 2003; Cadogan et al. 2001; Defoort 2005).

#### EXAMPLES

The most promising research in this field was performed by ILC Dover several years ago. They developed an UV curable boom which is "Rigidizable On Command" (ROC). They used a UV curable epoxy reinforced with high strength fibreglass and carbon fibre in a isogrid pattern. Both the bladder and the restraint layer were fabricated using 1 mm Mylar.



Figure 4.22: Sample of an UV cured composite by ILC Dover inc. (Allred et al. 2002)

#### ADVANTAGES

- Indefinite storage life
- Minimal energy required for rigidization (solar UV)
- Simple process when using solar UV
- Controlled rigidization process when using internal UV source
- Rapid rigidization possible

#### DISADVANTAGES

- Irreversible
- complex manufacturing process when using internal UV source
- Uncontrolled rigidization process when using solar UV
- Limited strength and stiffness

Material used	
Matrix	- Epoxy - Polyester
Reinforcement	- Glass - Quartz - Carbon - PBO - Kevlar
Supporting films	- Kapton - Mylar

Table 4.5: Materials used in UV cured composites

#### 4.4.6 INFLATION GAS REACTION COMPOSITES

The rigidization of a laminate structure similar to that of SOTC, thermal curing and UV curing can also be initiated using a catalyst carried by the inflation gas. This gaseous catalyst can either trigger the rigidization process itself, or can be used to accelerate the rigidization of a thermally cured thermoset composite. The main difference in the structure of the laminate is the fact that the bladder needs to be highly permeable to the inflation gas. The thickness of the laminate is also limited to ensure a full penetration of the inflation gas. Therefore, the structural performance of this rigidizable material is also limited, even though it can be tailored by using high tenacity fibres. Since the inflation gas itself triggers the curing of the composite, the rigidization process starts as soon as the structure is deployed (Cadogan et al. 2001; Marcos 2003; Defoort et. al 2005).

#### EXAMPLES

Contraves AG performed a case study in the 1980's into the development of inflatable reflectors and sunshields. They developed a thermally cured reflector which used the sun's heat and a catalyst carried by the inflation gas to accelerate the rigidization process.

The catalyst reduced the curing time from 120 °C for six hours to 80 °C for three hours. Kevlar was used for reinforcement of the matrix.

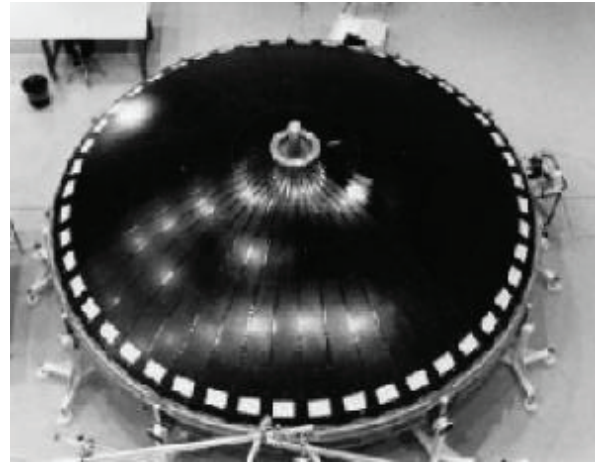


Figure 4.23: Gaseous catalyst cured reflector by Contraves (Cadogan et al 2001)

#### ADVANTAGES

- Minimum energy required
- Long storage life

#### DISADVANTAGES

- Limited structural performance due to thickness limitations
- Uncontrolled rigidization process
- Irreversible
- Complexity of the system

Material used	
Matrix	- Epoxy
Reinforcement	- Glass - Kevlar - PBO - Vectran - Carbon
Supporting films	- Kapton - Mylar

Table 4.6: Materials used in inflation gas reaction composites

#### 4.4.7 FOAM RIGIDIZATION

Foam rigidization is a method which has undergone extensive research in the space industry, but also found its way to the construction industry.

- *Foam rigidization in the space industry*

The study into the rigidization of inflatable structures for space applications using foam started in the 1960's. For Gossamer structures, foam is either used to fill the cavities of the membrane, or as a secondary system to enhance the structural performance of the primary rigidizable material. The foam can be



used as an inflation device, where it is mixed and then pumped into the structure. Also, the foam can be frozen and predistributed in the structure, where it can be activated by heat (Schnell et al. 2002).

Many different foams have been studied thus far; including two- or one part polyurethane foams and solvent expanded polystyrene and polyurethane that foams when exposed to a vacuum. In general, all foams that are studied for Gossamer structures have inferior structural properties compared to the other rigidizable materials. Therefore, they are often used in combination with a primary structure (Cadogan et al. 2001).

#### EXAMPLES

The Science Applications International Corporation (SAIC) developed a solar concentrator using foam rigidization in 1989 (Figure 4.24). The struts and outer perimeter ring are injected with a polyester foam. This initiates deployment and rigidizes the structure. In this case, the foam and the membrane material (silicon coated glass fiber) function as the primary load bearing mechanism (figure 4.24).

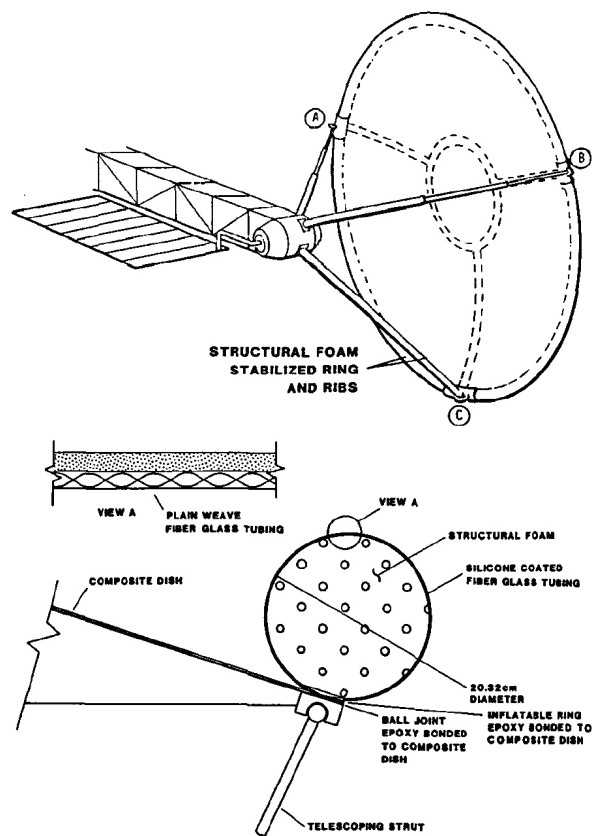


Figure 4.24: TOP; Solar concentrator by SAIC BOTTOM; detail of inflated structure components (Beninga & Davenport 1989)

#### ADVANTAGES

- Enhancing structural stiffness
- Relatively simple to manufacture, good availability of materials

#### DISADVANTAGES

- Limited structural performance
- Uncontrolled rigidization process (uniformity)
- Limited storage life
- Longer rigidization time
- Pumping and mixing system sometimes required

#### • Foam rigidization in the construction industry

In the seventies, Thomas Herzog supervised a group of students from the University of Kassel with the development of light weight external walls, constructed of standard membranes which were rigidized using expanded polyurethane foam (Koch & Habermann 2004). They constructed and tested multiple prototypes, which were fixed in wooden frames. Figure 4.25 shows this process, and figure 4.26 shows a detailed section.



Figure 4.25: Experimental building using the foam rigidized membranes (Koch & Habermann 2004)

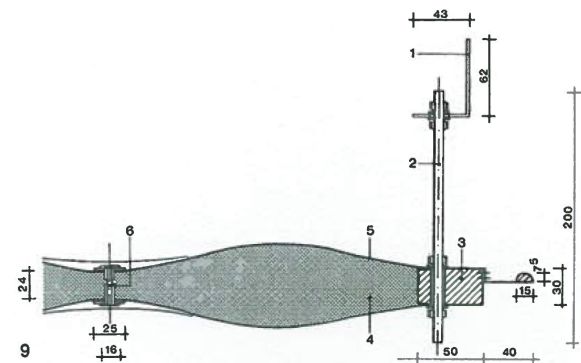


Figure 4.26: Section of a part of one wall panel (Koch & Habermann 2004)



#### 4.4.8 MULTI CRITERIA ANALYSIS

Rigidizable materials for Gossamer structures is a specific class of materials which have been studied extensively in the space industry over the last 50 years. This industry is typically characterized by high technology and high cost, where the construction industry is characterized by low technology and lower cost. Therefore, one might look in other directions than the space industry when searching for innovations in the construction industry. However, many of the performance objectives which apply for space structures also apply for the construction sector; e.g. low weight, high structural performance, reduced on sight labour, increased durability and low maintenance (van Dessel et al. 2003). Therefore, rigidizable materials hold the potential for being a successful technology transfer from the space industry to the construction industry, especially when used for the construction of optimized structures.

From the previous paragraphs, three main groups of rigidizable materials can be derived;

1. Aluminium and thin film laminates
2. Polymer composites
3. Foam rigidized structures

Aluminium laminates and foam rigidized structures differ from other rigidizable materials by their mechanism of rigidization which is distinctively different from polymer composites. The latter is classified by similar structures, with a similar material choice. All methods use a fibre reinforced matrix which is sandwiched in between two layer of film. The main difference between the methods is the outside influence which induces rigidization. This influence is either;

- The cooling of a thermoplastic below its  $T_g$
- The evaporation of a matrix softening component
- Heat
- Ultra-Violet light
- A catalyst in the inflation gas

Depending on the influence that induces rigidization, different requirements apply to the materials that are used. Therefore, the method of rigidization has a large influence on material choice and vice versa. In the decision making process of this research, the method of rigidization is leading.

#### CRITERIA

In paragraph 4.2.2 the requirements or performance objectives for rigidizable materials in terms of Gossamer structures were explained. Here, we showed that the space industry and the construction industry share many of the same objectives. However,

some requirements are very important in space applications, while having no significant meaning for the construction sector. For example, one of the most important requirements for rigidizable materials for Gossamer structures is a very high resistance to the space environment. Space structures are often engineered for end-of-life performance (EOL), meaning they must show a high resistance to the space environment as long as possible. Naturally, this requirement does not apply for earth bound applications. Also, Gossamer structures must have a high dimensional stability, since there are often very small tolerances. Therefore, the CTE of the material must be as low as possible. This requirement is of less importance for our case, since it has larger tolerances. This consideration can be made with every requirement as described in paragraph 4.2.2, leading to requirements for rigidizable materials for our case, with their corresponding weight factors. Naturally, this consideration is somewhat subjective since the transfer of rigidizable material technology to the construction sector has not yet been made.

1. Predictable and controlled rigidization process
2. Simple to manufacture / availability
3. High specific strength and stiffness materials
4. Rapid rigidization process
5. Low cost
6. Reversible
7. Minimal energy required for deployment and rigidization
8. Allow rigidization in a wide range of thermal environments
9. Long storage life (2+ years)
10. Compaction ability
11. No adverse effects from packaging or deployment

The eleven criteria described above are deemed essential for a balanced consideration of rigidizable materials for our case. As one might notice, several criteria that are considered in the case of Gossamer structures were omitted. As explained earlier, the resistance against the space environment and a near zero CTE are criteria that do not play a role in this research. For a similar reason, outgassing is also excluded from the consideration. The criterium that the materials must be as light as possible is not necessary since every material is already light weight compared to traditional construction materials. The criteria that deal with the possibility of upscaling, compatibility with associated materials and the shape deformation from deployment were also omitted due to lack of information to judge them individually. It was found that the compatibility with associated materials is already covered by the criterium manufacturability / availability, and that shape deformation due to



deployment or rigidization can be considered an adverse effect from packaging and deployment. Finally, a controlled and rapid rigidization process has been split into two criteria since they can both occur either simultaneously or separately.

#### WEIGHT FACTORS

The criteria described on the left are ordered from the most important to the least important. Several different weighing factors were considered and tested, which all gave similar results. The final method is based on a method used by Marcos (2003) and incorporates four possible values per criterium; bad, acceptable, good and excellent. Here every rigidizable material can take any value per criterium, with the exception that only one material can score excellent in any given criterium. Hereby, the result become better balanced since a material gets rewarded when it outperforms all the other on a certain criterium. The weight factors are as follows:

Criteria	Weight factor
1,2	3
3,4,5,6	2
7,8,9,10,11	1

Table 4.7: Weight factors

Within the scope of this research, the controllability and manufacturability of the rigidizable material that is going to be used if believed to be the most important criteria. Since the construction industry is characterized by low technology and low cost (van Dessel et al. 2003), it is important that the selected materials are commercially available, and are compatible with existing manufacturing techniques. In addition, a decisive criterium is the ability to rigidize the structure on command. An important feature of the design is the fact that the user can decide whether or not the structure needs rigidization. For example, for temporary applications an 100% inflated structure could prove more effective. When the structure has a (semi)-permanent nature it could be more efficient to rigidize the inflatable.

Several other criteria can be categorized as important although not imperative. This means that the consequences for scoring "bad" on one of these criteria will be less than the in the case of the previously discussed criteria. These criteria, 3,4,5 and 6, are assigned a weight factor of two. The last 5 criteria have a weight factor of one. The represent requirements of the rigidizable materials that have to be considered in the decision making process, but are of lesser importance.

#### RESULTS

The result of the multi- criteria analysis is shown in figure 4.27. Initially, all rigidizable materials are considered despite the fact that several candidates can be omitted on beforehand based on their key characteristics. This was done to provide a complete overview, and show that the results of the analysis are not definitive.

The analysis is based on data acquired during the literature study into rigidizable materials which was explained in the previous paragraphs. 70 % of the necessary data was found directly in the literature, 21 % of the data could not be found directly but was derived out of the context, and 9 % of the data (i.e. the information regarding the costs) was determined by the authors themselves.

Based upon the results of the multi- criteria analysis and the literature study an overview of plausible rigidizable materials can be made. Therefore three materials will be excluded from further elaboration based on their key characteristics;

- *Aluminium and thin film laminates*

A key characteristic of aluminium and thin film laminates is the fact that their rigidization pressure, thus operating pressure, is very close to their burst pressure. Load cases commonly found in the construction industry have a very dynamic nature, e.g. wind or traffic over a bridge. With respect to the strong safety regulations for building and civil structures, the use of aluminium and thin film laminates for the construction industry is therefore not plausible.

- *Seconder order transition change composites and shape memory polymers*

This class of rigidizable materials needs to be heated above its glass transition temperature to become flexible and inflated. When the materials is cooled below its  $T_g$  again, rigidization is achieved. This means that for applications where rigidization is not necessary, the structure needs to be heated continuously to avoid rigidization. Moreover, the materials associated with this type of rigidization, i.e. (shape memory) thermoplastics, can be considered to specific and underdeveloped for our study. These are the main reasons that this rigidizable material has one of the lowest total scores: 35.

- *Gas reaction composites*

A combination of characteristics make this rigidizable material not suited for our purpose. Due to the sophistication in material choice and limitations in process control, which are the two most important criteria for this study, this material is also excluded from further elaboration.

	W.F	Aluminium laminates	SOTC / SMP	Boil off composites	Heat cured composites	UV cured composites (solar)	UV cured composites (internal source)	Gas reaction composites	Foam rigidization
Predictable and controlled rigidization process	3	good <sup>1,2,4</sup>	bad <sup>4</sup>	bad <sup>1</sup>	excellent <sup>1,2</sup>	acceptable <sup>1,2</sup>	good <sup>1,2</sup>	bad <sup>1,2</sup>	bad <sup>1,4</sup>
Simple to manufacture / availability	3	acceptable <sup>1,2,4</sup>	bad <sup>1,4</sup>	good <sup>1</sup>	bad <sup>2</sup>	good <sup>1,2</sup>	bad <sup>1,2</sup>	bad <sup>1</sup>	excellent
High specific strength and stiffness materials	2	bad <sup>1,2,5</sup>	good <sup>1,6</sup>	acceptable <sup>1,2</sup>	excellent <sup>1</sup>	acceptable <sup>1,2,7</sup>	acceptable <sup>1,2</sup>	acceptable <sup>1,2</sup>	bad <sup>1,2</sup>
Rapid rigidization process	2	excellent <sup>1,2,4</sup>	acceptable	acceptable	good <sup>1</sup>	good <sup>1,2</sup>	good <sup>1,2</sup>	acceptable	acceptable <sup>8</sup>
Low cost	2	acceptable	bad	bad	bad	bad	bad	bad	excellent
Reversible	2	acceptable <sup>1,2,3,4</sup>	good <sup>1,2,4,6</sup>	excellent <sup>1,2,4,5</sup>	bad <sup>1,2,3</sup>	bad <sup>1,2,3</sup>	bad <sup>1,2,3</sup>	bad <sup>1,2</sup>	bad <sup>1,2</sup>
Minimal energy required for deployment and rigidization	1	good <sup>1,2,4,5</sup>	bad <sup>1,2,6</sup>	good	bad <sup>1,2,4</sup>	excellent <sup>1</sup>	bad <sup>1</sup>	good <sup>1,2</sup>	bad <sup>8</sup>
No adverse effects from packaging or deployment	1	bad <sup>1,2</sup>	good <sup>1,2</sup>	good <sup>1</sup>	good <sup>1</sup>	good	good	good	excellent
Long storage life (2+ years)	1	good <sup>1,2</sup>	good <sup>1,2,6</sup>	acceptable	acceptable <sup>1,2</sup>	excellent <sup>2,7</sup>	good <sup>2</sup>	good <sup>1,2</sup>	bad <sup>1,2</sup>
Compaction ability	1	acceptable <sup>3,5</sup>	good <sup>3</sup>	good <sup>1,3</sup>	good <sup>3</sup>	good <sup>3</sup>	good <sup>3</sup>	good	excellent
Allow rigidization in a wide range of thermal environments	1	acceptable	bad <sup>1,6</sup>	bad <sup>1</sup>	good	good <sup>7</sup>	excellent	good	acceptable
		<b>44</b>	<b>35</b>	<b>42</b>	<b>45</b>	<b>46</b>	<b>40</b>	<b>33</b>	<b>43</b>
<b>TOTAL POINTS</b>		<b>44</b>	<b>35</b>	<b>42</b>	<b>45</b>	<b>46</b>	<b>40</b>	<b>33</b>	<b>43</b>

The top five is as follows;

1. UV cured composites (solar) 46
2. Heat cured composites 45
3. Foam rigidization 44
4. Boil off composites 43
5. UV cured composites (internal) 42

The difference in total points is too little to determine if there is a rigidizable material which can be transferred directly to the construction industry. Therefore, the criteria, weight factors and analysis were presented to several experts<sup>1</sup> in the field of rigidizable materials. These expert meetings led to the conclusion that rigidizable materials as studied for Gossamer structures are not yet ready for a transfer to the construction industry.

- 1) Cadogan & Scarborough 2001  
2) Markos 2003  
3) Freeland 1998  
4) Defoort et al. 2005  
5) Chmielewski & Jenkins 2005  
6) Guidanean & Lichodziejewski 2002  
7) Allred et al. 2002  
8) Schnell et al. 2002
- Value derived out of the literature  
Value determined by authors
- excellent 4 points  
good 3 points  
acceptable 2 points  
bad 1 point

1. 1) Tiziane Cardone, ESA ESTEC, Noordwijk, the Netherlands  
2) Marco Straubel, Deutsches Zentrum für Luft- und Raumfahrt, Braunschweig, Germany  
3) Marcelo Muller, Nationaal Lucht- en Ruimtevaartlaboratorium, Amsterdam, the Netherlands

The main goal of this chapter was to reveal which rigidizable materials exist, and to determine which method is best suited for our purpose;

#### Which rigidization method is best suited for producing the case derived in RQ1?

Artificial composites, such as the fibre reinforced composites discussed in this research, have been used since the invention of Bakelite in 1909. A composite obtains its strength through the principle of combined action, where the combination of the different materials is stronger than the sum of the parts comprising it. Any fibre reinforced composite consists of a matrix material, often thermoset, and a fibrous reinforcement, often glass, graphite, aramid or polypropylene. They are characterized by their extremely high specific stiffness, high degree of tailoring, and large freedom of possible shapes. Multiple commercial manufacturing techniques exist, developed for different purposes. For our purpose, it was shown that hand lay-up, resin transfer moulding and vacuum infusion are the most promising due to their simplicity and relatively low cost.

The use of composites is not limited to terrestrial applications, but has also been studied for more than 60 years in the aerospace industry. Here, inflatable structures are used for quick deployment in space (Gossamer structures) and are subsequently rigidized to make the structure independent of air pressure. Seven rigidization techniques were found in the literature, which can be classified into three groups based upon their structure.

- Aluminum and thin film laminates
- Foam rigidized structures
- Polymer composites (Figure 4.28)

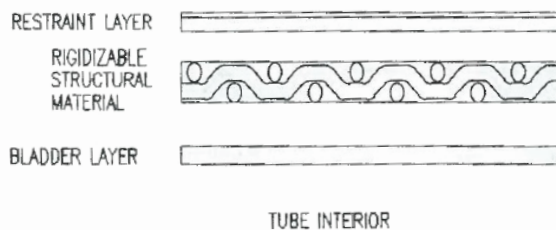


Figure 4.28: Typical cross section polymer composite used for Gossamer structures (Jenkins 2005)

The polymer composites used and studied for space applications differ from each other due to the external influence that induces rigidization. This influence is either heat, UV light, evaporation of a solvent, cooling below  $T_g$  and the reaction with a catalyst. The basic structure of these composites however, is always the same. An inner bladder ensures an airtight seal between the inflation medium and the rigidizable

layer. The restraint layer on the outside protects the structure from harmful outside influences and gives the part its final shape.

A multi criteria analysis was performed to determine which of the rigidizable materials used in space was the most promising for use in the construction industry. The results of this analysis showed to little difference to make a balanced decision. Meetings with several experts in the field of rigidizable materials showed that currently there are no rigidizable materials as studied for space applications suited for a transfer to the construction sector. Most techniques are still under development and are patented. In addition, the forces which act on a space structure are much lower than those on a terrestrial structure. These influences on the rigidized structure still have to be studied.

Despite the fact that a rigidizable material as used in space can not be transferred directly to the construction sector, the basic structure is very useful. The main advantage of the space materials is the possibility to rigidize on command (ROC), and the integration of all the component parts into one package. Methods for producing this structure, bladder-rigidizable material-restraint layer, do exist. Several manufacturers in the Netherlands, e.g. Eurocarbon, are able to braid fibres around a layer or mould. The result is the same structure as shown in figure 4.28, but without a resin already impregnated in the fibres. However, this process is compatible with commercial manufacturing techniques such as resin transfer moulding or vacuum infusion. Also, when the outer restraint layer is omitted, hand lay-up can be used.

Even though the space materials can not be used directly, their main advantages can be utilized when combining their structure with commercial manufacturing techniques. Therefore, the optimized shape derived in RQ1 will be fabricated using a combination of rigidizable materials used in space, and commercial fabrication techniques.



## 5.1 INTRODUCTION

In the first chapter of this thesis the main goal of this research was introduced; a new production method for structurally optimized section active structure systems. The rationale behind this was the fact that current production methods based on fabric formwork require large amounts of additional falsework. Therefore, the goal in this research is to develop a production method where the formwork of the 3D structure consists entirely of inflatables and is thus entirely based on form active principles.

The starting point for the development of the case were the section active structure systems defined by Engel (1997). These systems were structurally optimized using Solidthinking Inspire 9.0 and the ParaGen method. Hereby, the section active structure systems behave more like vector active structure systems. The main contribution of this thesis, besides revealing the morphological features of these section active structure systems, is to develop a production method which can produce these optimized elements more efficiently than current production methods. This is done using only inflatable structure. In other words;

*The use of form active principles to make a section active structure system vector active.*

The research is split into three succeeding phases. The first phase was explained in chapter one, describing the research plan. The second phase, describing the research phase, was explained in chapter two, three and four, and forms the basis for the development phase where scale models and a prototype will be fabricated. This chapter gives an overview of the most important conclusions of the research phase.

The basic approach to the production method that is proposed in the thesis is a 3d structure constructed out of a formwork which consists entirely out of inflatable structures. Therefore, not only the primary

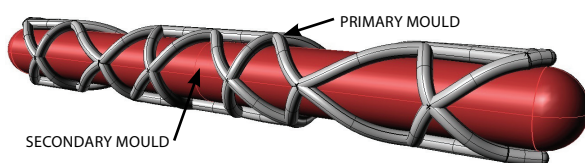


Figure 5.1: Concept explaining the proposed production method

mould, which is the structural rigidizable material, but also the secondary mould, i.e. the falsework, is based on form active principles.

The production method consists of two separate parts or stages. Naturally, the two stages have some interdependence, e.g. the material that is used for rigidization influences the height of the pressure difference in the secondary mould. But in general, decisions corresponding to the primary mould will follow after decisions concerning the secondary mould are made. Any design process, after recognizing the need for a device and defining specifications and functional requirements, starts with a conceptual phase and subsequently a detailed phase. During the conceptual phase the overall form is established and checked to see if meets predetermined requirements. Is so, the design moves towards a detailed phase where it is optimized for detailed requirements and manufacturability (Chapman 1994). In this research, the form finding process was performed in chapter three; Structural optimization, in order to answer the first research question.

### RQ1:

*Which structurally optimized section active structure system can best be used as a case?*

The first step towards the answer of this question was given by an in depth literature review into the fundamentals of structural optimization. The different optimization categories and optimization routine were explained. In addition, the algorithms for structural optimization were explained in order to analyse the outcome of the optimization software. Topology optimization was performed on the four section active structure systems using Solidthinking Inspire 9.0, validated by Topostruct. The morphological features of every separate structure system were revealed and compared to determine the general morphological features of optimized section active structure systems. These empirical case studies showed that an optimized one-bay beam reflected most of the general features, and that it forms the basis for all other optimized section active systems. Therefore, the optimized one-bay beam was chosen as the case for the remainder of the research.

The second step in the form finding process, the shape optimization, was performed using the Para-



Gen method. The optimized three dimensional beam was used as a basis for the development of the parametric model, which in turn forms the basis for the ParaGen method. ParaGen generated 1276 individual solutions with specific stiffness as the fitness function. The lead to three best fit solutions, where ID: 1269 was chosen as the case for the proposed production method, completing the form finding process and thus the answer to the first research question. Size optimization of the geometry will be discussed in chapter six, when detailed requirements and conditions are known.

In order to manufacture the complex shape derived in chapter two, a production method based entirely on inflatables is proposed. The falsework is also based on form active principles and has to support the primary mould, which represents the optimized shape. Therefore, in depth literature reviews were performed into pneumatic structures in chapter three in order to answer the second research question;

**RQ 2:**

*In which way can an inflatable structure be used as falsework for the production of structurally optimized section active elements?*

In order to answer this question the properties and characteristics of inflatable structures were revealed. First the historical development of pneumatic structures in general was explained, followed by the general characteristics of inflatables. The study showed that inflatables can be classified according to several different criteria, which led to five typologies of inflatable structures. These five typologies were assessed according to four morphological indicators. The four optimized section active structure systems were assessed according to the same indicators in order to compare the inflatable typologies to the optimized structures. The resulting matrix showed which inflatable typology was most promising to use as falsework for a specific optimized structure. In addition, an in depth literature review into envelope materials revealed the properties and characteristics of membrane materials in general. Moreover, it showed that, according to ten criteria relevant to our research, PVC coated polyester could best be used for the secondary mould.

The primary mould represents the optimized structure and is inflated before being rigidized to make the structure independent of air pressure. Several methods exist for the rigidization of a membrane, studied in different disciplines. Therefore, literature reviews were performed to determine which method is best suited for producing the geometry derived in the first research question;

**Which rigidization method is best suited for producing the case derived in RQ1?**

The road towards the answer to this question started with a study into the fundamentals of polymer composites. Subsequently, commercial manufacturing methods of polymer composites were explained and assessed. Besides these commercial methods, methods studied for space applications were also researched and assessed according to criteria which are relevant for this research. The outcome of this multi criteria analysis showed no clear results. Therefore, several experts in the field of rigidizable materials for space applications were consulted. These expert meetings showed that no single rigidizable material for space applications can be transferred to the construction industry directly. However, their main advantages, e.g. rigidization on command, can be utilized when combining their structure with commercial manufacturing methods such as resin transfer moulding or vacuum infusion.

With the answers to these three research question, the theoretical basis for the production method is made. The syntheses of the different chapters, and this synthesis form the basis for the development phase where initially a full structural analysis will be performed. This is followed by the fabrication and testing of the scale models. The analysed results of these models will, together with the previously discussed syntheses, form the basis for the development of the prototype.







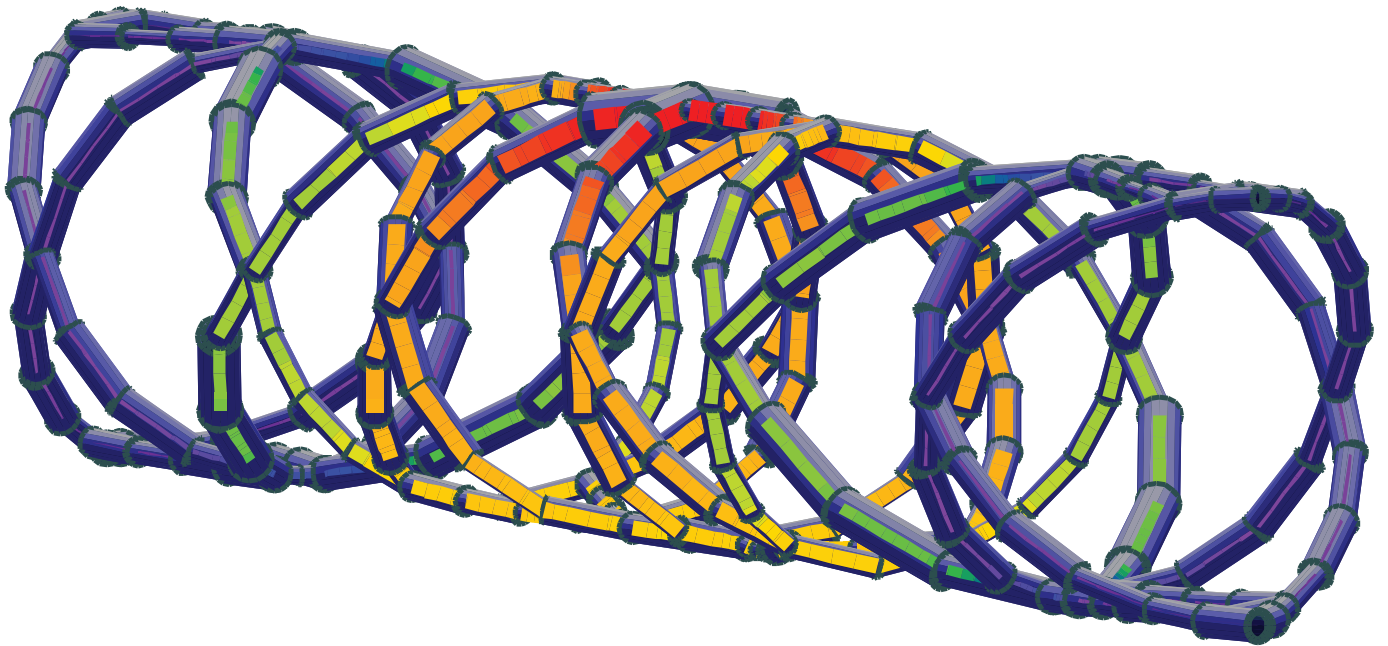
C

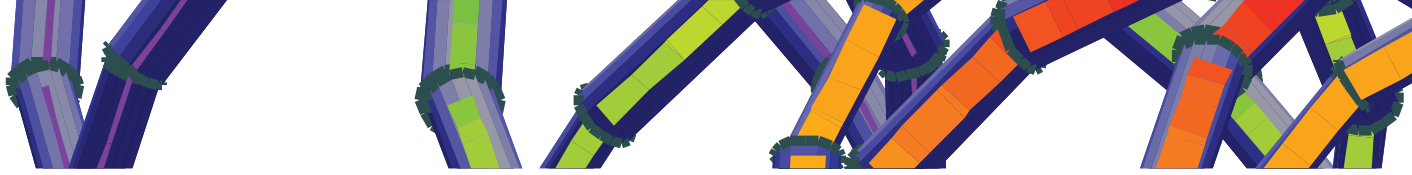
## Development phase



# 6

## Structural analysis





Out of the geometries produced by the Paragen method the id 1269 will serve as the case for further research. The performance of this case is based on a beam with straight members, however the final case is based on curved members and therefore further analysis and optimization is required.

The Paragen method resulted in a total of 1276 model numbers, each with a different size and shape. The members of the models with straight lines are optimized on their size by an iterative process of analysing the results and simultaneously optimizing the section diameters with Staad Pro. Eventually, this will lead to a final model with several section diameters that is upload on the interface with all related data. Finally, the model number 1269 proved to be the best performing geometry on the combination of the following fitness functions; least weight and highest stiffness.

On the University of Technology Eindhoven structural analysis of lightweight structures are mainly performed by Oasys' GSA Analysis. Since the models of the Paragen method are only analysed by Staad pro, the best performing model will also be analysed by GSA to compare the results. If this will lead to similar results, then the results are validated and the next step in the optimization process can start.

Eventually, the analysed results of the models with straight lines will not be representative for a model with curved members. Therefore, the members of model number 1269 will be divided in four equal parts and the knots are placed on a hypothetical tube. Then, the model will be analysed with Staad Pro and GSA and another comparison of results is made.

For the final case, and the production method of this case, composites are applied. Therefore, a structural analysis of the optimized beam is required by using the material properties of composites. These result will be compared with the results of a similar optimized beam with the material properties of steel.

Chapter 8 is about the production and testing of concrete scale models. For this research four geometries are produced with concrete and lycra. The test results of these concrete scale models are compared with the results of optimized scale models which are analysed with Staad Pro.

## 6.2.1 METHOD

The iterative analysis of geometries in the Paragen method is performed with a parametric model with linear members that connect the nodes. This is a simplification of the final model. Therefore, an structural analysis of a linear member model as well as a curved member model needs to be performed. At first Staad Pro is used to analyse the models, and model number 1269 is the best performing geometry when a 50 KN point load is applied on a steel beam with fixed supports.

The structural analysis of the model is performed with a non-linear static analysis. For our structure the geometric non-linearity and the material non-linearity are applicable;

- **Geometric non-linearity**, i.e. *P-delta analysis*, takes account of the third-order effects, such as the additional lateral rigidity and stresses resulting from deformation. This effect considers additional forces arising in a deformed structure such as a beam with fixed supports on both ends, loaded by a vertical load, longitudinal forces arise and the deflection decreases. (Autodesk, 2013)
- **Material non-linearity**, i.e. *non-linear static analysis*, takes account of the second-order effects, such as changing the stiffness of the element under the influence of the stress state in the element. At the same time, this analysis considers generation of moments resulting from the action of vertical forces at the nodes displaced horizontally.

During these analysis, an iterative process starts for optimizing the model on size with Staad Pro. This iterative process will eventually result in a size optimized beam.

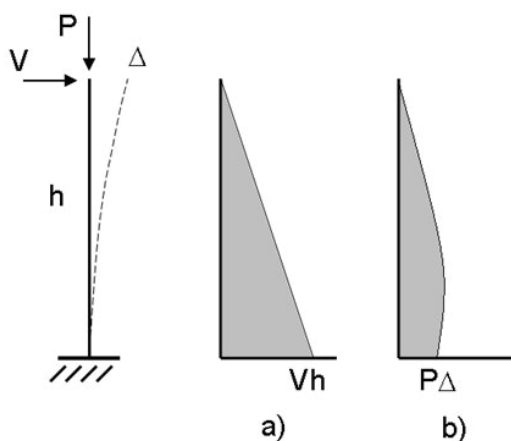


Figure 6.1: Moment diagrams for a cantilever column for a) First-order effects only and, b) P-Δ effects only. (Bentley, 2013)

The first analysis will be performed with the material properties of steel, since these properties were also applied in the Paragen Method. The member sizes are based on the AISC coding of steel pipe sizes. The material properties of steel are (Standard Oasys GSA):

Young's modulus:	205000 N/mm <sup>2</sup>
Poisson's ratio:	0,3
Density:	7850 kg/m <sup>3</sup>

Eventually, the analysis will be performed with the material properties of E-Glass Epoxy. The member sizes require a more complicated solution. The material properties of E-glass epoxy are (Budinski and Budinski, 2002):

Tensile strength:	482 MPa
Young's modulus:	31020 N/mm <sup>2</sup>
Poisson's ratio:	0,3
Density:	2140 Kg/m <sup>3</sup>
Flexural modulus (applied):	11800 N/mm <sup>2</sup>

The flexural modulus of E-glass epoxy is 17,37 times smaller than the Young's modulus of steel. To determine the member sizes for the composite material the ratio between diameter and wall thickness is of importance; the wall thickness is dependent on the diameter of the hollow tube. Conform the AISC 14th manual, section F8, the limit of round hollow structural section members is determined by the D/t ratio (Diameter / wall thickness). The D/t ratio should be less than:

$$0.45 * E / F_y$$

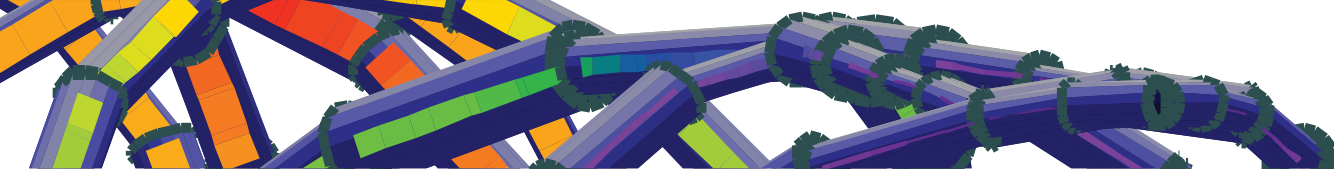
$$0.45 * \text{Modulus} / \text{Tensile strength}$$

For the E-glass epoxy this will be:  
 $0,45 * (11,8) / 0,482 = 11,01 \%$

With this formula the wall thicknesses are determined per diameter as shown below (Appendix C)

Diameter	Wall Thickness	Area
20	4	301,592
30	4	552,920
40	4	804,247
50	6	1432,566
60	6	1809,557
70	8	2714,336
80	8	3216,990
90	10	4398,229
100	10	5026,548
110	12	6484,247
120	12	7238,229

Table 6.1: Diameter / wall thickness of composites members



## 6.2.2 LINEAR MEMBER MODEL

The geometries out of the Paragen method were linear member models. Based on these models the best performing geometry was ID\_1269. By an iterative process the members are optimized on size (Figure 6.2 & Appendix D.3). In both structural analysis programs this model is **non-linear static** analysed, with the 50 kN point load and fixed supports applied, resulting in the following outcomes:

Weight:	132,8 kg
Deflection:	13,22 mm
Frequency:	32,5 Hz
Axial tensile force:	44,24 kN
Axial compressive force:	-37,46 kN
C1 Combined maximum stress:	303,4 N/mm <sup>2</sup>
C1 Combined minimum stress:	-133,4 N/mm <sup>2</sup>
C2 Combined maximum stress:	115,3 N/mm <sup>2</sup>
C2 Combined minimum stress:	-291,9 N/mm <sup>2</sup>

Three typical visualisations of the analysis are shown below; deflection, axial forces and combined stresses. These visualisations give a good interpretation of the behaviour of the mean under load.

The deflection is visualised in figure 6.3, and shows the highest deflection at the point load in the upper part of the beam. The maximum deflection at this point is 13,22 mm. Remarkable is that the lower center part has a small deflection, possibly caused by the compressing of the beam to a more oval shape.

In figure 6.4 the axial forces are shown, the red and orange suggest tension forces, and the blue and green suggest compressive forces. If this image is compared with the moment diagram of the 2D-beam in chapter 2.5 at the point where the moment is zero, the tension and compressive forces change side in this model. The tension and compression lines are clearly visible and show that the tension starts in the top and is at the bottom side in the center with the point load.

The figure 6.5 shows the combined forces in the model. So bending, shear and axial forces are combined in this image, and the largest moment occurs at the intersections close to the center of the beam. Also the tension and compressive lines are clearly visible in this figure. The maximum force that occurs is 303,4 N/mm<sup>2</sup>, in comparison steel qualities are in between 235 and 355 N/mm<sup>2</sup>.

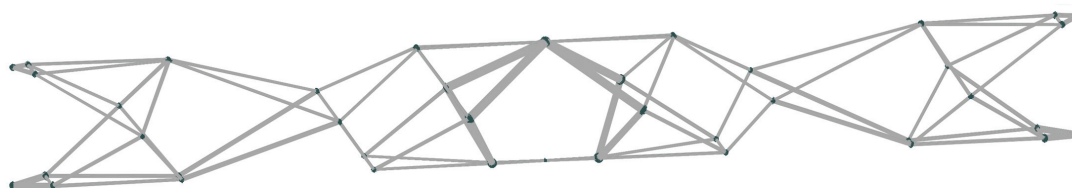


Figure 6.2: Linear member model - Members optimized on size



Figure 6.3: Linear member model - Deflection

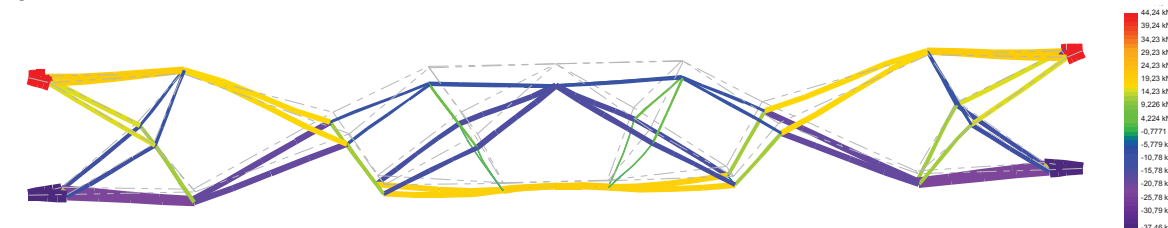


Figure 6.4: Linear member model - Axial force

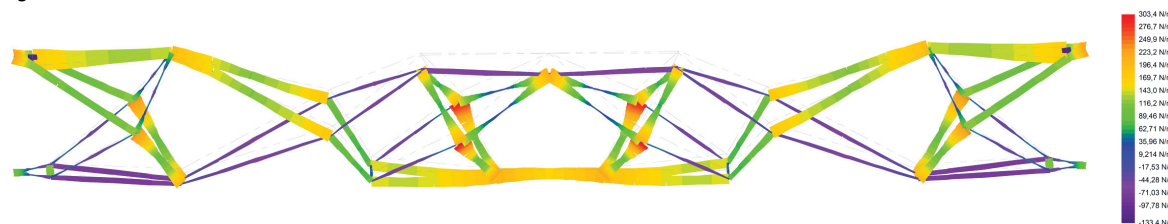


Figure 6.5: Linear member model - C1 Combined Stress



### 6.2.3 CURVED MEMBER MODEL

The analysis of the straight member model in both structural programs resulted in similar results. Therefore, it can be stated that the programs give the same outcomes for our case. Eventually, the analysed results of the models with straight lines will not be representative for a model with curved members. Therefore, the members of linear member model will be divided in four equal parts and the knots are placed on a hypothetical tube. Another optimization cycle takes place with Staad Pro to determine the member size using the AISC coding of steel pipe sizes, the result is shown in figure 6.6 and appendix D.2.

Again, this model is **non-linear static** analysed using both structural analysis programs, with the 50 kN point load and fixed supports applied, resulting in the following outcomes:

Weight:	193,3 kg
Deflection:	28,34 mm
Frequency:	24 Hz
Axial tensile force:	43,93 kN
Axial compressive force:	-37,47 kN
C1 Combined maximum stress:	308,6 N/mm <sup>2</sup>
C1 Combined minimum stress:	-114,2 N/mm <sup>2</sup>
C2 Combined maximum stress:	140,0 N/mm <sup>2</sup>
C2 Combined minimum stress:	-338,6 N/mm <sup>2</sup>

In the figures below the results of the analysis in GSA and Staad Pro are graphically visualized. In figure 6.7 the deflection of the beam is shown. It is clearly visible that in the center-upper part of the beam, where the point load is applied, the deflection is the highest. The maximum deflection at this point is 28,34 mm, which is twice as high as from the beam with straight members. This is probably the cause of the greater bending moments in the Y direction which is almost five times as high in the model with straight members.

The axial forces are shown in figure 6.8 and show only small differences with the straight member model, the compressive and tensile forces are almost similar. The direction of axial force is the same in each member and only small differences are shown in the size of the forces. The only member with significant difference is the member at the bottom side of the beam which has an increase in tensile force.

The combined stress of the beam with curved members is overall between -120 N/mm<sup>2</sup> and 340 N/mm<sup>2</sup>. In a previous optimization two small members exceeded the maximum stress to 500 N/mm<sup>2</sup>, by redesigning this point to one single node this peak stress is solved. The orange and purple parts are most likely to be weakest spots in the beam and require additional thickness.

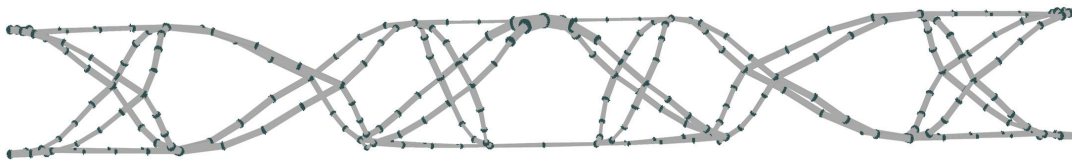


Figure 6.6: Curved member model - Members optimized on size

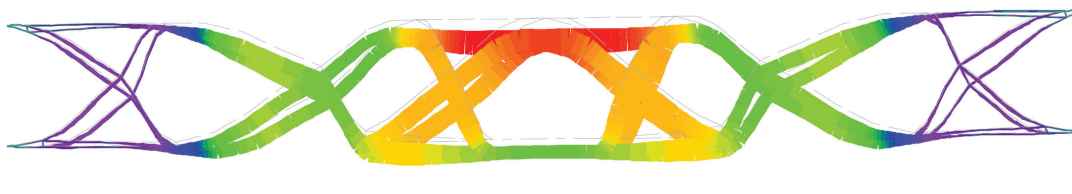


Figure 6.7: Curved member model - Deflection

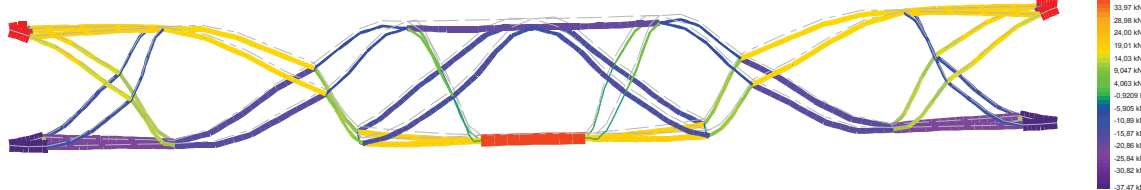


Figure 6.8: Curved member model - Axial force

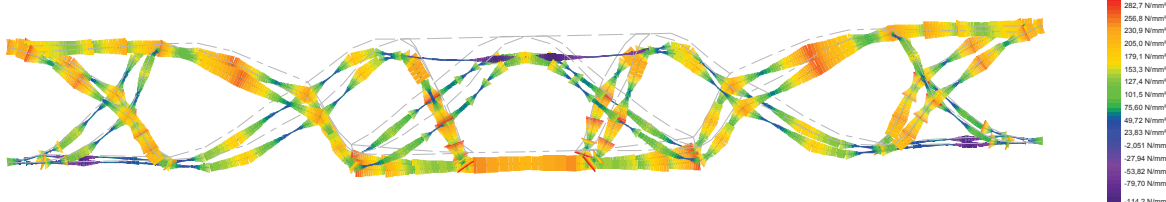
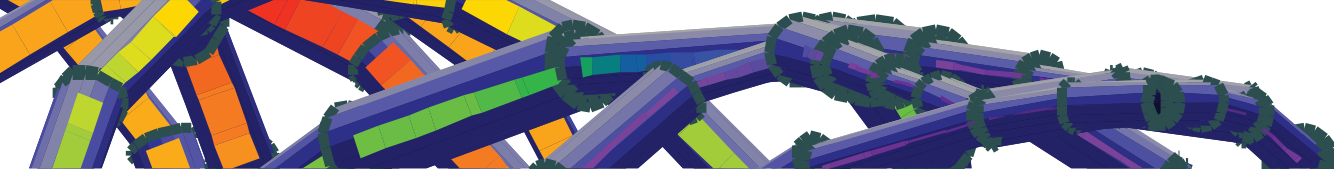


Figure 6.9: Curved member model - C1 Combined Stress



## 6.2.4 COMPOSITE CURVED MEMBER MODEL

After analysing the linear and curved member models with the properties of steel, an analysis of the curved member models is performed with the properties of E-glass epoxy.

The flexural modulus is applied in the analysis, because the tension does not seem to be the dominant stress. In most cases the tensile and compressive stress are similar and in some cases compressive stress is even higher, which would indicate flexural stress as dominant over axial (tensile) stress.

With the diameters and wall thicknesses in table 6.1 for composite members the iterative optimization process for size is performed with Staad Pro. For this optimization a non-linear static analysis and a P-delta analysis are performed on the structure.

The differences are visible in the member sizes, which results in a stiffer structure with less deflection for the P-delta analysis. Therefore, the size optimization by the P-delta analysis is used for further research. The result of this size optimization is shown in figure 6.10 and appendix D.1.

With the size optimized model, the analysis of the rigidized composite beam can start. To compare the differences with the steel beam, an analysis with the material properties of steel is also performed on this size optimized model. The modulus of the composite compared to the modulus of steel is very low and therefore the differences are great. The modulus of other composites can be much higher, but since the E-glass Epoxy will be applied in the prototype these performances are used in the analysis.

In both structural analysis programs the **composite model** is non-linear static analysed, with the 50 kN point load and fixed supports applied, resulting in the following outcomes:

Weight:	165,81 kg
Maximum deflection:	87,51 mm
Highest frequency:	34,943 Hz
Axial tensile force:	42,70 kN
Axial compressive force:	-37,54 kN
C1 Combined maximum stress:	141,0 N/mm <sup>2</sup>
C1 Combined minimum stress:	-41,66 N/mm <sup>2</sup>
C2 Combined maximum stress:	64,68 N/mm <sup>2</sup>
C2 Combined minimum stress:	-159,4 N/mm <sup>2</sup>

The steel model is non-linear static analysed with GSA to compare the results.

Weight:	607,14 kg
Maximum deflection:	5,11 mm
Axial tensile force:	42,07 kN
Axial compressive force:	-37,69 kN
C1 Combined maximum stress:	308,6 N/mm <sup>2</sup>
C1 Combined minimum stress:	-114,2 N/mm <sup>2</sup>
C2 Combined maximum stress:	140,0 N/mm <sup>2</sup>
C2 Combined minimum stress:	-338,6 N/mm <sup>2</sup>

At first the deflection will be analysed, followed by the axial and bending stresses. Then, the torsion and shear stress will be analysed, and eventually the combined stresses will conclude this paragraph.

The deflection of the composite model is 87,51 mm over a span of 8 meters (Figure 6.11). This is a huge increase relative to the previous optimized steel beams, and the similar member sized model in steel (Figure 6.17), which has a deflection of 5,11 mm. This is a deflection of about 17 times as high due to the material properties. It has to be noted that the composite material properties are relatively low, compared to other composite materials. Furthermore, the deflection in the upper center part is the largest, due to the effect of the point load.

The axial force is similar to previous analysis, the force of 50 kN is transferred to the support points by an tensile and compressive line, in which the blue and purple lines transfer the compressive forces, and the red, orange and yellow lines transfer the tensile forces.

The resolved element rotation option gives an overview of the rotation of each element in radians. The effect of the rotation of elements results in bending stresses. By applying a point load on the circular beam, the force will deform the beam to an oval shape, the most effect will take place at the red and orange indicated members. (Figure 6.13)

The bending stress has four output files, two in the Z-direction and two in the Y-direction, the files in the same direction give the same results, but in opposite direction. The maximum bending stress in the Z-direction is 139,7 N/mm<sup>2</sup>, and the minimum bending stress is -125,4 N/mm<sup>2</sup>. In the Z-direction the overall bending stress is normal, except for two points in the upper part of the beam, which have peak values. In the vertical, Y-direction, the maximum bending stress

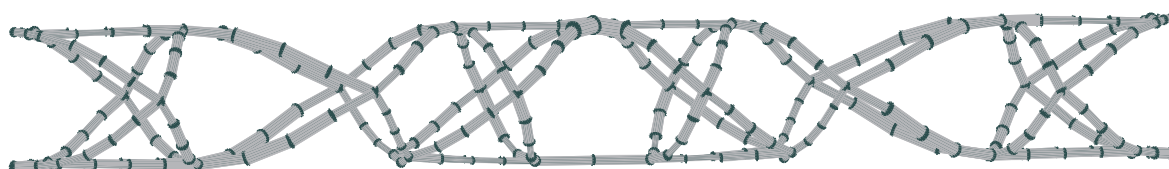
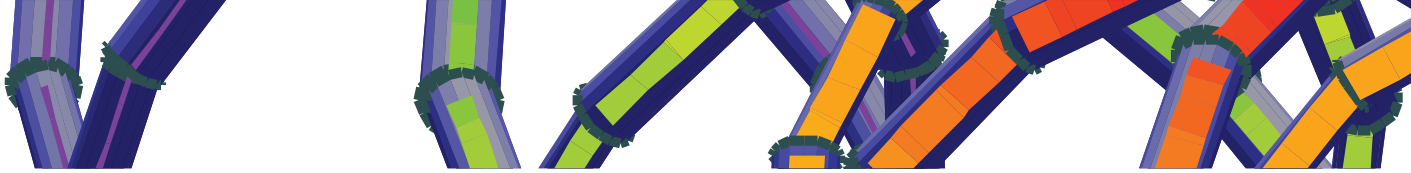


Figure 6.10: Composite model - Members optimized on size



is 82,52 N/mm<sup>2</sup>, and the minimum bending stress is -82,52 N/mm<sup>2</sup>. In the Y-direction the peak stresses are located at the knots in the center part of the beam. The point load is compressing the beam to a more oval shape, this will cause the larger stresses at these knots.

Torsion appears mainly in the members in the upper part of the beam. In the lower part a peak torsion appears in the members between the first and second "X", this peak torsion might be due to the single knot, at the second "X", that transfers the torsion, forces and stresses to the support points. (Figure 6.16)

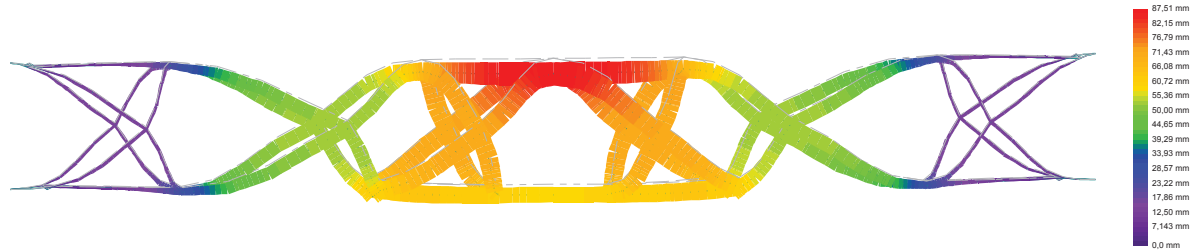


Figure 6.11: Composite model - Deflection

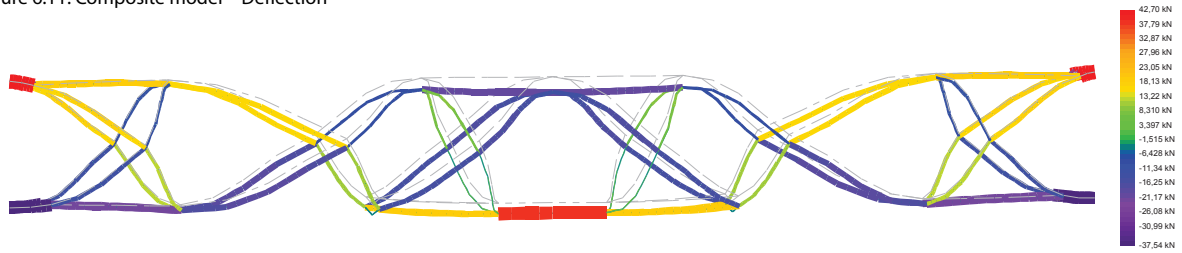


Figure 6.12: Composite model - Axial force

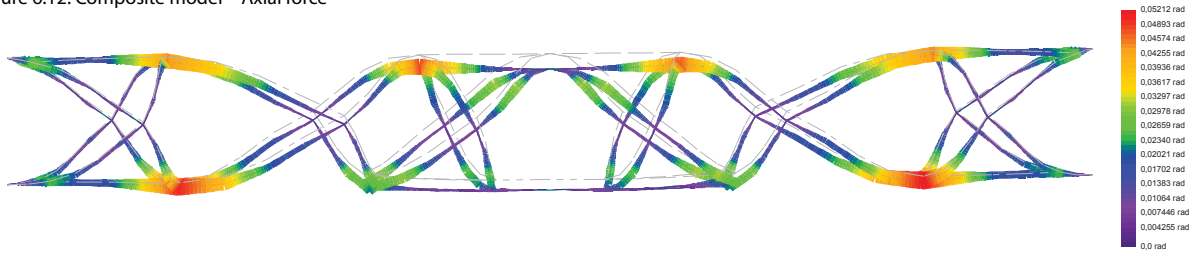


Figure 6.13: Composite model - Element rotation

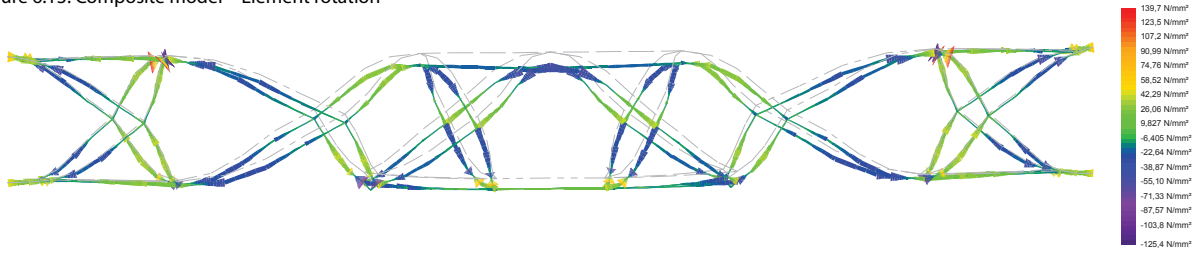


Figure 6.14: Composite model - Bending stress, Z-direction

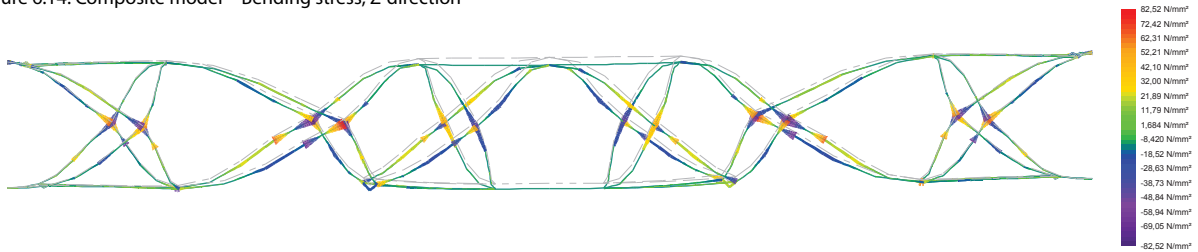


Figure 6.15: Composite model - Bending stress, Y-direction

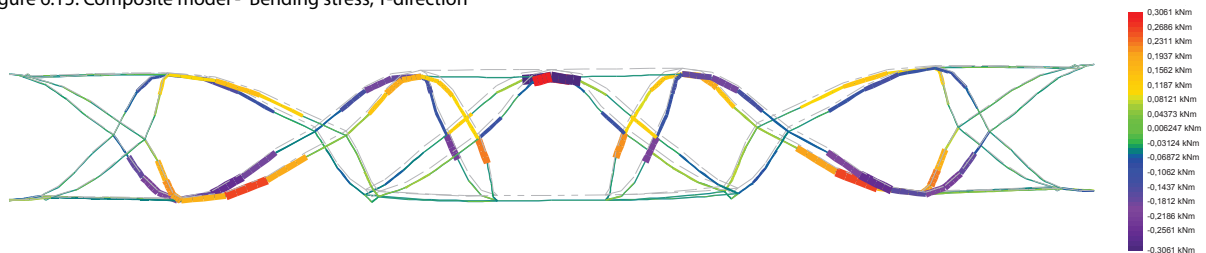


Figure 6.16: Composite model - Torsion

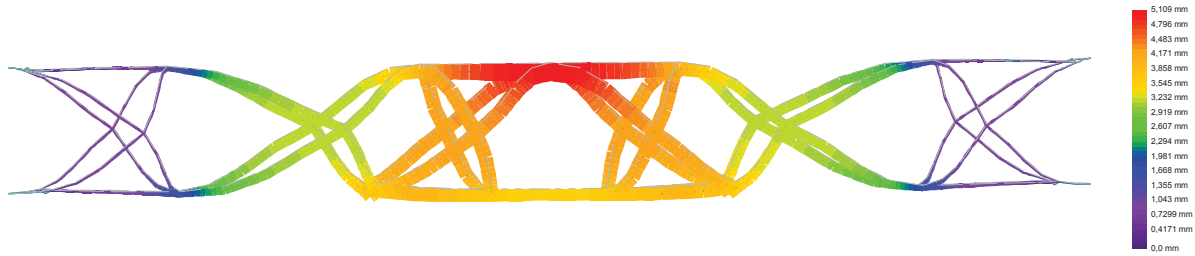
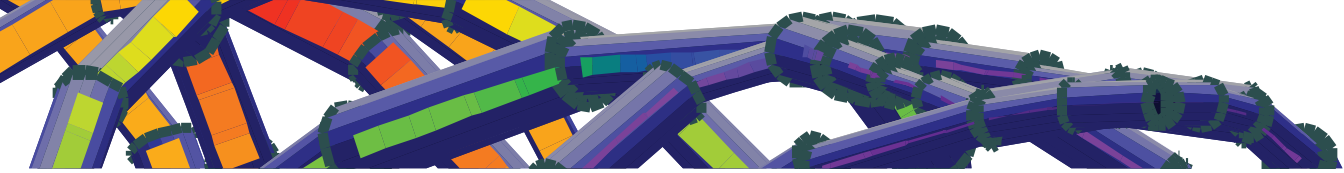


Figure 6.17: Steel model - Deflection

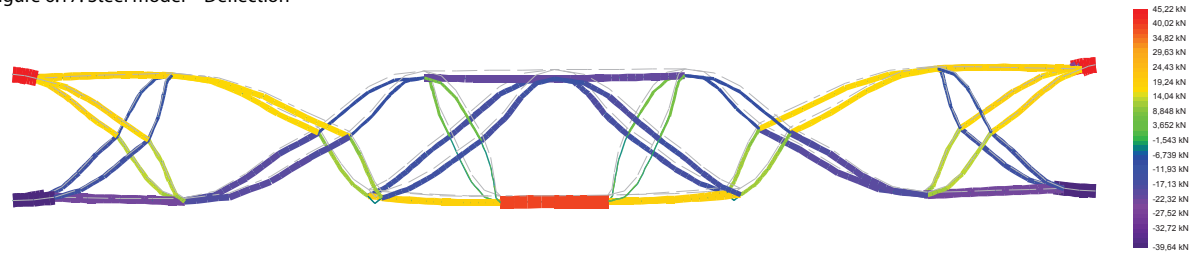


Figure 6.18: Steel model - Axial force

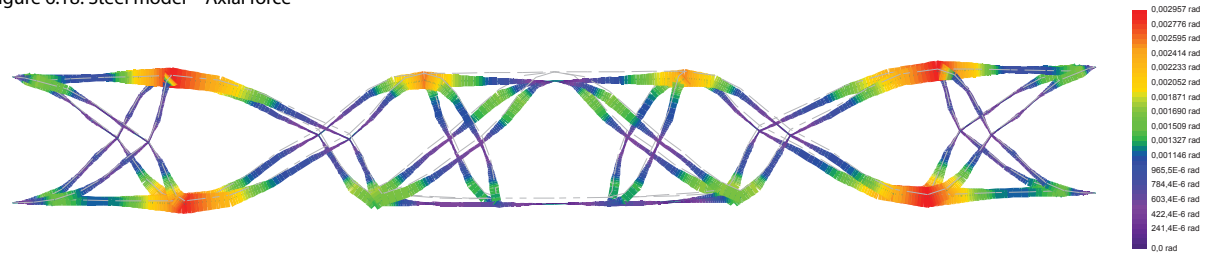


Figure 6.19: Steel model - Element rotation

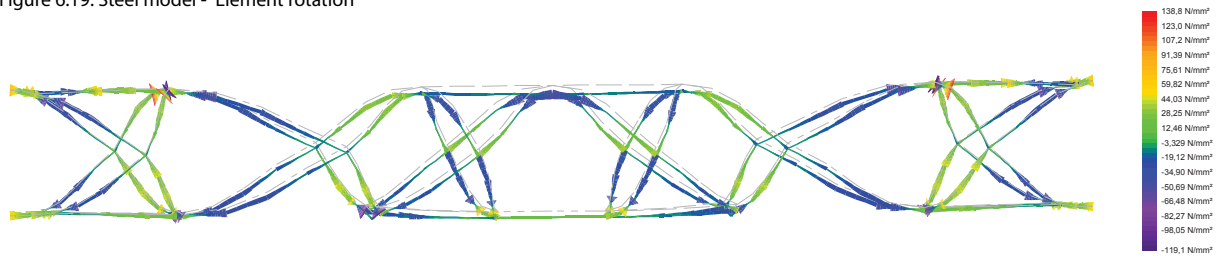


Figure 6.20: Steel model - Bending stress, Z-direction

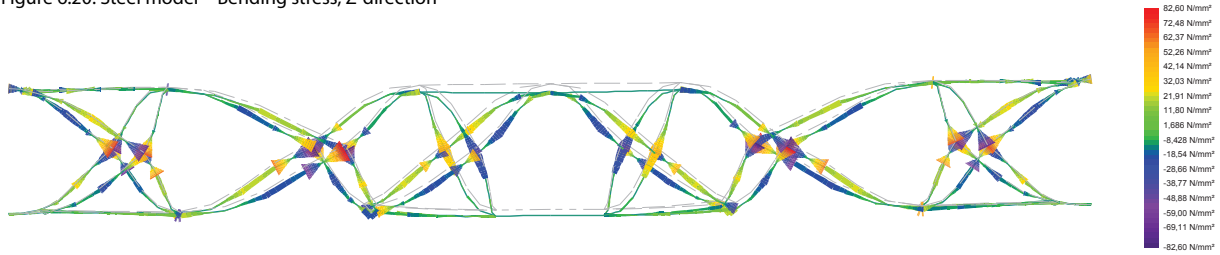


Figure 6.21: Steel model - Bending stress, Y-direction

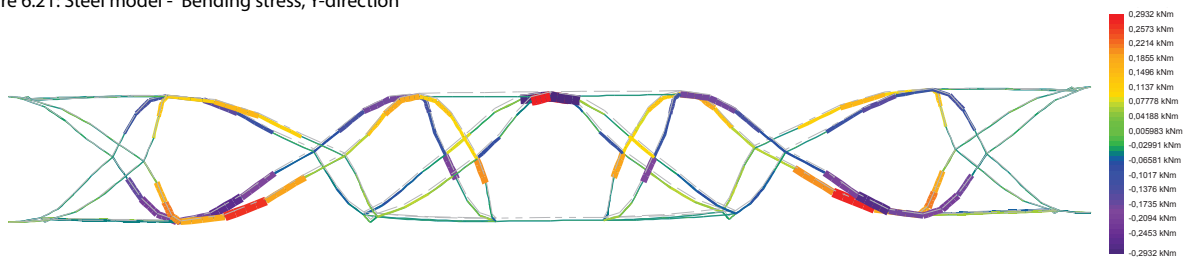
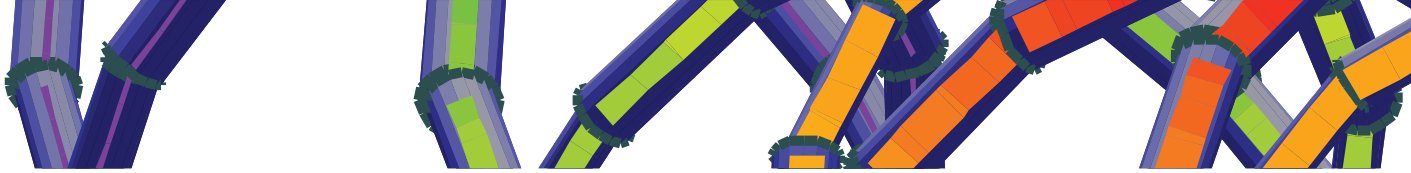


Figure 6.22: Steel model - Torsion



In the Y-direction the moments are relatively small, the largest moments are in the vertical Z-direction, and appear at the center knots of the beam with maximum moments of 1,412 kNm. This is also due to the point load that is deforming the beam to an oval shape. (Figure 6.23)

The largest shear stress and shear force in the y-direction are visual at the knots in the middle of the beam, which are the furthest out of the center of the beam for the y-direction. Tensile and compressive stresses and forces cross at these knots and therefore a large shear stress applies. The shear stresses are about + and - 11 kN/mm<sup>2</sup>, and the shear forces are + and - 5,73 kN. (Figure 6.24 & 6.25)

For the shear stress and shear force in the z-direction, the largest stresses and forces are at the upper and bottom part of the beam. This is due to its large distance from the center of the beam in the z-direction. The maximum shear force is 3,94 kN and the minimum shear force is -11,43 kN. The shear stress has a maximum of 9,763 N/mm<sup>2</sup> and a minimum shear stress of 19,49 N/mm<sup>2</sup>. The shear forces are similar in the steel and composite model, even though the shear stresses in the steel model are slightly higher, this might be the cause of the different values of the young's modulus and shear modulus. (Figure 6.29 & 6.30)

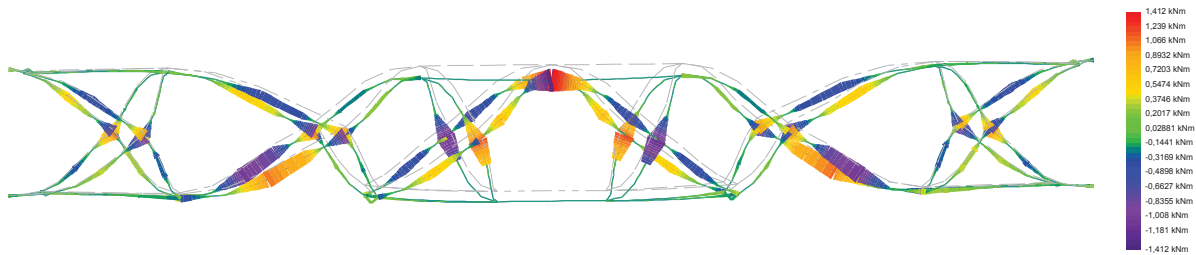


Figure 6.23: Composite model - Moment, Z-direction

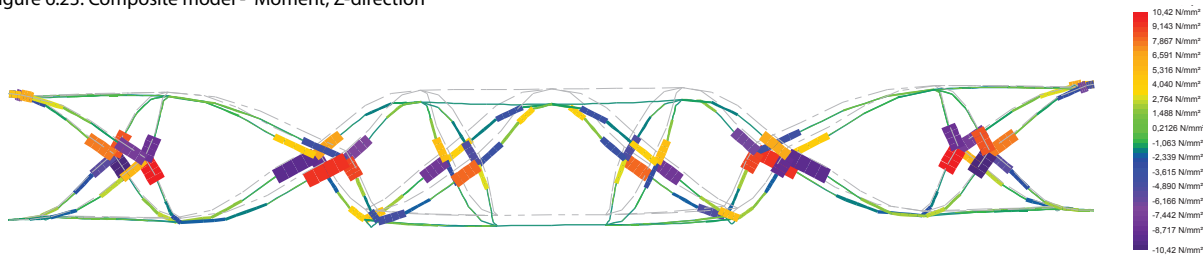


Figure 6.24: Composite model - Shear stress, Y - direction

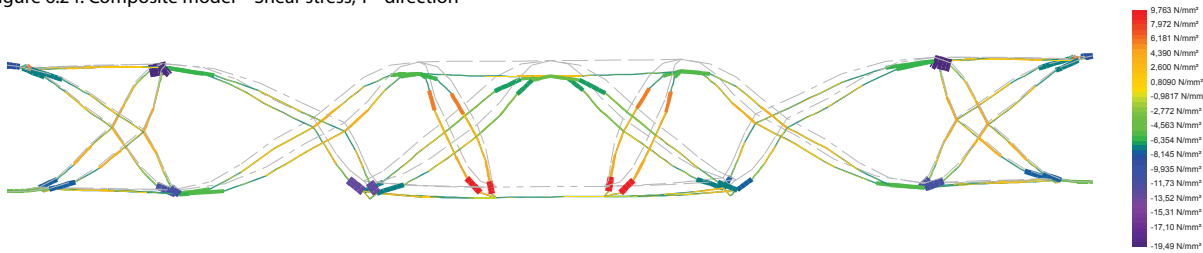


Figure 6.25: Composite model - Shear stress, Z - direction

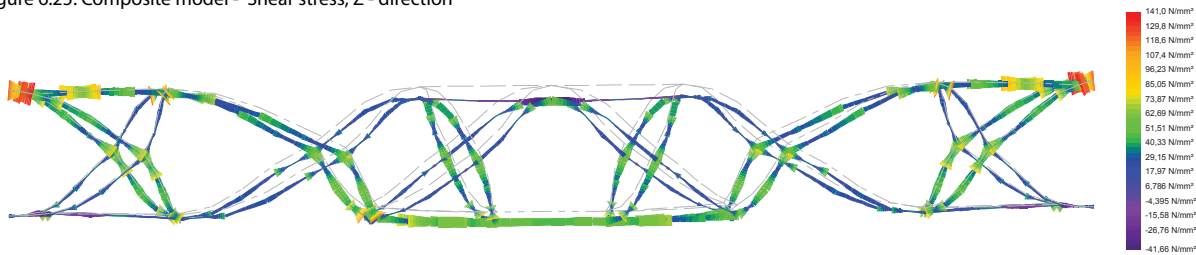


Figure 6.26: Composite model - Combined stress, C1

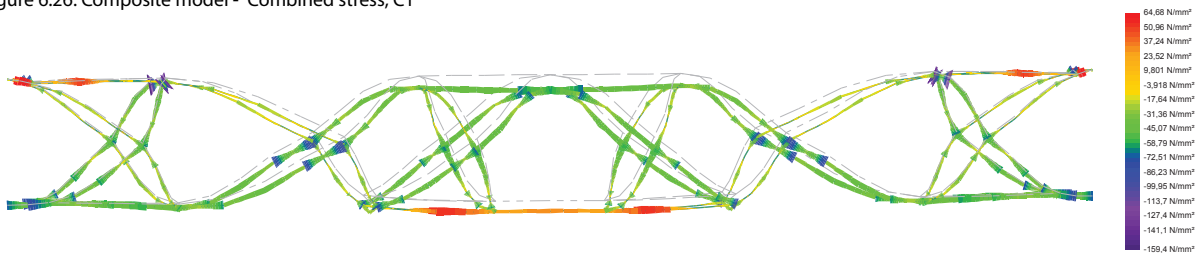
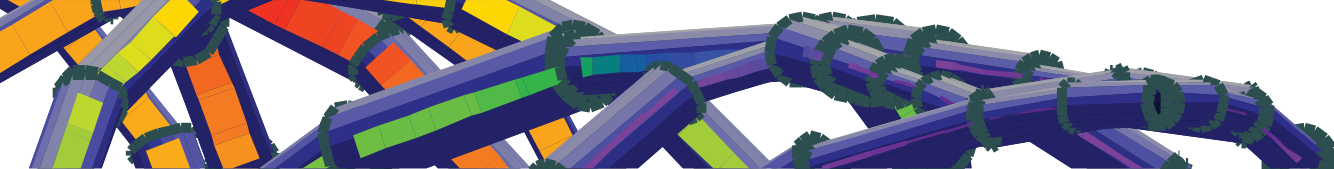


Figure 6.27: Composite model - Combined stress, C2



Eventually, the visualisation of the combined stresses gives a valuable output for this research. It is important that the topology, shape and size optimization has led to a optimized shape with no peak stresses. In figure 6.26 and 6.27 the visualisations of the combined stresses in both direction are shown. Since the overall parts of the beam show no peak stresses it can be concluded that the optimization on size has led to a stable shape, with maximum stresses of 141,0 N/mm<sup>2</sup> near the support points and in most members stresses of less then 70 N/mm<sup>2</sup>. These results are similar to the results of the optimized beam with steel properties. This rigid composite model should be able to transfer the point load of 50 kN to the support points.

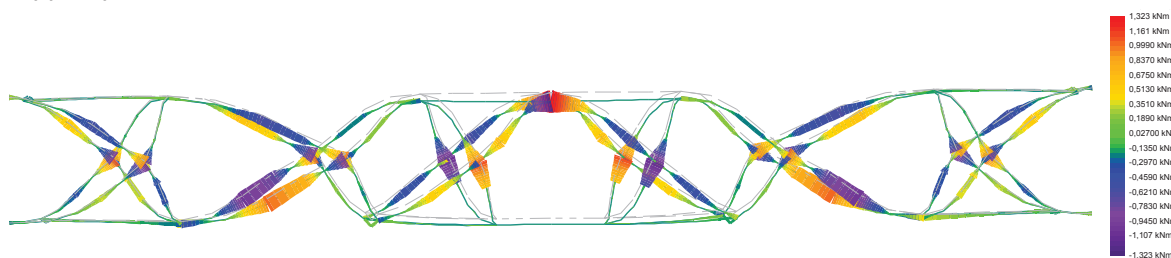


Figure 6.28: Steel model - Moment, Z-direction

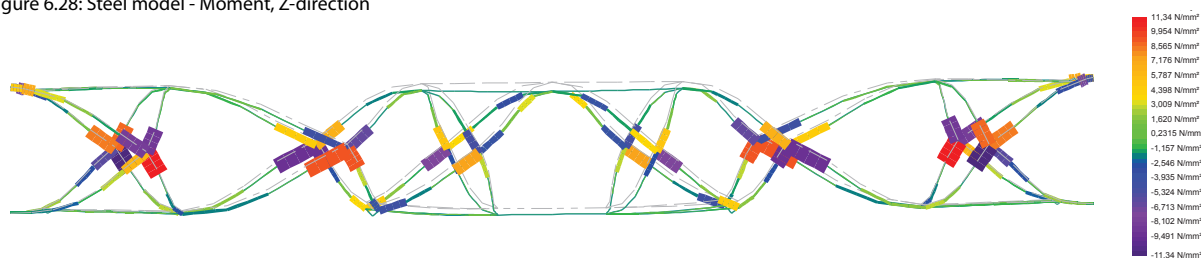


Figure 6.29: Steel model - Shear stress, Y-direction

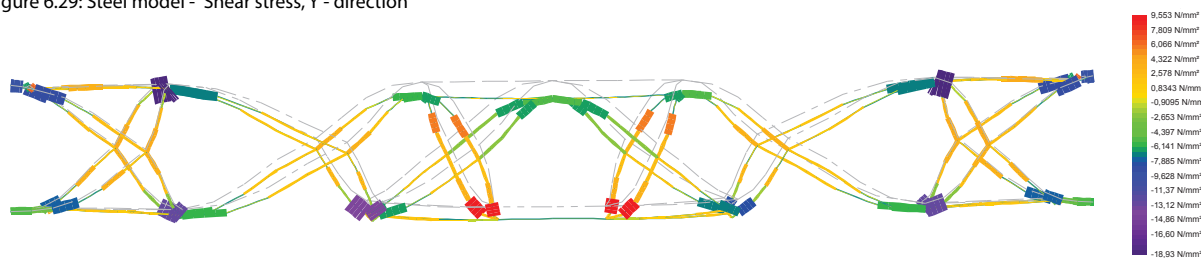


Figure 6.30: Steel model - Shear stress, Z-direction

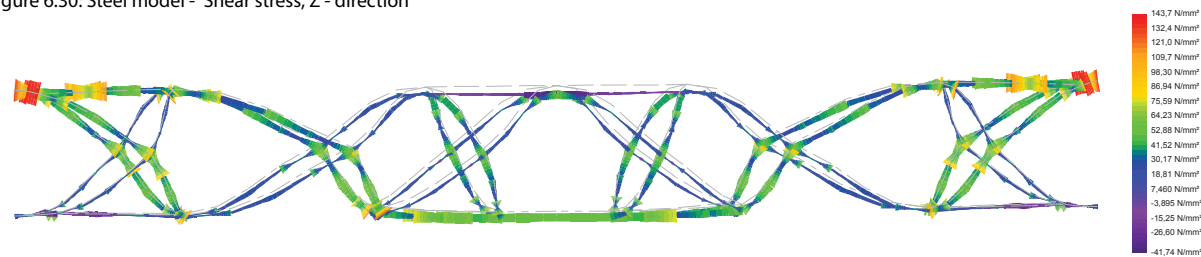


Figure 6.31: Steel model - Combined stress, C1

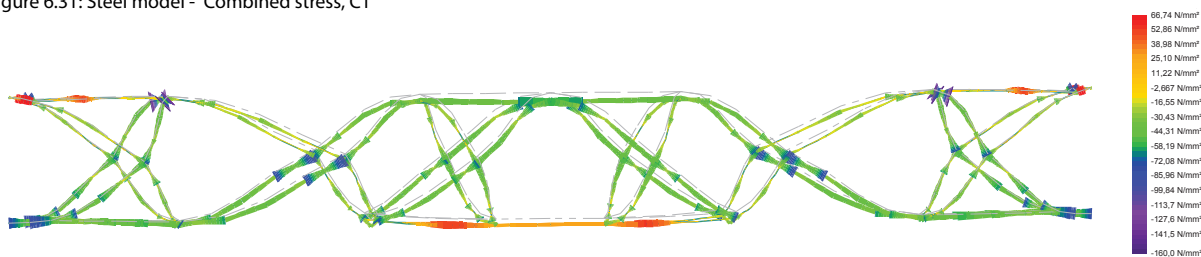


Figure 6.32: Steel model - Combined stress, C2

6.3.1 CONVENTIONAL CONCRETE BEAM

The conventional concrete beam can be calculated using the rules of thumb. For a normal beam, the height of the beam can be calculated by the formula:

$$1/10 * L = H \quad 1/10 * 8 = 0,8 \text{ m}$$

The width can be calculated by the formula:

$$1/5 - 1/3 * H = W \quad 1/3 * 0,8 \approx 0,3 \text{ m}$$

With these dimensions the volume is 1,92 m<sup>3</sup>, and the weight of pre-mixed concrete is 4090 kg. In comparison to the weight of the optimized beam, 165,8 kg, this is a difference of about 25 times as heavy. With these properties the moment and displacement of a concrete beam can be calculated.

**Beam characteristics:**

- P = 50 kN concentrated load
- L = 8 m beam length
- E = 14000000 kN/m<sup>2</sup> young's modulus
- I = 1280000 cm<sup>4</sup> moment of inertia

**Shears, moments and deflections**

$$R = V = P/2 = 25 \text{ kN} \quad \text{support reactions}$$

$$M_{\text{max}} = P * L / 4 = 100 \text{ kNm} \quad \text{max. moment}$$

$$\hat{\delta}_{\text{max}} = P * L^3 / 48 EI = 2,98 \text{ mm} \quad \text{max. deflection}$$

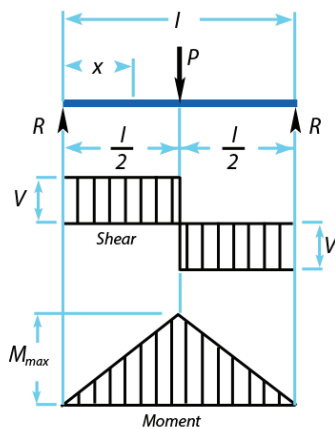


Figure 6.33: Shear, moment and deflection calculation

	Material	Staad Pro	GSA	Scalemodels
Linear	Steel	✓	✓	
	Concrete			
	Composite	✓		
Curved	Steel	✓	✓	
	Concrete	✓	✓	✓
	Composite	✓	✓	

Table 6.2: Analysis performed with software and testing

6.3.2 GENERAL CONCLUSIONS

For the structural analysis of the beams two software programs are used; Staad Pro and GSA. By comparing the results of the analysis it can be stated that these programs give the same results.

The output of the Paragen method was a size optimized linear member model with the material properties of steel, which is not representative for the final case that has to conform to the funicular shapes of inflatables. Therefore, a curved member model with the material properties of steel is optimized on size and analysed using Staad Pro and GSA, and the results are compared. Due to this curving of the model the deflection is increased from 13,22 mm to 28,34 mm, and the frequency is decreased from 32,5 Hz to 24 Hz. The model is less stiff and has a larger deflection.

Further research had to be made by replacing the material properties of steel to the material properties of composites. Therefore, the material properties of E-glass epoxy are applied, since this material will be applied in the prototype. By changing the material properties a new iterative cycle of determining the diameter and wall thickness is necessary. The outcome is a structurally optimized beam (topology, shape and size) with for a composite beam. To compare the results with previous analysis, this optimized beam is also analysed with the material properties of steel. With these analysis in Staad Pro, GSA and by testing scale models, the results are validated as shown in table 6.2.

The deflection is largely increased in comparison to previous analysis, and in comparison with the same optimized beam with steel properties. The deflection of the composite model with a 50 kN point-load applied is 87,51 mm.

The axial forces are distributed by clear tension and compressive lines, and give similar results in all analysis.

Due to the point-load the circular beam is deforming to an oval shape, this is visual by the bending stresses, element rotation and shear stresses. This is also visible in the tests with the scale models.

The stresses in the composite and steel model are similar and no large differences are shown. The combined stresses show a balanced structure, with low peaks and evenly distributed stresses. This is the result of the optimization on size and shape. Therefore, it can be stated that the optimization is performed accurate.

7

# Scale models





## 7.1.1 FRAMEWORK

Several different geometries were used as cases for the fabrication and testing of scale models. The geometries were derived using the database created with the ParaGen method. The cases were selected based on the different criteria which are relevant in the frame of this research, i.e. low and high frequency, low deflection and lowest weight<sup>1</sup> with highest frequency. The four different cases corresponding to these criteria were all fabricated and tested three times to reduce the chance on abnormalities. All the scale models were tested using a 3 point bending test in the van Mussenbroek laboratory at Eindhoven Technical University.

The results of the bending test are finally compared to each other to determine which geometry is the strongest. The method used for the fabrication of the models is not at all comparable with the actual production method proposed in this thesis. Therefore, it is important to note that this experimental study is primarily aimed at comparing different geometries to validate ParaGen and explore the differences between linear and curved members and secondarily to gain hands on experience with fabric formwork.

## 7.1.2 GEOMETRIES

The cases were derived using the ParaGen online database. The decision for which case to use was based on the four criteria explained in the previous paragraph. The choice was not merely based on the best or worst performing solution in a specific criterium. It was also important that the morphology of the four cases had some significant differences. In this way the test results of the models can be compared more easily, since slight manufacturing deviations have less influence. The four cases that will be manufactured are the following;

1. idtag 1269: Lowest weight<sup>1</sup> with highest stiffness
2. idtag 799: Large deflection, ;low stiffness
3. idtag 1249: Lowest deflection
4. idtag 1259: Highest stiffness

Table 7.1 shows the key performance values of these four cases. Based on these performance values we expect that id 799 will be the weakest based on its lower frequency and thus stiffness. The other three have almost identical frequency values, ranging between 30.3 and 33.7 Hz. In addition, the weight and deflection are also not far apart. The relevance of the

idtag	deflection (-Y) [cm]	Weight [kg] <sup>1</sup>	Modalfrequency [Hz]
1269	1.33	132.8	32.5
799	2.49	330.6	7.6
1249	1.15	143.2	30.3
1259	1.43	146.6	33.7

Table 7.1: The four cases for the scale models with their key performance values

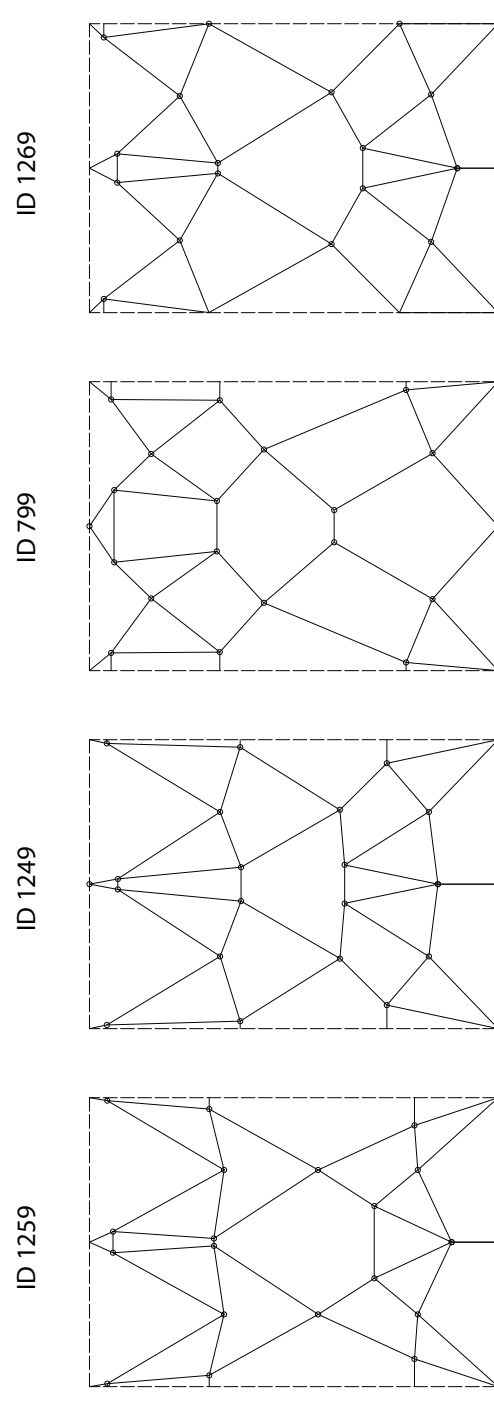


Figure 7.1: Unrolled pattern of the four cases.

1. The weight of these geometries is based on steel tubes with a variable diameter and wall thickness resulting from the FEA using StaadPro.

fabrication of these models can be found in the difference between the linear line model given by ParaGen and the curved members of the actual scale model. ParaGen uses straight linear members as a simplification of the real model. Linear members transfer loads more efficiently, which might render the illusion of an optimal geometry. When using curved members, id 1259 could prove to be less stiff than id 1249 even though it has a higher theoretical modal frequency. Figure 7.2 shows both geometries underneath one another. The blue circles indicate the location of the largest difference in morphology.

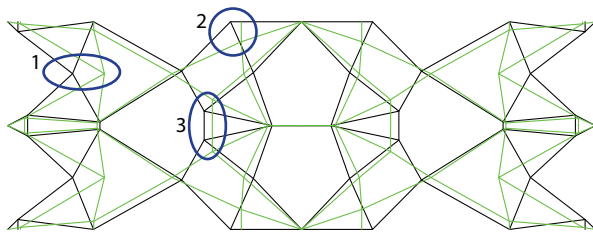


Figure 7.2: Pattern of id 1269 (black) and 1259 (green) and their main morphological differences

Figure 7.2 illustrates the hypothesis explained above. The main difference between the linear computer model and the curved scale model will be in areas one and two in the case of id 1259. Here, shear forces will not be transported efficiently since the members are bound to the surface of the inner tube. This prevents the ability to take the shortest, most efficient route as in the computer model.

### 7.1.3 MANUFACTURING METHOD

The manufacturing method was developed in a way to control the different parameters as much as possible. In this way, the only difference between the models is the geometry. Every geometry was manufactured three times to give significant results. ID 1269 was only tested two times since one beam was kept as a show model. The models were cast in 2 weeks, casting one model every morning. The following morning, the beam was removed from the falsework and put aside to continue drying. The beams were tested using a 5-point bending test in sets of 3 after 13, 14 or 15 days drying. Also, standardized mortar bars were made with every cast according to NEN 3835 to test inconsistencies in the concrete composition. The low viscosity concrete mixture for ten litres is shown in table 7.2.

The production technique used for the fabrication of the scale models was based on a method described by Dominicus et al. (2008) for producing concrete bone structures. The moulds for the concrete beams were constructed of multiple layers of PVC piping. Ini-

tially, clamps which represent the inverse of the beam were sawn out of standard PVC pipes with a diameter of 160 mm. Two layers of these clamps were mounted to a PVC pipe of 1.4 meters long. Then, two layers of high tenacity Lycra fabric were pulled over the PVC, followed by a third and final layer of clamps (Figure 7.3). The mould was then mounted in a steel bracket keeping it in place during the cast, and allowing the model to rotate about its axis to prevent sagging of the uncured concrete (Figure 7.3). Treaded rod was mounted into the top and bottom ends of the model, allowing every model to be fixed identically in the bending test. Since the model was pinned at the top and bottom of each side, the two form a force couple. A detailed manual of the manufacturing method is shown in Appendix F.

Material	Amount [Kg]
Cem I 52.5 R	9.5
Limestone flour	3
Glenium 27 con. 20%	0.45
Water	2.66
Polypropylene fibre (12 mm)	0.114
Sand 0.125 - 0.25	2.144
Sand 0.25 - 0.5	3.369
Sand 0.5 - 1	0.612

Table 7.2: Concrete composition for 10 litres



Figure 7.3: 1: Mounting clamps on the PVC piping, 2: Finished mould in the falsework, 3: Casting of the concrete

ID: 1269



ID: 799



ID: 1259



ID: 1249



## 7.2.1 INTRODUCTION

As explained earlier, every geometry was fabricated three times. All the beams were tested using a five-point bending test in a 100 kN pressure bench located at the van Musschenbroek laboratory at the TU campus. Concrete test samples of every cast were fabricated and tested according to NEN 3835. First, the three beams with a similar geometry are compared to each other in order to determine the failing pattern. Ultimately the four different geometries are compared to each other.

## 7.2.2 ID 1269

For this geometry a set of three beams were fabricated of which only two were tested. Since this geometry serves as a case for the proposed production method, one beam will be used as a show model. The crack pattern of the two tested beams is shown in figure 7.5, and the force-deflection diagram in figure 7.4. Beam 0 failed at a maximum force of 4.99 kN with a corresponding deflection of 17.55 mm, and beam 1 at 6.74 kN at 18.9 mm deflection. An overview of the data of id 1269 is given in table 7.3.

Figure 7.5 shows that the beams fail at the members which are mostly subjected to tension (¶ 7.1.3), which correlates with the fact that concrete is poor at absorbing tensile forces. Members always fail near the nodes, and almost never in the middle. This is due to the fact that the moments are often the largest near the nodes (chapter 6).

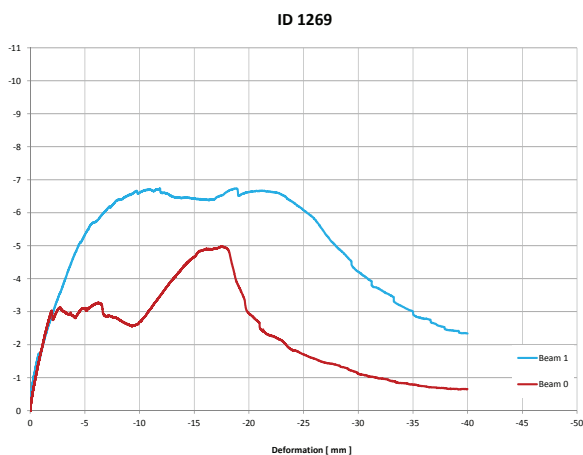


Figure 7.4: Force- deflection diagram of id 1269

	FEM model	Beam 0	Beam 1
Weight [kg]		23.57	33.29
Drying time [days]	-	11	15
Maximum force [kN]	8	4.99	6.74
Deflection at max. force [mm]	-	17.55	18.9
Force at 1st crack [kN]	-	3.03	1.74
Deflection at 1st crack [mm]	-	1.98	0.82

Table 7.3: Results of id: 1269

Members are linked by fixed moment connections, meaning that forces have to be transferred from one member to the other near the nodes. Beam 0 also cracked at a cross member in the bottom, which means that the shear forces might be higher than expected on beforehand. In general, it can be said that the crack pattern correlates with the structural analysis performed in chapter 7. It has to be noted that the first few cracks are often the ones on which the beam will fail eventually. When a crack occurs, a small “dip” is visible in the force-deflection diagram. For example, the first crack which occurred in beam 1 is clearly visible in figure 7.4 near 0.8 mm deflection and a force of 1.74 kN. An important observation is the fact that the graphs of beam 0 and 1 were almost identical up to the point that the first crack occurred in beam 0. The angle of inclination is very similar meaning that until a crack occurs the beams behave similar.

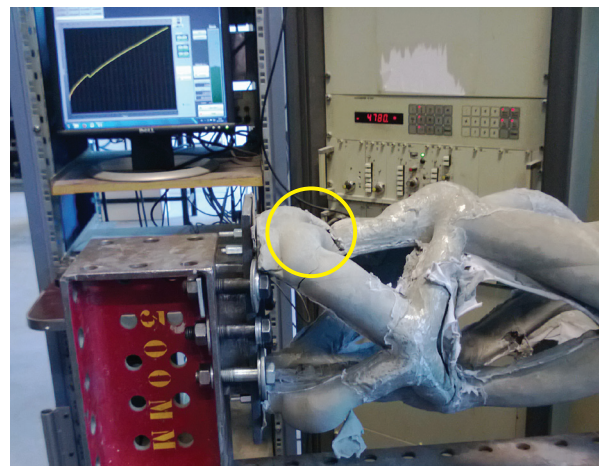


Figure 7.6: Testing beam 1: first crack

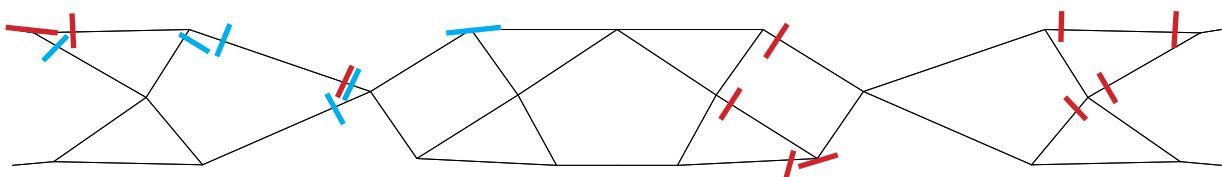


Figure 7.5: Crack pattern of id 1269; red: beam 0, blue: beam 1

The main difference in the test results of id:1269 is the maximum force (Table 7.3). Beam reached a maximum force of 6.75 kN which is 35% more than beam 0. However, the deflection due to these forces shows less difference; only 7.5%. When we state that the deflection of the two beams stayed constant, the difference in maximum force has to be caused by something else. The answer can be found in the relation between the deflection of point loaded fixed beam and its stiffness [8.1];

$$\delta_{\max} = \frac{Fl^3}{192EI} \quad 8.1$$

Where;

- $\delta_{\max}$  = Maximum elastic deflection
- F = Center point load acting on the beam
- L = Length of the beam
- E = Elasticity modulus
- I = Second moment of area

In our case, the deflection  $\delta_{\max}$ , the length L and Young's modulus E are constant. The force F is 35% higher in the case of beam 1. To compensate, the second moment of area I also has to be higher in beam 1. This is correct since beam 1 is almost ten kilograms heavier than beam 0. The density of the concrete mixture is constant which means that the members of beam 1 are thicker than those of beam 0, causing a higher second moment of area.

The force-deflection diagram also shows that the beams possess a very large residual strength due to the polypropylene fibres. Even though the concrete has cracked at numerous places, the fibres still possess enough strength to prevent the beam from sudden collapse, which is an advantage with respect to safety. However, this also renders fibre reinforced concrete difficult to standardize, since its behaviour is difficult to predict.

### 7.3.3 ID 799

This candidate solution was included in the fabrication and testing of the scale models since its geometry and topology is very different compared to the other three cases. During shape optimization the bottom horizontal members moves upwards

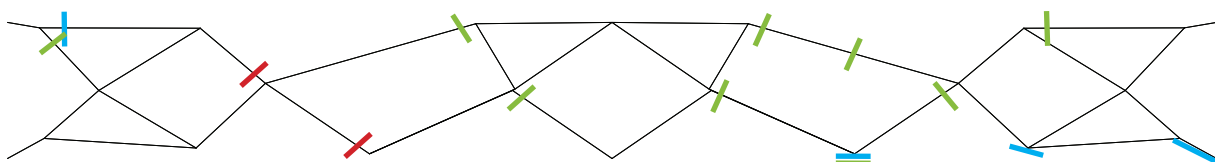


Figure 7.7: Crack pattern of id 799; red: beam 3, blue: beam 4; green: beam 5

against the diagonal members, changing the topology of the beam. According to the ParaGen analysis, this geometry is the weakest of the four since it has a much lower modal frequency (approximately 22% of id 1259). In addition, its theoretical deflection is also approximately twice as large as the other beams. Figures 7.7, 7.8 and table 7.4 show the crack pattern and corresponding data of id 799.

	FEM model	Beam 3	Beam 4	Beam 5
Weight [kg]		29.33	25.32	23.94
Drying time [days]	-	15	14	17
Maximum force [kN]	4	10.14	8.24	4.61
Deflection at max. force [mm]	-	23.04	10.36	14.94
Force at 1st crack [kN]	-	4.13	6.92	2.88
Deflection at 1st crack [mm]	-	3.47	5.69	3.65

Table 7.4: Results of id: 799

Between the three tested beam with this geometry, no clear crack pattern can be recognized. Again, members almost always crack near the nodes due to higher stresses, but not at the same locations. It seems that the weak points of this geometry are the cross members at the bottom of the beam. This was the location of the first cracks of both beam four and five (Figure 7.7). However, the results of this beam are completely the opposite of the expectations,

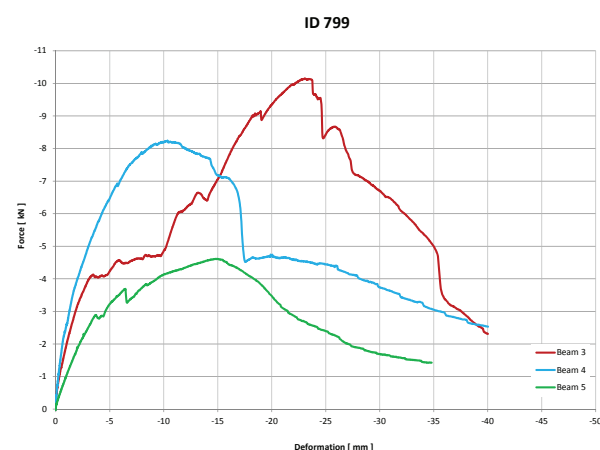


Figure 7.8: Force- deflection diagram of id 799

and therefore contradict the hypothesis of being the weakest. Instead of being the weakest and having the highest deflection, two of the three beams tested showed a larger maximum force than all the other beams. Beam four has one of the highest forces with one of the least deflections. Beam three has a high deflection which was expected, but also a maximum force of 10.14 kN. This is approximately twice the force of the other geometries, which are theoretically stiffer. The force-deflection diagrams of the three beams show different patterns. No generalizations can therefore be made regarding maximum force and deflection, or force and deflection at the first crack, since the data shows too much variation. No single explanation can be given regarding the reason of these deviating results. The total weight of the beams does not differ enough from the other beams to cause the difference. Also, the density, flexural strength, compressive strength and Young's modulus of the concrete mixture show no significant variations compared to the mixture of the other beams (Appendix G). Therefore, the difference is either caused by a very optimal distribution of material during fabrication resulting in a size optimized beam, or this might be due to the theoretical optimization with steel and linear members, while the scale models have curved members and are produced with concrete.

#### 7.2.4 ID 1259

According to the analysis performed using the ParaGen method, this geometry possesses the highest modal frequency of the four. Since the deflection and stiffness are roughly the same as id 1269, it should perform in a similar way as id 1269. However, in the crack pattern of id 1269 we saw that cross members are more likely to fail due to shear forces locally. This geometry includes certain cross members which are prone to fail when subjected to large shear forces, due to the fact that their radius of curvature is smaller. Figure 7.9 shows the crack pattern of beams six through 8, with the corresponding data in table 7.5 and the force-deflection diagram in figure 7.10.

Contrary to the tested beams with id 1269, the beams with id 1259 showed no cracks near the cross members. This could mean that the beam is weaker somewhere else, or the shear forces are less than in id 1269. The crack pattern of the three beams (Figure 7.9) shows that all the beams fail near the node in the

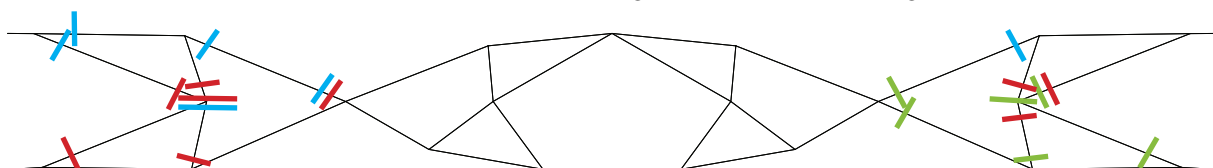


Figure 7.9: Crack pattern of id 1259; blue: beam 6; red: beam 7; green: beam 8

first and last quarter. It was already shown that forces accumulate near the nodes due to the fixed moment connections. However, according to the finite element model stresses are the highest in the tension and pressure zones near the middle of the beams. The crosses which connect the upper and lower members near the supports are typically under less stress. The failure of the beams near these points is therefore due to the disadvantageous geometry locally. Here, the angle of the members is too large which prevents the four members from forming a stable cross, as is the case in id 1269 (Figure 7.11). The node fails due to buckling and not because the stress in the node reaches the yield limit of the material.

	FEM model	Beam 6	Beam 7	Beam 8
Weight [kg]		25.51	24.05	28.38
Drying time [days]	-	15	14	13
Maximum force [kN]	7	4.20	5.06	3.81
Deflection at max. force [mm]	-	11.57	10.16	12.05
Force at 1st crack [kN]	-	3.54	3.36	2.8
Deflection at 1st tear [mm]	-	6.34	5.19	6.08

Table 7.5: Results of id: 1259

The three beams behave identically until the first crack occurs, which is near a deflection of 5.87 mm at 3.23 kN of pressure. After the first crack, the forces are transferred via different members until the stress

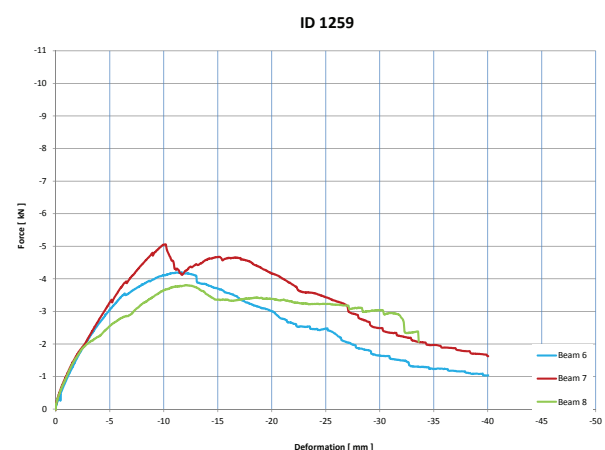


Figure 7.10: Force-deflection diagram of id 1259

reaches the yield limit of the material, which is around  $7.34 \text{ N/mm}^2$  for beams six, seven and eight (Appendix G). The maximum force is on average  $4.36 \text{ kN}$ , at an average maximum deflection of  $11.26 \text{ mm}$ . The relatively small differences in these values are not caused by the weight differences of the beams, but is mainly due to an advantageous distribution of material during fabrication.

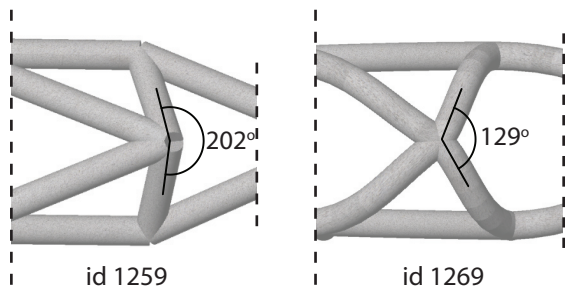


Figure 7.11: Disadvantageous geometry of id 1259 near the supports.

### 7.2.5 ID 1249

This geometry is similar to id 1269, with the largest differences located in the cross near the supports and the lower flange near the zero-moment area. According to the finite element analysis, this geometry should show the least deflection. However, the differences are small and will only show in an optimal model. The crack pattern and corresponding data are shown in figure 7.12 and 7.13 and table 7.6.

Compared to the other geometries, id 1249 shows a more elaborate crack pattern. The weakest part of the models is located around the supports. Similar to id 1259, the geometry of the cross is disadvantageous. It has to be noted that beam nine was already cracked during demoulding and is therefore not representative. Members almost always fail near the nodes like the other tested beams. The force deflection diagram of beam 10 is shorter due to a sudden detachment of the deflection meter plate during the test. However, a third deflection meter integrated in the pressure bench showed that the beam had already failed which renders the rest of the graph of less importance. Beams 10 and 11 failed at an average force of  $4.09 \text{ kN}$  at  $12.13 \text{ mm}$  deflection. Beam 11 shows a

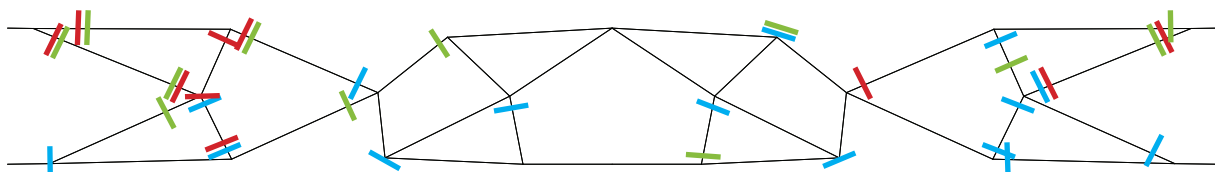


Figure 7.12: Crack pattern of id 1249; blue: beam 9, red: beam 10; green: beam 11

second peak around  $28 \text{ mm}$  deflection and  $3.8 \text{ kN}$  of pressure. However, this value is merely achieved by the residual value of the polypropylene fibres. Here, the stress in the material has already exceeded the flexural strength of the material. Therefore, the maximum force which is of interest in our case is near the first peak in the graph. Also, it has to be noted that a different plasticizer was used for the concrete mixture of beams nine through eleven<sup>1</sup>. Due to this plasticizer the concrete mixture has a lower flexural strength;  $5.16 \text{ N/mm}^2$  versus  $7.01 \text{ N/mm}^2$  (Appendix G). Therefore, when the same mixture was used the tested beams would show higher stiffness properties.

	FEM model	Beam 9	Beam 10	Beam 11
Weight [kg]		25.28	27.04	20.39
Drying time [days]	-	15	14	13
Maximum force [kN]	7	2.79	4.67	3.50
Deflection at max. force [mm]	-	24.44	13.73	10.53
Force at 1st crack [kN]	-	2.06	3.52	1.63
Deflection at 1st tear [mm]	-	11.01	6.38	2.98

Table 7.6: Results of id: 1249

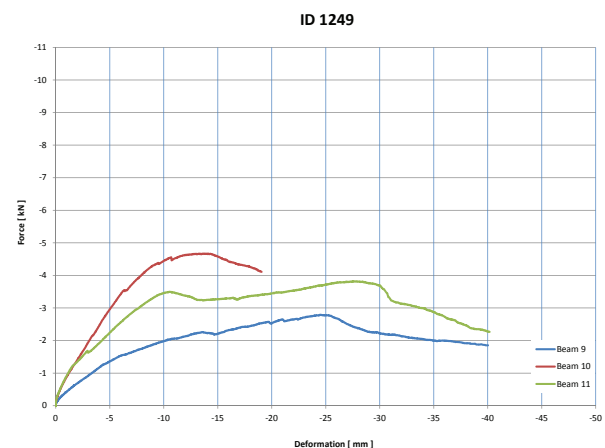


Figure 7.13: Force-deflection diagram of id 799

1. In the first 8 beams Glenium 27 con. 20% was used, for the beams with id 1249 Glenium 51 con. 35% was used.

### 7.2.6 AVERAGE LINEAR ELASTIC REGIONS

In the previous paragraphs all the data gathered during the testing of the beams was explained and analysed on geometry at a time. The goal of this chapter however was to compare the different geometries to each other to determine their relative stiffness. The most important part of the force-deflection diagrams is the linear elastic region where the material deforms elastically. This means that no permanent deformation takes place within this region, and the beam will return to its original form when the force is removed. According to Hooke's law, the relation between the force applied and the deformation is linear;

$$E = \sigma / \varepsilon \quad 8.2$$

Where;

- E = Elasticity modulus
- $\sigma$  = Stress
- $\varepsilon$  = Strain

The linear elastic region of every tested beam was approached using trendlines and its linear equation was subsequently determined. In this way, all the Y-values (Force) could be interpolated to the same X-value (Deformation), allowing us to determine the average of a set of beams with the same geometry. The plastic region of the diagrams are not relevant, since the stiffness of an element is determined within the elastic region. In addition, there are very large differences in the plastic regions of the beams. Even within the same geometry the behaviour is hard to predict due to the use of fibres, and fabrication variations between the beams themselves.

The four graphs representing the elastic regions of the four geometries are shown in figure 7.14. The graphs do not start in the origin since every beam can absorb a certain amount of stress within deflecting. The stiffness of a geometry is determined by the angle  $\alpha$ . The larger the angle, the larger the modulus of elasticity and thus stiffness, and the smaller the deformability. Following this analogy, ID 1269 is the stiffest, followed by ID 799. ID 1259 is slightly stiffer than ID 1249. However, when corrected with respect to its lower flexural strength it will be the other way round.

These results differ from the hypothesis based on the ParaGen results. This is mainly due to the difficulty of controlling all the variables during manufacturing. ID 1269, 1259 and 1249 possess very similar stiffness properties, which renders them susceptible for manufacturing variations. However, the results do confirm that ID 1269 is the best choice as a case to base the production method on, confirming the most important part of the hypothesis.

Average linear elastic regions

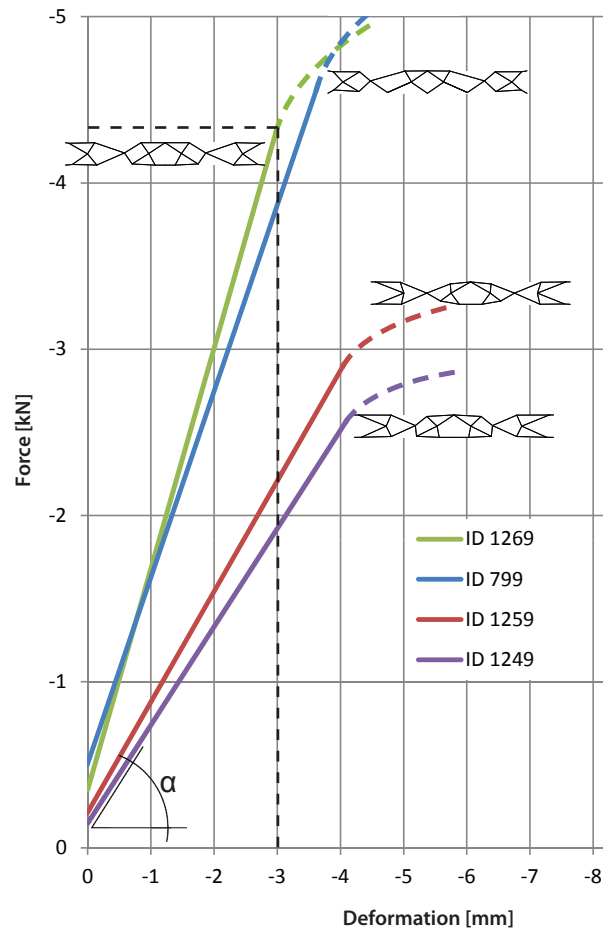


Figure 7.14: Average linear elastic regions of the four geometries.



All the scale models were tested in a 100 kN pressure bench at the van Musschenbroek laboratory at the TU/e campus. The weight of the beams varied between 23 and 33 kg due to member size fluctuations in the moulds. However, the distribution of the material within the model influenced the outcome more than the weight. The results of the mortar bars showed no significant variations with respect to the material density and yield strength. However, the flexural strength of the concrete mixture for id: 1249 was 27% less than the mixture for the other geometries due to the use of a different plasticizer (Glenium 51 con. 35%). Therefore, this id would probably perform better when concrete was used with the same flexural strength as the previous models.

ID: 1269 failed in all the beams in the tension zone which runs helically around the beam. This is natural given the properties of concrete, and means that there are no clear weak parts in the geometry. In every geometry, the members always fail near the nodes. The structural analysis performed in GSA and Staad PRO showed that stresses are the highest near the nodes due to the fixed moment connections, which explains the crack pattern of the scale models. ID: 1259, and to a lesser extent id: 1249, showed a concentrated crack pattern near the cross members at the supports. The morphology of the members prevents the formation of a stable cross locally, causing the node to fail due to buckling and not because the yield limit of the material is reached. Therefore, large angles between members should be avoided to prevent the nodes from local buckling, and the member length in transverse direction should be minimized.

To determine the stiffness of the four different geometries, the linear elastic region of every beam was determined using trendlines. In this region, according to Hooke's law, the deformation  $\varepsilon$  is proportional to the force  $F$ . All the beams showed this linear behaviour until a first crack occurred, which caused the deformation-force diagram to behave unpredictably due to the use of polypropylene fibers. The angle  $\alpha$  in Figure 7.14 is used as a measure for the stiffness. This confirms that ID: 1259 indeed has a disadvantageous geometry with respect to curved members, since it was initially optimized for straight linear members. Now, ID:1269, which is also the case for the remainder of the research, has the highest stiffness. It has to be noted that ID:799, which had the lowest theoretical stiffness, is the second stiffest geometry according to these results. This might be due to the theoretical optimization with steel and linear members, while the scale models have curved members and are produced with concrete.

8

# Prototype





## 8.1 INTRODUCTION

As a final step of the development phase, a full size prototype was fabricated. This prototype was fabricated to demonstrate the proposed production method. The fabrication was labour intensive due to limitations in commercial fabrication techniques and the equipment which was available to us. However, the manufacturing process resembled the proposed production method in many ways.

The structure is eight meters long and has an internal diameter of one meter. The morphology of the beam was determined in chapter two of this thesis. The wall thickness of the members was a result of the amount of material available to us. Therefore, the wall thickness of the members of the prototype do not correlate with the ideal wall thickness resulting from the structural analysis. However, the structure is still easily strong enough to support its own weight. The

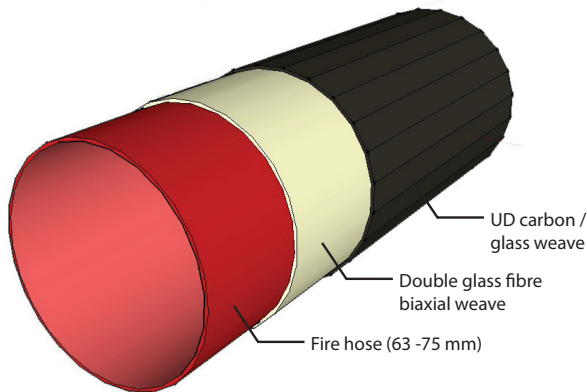


Figure 8.1: Laminate design of the prototype

laminates design of the members is shown in figure 8.1.

The members were constructed in different stages to realize the laminate design. Thanks to Eurocarbon, different fibres and weaves could be used to increase the modulus of the composite. The different materials used were the following;

- Fire hoses (63 and 75 mm)
- Poly urethane tubes (70 mm)
- PVC coated polyester inflatable tube
- Glass fibre chopped strand mat
- Glass fibre biaxial weave
- Carbon/glass unidirectional tape
- Polyester resin

## 8.2 FABRICATION

The first step in the fabrication process was the inflation and positioning of the secondary mould. Initially this inflatable tube was supported temporarily



Figure 8.2: Inflated secondary mould

The pattern of the structure was transferred to the inflatable tube using tape. Subsequently, fire hoses representing the main pressure and tension lines were mounted to the inflatable. These four hoses were interconnected to allow simultaneous inflation. They were designed for an overpressure of 10 bar. However, for our purpose a low pressure of 0.5 bar was used to allow easy manipulation of the hoses. For the crosses between the main pressure and tension lines poly urethane tubes were used (Figure 8.3). The variant with 100 % inflatable members proved to be difficult to maintain a constant pressure throughout all the tubes.

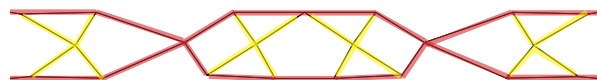


Figure 8.3: Fire hoses (red) and poly urethane tubes (yellow)



Figure 8.4: Inflated unfixed fire hoses with double glass fibre biaxial weave



Figure 8.5: Fixed inflated fire hoses



Figure 8.6: Support with welded steel nozzles

A double layer of glass fibre biaxial weave was pulled over the fire hoses before they were inflated and positioned in the correct place (Figure 8.5). To reduce the amount of junctions, the hoses only crossed near the zero moment. In the top and bottom of the middle of the structure the hoses were connected but did not overlap. Therefore, the hoses only needed to be fixed at the ends, and in the middle where they connected. In this manner, the hoses followed the pattern naturally. The junction of the top and bottom hoses were realized using metal wire. Hereby, the section of the cross was limited causing the two hoses to merge upon inflation (Figure 8.8). The fire hoses were finally rigidized using a polyester resin with 2% curing agent. This was done before the crosses were mounted to make the structure independent of air pressure as soon as possible. Since glass fibre becomes transparent after impregnation with a resin, the red fire hose became visible again.



Figure 8.7: fabrication of the crosses

The crosses were made of PU tubes covered with a double layer of biaxial glass fibre weave, and were rigidized with the same polyester resin (Figure 8.7). The nodes and junction of the resulting structure were reinforced using glass fibre chopped strand mats. After these reinforcements the secondary mould was removed, leaving the rigidized open cell structure (Figure 8.8).

The final step in the fabrication of the prototype was the application of a final unidirectional layer of carbon and glass fibre tapes (Figure 8.9). Since the fibres of this tape are placed in the longitudinal direction, they absorb bending forces more efficiently, making the structure much stronger. With this final layer, the laminate as shown in figure 8.1 is complete.



Figure 8.8: Junction between two fire hoses



Figure 8.8: Deflation of the secondary mould



Figure 8.9: Application of the UD carbon/glass layer

### 8.3 CONCLUSION

With the fabrication of the prototype the proposed production method was demonstrated. An inflatable secondary mould was successfully used as falsework. The primary structure was partially inflatable and subsequently rigidized, demonstrating the proposed method. In this case, hand lay up was used as a rigidization technique. However, when using techniques such as resin transfer moulding or vacuum infusion, fabrication time and especially surface quality can be greatly improved. When the production method is optimized for industrial fabrication techniques, it could be a very rapid deployable system. Especially when rigidizable materials used for Gossamer structures can be utilized.

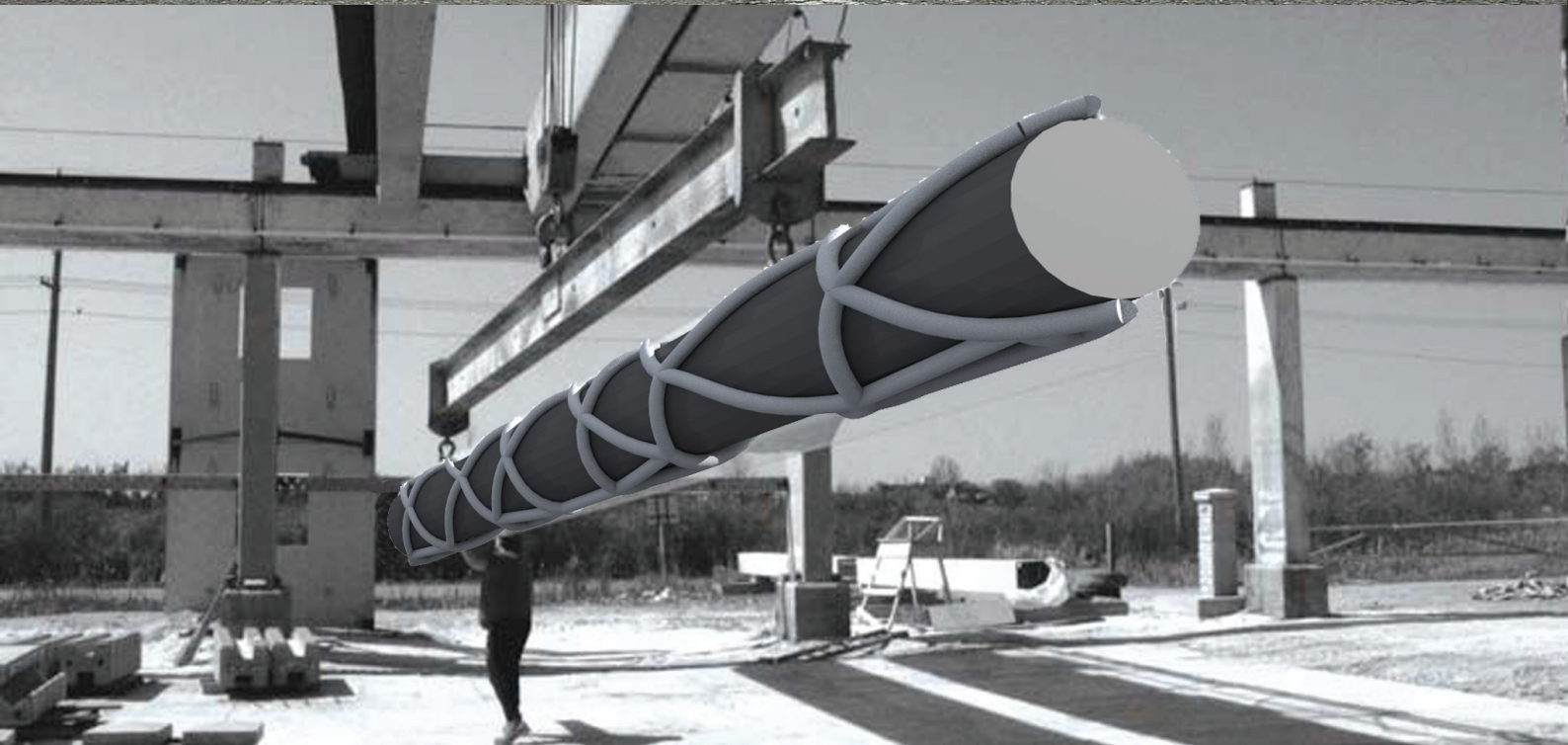
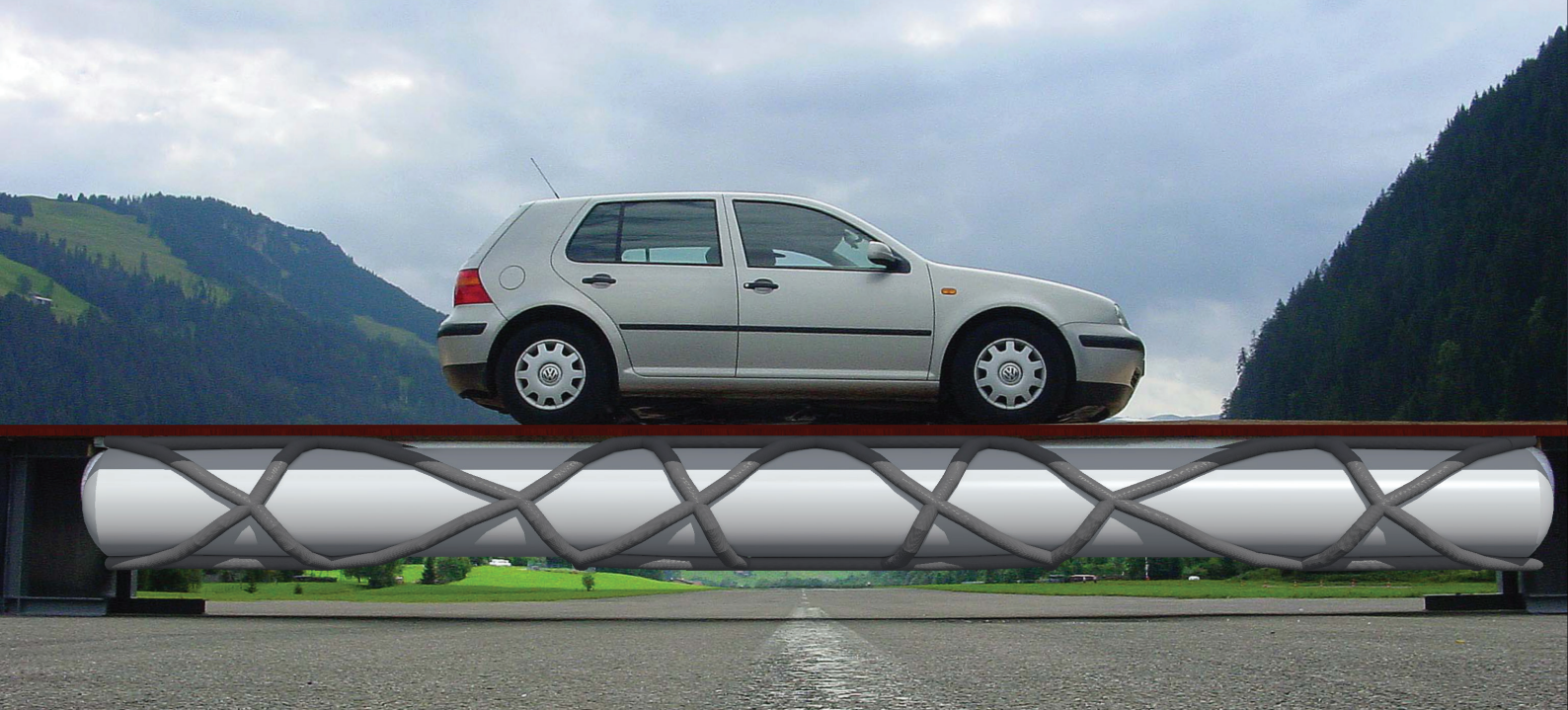
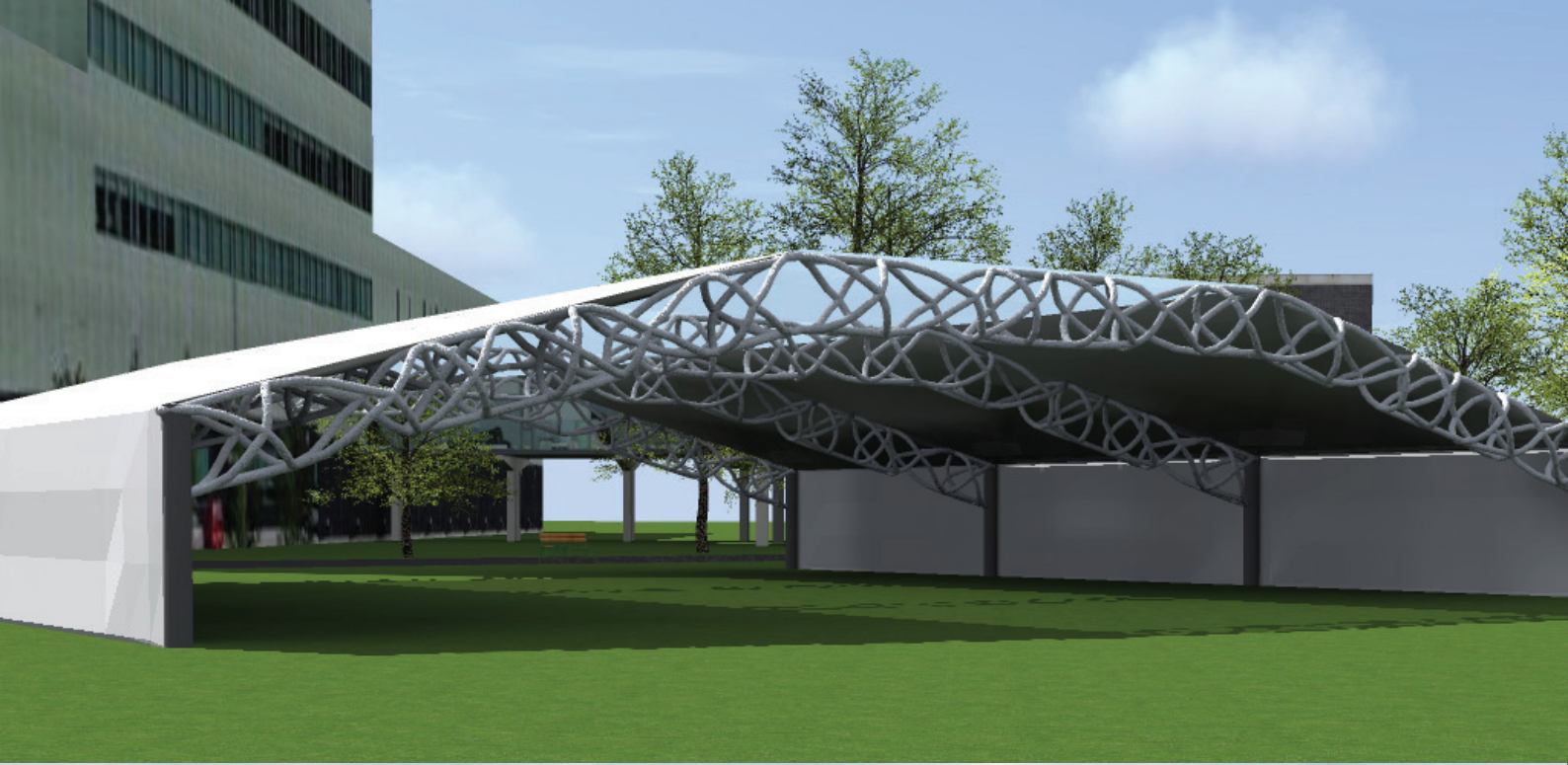












### CONCLUSIONS

The meta objective of this research was to contribute to the current global sustainability by reducing the amount of material used for structural elements in the construction sector. Therefore, the goal in the research was to develop a production method for structurally optimized section active structure systems, by using a rigidized inflatable structure. To reach this goal, several sub goals were defined corresponding to the different research objects. Between the different literature reviews, case studies, structural analyses, and experimental research a very integral and complete study was performed where an innovative production method was developed. Therefore, we can say that the goals and objectives set at the beginning of the study were achieved.

The research started with empirical case studies of section active structure systems to determine their general morphological features. This showed that the optimized beam is the basis for all other optimized systems, and was therefore used to perform shape optimization using the ParaGen method. This topologically and shape optimized model was finally size optimized using GSA and STAADpro. Literature reviews into inflatables structures resulted in the most suited typology and envelope material to use for the secondary mould. Where the study into rigidizable materials showed that no single rigidizable material used in the space industry can be transferred directly to the construction sector. Therefore, the strong attributes of these materials were utilized in combination with commercial fabrication methods.

With the structural analysis the exact force distribution was revealed, and translated to optimal member sizes. With the fabrication of the scale models an existing method was refined to produce concrete open cell structures. The test results of these models were used to validate the results of the different computer models. With these results, a prototype was finally made to demonstrate the production method in full size.

With this research it was shown that rigidized inflatables may be a step forward in the development of construction techniques for spatial structures subjected to structural optimization. The method eliminates the need for large amounts of falsework, rendering very rapid deployable elements. In addition, the method produces extremely light weight structures due to the multiple levels of optimization. The final production method is a synthesis between the optimization of structural elements, and the optimization of fabric formwork.

### RECOMMENDATIONS

This aim of this thesis was to give a complete overview of the problem, and the road towards the solution to that problem. However, there are several aspects that are still worth investigating;

- It should be clearly identified which applications are suited for fully inflatable, partial rigidization and /or full rigidization. In this way, a broad range of possible applications can be accommodated.
- The influence of an inner inflatable on the strength of the structure still has to be researched. The inner inflatable together with the rigidized outer structure will act as a tensairity. The inflatable prevents the outer members from buckling. Therefore, these members can be loaded to their yield limit since buckling is no longer the failure mode. Following the principle of combined action, the strength of the whole will be larger than the sum of the individual parts. A downside of course is the fact that this structure no longer is independent of air pressure.
- Many bridges in the Netherlands no longer meet the current safety codes, since traffic has increased over the years. These bridges are no being reinforced using carbon fibre mats which are glued to the structural members. This process could be much faster when using a form of rigidized inflatables.
- The implementation of rigidizable materials used in the space industry have to be studied when they are sufficiently developed for implementation in other industries. These materials could make the method even faster and less involved
- With the inspire case studies it was shown that method should be suited to produce elements which are optimized with different boundary conditions. To prove this, multiple prototype have to be manufactured.
- One optimization level can still be researched. This includes the translation of the structural analysis to the fibre orientation of the composite layers.



## REFERENCES

- Allred, R.E., Hoyt, A.E., McElroy, P.M., Scarborough, S., Cadogan, D.P., UV rigidizable carbon-reinforced isogrid inflatable booms, 2002, American Institute of Aeronautics and Astronautics, USA
- Ant Farm, *the Inflatocookbook*, 1973, Ant Corps, California, USA
- Bailiss, J.: *Fabric-formed concrete beams: Design and analysis*, MEng Thesis, Department of Architecture and Civil Engineering, Bath, University of Bath, 2006
- Bektesevic, A.: *Complexe vormen & Pneumatische Constructies; ontwerp voor een complexgevormd, pneumatisch en mobile paviljoen*, 2010, Eindhoven University of Technology, Eindhoven, The Netherlands
- Bendsoe, M.P.: *Optimization of Structural Topology, Shape and Material*, 1995, Berlin, Germany
- Beninga, K., Davenport, R., *An advanced concentrator for solar dynamic power systems in space*, 2002, Science Applications International Corporation, San Diego, USA
- Bond Nederlandse Architecten, *NL/SfB-tabellen*, 2005, Amsterdam, The Netherlands
- Budinski & Budinski, *Engineering materials: properties and selection*, 2002, Prentice Hall, UK
- Buelow, P., *ParaGen: Performative exploration of generative systems*, 2012, University of Michigan, Ann Arbor, USA
- Cauberg, N.: Parmentier, B., Janssen, D., Mollaert, M., *Fabric formwork for flexible Architectural concrete*, 2008, Londen
- Cadogan, D.P.: Scarborough, S.E.: *Rigidizable Materials for use in Gossamer Space Inflatable Structures*, 2001, ILC Dover, Frederica, USA
- Chapman, C.D., *Structural optimization via the genetic algorithm*, 1994, Massachusetts Institute of Technology, Boston, USA
- Christensen, P.W., Klarbring, A., *An Introduction to Structural Optimization*, 2009, Division of Mechanics, Linköping University, Linköping, Sweden
- Dantzig, J.A.: Rappaz, M., *Solidification*, 2009, EPFL
- Defoort, B., Peypoudat, V., Bernasconi, M.C., Chuda, K., Coqueret, X., *Recent advances in the rigidization of Gossamer Structures*, Textile composites and inflatable structures, p259-283, 2005
- Dombernowsky, P., Sondergaard, A., *Three-dimensional topology optimization in architectural and structural design of concrete structures*, 2009, Aarhus School of Architecture, Aarhus, Denmark
- Dominicus M.M.T., Ketelaats J., van Laerhoven P., Pronk A.D.C., *The production of freeform concrete elements in a flexible mould*, 2008, IASS, Acapulco
- DuPont, Summary of properties for Polyimide Kapton films, Wilmington
- DuPont Teijin Films, Physical, Thermal, Electrical and Chemical properties of Mylar, Hopewell, 2003
- Engel, H.: *Structure Systems*, 1997, Ostfildern-Ruit, Germany
- European Commission: *A strategy for smart, sustainable and inclusive growth*, 2010, Obtained from <http://eur-lex.europa.eu/LexUriServ/LexUriServ.do?uri=COM:2010:2020:FIN:EN:PDF> on 17 October 2012
- European Commission: *Roadmap to a Resource Efficient Europe*, 2011, Obtained from [http://ec.europa.eu/environment/resource\\_efficiency/pdf/com2011\\_571.pdf](http://ec.europa.eu/environment/resource_efficiency/pdf/com2011_571.pdf) on 17 October 2012
- Frattari, L.: *The Structural Form; Topology Optimization in Architecture and Industrial Design*, 2011, University of Camerino, Ascoli Piceno, Italy
- Freeland, R.E., Bilyeu, G.D., Veal, G.R., Mikulas, M.M., *Inflatable deployable space structures technology summary*, 1998, proceedings of the 49<sup>th</sup> International Astronautical Congress, Melbourne, Australia
- Garbett, J.: *Bone growth analogy for optimising flexibly formed concrete beams*, MEng Thesis, Dept for Architecture and Civil Engineering, Bath, University of Bath, 2008
- Groot, de A.D.: *Methodologie; Grondslagen van onderzoek en denken in de gedragswetenschappen*, 1994, Van Gorcum, Assen, The Netherlands
- Guidanean, K., Lichodziejewski, D., *An Inflatable Rigidizable Truss Structure Based on New Sub-Tg Polyurethane Composites*, 2002, L'Garde Inc., USA
- Habraken, A., *Reader lightweight structures*, 2010, Eindhoven University of Technology, Eindhoven,



the Netherlands

- Haerle, J.W.S., Grosberg, P. and Backer, S.: Structural mechanics of fibres, yarns and fabrics. Vol.1, New York, 1969.
- Hanks, P., *The New Oxford Dictionary of English*, 1998, Clarendon Press, Oxford, United Kingdom
- Harris, C.M.: *Dictionary of Architecture and Construction*, 2006
- Herzog, T.: *Pneumatic Structures*, 1976, Oxford University Press, Oxford, United Kingdom
- Holslag, A., Westenbrugge, S., *Pneumatische Konstrukties*, 1972
- Houtman, R., Orpana, M.: *Materials for Membrane Structures*, Textile Roofs 2000, Berlin, 2000
- Houtman, R.: From computer model to realized structure, TU Delft, Delft, 1996
- Jenkins, C.H.M., *Gossamer spacecraft*, Compliant structures in nature and engineering, 2005, Montana State University, USA
- Kakani & Kakani, *Material Science*, 2004, New Age International, New Delhi, India
- Koch, K.M., Habermann, K.J., *Membrane Structures: The Fifth Building Material*, 2004
- Krog, L., Tucker, A., Rollema, G., *Application of topology, sizing and shape optimization methods to optimal design of aircraft components*, Airbus UK Ltd, Advanced Numerical Solutions Department, Bristol, United Kingdom
- Kumar, A. V., *Shape and topology synthesis of structures using a sequential optimization algorithm*, 1993, Massachusetts Institute of Technology, Boston, USA
- Kuraray America, Inc.: Vectran liquid crystal polymer Fiber: a unique combination of properties for demanding applications, Fort Mill, 2006
- Lee, K.H., Shin, J.K, Song, S.I., Yoo, Y.M., Park, G.J., *Automotive door design using structural optimization and design of experiments*, 2003, Department of Mechanical Engineering, Hanyang University, Ansan, Kyunggi-Do, South Korea
- Lichtenberg, J.: *Slimbouwen, a strategy for efficient and sustainable building innovation*, 2006, Eindhoven University of Technology, Eindhoven, the

Netherlands

- Luchsinger, R.H., Pedretti, M, Reinhard, Andreas, *Pressure induced Stability; From pneumatic Structures to Tensairity*, Prospective concepts ag, Glattbrugg, Switzerland
- Marcos, J., *Materials and Curing Systems for Inflatable Materials*, 2003, Inasmet fundacion, San Sebastian, Spain
- Meijer, H. Tape making for sailing, TU/e Eindhoven, Eindhoven, 2007
- Motro, R., *An approach to structural morphology*, 2009, Laboratoire de Mécanique et Génie Civil, Université de Montpellier, Montpellier, France
- Nederlands Normalisatie Instituut, *NEN 3835: Mortels voor metselwerk van stenen, blokken of elementen van baksteen, kalkzandsteen, beton en gasbeton*, 1991, Delft, The Netherlands
- Olason, A. & Tidman, D., *Methodology for Topology and Shape Optimization in the Design Process*, 2010, Department of Applied Mechanics, Chalmers University of Technology, Göteborg, Sweden
- Otto, F.: *IL 35; Pneu und Knochen*, 1995, University of Stuttgart, Stuttgart, Germany
- Rao, S.S., *Engineering Optimization: Theory and practice*, 1996, third edition, New Age International Publishers
- Read, T., O'Brien, T.: Coated fabrics for lightweight structures
- Rozvany, G.I.N., *A critical review of established methods of structural topology optimization*, 2001, Department of Structural Mechanics, Budapest University of Technology and Economics, Budapest, Hungary
- Rozvany, G.I.N., *Aims, scope, methods, history and unified terminology of computer-aided topology optimization in structural mechanics*, 2001, Department of Structural Mechanics, Budapest University of Technology and Economics, Budapest, Hungary
- Schnell, A.R., Leigh Jr, L.M., Tinker, M.L., *Deployment, foam rigidization, and structural characterization of inflatable thin-film booms*, 2002, American Institute of Aeronautics and Astronautics, USA
- Skelton, J.: Comparison and selection of materi-



als for air-supported structures. *Journal of coated fibrous materials*.

*the evolution of pneumatic structures*, University of São Paulo, São Paulo, Brazil

- Sobek, W., Speth, M.: Von der Faser zum Gewebe, *Textile werkstoffe im bauwesen*, nr 9 September, 1993
- Thomke, S.H.: *Experimentation matters*, 2003, Harvard Business School, Boston, Massachusetts, USA
- Toyobo Co. Ltd.: PBO fiber Zylon, Osaka, 2005
- United Nations: *Kyoto protocol to the United Nations Framework convention on climate change*, 1998, Obtained from <http://unfccc.int/resource/docs/convkp/kpeng.pdf> on 17 October 2012
- United Nations: *United Nations Framework convention on climate change*, 1992, Obtained from <http://unfccc.int/resource/docs/convkp/con-veng.pdf> on 17 October 2012
- van Dessel, S., Messac, A., Muller, A.A., Farina, A.A., *Feasibility and Optimization of Rigidified Inflatable Structures for Housing*, 2003, Department of Mechanical and Aerospace Engineering, Syracuse University, Syracuse, New York, USA
- Veldman, S.L.: *Design and Analysis Methodologies for Inflatable Beams*, Thesis at TU Delft, Delft University Press, Delft, 2005
- Verenigde Textielindustrie Nederland, *Plan van aanpak Routekaart Textiel*, 2011, Zeist, The Netherlands
- Wesdorp, G.: *Lintijsbaan*, Graduation project TU/e Eindhoven, Eindhoven, 2005
- West, M.: *Fabric Formwork for reinforced concrete and Architecture*, 2010, Centre for Architectural Structures and Technology, University of Manitoba, Winnipeg, Canada
- West, M.: *Material Reduction - Efficient Fabric-Formed Concrete*, 2006, Winnipeg, Canada
- World Business Council for Sustainable Development: *Vision 2050; the new agenda for business*, 2010, Brussels, Belgium
- Yamashita, Y., Kawabata, S., Okada, S. and Tanaka, A.: *Mechanical Characteristics of PBO Single Fiber*, the University of Shiga Prefecture, Hikone, 2003
- Yun Chi, J.: Oliveira Pauletti, M de, *An outline of*

#### Internet sources

- <https://britannica.com/EBchecked/topic/392797/morphology>, consulted at 16/01-2013
- [http://www2.dupont.com/Teflon\\_Industrial/en\\_US/tech\\_info/techinfo\\_compare.html](http://www2.dupont.com/Teflon_Industrial/en_US/tech_info/techinfo_compare.html)
- <http://www.pvc.org/en/p/pvc-strength>
- <http://communities.bentley.com>
- <http://www.compositesworld.com/articles/fabrication-methods>
- <http://www.autocomposites.org/composites101/manufacturing.cfm#introduction>